Parasites, Hosts and Diseases

Volume 64 • Number 3 • July 2026

CONTENTS

http://parahostdis.org

The Korean Society for Parasitology and Tropical Medicine

Parasites, Hosts and Diseases

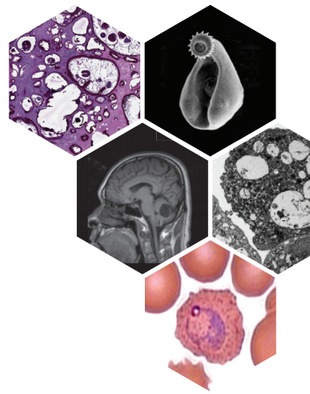

Parasites, Hosts and Diseases

pISSN 2982-5164 eISSN 2982-6799

Volume 64 • Number 3 • July 2026

Volume 64 • Number 3 • July 2026

http://parahostdis.org

The Korean Society for Parasitology and Tropical Medicine

Parasites, Hosts and Diseases

pISSN 2982-5164
eISSN 2982-6799

Volume 64 • Number 3 • July 2026

Parasites, Hosts and Diseases (Parasites Hosts Dis, PHD) is a peer-reviewed, open-access journal published quarterly on the last day of January, April, July, and October. Established in 1963 as *The Korean Journal of Parasitology*, the journal transitioned to an online-only publication starting with Vol. 53 in 2015, and adopted its current title in 2023. As the official publication of The Korean Society for Parasitology and Tropical Medicine, PHD is dedicated to advancing knowledge on human and animal parasites, disease vectors, host-parasite interactions, zoonoses, and tropical medicine. The journal publishes original articles, review articles, case reports, brief communications, letters to the editor, and book reviews.

Abstracting and Indexing Services

A part of articles, metadata, or full text is available from KoreaMed (1963–), CrossRef metadata (1963–), Korea Citation Index (2002–), Science Citation Index Expanded (2008–), MedLine (1993–), PubMed Central (1998–), PubMed (1993–), Scopus (1977–), and EMBASE (2023–).

Publisher The Korean Society for Parasitology and Tropical Medicine
Editor-in-Chief Myeong Heon Shin, MD, PhD

Editorial Office The Korean Society for Parasitology and Tropical Medicine
Department of Tropical Medicine, Yonsei University College of Medicine, Yonsei-ro 50-1, Seodaemun-gu, Seoul 03722 Korea
Tel: +82-2-2228-1844 E-mail: support@parahostdis.org

Publishing Office M2PI
#805, 26 Sangwon 1-gil, Seongdong-gu, Seoul 04779, Korea
Tel: +82-2-6966-4930 Fax: +82-2-6966-4945 E-mail: support@m2-pi.com

This journal was supported by the Korea Association of Health Promotion, National Research Foundation of Korea (NRF) grant and the Korean Federation of Science and Technology Societies (KOFST) grant funded by the Korean Government.

Parasites, Hosts and Diseases

pISSN 2982-5164
eISSN 2982-6799

Volume 64 • Number 3 • July 2026

Editorial Board

Parasites, Hosts and Diseases

pISSN 2982-5164
eISSN 2982-6799

Volume 64 • Number 3 • July 2026

Contents

Original Articles

Brief Communications

Parasites, Hosts and Diseases

pISSN 2982-5164
eISSN 2982-6799

Volume 64 • Number 3 • July 2026

Case Reports

Original Article

Parasites Hosts Dis 2026;64(3):195-202
https://doi.org/10.3347/PHD.26007

Parasites, Hosts and Diseases

pISSN 2982-5164 • eISSN 2982-6799

Infection characteristics of *Diplostomum* species (Digenea: Diplostomidae) metacercariae in fishes from Korea

Woon-Mok Sohn[1,*], Byoung-Kuk Na[1,2], Jung-A Kim[1,2], Hee-Ju Kim[1]

[1]Department of Parasitology and Tropical Medicine, Institute of Medical Science, Gyeongsang National University College of Medicine, Jinju, Korea; [2]Department of Convergence Medical Science, Gyeongsang National University, Jinju, Korea

Infection characteristics of *Diplostomum* spp. metacercariae (DsMc) were analyzed in fishes from 9 major water systems of Korea. A total of 15,879 fishes in 79 species were examined by the artificial digestion method for 8 years (2013–2020). DsMc were detected in 48 (60.8%) out of 79 fish species examined. The prevalence was higher in *Pseudogobio esocinus* (61.5%), *Squalidus chankaensis* (56.9%) and *Zacco platypus* (44.8%). The infection intensities were 22.1, 9.4, 7.5 and 6.7 per fish infected in *Hemibarbus longirostris*, *P. esocinus*, *Z. platypus*, and *S. chankaensis* respectively. The higher prevalence was shown in fishes from Yeongsan-gang (59.3%) and the middle reaches of Seomjin-gang (48.0%), and the higher infection intensities were revealed in fishes from above 2 regions and streams in east coast (83.1, 7.5, and 11.3 per fish infected). In index fish, *Z. platypus*, overall prevalence was 44.8% and the higher prevalence were revealed in the middle reaches of Seomjin-gang (79.6%), Geum-gang (79.2%) and Tamjin-gang (64.7%). The susceptibility index in index fish was highest in fish from the streams in east coast (13.64), and followed by fish from the middle reaches of Seomjin-gang (7.56) and Mangyeong-gang (4.75). This study provides several novel characteristics of DsMc infection in fishes with a report of 30 new second intermediate host of *Diplostomum* spp. in Korea.

Keywords: *Diplostomum* spp., metacercaria, susceptibility index, endemicity, second intermediate fish host

Introduction

Digenetic trematodes (subclass Digenea) are a larger taxonomic group, and they have 2 intermediate and 1 definitive hosts in their life cycle. Various species of vertebrates, i.e., fish, amphibian, reptilian and arthropod, act as the second intermediate hosts, which retained the infective larvae, metacercariae. Digenetic trematode metacercariae (DTM) are mainly inhabited in fish intermediate hosts, and they are microscopically distinguished by the morphological characteristics [1-3]. In Korea, since Chun [4] reported various DTM in 16 fish species collected from streams and ponds in adjacent areas of Nakdong-gang (gang means river), many Korean workers have been investigated the infection status with DTM in fishes from various local areas [5-14]. Especially, they have frequently surveyed the infection status of fishborne zoonotic trematodes, i.e., *Clonorchis sinensis*, *Metagonimus* spp. including *M. yokogawai*, *Centrocestus armatus*, *Isthmiophora hortensis* and *Clinostomum complanatum*, metacercariae in Korea [15-32]. Meanwhile, the metacercarial surveys on the infection status of non-human infecting species including *Diplostomum* spp. have not been widely conducted in fish hosts of Korea [4-14].

In the genus *Diplostomum* von Nordmann 1832, more than 40 nominal species have been described in the world [1,33].

Received: January 15, 2026 Accepted: May 9, 2026
*Correspondence: wmsohn@gnu.ac.kr

Citation
Sohn WM, Na BK, Kim JA, Kim HJ. Infection characteristics of *Diplostomum* species (Digenea: Diplostomidae) metacercariae in fishes from Korea. Parasites Hosts Dis 2026;64(3):195-202.

However, the debate on the species validity existed long time because of taxonomic problems. Recently, several species including *D. spathaceum* (Rudolphi, 1819), *D. pseudospathaceum* Niewiadomska, 1984, *D. ardeae* Dubois, 1969 and *D. baeri* Dubois, 1937 were identified with the morphological and molecular studies [33,34]. In Korea, *D. spathaceum* adults recovered in the intestines of a herring gull, *Larus argentatus*, were only reported by Lee et al. [35]. The metacercariae of *Diplostomum* spp. (DsMc) were first described from catfish, *Parasilurus asotus* (= *Silurus asotus*) by Chun [4]. After that, several Korean workers reported the infection status of DsMc together with other DTM in fishes from specific limited regions of Korea [6,8,9-14]. On the other hand, our team had conducted the surveys on the metacercarial infections of *C. sinensis* in fishes from 9 wide water systems, i.e., Hantan-gang and Imjin-gang, Han-gang, Geum-gang, Mangyeong-gang, Yeongsan-gang, Tamjin-gang, Seomjin-gang, Nakdong-gang and streams in east coast, of Korea for a long time [11,14-24]. Among the data of these surveys, only the infection data of DsMc were gathered and arranged to report them here after excluding the our previous studies with DsMc data [11,13,14].

Methods

Ethics statement

Not applicable.

Fish collection and examination for DsMc

A total of 15,879 fishes in 79 species were collected and examined from 9 major water systems, i.e., Hantan-gang and Imjin-gang, Han-gang, Geum-gang, Mangyeong-gang, Yeongsan-gang, Tamjin-gang, Seomjin-gang, Nakdong-gang and streams in east coast, of Korea. The information on the fishes examined by the survey localities was detailedly shown in Supplementary Tables S1-S13, respectively. The survey localities on the map were nearly included in the map of Sohn [29].

All collected fishes with ice were transported to the laboratory of the Department of Parasitology and Tropical Medicine, Gyeongsang National University College of Medicine, Jinju, Korea. The fish species was identified, after which individual fish was finely ground in a mortar with pestle. The ground fish meat was mixed with artificial gastric juice, and incubated at 36°C for about 2 h. The digested material was filtered through a mesh (pore size 1×1 mm) and washed with 0.85% saline until the supernatant became clear. The sediment was carefully examined under a stereomicroscope. DsMc were separately collected according to a previously described method [3]. The morphologies of 45 DsMc from *Pseudogobio esocinus*, *Squalidus chankensis* and *Zacco platypus* were observed under a light microscope (Olympus BH-22, Olympus) with a micrometer after the previously described procedures for specimen [2,3]. The measurement unit for the morphologies of DsMc was designated with μm. DsMc detected from each fish were counted to determine the infection rate (No. of fish with DsMc/No. of fish examined × 100) and intensity (No. of DsMc detected/No. of fish infected) by fish species and survey localities. The susceptibility index (SI) of DsMc in index fish, *Zacco platypus* was calculated by the formula, prevalence/100 × mean metacercarial intensity per fish infected (PFI).

Results

Morphology of *Diplostomum* spp. metacercariae (*n*=45)

Body elongate-oval, dorso-ventrally flat, 327–480 (376) × 225–297 (263) with a primordial hindbody. Oral sucker oval, 38–50 (45) × 35–50 (43). Two contractile lappets (pseudosuckers) present on each side of oral sucker. Prepharynx very short; pharynx elongate-oval, 15–50 (36) × 13–32 (18); oesophagus short; ceca long, wide, reach posterior to tribocytic (holdfast) organ. Ventral sucker transversely oval, 28–50 (41) × 45–63 (54). Tribocytic organ large, transversely oval, 53–85 (62) × 43–106 (80). Reserve excretory system with numerous, relatively large excretory granules, distributed in a median and 2 lateral fields (Fig. 1).

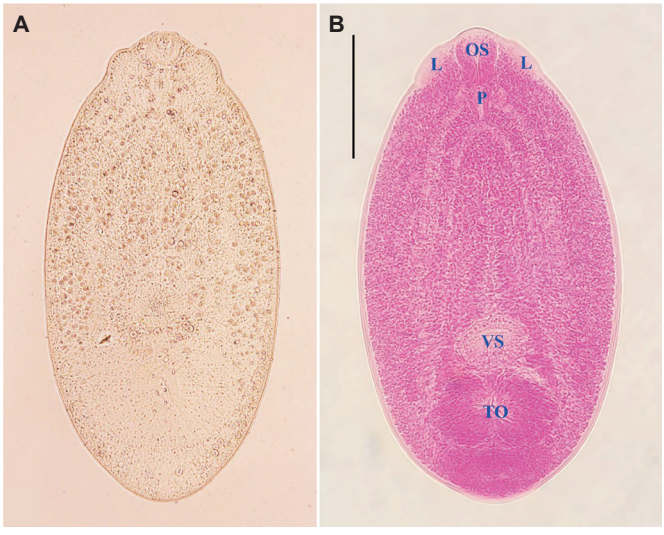

Fig. 1. *Diplostomum* sp. metacercariae detected in a pale chub, *Zacco platypus*, from Deokcheon-gang, a branch stream of Nakdong-gang, in Sancheong-gun, Gyeongsangnam-do, Korea. (A) Fresh unstained and (B) acetocarmin stained. L, lappet; OS, oral sucker; P, pharynx; VS, ventral sucker; TO, tribocytic organ. Scale bar=100 μm.

https://doi.org/10.3347/PHD.26007

Overall infection status with DsMc by positive fish species

DsMc were detected in 3,831 (24.1%) out of 15,879 fishes in 79 fish species examined. The overall infection status of DsMc by the fish species was detailedly revealed in Table 1. No DsMc were detected from 386 fishes in 31 spp., i.e. *Gnathopogon strigatus* (*n*=45), *Mugil cephalus* (39), *Microphysogobio yaluensis* (34), *Ladislabia taczanowskii* (34), *Cobitis sinensis* (22), *Misgurnus anguillicaudatus* (21), *Iksookimia koreensis* (20), *Liobagrus mediadiposalis* (20), *Erythroculter erythropterus* (20), *Liobagrus andersoni* (18), *Chaenogobius castaneus* (17), *Pseudobagrus fulvidraco* (16), *Cottus hangiongensis* (13), *Rhodeus pseudosericeus* (10), *Iksookimia longicorpa* (9), *Liobagrus somjinensis* (9), *Culter brevicauda* (5), *S. asotus* (5), *Cobitis lutheri* (5), *Acanthogobius flavimanus* (4), *Koreocobitis naktongensis* (4), *Hypomesus nipponensis* (3), *Cobitis tetralineata* (2), *Squalidus multimaculatus* (2), *Koreocobitis rotundicaudata* (2), *Hemiculter leucisculus* (2), *Microphysogobio jeoni* (1), *Acheilognathus signifer* (1), *Orthrias nudus* (1), *Misgurnus mizolepis* (1), and *Phoxinus phoxinus* (1). The infection status by the fish species and survey localities was detailedly shown in Supplementary Tables S1-S13, respectively.

Infection status with DsMc by survey localities

DsMc were detected in 3,831 (24.1%) out of 15,879 fishes examined and their infection intensity was 7.2 PFI in average. The prevalence was highest in fishes from Yeongsan-gang (59.3%) and followed by the middle reaches of Seomjin-gang in Gokseong-gun (gun means county) and Gurye-gun, Jeollanam-do (do means province) (48.0%) and Geum-gang (32.3%). That of remain 10 localities was 1.1%–31.3% respectively. The intensity of infection was also highest, 83.1 PFI, in fish from Yeongsan-gang. That of streams in east coast was 11.3 PFI and those of remain 11 localities were 2.1–7.5 PFI respectively. The infection status with DsMc by the survey localities was revealed in Table 2 in detail.

Infection status with DsMc in index fish, *Z. platypus*, by survey localities

DsMc were detected in 1,038 (44.8%) out of 2,319 *Z. platypus* examined and their infection intensity was 7.5 PFI in average. The higher prevalence was revealed in the middle reaches of Seomjin-gang (79.6%), Geum-gang (79.2%), and Tamjin-gang (64.7%). SI in index fish was highest (13.64) in 69 (48.9%) out of 141 *Z. platypus* from streams in east coast, followed by the middle reaches of Seomjin-gang in Gokseong-gun and Gurye-gun, Jeollanam-do (7.56) and Mangyeong-gang (4.75). That of remain 10 localities was 0–3.88 respectively. The infection status with DsMc in index fish, *Z. platypus*, was detailedly shown in Table 3.

Discussion

We described the morphologies of DsMc collected from 3 fish species, i.e., *P. esocinus*, S. *chankensis* and *Z. platypus*, which were susceptible hosts to obtain DsMc specimens easily, in this study. Among 14 genus in Diplostominae, 2 ones, genus *Diplostomum* and *Tylodelphys*, have the possibility to be present in Korean peninsula by the closely related biological factors, the geographical distribution and second intermediate hosts (fish) [1]. The metacercariae of *Diplostomum* spp. have been well known, already reported by many Korean workers and they have been detected only in fishes [4,6,8,11-14]. However, those of *Tylodelphys* spp. have not been reported yet in Korea and they have been found in fishes and amphibians. The metacercarial morphologies of *Tylodelphys* spp. are obviously differentiated from *Diplostomum* spp. metacercariae by the more slender body, no lappets on each side of oral sucker and a long elliptical tribocytic organ [1]. Interspecies differentiation of *Diplostomum* spp. metacercariae is not easy only with morphological characters. Several species of *Diplostomum* metacercariae, i.e., *D. spathaceum*, *D. pseudospathaceum*, *D. ardeae*, *D. baeri*, and *D. phoxini*, were identified with the morphological and molecular studies [33,34]. Therefore, the morphological and molecular studies on the species-validity of DsMc detected by the fish species and survey localities should be performed in the future in Korea.

The DsMc were detected from 48 (60.8%) out of 79 fish species examined in this study. Among 48 positive fish species (PFS), 18 ones, *Abbotina revularis*, *Acanthorhodeus gracilis*, *A. macropterus*, *Acheilognathus koreensis*, *Carassius auratus*, *Cyprinus capio*, *Hemibarbus labeo*, *H. longirostris*, *Hemiculter eigenmanni*, *Lepomis macrochirus*, *Microphysogobio longidorsalis*, *P. esocinus*, *Pseudorasbora parva*, *Pungtungia herzi*, *Rhodeus ocellatus*, *Tribolodon hakonensis*, *Z. platypus*, and *Z. temminckii* (= *Nipponocypris temminckii*), were already reported as the 2nd intermediate hosts of *Diplostomum* spp. in Korea [4-14]. The remaining 30 fish species are regarded as new second intermediate hosts of *Diplostomum* spp. in Korea. In previous studies, a total of 4 fish species (DsMc negative in this study: *S. asotus*, *M. anguillicaudatus*, and *E. erythropterus*, and not examined in this study: *Hemibarbus mylodon*) were revealed as additional second intermediate hosts of *Diplostomum* spp. [4,6,8-11,14]. Accordingly, a total of 52 fish species is listed as

Table 1. Overall[a] infection status of DsMc by the fish species

Positive fish species	No. of fish examined	No. (%) of fish infected	No. of DsMc detected	
			Range	Average
Zacco platypus	2,319	1,038 (44.8)	1–282	7.5
Pungtungia herzi	2,144	124 (5.8)	1–49	3.8
Nipponocypris temminckii	1,033	398 (38.5)	1–60	4.1
Pseudogobio esocinus	1,032	635 (61.5)	1–56	9.4
Carassius auratus	870	63 (7.2)	1–11	2.1
Nipponocypris koreanus[b]	848	363 (42.8)	1–31	5.8
Hemibarbus longirostris	620	137 (22.1)	1–452	22.1
Acheilognathus koreensis	551	164 (29.8)	1–94	5.1
Coreoperca herzi[b]	532	21 (3.9)	1–7	1.8
Squalidus japonicus coreanus[b]	447	146 (32.7)	1–33	6.6
Sarcocheilichthys variegatus[b]	402	3 (0.7)	-	1.0
Odontobutis platycephala[b]	386	32 (8.3)	1–20	3.5
Plecoglossus altivelis[b]	348	20 (5.7)	1–4	1.7
Acheilognathus yamatsutae[b]	345	77 (22.3)	1–29	4.8
Acheilognathus lanceolatus[b]	330	118 (35.8)	1–28	3.5
Acheilognathus rhombeus[b]	316	21 (6.6)	1–16	3.4
Coreoleuciscus splendidus[b]	256	32 (12.5)	1–7	2.4
Acheilognathus majusculus[b]	213	38 (17.8)	1–13	2.7
Squalidus gracilis majimae[b]	207	57 (27.5)	1–32	3.2
Hemibarbus labeo	205	78 (38.0)	1–14	3.5
Squalidus chankaensis[b]	188	107 (56.9)	1–47	6.7
Sarcocheilichthys nigripinnis[b]	169	3 (1.8)	-	1.0
Pseudorasbora parva	159	5 (3.1)	1–2	1.4
Micropterus salmoides[b]	153	2 (1.3)	-	1.0
Coreoperca kawamebari[b]	130	2 (1.5)	-	1.0
Odontobutis obscurus[b]	125	6 (4.8)	1–4	1.8
Opsariichthys uncirostris[b]	122	18 (14.8)	1–4	1.9
Rhynchocypris oxycephalus[b]	111	12 (10.8)	1–5	3.4
Lepomis macrochirus	105	1 (1.0)	-	2.0
Siniperca scherzeri[b]	90	2 (2.2)	-	1.0
Acanthorhodeus gracilis	89	7 (7.9)	1–22	8.9
Microphysogobio longidorsalis	82	14 (17.1)	1–12	3.0
Acanthorhodeus macropterus	81	19 (23.5)	1–5	1.7
Microphysogobio koeensis[b]	75	24 (32.0)	1–11	3.4
Rhodeus ocellatus	57	4 (7.0)	1–1,245	312.0
Hemiculter eigenmanni	52	4 (7.7)	1–3	1.5
Abbottina springeri[b]	47	4 (8.5)	1–2	1.5
Pseudobagrus koreanus[b]	46	1 (2.2)	-	1.0
Tribolodon hakonensis	41	2 (4.9)	1–2	1.5
Abbottina rivularis	38	11 (28.9)	1–70	15.5
Cyprinus capio	38	3 (7.9)	1–4	2.0
Chaenogobius urotaenia[b]	20	2 (10.0)	-	1.0
Tridentiger brevispinis[b]	19	3 (15.8)	1–5	3.3
Acheilognathus somjinensis[b]	18	2 (11.1)	-	1.0
Onchorhynchus masou masou[b]	14	3 (21.4)	1–2	1.3
Acanthogobius lactipes[b]	10	3 (30.0)	1–6	4.3
Channa argus[b]	8	1 (12.5)	-	4.0
Lateolabrax japonicus[b]	2	1 (50.0)	-	5.0
Total	15,879[c]	3,831 (24.1)	1–1,245	7.2

DsMc, *Diplostomum* spp. metacercariae.

[a]A total of 48 fish species was positive with DsMc; [b]Thirty fish intermediate hosts of *Diplostomum* spp. newly listed in this study; [c]A total of 386 DsMc negative fishes (31 species) was included.

https://doi.org/10.3347/PHD.26007

Table 2. Infection status of DsMc by the survey locality in Korea

Survey locality	No.[a] of fish examined	No. (%) of fish infected	No. of DsMc detected	
			Range	Average
Hantan-gang and Imjin-gang	1,323	275 (20.8)	1–48	5.2
Han-gang	707	124 (17.5)	1–54	4.2
Geum-gang	830	268 (32.3)	1–28	4.3
Mangyeong-gang	927	223 (24.1)	1–59	6.4
Yeongsan-gang	86	51 (59.3)	1–1,245	83.1
Tamjin-gang	2,201	563 (26.6)	1–52	5.5
Seomjin-gang (upper reaches)[b]	1,259	347 (27.6)	1–47	6.7
Seomjin-gang (middle reaches)[c]	1,276	613 (48.0)	1–106	7.5
Seomjin-gang (lower reaches)[d]	1,161	363 (31.3)	1–40	4.3
Nakdong-gang (upper reaches)[e]	1,179	269 (22.8)	1–94	6.8
Nakdong-gang (middle reaches)[f]	1,647	18 (1.1)	1–6	2.1
Nakdong-gang (lower reaches)[g]	2,057	456 (22.2)	1–65	4.3
Streams in east coast	1,226	261 (21.3)	1–282	11.3
Total	15,879	3,831 (24.1)	1–1,245	7.2

DsMc, *Diplostomum* spp. metacercariae.
[a]No. of fish (No. of fish species) in DsMc negative: 573 (23), 289 (19), 176 (16), 96 (19), 8 (3), 322 (12), 186 (18), 188 (8), 214 (19), 177 (19), 990 (31), 142 (11), and 147 (15) by the survey localities from upper to bottom; [b]Seomjin-gang in Jeollabuk-do; [c]Seomjin-gang in Jeollanam-do; [d]Seomjin-gang in Gyeongsangnam-do; [e]Nakdong-gang in Gyeongsangbuk-do; [f]Nakdong-gang (Wi-cheon) in Gyeongsangbuk-do; [g]Nakdong-gang in Gyeongsangnam-do.

Table 3. Infection status of DsMc in the index fish, *Zacco platypus*, by the survey locality in Korea

Survey locality	No. of fish examined	No. (%) of fish infected	No. of DsMc detected		
			Range	Average	SI[a]
Hantan-gang and Imjin-gang	289	134 (46.4)	1–18	3.4	1.58
Han-gang	85	28 (32.9)	1–5	2.1	0.69
Geum-gang	101	80 (79.2)	1–22	4.9	3.88
Mangyeong-gang	100	44 (44.0)	1–59	10.8	4.75
Yeongsan-gang	30	3 (10.0)	1–2	1.3	0.01
Tamjin-gang	266	172 (64.7)	1–49	5.2	3.36
Seomjin-gang (upper reaches)[b]	182	76 (41.8)	1–34	6.8	2.84
Seomjin-gang (middle reaches)[c]	206	164 (79.6)	1–106	9.5	7.56
Seomjin-gang (lower reaches)[d]	185	87 (47.0)	1–21	2.9	1.36
Nakdong-gang (upper reaches)[e]	211	97 (46.0)	1–64	8.1	3.73
Nakdong-gang (middle reaches)[f]	326	6 (1.8)	1–3	1.5	0.00
Nakdong-gang (lower reaches)[g]	197	78 (39.6)	1–65	5.3	2.10
Streams in east coast	141	69 (48.9)	1–282	27.9	13.64
Total	2,319	1,038 (44.8)	1–282	7.5	3.36

DsMc, *Diplostomum* spp. metacercariae; SI, susceptibility index.
[a]Prevalence/100 × mean metacercarial intensity per fish infected; [b]Seomjin-gang in Jeollabuk-do; [c]Seomjin-gang in Jeollanam-do; [d]Seomjin-gang in Gyeongsangnam-do; [e]Nakdong-gang in Gyeongsangbuk-do; [f]Nakdong-gang (Wi-cheon) in Gyeongsangbuk-do; [g]Nakdong-gang in Gyeongsangnam-do.

the second intermediate hosts of *Diplostomum* spp. by the present and previous studies in Korea.

In this study, the number of fish examined was 2–2,310 (322.8 in average) in 48 fish species of DsMc positive group, but that was 1–45 (12.5 in average) in 31 fish species of DsMc negative group. The number of fish examined was quite different between 2 groups. Fish species in DsMc negative group were not collected a lot in this study. The reason why they might be less prevalent in the water systems surveyed. The fish catching methods, mainly by netting and casting net, and

the fish ecology, especially the high prevalence of predatory fish species, i.e., snake head (*Channa argus*), Mandarin fish (*Siniperca scherzeri*), Korean aucha perch (*Coreaperca herzi*), large mouth bass (*M. salmoides*) and blue gill (*L. macrochirus*), might be partly affected the small number of fish examined and of even DsMc negative group in some localities. If the fish species in negative group were examined enough, some of them could be convert to the DsMc positive species.

The overall prevalence of DsMc was 24.1% and the infection intensity was 7.2 PFI in average in 48 PFS in this study. Among 48 PFS, the prevalence was highest in *P. esocinus* (61.5%) and followed by that in *S. chankaensis* (56.9%), *Z. platypus* (44.8%), *Nipponocypris koreanus* (42.8%), *N. temminckii* (38.5%), *H. labeo* (38.0%), *Acheilognathus lanceolatus* (35.8%), and *Squalidus japonicus coreanus* (32.7%). The mean infection intensity was highest in *R. ocellatus* (312.0), followed by in *H. longirostris* (22.1), *A. rivularis* (15.5), *P. esocinus* (9.4) and *A. gracilis* (8.9). In case of *R. ocellatus*, DsMc were detected in 4 (7.0%) out of 57 fish examined and 1,245 DsMc were extraordinally detected from only 1 fish, which will be the cause of the highest infection intensity. The most susceptible fish with DsMc was *P. esocinus* (61.5% prevalence and 9.4 infection intensity) in this study. It was previously confirmed by Sohn et al. [11]. They reported 53.8% and 66.7% DsMc prevalence and 8.1 and 28.0 infection intensity in *P. esocinus* from Hantan-gang and Imjin-gang respectively. On the other hand, Sohn and Choi [8] reported 85.0% and 73.0% DsMc prevalence and 9.5 and 12.0 infection intensity in 2 species of cultrinid fish, *E. erythropterus* and *H. eigenmanni*, from Junam-jeosuji (jeosuji means reservoir) in Uichang-gun, Gyeongsangnam-do, Korea. Interestingly, DsMc were found in pond smelt, *Hypomesus olidus* (= *H. nipponensis*) [9,10] and sea rundace, *T. hakonensis*, from 3 coastal lakes in Gangwon-do [13]. From the present and previous studies, we can know that the prevalence and infection intensity of DsMc are somewhat affected by the fish species, the susceptible fish species aforementioned.

The prevalence with DsMc was more or less higher in fishes from Yeongsan-gang (59.3%) and middle reaches of Seomjin-gang (48.0% in Gokseong-gun and Gurye-gun in Jeollanam-do). The intensity of infection with DsMc was much higher in fishes from Yeongsan-gang (83.1 FPI) than in fishes from middle reaches of Seomjin-gang (7.5 FPI). Meanwhile in fishes from streams in east coast, the prevalence (21.3%) was similar with the overall prevalence, but the infection intensity (11.3 PFI) was relatively high. On the other hand, Sohn et al. [11] reported 17.6% DsMc prevalence and 6.9 infection intensity in fishes from Hantan-gang and Imjin-gang. In this study, the prevalence was 20.8%, and the mean infection intensity was 5.2 PFI in fishes from Hantan-gang and Imjin-gang. Sohn and Choi [8] reported 42.3% DsMc prevalence and 10.5 mean infection intensity in 130 fish of 5 species, i.e., *E. erythropterus*, *H. eigenmanni*, *C. auratus*, *P. parva* and *A. macropterus*, from Junam-jeosuji. In the same survey locality, Junam-jeosuji, Sohn and Na [14] detected a total of 46 DsMc (2.7 in average) in 17 (7.7%) out of 220 fish in 7 species examined. They also reported 33.9% DsMc prevalence and 2.4 mean infection intensity in 127 fish of 7 species, i.e., *E. erythropterus*, *H. eigenmanni*, *P. parva*, *C. auratus*, *C. carpio*, *L. macrochirus*, and *Micropterus salmoides*, from Woopo-neup (neup means swamp) in Changnyeong-gun, Gyeongsangnam-do [14]. Choe et al. [12] reported 5.7% DsMc prevalence and 7.3 mean infection intensity in 314 fish of 7 species, *Z. platypus*, *C. auratus*, *H. longirostris*, *P. esocinus*, *P. herzi*, *L. macrochirus* and *M. salmoides*, from Daecheong-ho (ho means lake) in Chungcheongnam-do. The prevalence and infection intensity of DsMc were much different by the survey localities in this study. However, those of all survey localities (Table 2) except for Nakdong-gang (middle reaches: Wi-cheon) were higher than those of previous studies.

The pale chub, *Z. platypus*, is widely distributed in the water systems of Korea. They were most dominantly collected in this study. The objective endemicity of DsMc infection was calculated from the index fish, *Z. platypus*, which was also recommended as the index fish for the infections of *Metagonimus* spp. metacercariae in Sohn [29]. A total of 2,319 pale chubs were examined, and they were 14.5% of total 15,985 in 48 PFS. The overall DsMc prevalence was 44.8%, the infection intensity was 7.5 PFI and the SI was 3.36 in average. The DsMc prevalence was relatively high in *Z. platypus* from Seomjin-gang (middle reaches in Jeollanam-do: 79.6%), Geum-gang (79.2%) and Tamjin-gang (64.7%). The infection intensity was somewhat higher in index fish from streams in east coast (27.9), Mangyeong-gang (10.8) and Seomjin-gang (middle reaches: 9.5). The SI was also higher in pale chubs from streams in east coast (13.64), Seomjin-gang (middle reaches: 7.56), and Mangyeong-gang (4.75). The endemicity of DsMc in the index fish (Table 3) was not coincided with that in all fish species examined (Table 2) except for that of Seomjin-gang (middle reaches). In case of all fish species examined, the number of DsMc negative fish is too much included and is affected the prevalence. On the other hand, Sohn et al. [11] reported 27.3% prevalence, 2.2 infection intensity and 0.60 SI in *Z. platypus* from Hantan-gang and Imjin-gang. In this study, the slightly higher endemicity (1.58 SI) was re-

https://doi.org/10.3347/PHD.26007

vealed in index fish from the same locality, Hantan-gang and Imjin-gang. Choe et al. [12] reported 26.0% prevalence, 10.0 infection intensity and 2.60 SI in *Z. platypus* from Daecheong-ho, Chungcheongnam-do, Korea. From the findings of present and previous studies, we can suppose that the endemicity with DsMc is much higher in index fish, *Z. platypus*, from streams of east coast and Seomjin-gang (middle reaches) in Jeollanam-do, Korea.

Conclusively, it was confirmed that DsMc are prevalent in various species of fishes in Korea although their prevalence and infection intensity are somewhat different by fish species and survey localities. And then the second intermediate hosts of *Diplostomum* spp. are obviously listed and consolidated by this study in Korea. The endemicity (SI) of DsMc in index fish, *Z. platypus*, is regarded as a useful comparative datum in the conjecture of epidemiological situation. Further studies are needed with regard to the species-diversity of *Diplostomum* spp. flukes in Korea. The species-validity for DsMc detected by the fish species and survey localities should be clarified by molecular genomic studies. Morphological characteristics on the adults recovered from the avian hosts, which are naturally and/or experimentally infected with DsMc, should be precisely described for the fauna of this fluke group in Korea.

Author contributions

Conceptualization: Sohn WM. Data curation: Sohn WM, Na BK, Kim JA. Formal analysis: Sohn WM, Na BK. Investigation: Sohn WM, Na BK, Kim JA, Kim HJ. Methodology: Sohn WM, Na BK, Kim JA. Project administration: Sohn WM, Kim JA. Supervision: Sohn WM. Validation: Sohn WM, Na BK. Visualization: Sohn WM. Writing - original draft: Sohn WM. Writing - review & editing: Sohn WM, Na BK.

Conflict of interest

Woon-Mok Sohn and Byoung-Kuk Na serve as editors of Parasites, Hosts and Diseases but had no involvement in the decision to publish this article. No other potential conflicts of interest relevant to this study were reported.

Supplementary information

Supplementary material is available with this article at https://doi.org/10.3347/PHD.26007.

ORCID

Woon-Mok Sohn, https://orcid.org/0000-0002-9795-9386
Byoung-Kuk Na, https://orcid.org/0000-0002-6734-1673

References

1. Gibson DI, Jones A, Bray RA. Keys to the trematoda. Vol. 1. CABI Publishing and the Natural History Museum; 2002.
2. Sohn WM. Invertebrate fauna of Korea. Vol. 6, No. 1. Trematodes. National Institute of Biological Resources; 2013.
3. Sohn WM. Fish-borne zoonotic trematode metacercariae in the Republic of Korea. Korean J Parasitol 2009;47 Suppl:S103-13. https://doi.org/10.3347/kjp.2009.47.S.S103
4. Chun SK. Studies on some trematodes whose intermediate hosts are fishes in the Naktong River. Bull Fish Coll 1962;4:21-38.
5. Rhee JK, Lee HI, Baek BK, Kim PG. Survey on encysted cercariae of trematodes from fresh-water fishes in Mangyeong riverside area. Korean J Parasitol 1983;21:187-92. https://doi.org/10.3347/kjp.1983.21.2.187
6. Rhee JK, Rim MH, Baek BK, Lee HI. Survey on encysted cercariae of trematodes from fresh-water fishes in Tongjin riverside areas in Korea. Korean J Parasitol 1984;22:190-202. https://doi.org/10.3347/kjp.1984.22.2.190
7. Kong HH, Choi BR, Moon CH, Choi DW. Larval digenetic trematodes from fresh water fish in River Miryang, Korea. Jpn J Parasitol 1995;44:112-8.
8. Sohn WM, Choi YS. Infection status with trematode metacercariae in the fresh-water fish from Chunamchosuchi (pond), Uichang-gun, Kyongsangnam-do, Korea. Korean J Parasitol 1997;35:165-70. https://doi.org/10.3347/kjp.1997.35.3.165
9. Nam HS, Sohn WM. Infection status with trematode metacercariae in pond smelts, *Hypomesus olidus*. Korean J Parasitol 2000;38:37-9. https://doi.org/10.3347/kjp.2000.38.1.37
10. Cho SH, Sohn WM, Shin SS, et al. Infection status of pond smelts, *Hypomesus olidus*, and other freshwater fishes with trematode metacercariae in 6 large lakes. Korean J Parasitol 2006;44:243-6. https://doi.org/10.3347/kjp.2006.44.3.243
11. Sohn WM, Na BK, Cho SH, et al. Trematode metacercariae in freshwater fish from water systems of Hantangang and Imjingang in Republic of Korea. Korean J Parasitol 2015;53:289-98. https://doi.org/10.3347/kjp.2015.53.3.289
12. Choe S, Park H, Lee D, et al. Infections with digenean trematode metacercariae in two invasive alien fish, *Micropterus salmoides* and *Lepomis macrochirus*, in two rivers in Chungcheongbuk-do, Republic of Korea. Korean J Parasitol 2018;56:509-13. https://doi.org/10.3347/kjp.2018.56.5.509
13. Sohn WM, Na BK, Cho SH, Lee SW. Infection status with digenetic trematode metacercariae in fishes from coastal lakes in Gangwon-do, Republic of Korea. Korean J Parasitol 2019;57:681-90. https://doi.org/10.3347/kjp.2019.57.6.681
14. Sohn WM, Na BK. Infections with digenetic trematode metacercari-

ae in freshwater fishes from two visiting sites of migratory birds in Gyeongsangnam-do, Republic of Korea. Korean J Parasitol 2019;57:273-81. https://doi.org/10.3347/kjp.2019.57.3.273
15. Cho SH, Lee WJ, Kim TS, et al. Prevalence of zoonotic trematode metacercariae in freshwater fish from Gangwon-do, Korea. Korean J Parasitol 2014;52:399-412. https://doi.org/10.3347/kjp.2014.52.4.399
16. Sohn WM, Na BK, Cho SH, et al. Endemicity of zoonotic trematode metacercariae in fish from Deokcheon-gang (river) in Sancheong-gun, Gyeongsangnam-do, Republic of Korea. Korean J Parasitol 2021;59:523-9. https://doi.org/10.3347/kjp.2021.59.5.523
17. Sohn WM, Na BK, Cho SH, et al. Survey of zoonotic trematode metacercariae in fish from irrigation canal of Togyo-jeosuji (reservoir) in Cheorwon-gun, Gangwon-do, Republic of Korea. Korean J Parasitol 2021;59:427-32. https://doi.org/10.3347/kjp.2021.59.4.427
18. Sohn WM, Na BK, Cho SH, et al. Prevalence and infection intensity of zoonotic trematode metacercariae in fish from Soyang-cheon (stream), in Wanju-gun, Jeollabuk-do, Korea. Korean J Parasitol 2021;59:265-71. https://doi.org/10.3347/kjp.2021.59.3.265
19. Cho SH, Sohn WM, Na BK, et al. Prevalence of *Clonorchis sinensis* metacercariae in freshwater fish from three latitudinal regions of the Korean Peninsula. Korean J Parasitol 2011;49:385-98. https://doi.org/10.3347/kjp.2011.49.4.385
20. Sohn WM, Na BK, Cho SH, et al. Prevalence of *Clonorchis sinensis* metacercariae in fish from water systems of Seomjin-gang (River). Korean J Parasitol 2017;55:305-12. https://doi.org/10.3347/kjp.2017.55.3.305
21. Sohn WM, Na BK, Cho SH, Ju JW, Son DC. Prevalence and intensity of *Clonorchis sinensis* metacercariae in freshwater fish from Wicheon stream in Gunwi-gun, Gyeongsangbuk-do, Korea. Korean J Parasitol 2018;56:41-8. https://doi.org/10.3347/kjp.2018.56.1.41
22. Yoon KB, Lim HC, Jeon DY, et al. Infection status with *Clonorchis sinensis* metacercariae in fish from Tamjin-gang (river) in Jeollanam-do, Republic of Korea. Korean J Parasitol 2018;56:183-8. https://doi.org/10.3347/kjp.2018.56.2.183
23. Sohn WM, Na BK, Cho SH, et al. High endemicity with *Clonorchis sinensis* metacercariae in fish from Yongjeon-cheon (stream) in Cheongsong-gun, Gyeongsangbuk-do, Korea. Korean J Parasitol 2021;59:97-101. https://doi.org/10.3347/kjp.2021.59.1.97
24. Sohn WM. Infection characteristics of *Clonorchis sinensis* metacercariae in fish from Republic of Korea. Korean J Parasitol 2022;60:79-96. https://doi.org/10.3347/kjp.2022.60.2.79
25. Yoo WG, Sohn WM, Na BK. Current status of *Clonorchis sinensis* and clonorchiasis in Korea: epidemiological perspectives integrating the data from human and intermediate hosts. Parasitology 2022;149:1296-305. https://doi.org/10.1017/S0031182022000798
26. Song CY, Lee SH, Jeon SR. Studies on the intestinal fluke, *Metagonimus yokogawai* Katsurada, 1912 in Korea. IV. Geographical distribution of sweetfish and infection status with *Metagonimus* metacercariae in south-eastern area of Korea. Korean J Parasitol 1985;23:123-38. https://doi.org/10.3347/kjp.1985.23.1.123
27. Cho SH, Kim TS, Na BK, Sohn WM. Prevalence of *Metagonimus* metacercariae in sweetfish, *Plecoglossus altivelis*, from eastern and southern coastal areas in Korea. Korean J Parasitol 2011;49:161-5. https://doi.org/10.3347/kjp.2011.49.2.161
28. Sohn WM, Na BK, Cho SH, et al. Infection status with *Metagonimus* spp. metacercariae in fishes from Seomjin-gang and Tamjin-gang in Republic of Korea. Korean J Parasitol 2018;56:351-8. https://doi.org/10.3347/kjp.2018.56.4.351
29. Sohn WM. Infection characteristics of *Metagonimus* species (Digenea: Heterophyidae) metacercariae in fish from major rivers of Korea. Parasites Hosts Dis 2024;62:1-29. https://doi.org/10.3347/PHD.23096
30. Sohn WM, Na BK, Cho SH, et al. Infections with *Centrocestus armatus* metacercariae in fishes from water systems of major rivers in Republic of Korea. Korean J Parasitol 2018;56:341-9. https://doi.org/10.3347/kjp.2018.56.4.341
31. Sohn WM, Na BK, Cho SH, Ju JW. Infection status of *Isthmiophora hortensis* metacercariae in dark sleepers, *Odontobutis* species, from some water systems of the Republic of Korea. Korean J Parasitol 2018;56:633-7. https://doi.org/10.3347/kjp.2018.56.6.633
32. Sohn WM, Na BK, Cho SH. Infection status with *Clinostomum complanatum* metacercariae in fish from water systems of Nakdong-gang (river) in Korea. Korean J Parasitol 2019;57:389-97. https://doi.org/10.3347/kjp.2019.57.4.389
33. Niewiadomska K, Laskowski Z. Systematic relationships among six species of *Diplostomum* Nordmann, 1832 (Digenea) based on morphological and molecular data. Acta Parasitol 2002;47:20-8.
34. Lebedeva DI, Chrisanfova GG, Ieshko EP, et al. Morphological and molecular differentiation of *Diplostomum* spp. metacercariae from brain of minnows (*Phoxinus phoxinus* L.) in four populations of northern Europe and East Asia. Infect Genet Evol 2021;92:104911. https://doi.org/10.1016/j.meegid.2021.104911
35. Lee YI, Seo M, Chai JY. Intestinal flukes recovered from a herring gull, *Larus argentatus*, in the Republic of Korea. Korean J Parasitol 2020;58:81-6. https://doi.org/10.3347/kjp.2020.58.1.81

Original Article

Parasites Hosts Dis 2026;64(3):203-214
https://doi.org/10.3347/PHD.26003

Parasites, Hosts and Diseases

pISSN 2982-5164 • eISSN 2982-6799

The therapeutic potential of green synthesized zinc oxide nanoparticles in murine schistosomiasis

Asmaa M. El-kady[1,*], Majed H. Wakid[2,3,*], Khalil Mohamed[4], Abdullah Alhazmi[4], Wafa Abdullah Al-Megrin[5], Hayam Elshazly[6], Eman Sayed[7], Matthew W. Spears[8], Hatem A. Elshabrawy[8,*], Eman Fathy Fadel[9], Marawan Khodary[10], Somia Mohammed El Hassan[11]

[1]Department of Medical Parasitology, Faculty of Medicine, Qena University, Qena, Egypt; [2]Department of Medical Laboratory Sciences, Faculty of Applied Medical Sciences, King Abdulaziz University, Jeddah, Saudi Arabia; [3]Special Infectious Agents Unit, King Fahd Medical Research Center, King Abdulaziz University, Jeddah, Saudi Arabia; [4]Department of Epidemiology and Medical Statistics, Faculty of Public Health and Health Informatics, Umm Al-Qura University, Makkah, Saudi Arabia; [5]Department of Biology, College of Science, Princess Nourah bint Abdulrahman University, Riyadh, Saudi Arabia; [6]Department of Biology, College of Science, Qassim University, Al-Qassim, Saudi Arabia; [7]Department of Parasitology, Faculty of Veterinary Medicine, Qena University, Qena, Egypt; [8]Department of Molecular and Cellular Biology, College of Osteopathic Medicine, Sam Houston State University, Conroe, USA; [9]Department of Medical Parasitology, Faculty of Medicine, Sohag University, Sohag, Egypt; [10]Faculty of Medicine, Qena University, Qena, Egypt; [11]Biology Department, Faculty of Science, Al-Baha University, Al-Baha, Saudi Arabia

Schistosomiasis remains a major neglected tropical disease, affecting approximately 600 million individuals worldwide and accounting for nearly 500,000 deaths annually. The principal causative species—*Schistosoma haematobium*, *S. mansoni*, and *S. japonicum*—drive significant morbidity through hepatomegaly, splenomegaly, and progressive hepatic fibrosis. Praziquantel (PZQ) remains the cornerstone of treatment; however, its limited efficacy against immature worms and eggs, combined with concerns over emerging drug resistance, underscores the urgent need for novel therapeutic alternatives. This study investigated the anti-schistosomal potential of green-synthesized zinc oxide (ZnO) nanoparticles (NPs) in a murine model of *S. mansoni* infection, benchmarked against PZQ. ZnO NPs were fabricated using ginger extract via an eco-friendly green synthesis approach. Fifty male BALB/c mice were randomly assigned to five groups (n=10): normal control, infected untreated control, infected treated with PZQ alone, infected treated with ZnO NPs alone, and infected treated with a PZQ–ZnO NP combination. Parasitological, histopathological, and fibrosis assessments were subsequently performed. All treatment groups demonstrated significant reductions in worm burden and tissue egg counts relative to infected untreated controls. Histopathological examination of untreated infected mice revealed extensive chronic granulomatous inflammation, concentric perioval fibrosis, fibroblast proliferation, hepatocellular necrosis, hydropic degeneration, marked collagen deposition, and portal-to-portal fibrous bridging. Treated groups, by contrast, exhibited marked hepatic improvement characterized by reduced granuloma size, diminished fibrosis, and decreased collagen deposition. Collectively, these findings indicate that green-synthesized ZnO NPs possess promising anti-schistosomal and antifibrotic properties, warranting further investigation as a potential adjunct or alternative therapeutic strategy for schistosomiasis management.

Keywords: Schistosomiasis, zinc oxide, nanoparticles, fibrosis, protective, hepatocytes

Received: January 7, 2026 Accepted: March 29, 2026
*Correspondence: ame, asmaa.elkady@med.svu.edu.eg; mhw, mwakid@kau.edu.sa; hae, hatem.elshabrawy@shsu.edu

Citation
El-kady AM, Wakid MH, Mohamed K, Alhazmi A, Al-Megrin WA, Elshazly H, Sayed E, Spears MW, Elshabrawy HA, Fadel EF, Khodary M, El Hassan SM. The therapeutic potential of green synthesized zinc oxide nanoparticles in murine schistosomiasis. Parasites Hosts Dis 2026;64(3):203-214.

Introduction

Schistosomiasis, often referred to as bilharziasis, is a tropical illness that is frequently overlooked regarding its significant public health implications in various areas, including South America, Asia, and particularly sub-Saharan Africa. This disease is caused by parasitic trematodes, commonly known as blood flukes, which belong to the genus *Schistosoma*. Each year, approximately 600 million individuals are affected by schistosomiasis globally, resulting in around 280,000–500,000 deaths fatalities each year [1]. The human form of schistosomiasis is attributed to 8 distinct species within the *Schistosoma* genus, with *S. mansoni*, *S. haematobium*, and *S. japonicum* being the most prevalent and pathogenic parasites. The disease is associated with a range of immunopathological alterations, with hepatosplenomegaly being a notable characteristic. Additionally, it is estimated that 90% of those infected experience hepatic fibrosis as a result of egg granulomas [2]. The widespread impact of schistosomiasis underscores the need for increased awareness and targeted interventions to mitigate its effects on affected populations.

The development of a vaccine for schistosomiasis has been extensively researched, yet none have achieved regulatory approval to date. Since the 1970s, praziquantel (PZQ) has served as the primary treatment option in numerous endemic areas. This oral medication is effective against all species of *Schistosoma* and is generally regarded as safe and well-absorbed [3]. Nevertheless, its efficacy is limited when it comes to targeting eggs and immature worms.

Moreover, the frequent administration of PZQ, particularly among school-aged children, raises concerns about its long-term effectiveness in regions where schistosomiasis is highly prevalent. As a result, several countries have reported less than satisfactory outcomes from PZQ treatments [4]. This situation underscores the need for ongoing evaluation and potential alternatives to enhance treatment efficacy in affected populations.

The emergence of nanotechnology as a precise, rapid, and cost-effective therapeutic option has garnered significant interest for addressing various infectious agents [5]. A nanoparticle (NP), measuring between 1 to 100 nanometers, possesses the ability to penetrate the tiniest capillaries in the body, thereby improving solubility, absorption, and overall uptake [6]. Furthermore, NPs demonstrate superior accumulation in targeted tissues compared to standard pharmaceuticals, resulting in a reduction in systemic toxicity. The synthesis of NPs using natural and environmentally friendly materials is referred to as green NP synthesis. This method presents several advantages over traditional chemical and physical synthesis techniques, such as reduced toxicity [7], lower environmental pollution [8], increased economic feasibility [9], and enhanced sustainability [10]. These benefits underscore the potential of green synthesis in advancing nanotechnology applications in medicine and various other domains.

Zinc plays an essential role in maintaining human health, and zinc oxide (ZnO) NPs demonstrate antimicrobial properties while being non-toxic to humans [11]. The diminutive size of ZnO particles enhances the surface area available for interaction, leading to a range of physical, chemical and biological effects at elevated concentrations [12]. Furthermore, ZnO NPs are generally well tolerated by human cells, and the safety of ZnO has been confirmed by the Food and Drug Administration [13]. ZnO NPs can generate reactive oxygen species, disrupt membranes, and interfere with parasite metabolism, while zinc itself has recognized antioxidant and tissue protective properties in various organ systems, including models of schistosomiasis related neuro and tissue injury [14].

The environmentally friendly and cost-effective green synthesis of ZnO NPs utilizing plant extracts eliminates the need for toxic reagents and frequently results in particles that exhibit excellent stability and bioactivity. ZnO NPs synthesized with ginger have demonstrated significant antioxidant and antimicrobial properties, potentially acting as a dual-action treatment that directly targets *Schistosoma* worms and their eggs, while also reducing oxidative stress, inflammation, and fibrosis—thus serving as an alternative or complementary option to PZQ in the treatment of schistosomiasis [15-17]. Finally, this study aimed to assess the therapeutic efficacy of green-synthesized ZnO NPs using ginger extract in treating *S. mansoni* infection in mice, in comparison to standard PZQ treatment.

Methods

Ethics statement

All animal experiments were approved by the institutional review board and ethics committee of the Faculty of Medicine at New Valley University, Egypt, granted approval for all animal experiments (NVREC-0232-2024-9) considering ARRIVE guideline compliance.

Preparation of ZnO NPs

ZnO NPs were prepared according to the methodology described previously [18]. Initially, dried ginger (0.5 g) was dissolved in 100 ml of ethanol and then mixed with 5 g of zinc ace-

https://doi.org/10.3347/PHD.26003

tate, which had been previously dissolved in 1,000 ml of boiled distilled water. The mixture was stirred for 30 min at 60°C. The pH was adjusted to 12 using sodium hydroxide, leading to the formation of ZnO NPs. Stirring continued for another hour to ensure complete reduction. Afterward, the mixture was centrifuged at 4,000 rpm, and the sediment was washed twice with distilled water and once with ethanol before drying and freezing to obtain the NPs.

Characterization of ZnO NPs

Examination of ZnO NPs by scanning electron microscopy (SEM) was done to determine the surface morphology of the NPs [19]. The samples were prepared by adhering lyophilized powder to stubs with carbon tape and then coating them with a thin gold layer to enhance conductivity. SEM imaging was conducted at high magnifications (up to 60,000 times) and imaged by scanning electron microscope (JEOL JSM-5500 LV, JEOL).

Determination of ZnO NPs size and distribution

This was conducted using photon correlation spectroscopy, which relies on quasi-elastic or dynamic light scattering techniques facilitated by a particle size analyzer known as ZetaSizer. This method provides essential metrics, including the mean particle size, particle diameter, and the polydispersity index, which serves as a dimensionless indicator of the variability within the particle size distribution as protocol provided previously [15]. In this process, 1 mg of ZnO NPs was dispersed in 5 ml of deionized water and agitated to achieve a homogeneous mixture.

The size measurements were conducted using disposable cuvettes, with a scattering angle set at 90° and the temperature maintained at 25°C. To ensure the reliability of the results, each sample was analyzed in triplicate, allowing for the calculation of average values and SD from the measurements obtained. This rigorous approach ensures a comprehensive understanding of the particle size characteristics and distribution of the ZnO NPs.

For a comprehensive assessment of the surface charge characteristics of the ZnO NPs, contributing valuable insights into their behavior in various applications, ZnO NPs was evaluated through laser Doppler anemometry utilizing a ZetaSizer device, following the previously outlined protocol. To conduct the analysis, the ZnO NPs suspension was diluted 100 times with deionized water and subsequently measured within a capillary cell, employing a detector angle of 90° of 633 nm wavelength at 25°C. Each measurement was performed in triplicate to ensure accuracy. The results obtained from these measurements were reported as mean ± SD [20].

Experimental animals and grouping

Fifty adult male BALB/c mice, each weighing between 18 and 20 g, were sourced from the Schistosome Biological Supply Program at Theodor Bilharz Research Institute located in Giza, Egypt. Mice were maintained and bred in specific pathogen-free conditions at the department of Parasitology, Faculty of Medicine, Qena University, Qena, Egypt. The mice were housed 3 per cage under a 12/12-h light/dark cycle at 22°C–23°C with 40%–70% humidity. They had free access to food and water and were acclimated for 1 week before the experiment. Regular monitoring allowed for the timely identification of any health issues, ensuring the welfare of the animals throughout the duration of the study. To ensure that the experimental mice were free of any intestinal parasitic infection, the feces were examined microscopically using various techniques, including direct wet smears, concentration using formal ether, and permanent staining [21,22]. The mice in the infected groups underwent percutaneous infection with approximately 60 ± 10 *S. mansoni* cercariae per mouse, utilizing the paddling method previously described [16].

Mice were assigned randomly into 5 distinct groups, each consisting of 10 animals: Group I, uninfected and untreated negative control; Group II, infected and untreated positive control; Group III, infected with *S. mansoni* cercariae and subsequently treated with PZQ, administered orally during the 6th week post-infection at a dosage of 1,000 mg/kg over 2 consecutive days [16,17]; Group IV, infected and treated with a homogenous suspension of powdered ZnO NPs [23], administered at a dosage of 10 mg/kg per day for 5 consecutive days [6,24]; and Group V, infected and treated with ZnO NPs+PZQ. At 8th week post-infection (10 days after the end of treatment), all mice were euthanized by cervical dislocation under isoflurane anesthesia for further analyses.

Worm burden and reduction percentage

The recovery of adult schistosomes was assessed using the porto-mesenteric perfusion technique, adapted from a method established previously [25]. A citrate saline solution was used to perfuse the adult worms. The recovered worms were transferred to a clean sieve that had been previously sanitized with 70% ethyl alcohol. The perfusion procedure concluded when the liver, kidneys, and intestines exhibited a pale appearance. The worms were subsequently washed 3 times with a phosphate buffer (pH 7.4), then counted [26], and the percentage reduction in worm burden was calculated using the formula provided below, as utilized previously [4,27].

$$\text{Worm burden reduction \%} = \frac{\text{Mean worms number in control group} - \text{mean worms number in treated group}}{\text{Mean worms number in control group}} \times 100$$

Egg counts in intestine and liver

The liver and intestine were extracted from all groups, cleaned, and weighed. Small pieces of both tissues were then separately digested in a 4% potassium-hydroxide solution at 37°C for 6–12 h. The tissue suspensions were then centrifuged at 1,500 rpm for 5 min and the supernatants were discarded. After 3 cycles of washing and centrifugation, the number of eggs in 2 100-μl aliquots was determined using a light microscope. The results were expressed as the mean number of eggs per gram of intestine and liver tissue [28].

Oogram pattern

The effect of the used formula on the degree of ova maturity and viability was calculated. Three parts of the small intestine (each 1 cm in length) were sliced longitudinally after perfusion, washed in saline, dried on filter paper and then squeezed between 2 glass slides. As a rule, in each fragment, one hundred eggs were counted and this was replicated with other fragments until a total of 300 eggs were collected and categorized into 3 types: immature, mature, and dead [29].

Histopathological examination

Following the sacrifice, a portion of the liver tissue was promptly fixed in a 10% buffered formalin solution and subsequently processed into paraffin blocks. Sections measuring 5 μm in thickness were prepared on albuminized glass slides and stained with hematoxylin-eosin for standard histopathological analysis, which included granuloma counting, measurement of granuloma diameter, and cellular profiling. Additionally, Masson's trichrome staining was employed to evaluate tissue fibrosis. The cellular profiles of liver egg granulomas were examined, with the calculation of the percentage of various cell types present within the granulomas across different groups. The classification of granulomas as cellular, fibrocellular, or fibrous was based on the ratio of cellular to fibrous components. Furthermore, the percentage of egg granulomas containing either intact or degenerated eggs was determined. Granulomas in the liver were counted across 5 consecutive low-power fields (10×), and their diameters were measured using graduated eyepiece lenses, focusing solely on lobular granulomas that contained central ova. Two perpendicular maximal diameters were recorded to calculate the mean diameter for each granuloma, followed by the computation of mean granuloma diameters for the group [30]. The preparations were examined using a microscope at a magnification of ×400.

Statistical analysis

The analysis of the results was conducted utilizing the statistical software package SPSS version 16 (SPSS Inc.). The data was presented as mean ± SD. To assess differences between groups, one-way analysis of variance was employed, along with the non-parametric Mann–Whitney *U*-test to compare the mean values of various variables between the treated and control groups in this study. A *P*-value of less than 0.05 was considered statistically significant. Reduction percentage in adult worms, egg and oogram count was calculated using the following formula:

$$\text{Efficacy (\%)} = \frac{\text{Mean count in control group} - \text{mean count in treated group}}{\text{Mean count in control group}} \times 100$$

Results

Characterization of ZnO NPs

The morphology and dimensions of the synthesized NPs were examined using SEM. Fig. 1 illustrates the successful synthesis of ZnO NPs. The ZnO NPs exhibited a non-spherical shape with consistent distribution. As indicated in Fig. 1, the size of the produced particles varied between 35.9 nm and 111.1 nm.

As shown in Fig. 2, the main peak is at about 1,352 nm in diameter, meaning most particles are a little over 1 μm in size. The Z-average size is 2,270 nm and the polydispersity index is 0.518, indicating a broad and somewhat heterogeneous size distribution rather than a very monodisperse sample. No secondary peaks are reported (Peak 2 and 3 are 0), so there is no clear evidence of separate smaller or larger particle populations, just 1 broad main population.

On the other hand, the zeta potential peak is at about +20.8 mV, with all of the area (100%) in this single peak. This value indicates a moderately positive surface charge: the particles have some electrostatic repulsion and colloidal stability, but they are not as strongly stabilized as systems with |ζ| above about 30 mV. The standard deviation of 5.76 mV shows a relatively tight distribution around this charge value, meaning most particles carry a similar surface charge.

S. mansoni adult worm burden

The administration of PZQ or ZnO NPs or the combination of both resulted in a substantial decrease in the overall worm burden, demonstrating statistical significance ($P<0.001$)

https://doi.org/10.3347/PHD.26003

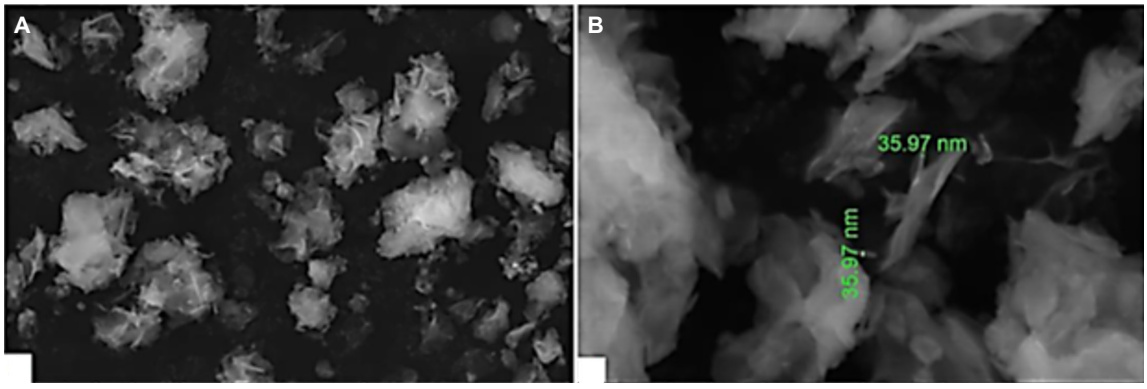

Fig. 1. The morphology and dimensions of the synthesized zinc oxide (ZnO) nanoparticles (NPs). (A) Scanning electron microscopy morphology of ZnO NPs showing non spherical structures. (B) The size of ZnO NPs as measured by scanning electron microscopy ranging from 35.9 to 111.1 nm (×60,000).

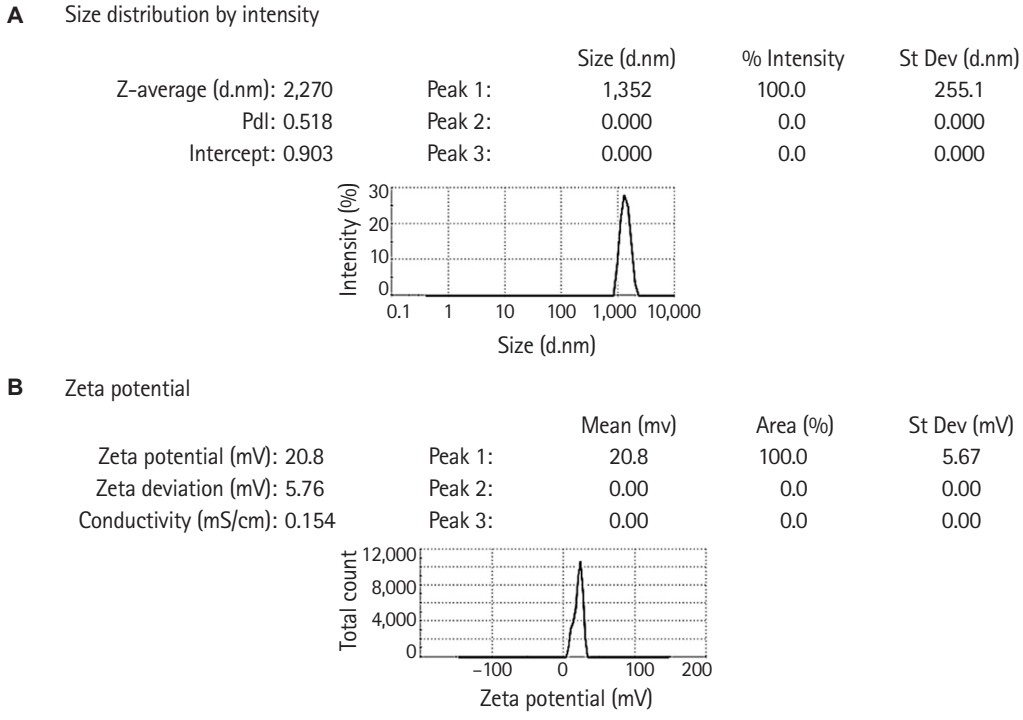

Fig. 2. Zeta potential characteristics of zinc oxide nanoparticles. (A) Size distribution by intensity. (B) Zeta potential as revealed by dynamic light scattering. The analysis revealed that the samples exhibited positive charges were measured 20.8±16.6 mV. The hydrodynamic diameters of the zinc oxide nanoparticles were determined to be 1,248 nm, with a polydispersity index (PDI) of 2,270.

when compared to the infected control group that did not receive treatment (Fig. 3).

Intestinal and hepatic egg count

In relation to the egg counts of *S. mansoni*, the animals that received treatment exhibited a significant decrease in both hepatic and intestinal egg counts with ($P<0.001$) when compared to the infected non-treated control group.

As shown in Fig. 4, animals that received a combination of both ZnO NPs and PZQ showed the highest reduction rate of total hepatic and intestinal egg counts (reduction of 95.4%) when compared to infected non-treated control group to those animals that received treatment. The group treated with PZQ demonstrated a substantial reduction in egg densities (reduction of 94.03%). This was followed by the animals treated with ZnO NPs, which showed a 63.9% reduction in total egg count.

As shown in Fig. 5, the 3 treatment regimens significantly changed the oogram patterns when compared to the infected-untreated group. The highest percentage of dead eggs was

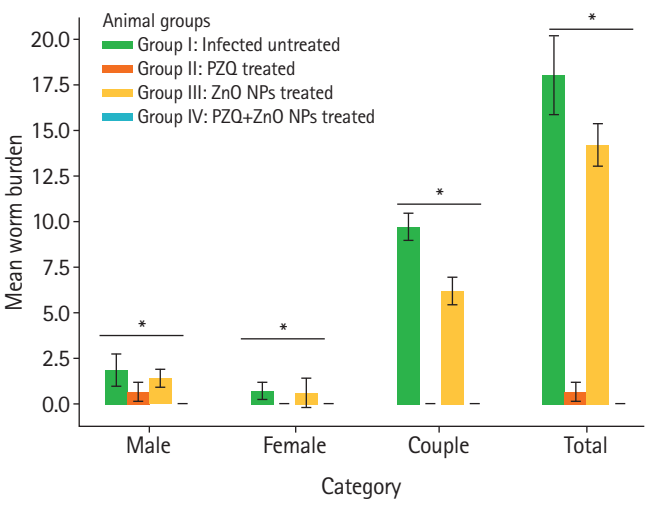

Fig. 3. *Schistosoma mansoni* worm burden and total reduction percentage in each animal group. Data are expressed as means (n=10) and were analysed using one-way analysis of variance and Tukey as a post hoc test. * indicates significant difference between the infected untreated animal group on one hand and the treated groups on the other hand. PZQ, praziquantel; ZnO, zinc oxide; NPs, nanoparticles.

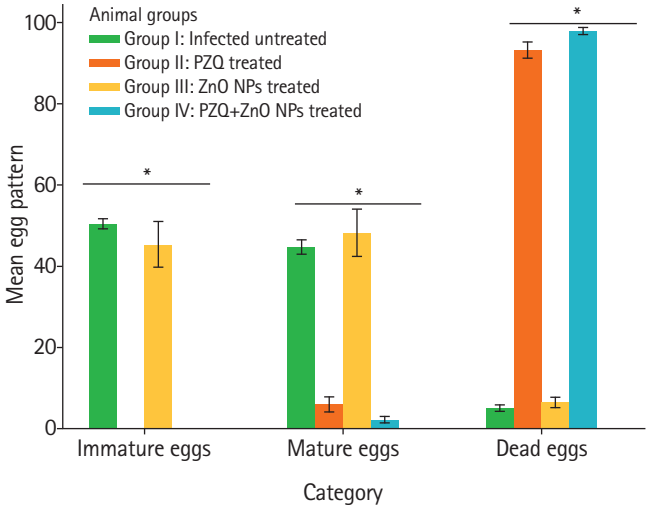

Fig. 5. Comparison of *Schistosoma mansoni* oogram patterns in treated and untreated animal groups. Data are expressed as means (n=10) and were analysed using one-way analysis of variance and Tukey as a post hoc test. * indicates significant difference between the infected untreated animal group on one hand and the treated groups on the other hand. PZQ, praziquantel; ZnO, zinc oxide; NPs, nanoparticles.

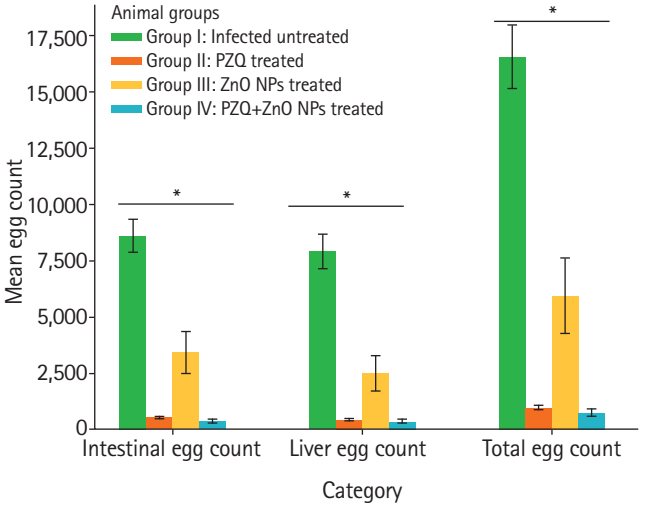

Fig. 4. Egg counts of *Schistosoma mansoni* in liver and intestinal tissues in each untreated and treated animal groups. Data are expressed as means (n=10) and were analysed using one-way analysis of variance and Tukey as a post hoc test. * indicates significant difference between the infected untreated animal group on one hand and the treated groups on the other hand. PZQ, praziquantel; ZnO, zinc oxide; NPs, nanoparticles.

recorded among ZnO NPs + PZQ-treated mice (97.8% versus 5% in infected untreated animals $P<0.002$), as compared to infected-untreated animals (1.60%).

Histopathological examination

Microscopic analysis of liver sections from normal mice revealed the typical cellular structure of hepatic lobules. The normal arrangement of hepatic cords radiating from the central veins to the lobule's periphery was evident, with narrow blood sinusoids lined by endothelial cells separating the cell cords. In contrast, the liver parenchyma of the infected untreated control group exhibited numerous chronic granulomatous lesions. These granulomas were primarily composed of parasite ova containing miracidia, surrounded by infiltrates of inflammatory cells. A notable feature of the granulomas was concentric fibrosis, characterized by numerous fibroblasts encircling the entrapped ova. Additionally, peri-granulomatous hepatocytes exhibited areas of necrosis and hydropic degeneration (Fig. 6).

Histological examination of liver sections from both the PZQ and ZnO NPs-treated groups showed a significant improvement compared to the non-treated infected group. This improvement was evidenced by a reduction in both the number and size of granulomas (Table 1). Moreover, there was a decrease in the number of bilharzial ova, the extent of hepatic fibrosis, and the infiltration of chronic inflammatory cells in these treated groups. Our results indicated a significant reduction in the average number of granulomas in both treated groups (Table 1).

Evaluation of the degree of liver fibrosis using Masson's trichrome-stained sections

Liver fibrosis was evaluated utilizing Masson's trichrome

https://doi.org/10.3347/PHD.26003

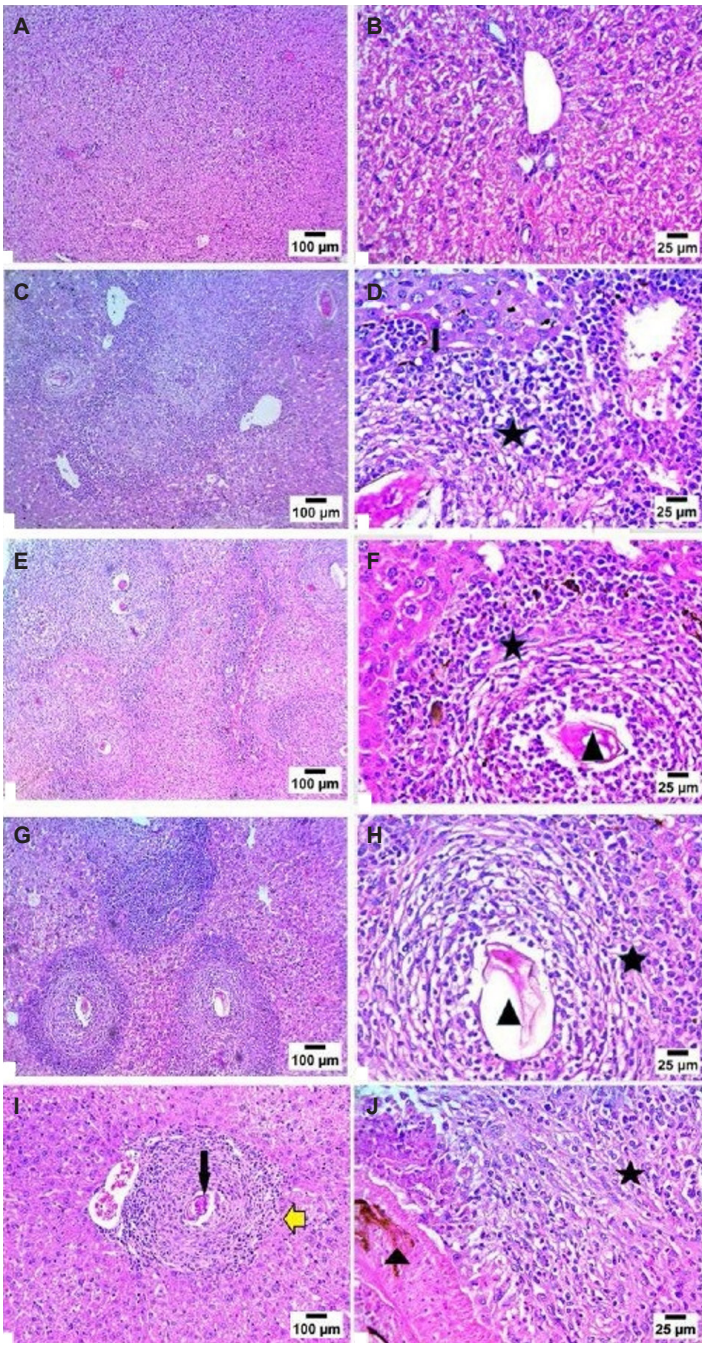

Fig. 6. Photomicrograph sections stained with hematoxylin-eosin showing the effect of various treatments on the *Schistosoma* induced hepatic granulomatous changes from each animal group investigated. (A, B) Sections from normal mice showing normal histological structure of the portal area. (C, D) Sections from *S. mansoni* infected untreated mice showing severe granulomatous changes in the portal triad, formed of fibrous connective tissue with inflammatory cells infiltration mainly eosinophils and lymphocytes (asterisk). (E, F) Sections from *S. mansoni* infected praziquantel treated mice with marked reduction of the number and diameter of *S. mansoni* egg granulomas in comparison with un-treated mice group. Liver sections showed granulomas in the portal triad, in which *S. mansoni* egg (arrowhead) is surrounded by fibrous connective tissue with inflammatory cells infiltration mainly eosinophils and lymphocytes (asterisk). (G, H) Sections from *S. mansoni* infected zinc oxide nanoparticles treated mice showing marked reduction of the number and diameter of *S. mansoni* egg granulomas in comparison with un-treated mice group. Sections showed granulomas change in the portal triad, in which *S. mansoni* (arrowhead) surrounded by fibrous connective tissue with inflammatory cells infiltration mainly eosinophils and lymphocytes (asterisk). (I, J) Sections from *S. mansoni* infected and treated with a combination of zinc oxide nanoparticle and praziquantel showing marked reduction of the number and diameter of *S. mansoni* egg granulomas in comparison with un-treated mice group. Sections showed granulomas change in the portal triad, in which adult *S. mansoni* (arrowhead) surrounded by fibrous connective tissue with inflammatory cells infiltration mainly eosinophils and lymphocytes (asterisk). (A, C, E, G, I) Magnification ×100, (B, D, F, H, J) Magnification ×400.

Table 1. Characteristics of the number and size of granulomas due to *Schistosoma mansoni* eggs in treated and untreated animal groups

Animal group	Count		Diameter		Cellular granuloma	Fibrocellular granuloma	Intact eggs	Degenerated eggs
	No.	Reduction	Size (μm)	Reduction				
Group I. Infected untreated	11.8	None	294.3	None	25	75	75	25
Group II. PZQ treated	4.8	59.3	200	31.9	5	95	25	75
Group III. ZnO NPs treated	9.7	17.8	261.7	11.1	40	60	75	25
Group IV. PZQ+ ZnO NPS treated	6.5	45	258.3	12.4	5	95	25	75

Values are presented as % unless otherwise indicated.
PZQ, praziquantel; ZnO, zinc oxide; NPs, nanoparticles.

staining. In the sections from the negative control group, the central vein and portal tract walls displayed a thin layer of collagen fibers, signifying normal collagen deposition. Conversely, the infected non-treated group revealed a significant increase in collagen fibers surrounding granulomas, as well as periportal fibrosis and portal-portal fibrous bridging. In contrast, both the PZQ and ZnO NPs-treated groups demonstrated a decrease in collagen deposition around the granulomas and portal tracts when compared to the infected untreated mice (Fig. 7).

Discussion

The present study demonstrates that green-synthesized ZnO NPs exert significant anti-schistosomal and hepato-protective effects in a murine model of *S. mansoni* infection, and that their combination with PZQ enhances therapeutic efficacy beyond PZQ monotherapy. The marked reduction in adult worm burden following treatment with PZQ, ZnO NPs, or their combination—each significantly lower than in infected untreated controls—confirms that both agents interfere with parasite survival. Of note, the ZnO NPs + PZQ regimen achieved nearly complete suppression of worm burden (99%), surpassing the already high efficacy of PZQ alone (96.28%), whereas ZnO NPs alone produced a smaller but still appreciable 21% reduction. This is consistent with previous research that has highlighted the anti-parasitic properties of various NPs, which are thought to induce oxidative stress and disrupt essential metabolic pathways in the parasites [6].

The decrease in hepatic and intestinal egg counts further supports the therapeutic potential of ZnO NPs. The combined ZnO NPs and PZQ treatment resulted in the most significant reduction in total egg burden (95.4%), closely followed by PZQ monotherapy (94.03%), while ZnO NPs alone achieved a 63.9% reduction. Because schistosomiasis pathology is primarily driven by the host's immune response to tissue trapped eggs, reducing egg deposition and viability is expected to attenuate granulomatous inflammation and subsequent fibrosis. Oogram analysis supports this idea: the ZnO NPs and PZQ group exhibited the highest rate of dead eggs (97.8% compared to 5% in infected untreated controls), and all treated groups showed a marked shift towards dead and degenerated eggs, which aligns with reduced egg viability or production.

Histopathological examination of liver tissue offers direct evidence of these protective effects. Infected untreated mice developed numerous chronic granulomas, characterized by schistosome eggs embedded in fibroblast rich concentric fibrosis, along with associated inflammatory infiltrates and zones of hepatocellular necrosis and hydropic degeneration. In contrast, livers from PZQ and ZnO NP treated animals demonstrated a notable improvement, with fewer and smaller granulomas, a reduced egg load, diminished inflammatory cell infiltration, and less extensive fibrosis. Quantitative evaluation confirmed a significant decrease in the mean number of granuloma in both treatment groups. Masson's trichrome staining further revealed that collagen deposition surrounding granulomas and portal tracts was considerably lower in treated mice compared to infected controls, highlighting the ability of ZnO NPs, similar to PZQ, to mitigate the development of schistosomal liver fibrosis—a crucial factor in morbidity associated with chronic infection [31,32].

The use of ginger extract for green synthesis adds a biocompatibility and sustainability advantage [14]. Ginger is rich in polyphenols, gingerols, alkaloids, and proteins that can act as reducing agents and surface capping ligands, facilitating the conversion of zinc ions to ZnO NPs and stabilizing the resulting NPs against aggregation. Such capping may also influence the biological activity of the NPs, potentially imparting antioxidants, anti-inflammatory, or antimicrobial properties that add to the intrinsic effects of ZnO. Although repeated washing

https://doi.org/10.3347/PHD.26003

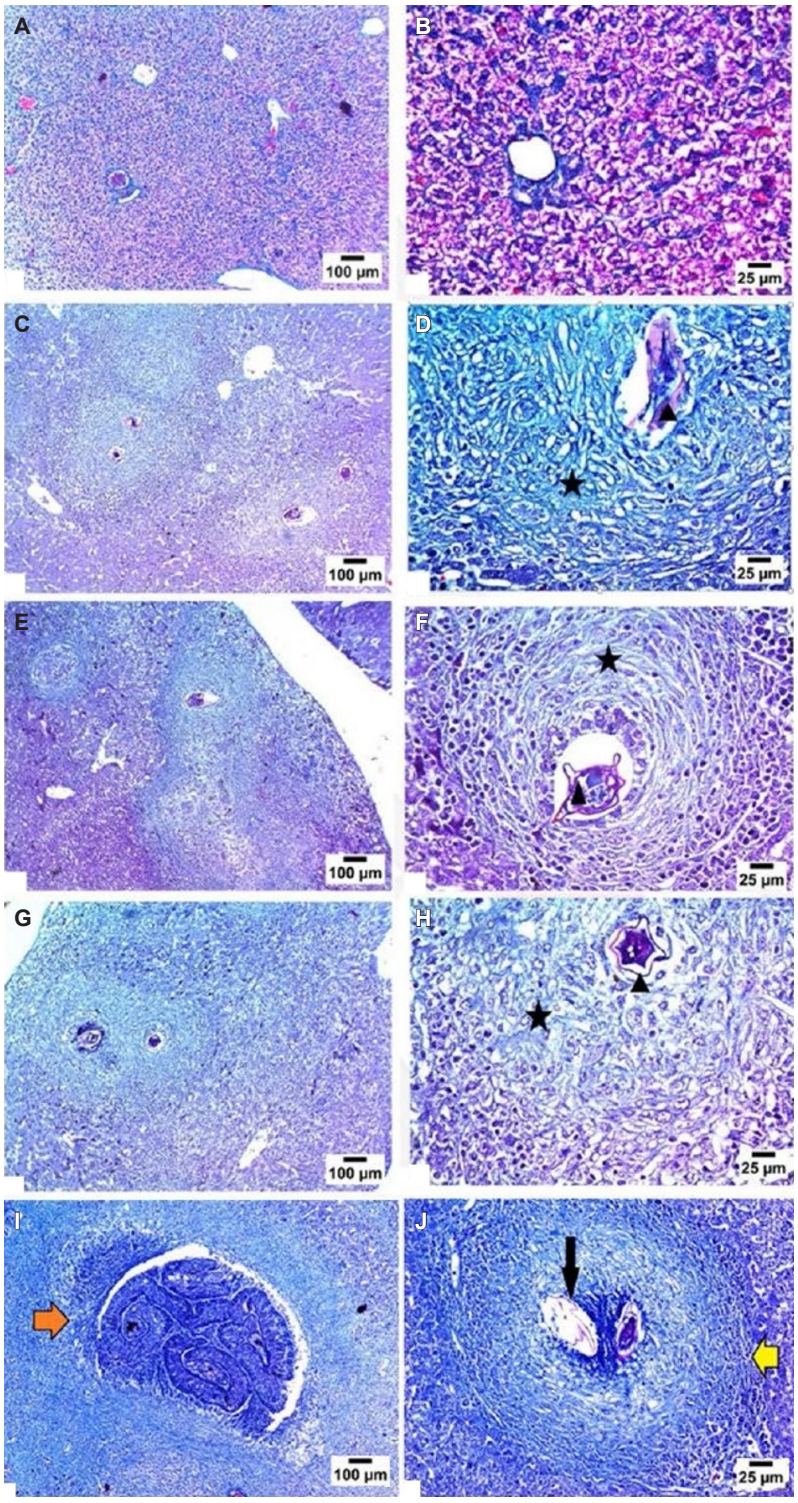

Fig. 7. Photomicrograph sections stained with Masson's trichrome evaluating hepatic fibrosis from each animal group investigated. (A, B) Photomicrograph showing normal histological structure of portal area with no fibrosis formation. (C, D) Photomicrograph showing *Schistosoma* parasite (arrowhead) granuloma with marked infiltration of fibrous connective tissue (asterisk). (E, F) Photomicrograph showing *Schistosoma* parasite (arrowhead) granuloma with significant reduction of fibrous connective tissue infiltration (asterisk) in comparison to infected untreated mice. (G, H) Photomicrograph showing *Schistosoma* parasite (arrowhead) granuloma with significant reduction of fibrous connective tissue infiltration (asterisk) in comparison to infected untreated mice. (I, J) Photomicrograph showing *Schistosoma* parasite (orange arrow) granuloma with significant reduction of fibrous connective tissue infiltration in comparison to infected untreated mice. (I, J) Sections from *S. mansoni* infected and treated with a combination of zinc oxide nanoparticle and praziquantel showing fibrocellular granulomas (yellow arrow) and a dead-worm granuloma (orange arrow). (A, C, E, G, I) Magnification ×100, (B, D, F, H, J) Magnification ×400.

and FTIR analysis did not show prominent peaks attributable to ginger derived organic moieties, trace phytochemical residues adsorbed on the NP surface cannot be entirely excluded and may have contributed to the observed anti-schistosomal and hepato-protective effects [31,33-35].

Several limitations should be acknowledged. The absence of a ginger extract only control and a group treated with chemically synthesized (non green) ZnO NPs precludes a clear dissection of the relative contributions of the inorganic ZnO core versus ginger derived surface components to the therapeutic outcome. Future work should include these controls to distinguish NPs-specific effects from those attributable to plant metabolites. Additionally, the mechanistic interpretation of liver protection is currently limited to histopathology and fibrosis scoring; inclusion of serum liver enzymes (e.g., alanine transaminase, aspartate transaminase), oxidative stress markers, antioxidants, and inflammatory mediators would provide a more comprehensive picture of the underlying molecular pathways. Finally, the observed aggregation in aqueous media suggests that formulation, dispersion behavior under physiological conditions, pharmacokinetics, and long term toxicity should be systematically evaluated before considering clinical translation.

In conclusion, green synthesized ZnO NPs represent a promising adjunct to PZQ therapy for schistosomiasis, exhibiting significant worm reduction, egg suppression, and anti fibrotic effects in a murine *S. mansoni* model. The combination of ZnO NPs with PZQ appears superior to PZQ monotherapy in several key parameters, warranting further investigation to optimize dosing regimens, clarify the detailed mechanisms of action, and assess safety for potential therapeutic use.

Author contributions

Conceptualization: El-kady AM, Khodary M. Data curation: El-kady AM, Wakid MH. Formal analysis: El-kady AM, Fadel EF. Funding acquisition: Al-Megrin WA, Elshabrawy HA. Investigation: Mohamed K, Alhazmi A, Elshazly H, Sayed E, Elshabrawy HA, El Hassan SM. Methodology: Spears MW, Khodary M, El Hassan SM. Project administration: El-kady AM, Wakid MH. Resources: El-kady AM. Software: El-kady AM, Fadel EF, Khodary M. Supervision: El-kady AM, Wakid MH. Validation: Alhazmi A, Elshazly H, Sayed E, Elshabrawy HA. Visualization: Mohamed K, Alhazmi A, Al-Megrin WA, Elshazly H, Sayed E, Spears MW. Writing – original draft: El-kady AM. Writing – review & editing: El-kady AM, Wakid MH.

Conflict of interest

The authors have no conflicts of interest to declare.

Funding

This work was supported by Princess Nourah bint Abdulrahman University Researchers Supporting Project number (PNURSP2026R39) at Princess Nourah bint Abdulrahman University, Riyadh, Saudi Arabia.

ORCID

Asmaa M. El-kady, https://orcid.org/0000-0002-9294-2630
Majed H. Wakid, https://orcid.org/0000-0003-4941-5373
Khalil Mohamed, https://orcid.org/0000-0002-0703-6757
Abdullah Alhazmi, https://orcid.org/0009-0001-4033-8722
Wafa Abdullah Al-Megrin, https://orcid.org/0000-0001-8011-8153
Hayam Elshazly, https://orcid.org/0000-0002-2892-9271
Eman Sayed, https://orcid.org/0000-0001-7007-4580
Matthew W. Spears, https://orcid.org/0009-0006-8562-186X
Hatem A. Elshabrawy, https://orcid.org/0000-0002-7771-113X
Eman Fathy Fadel, https://orcid.org/0000-0002-3264-1887
Marawan Khodary, https://orcid.org/0009-0004-0363-679X
Somia Mohammed El Hassan, https://orcid.org/0009-0003-2045-5053

References

1. LoVerde PT. Schistosomiasis. In: Toledo R, Fried B, editors. Digenetic trematodes. Springer; 2024. p. 75-106.
2. Song LJ, Yin XR, Mu SS, et al. The differential and dynamic progression of hepatic inflammation and immune responses during liver fibrosis induced by *Schistosoma japonicum* or carbon tetrachloride in mice. Front Immunol 2020;11:570524. https://doi.org/10.3389/fimmu.2020.570524
3. Doenhoff MJ, Cioli D, Utzinger J. Praziquantel: mechanisms of action, resistance and new derivatives for schistosomiasis. Curr Opin Infect Dis 2008;21:659-67. https://doi.org/10.1097/QCO.0b013e328318978f
4. Melman SD, Steinauer ML, Cunningham C, et al. Reduced susceptibility to praziquantel among naturally occurring Kenyan isolates of *Schistosoma mansoni*. PLoS Negl Trop Dis 2009;3:e504. https://doi.org/10.1371/journal.pntd.0000504
5. Kaittanis C, Santra S, Perez JM. Emerging nanotechnology-based strategies for the identification of microbial pathogenesis. Adv Drug Deliv Rev 2010;62:408-23. https://doi.org/10.1016/j.addr.2009.11.013
6. Dkhil MA, Al-Quraishy S, Wahab R. Anticoccidial and antioxidant activities of zinc oxide nanoparticles on *Eimeria papillata*-induced infection in the jejunum. Int J Nanomedicine 2015;10:1961-8. https://doi.org/10.2147/IJN.S79944
7. Devi HS, Boda MA, Shah MA, Parveen S, Wani AH. Green synthesis

of iron oxide nanoparticles using *Platanus orientalis* leaf extract for antifungal activity. Green Process Synth 2019;8:38-45. https://doi.org/10.1515/gps-2017-0145
8. Alsammarraie FK, Wang W, Zhou P, Mustapha A, Lin M. Green synthesis of silver nanoparticles using turmeric extracts and investigation of their antibacterial activities. Colloids Surf B Biointerfaces 2018;171:398-405. https://doi.org/10.1016/j.colsurfb.2018.07.059
9. Kataria N, Garg VK. Green synthesis of Fe3O4 nanoparticles loaded sawdust carbon for cadmium (II) removal from water: regeneration and mechanism. Chemosphere 2018;208:818-28. https://doi.org/10.1016/j.chemosphere.2018.06.022
10. Nasrollahzadeh M, Mohammad Sajadi S. Pd nanoparticles synthesized in situ with the use of *Euphorbia granulate* leaf extract: catalytic properties of the resulting particles. J Colloid Interface Sci 2016;462:243-51. https://doi.org/10.1016/j.jcis.2015.09.065
11. Chitra K, Annadurai G. Antimicrobial activity of wet chemically engineered spherical shaped ZnO nanoparticles on food borne pathogen. Int Food Res J 2013;20:59-64.
12. Dwivedi S, Wahab R, Khan F, et al. Reactive oxygen species mediated bacterial biofilm inhibition via zinc oxide nanoparticles and their statistical determination. PLoS One 2014;9:e111289. https://doi.org/10.1371/journal.pone.0111289
13. Emamifar A, Kadivar M, Shahedi M, Soleimanian-Zad S. Evaluation of nanocomposite packaging containing Ag and ZnO on shelf life of fresh orange juice. Innov Food Sci Emerg Technol 2010;11:742-8. https://doi.org/10.1016/j.ifset.2010.06.003
14. Król G, Fortunka K, Majchrzak M, et al. Metallic nanoparticles and core-shell nanosystems in the treatment, diagnosis, and prevention of parasitic diseases. Pathogens 2023;12:838. https://doi.org/10.3390/pathogens12060838
15. Ranjan AP, Mukerjee A, Helson L, Vishwanatha JK. Scale up, optimization and stability analysis of Curcumin C3 complex-loaded nanoparticles for cancer therapy. J Nanobiotechnology 2012;10:38. https://doi.org/10.1186/1477-3155-10-38
16. Abd El Wahab WM, El-Badry AA, Mahmoud SS, et al. Ginger (Zingiber Officinale)-derived nanoparticles in *Schistosoma mansoni* infected mice: hepatoprotective and enhancer of etiological treatment. PLoS Negl Trop Dis 2021;15:e0009423. https://doi.org/10.1371/journal.pntd.0009423
17. Muchirah PN, Yole D, Kutima H, et al. Determination of effective praziquantel dose in different mouse strains: BALB/c and Swiss mice in treatment of *Schistosoma mansoni*. J Clin Immunol Immunopathol Res 2012;4:12-21. https://doi.org/10.5897/JCIIR12.004
18. Melk MM, El-Hawary SS, Melek FR, et al. Antiviral activity of zinc oxide nanoparticles mediated by *Plumbago indica* L. extract against herpes simplex virus type 1 (HSV-1). Int J Nanomedicine 2021;16:8221-33. https://doi.org/10.2147/IJN.S339404
19. Rescignano N, Amelia M, Credi A, Kenny JM, Armentano I. Morphological and thermal behavior of porous biopolymeric nanoparticles. Eur Polym J 2012;48:1152-9. https://doi.org/10.1016/j.eurpolymj.2012.05.005
20. Cohen-Sela E, Chorny M, Koroukhov N, Danenberg HD, Golomb G. A new double emulsion solvent diffusion technique for encapsulating hydrophilic molecules in PLGA nanoparticles. J Control Release 2009;133:90-5. https://doi.org/10.1016/j.jconrel.2008.09.073
21. Al-Refai MF, Wakid MH. Prevalence of intestinal parasites and comparison of detection techniques for soil-transmitted helminths among newly arrived expatriate labors in Jeddah, Saudi Arabia. PeerJ 2024;12:e16820. https://doi.org/10.7717/peerj.16820
22. Bahwaireth EO, Wakid MH. Molecular, microscopic, and immunochromatographic detection of enteroparasitic infections in hemodialysis patients and related risk factors. Foodborne Pathog Dis 2022;19:830-8. https://doi.org/10.1089/fpd.2022.0024
23. Campbell WC. *Trichinella* and trichinosis. Springer Science & Business Media; 2012.
24. El-kady AM, Hassan AS, Mohamed K, et al. Zinc oxide nanoparticles produced by *Zingiber officinale* ameliorates acute toxoplasmosis-induced pathological and biochemical alterations and reduced parasite burden in mice model. PLoS Negl Trop Dis 2023;17:e0011447. https://doi.org/10.1371/journal.pntd.0011447
25. Duvall RH, DeWitt WB. An improved perfusion technique for recovering adult schistosomes from laboratory animals. Am J Trop Med Hyg 1967;16:483-6. https://doi.org/10.4269/ajtmh.1967.16.483
26. Kamel IA, Cheever AW, Elwi AM, Mosimann JE, Danner R. *Schistosoma mansoni* and *S. haematobium* infections in Egypt. I. Evaluation of techniques for recovery of worms and eggs at necropsy. Am J Trop Med Hyg 1977;26:696-701. https://doi.org/10.4269/ajtmh.1977.26.696
27. Muema JM, Obonyo MA, Njeru SN, Mwatha JK. Antischistosomal effects of selected methanolic plant extracts in Swiss Albino mice infected with *Schistosoma mansoni*. Eur J Med Plants 2015;9:1-11. https://doi.org/10.9734/EJMP/2015/16953
28. Jatsa HB, Kenfack CM, Simo DN, et al. Schistosomicidal, hepatoprotective and antioxidant activities of the methanolic fraction from *Clerodendrum umbellatum* Poir leaves aqueous extract in *Schistosoma mansoni* infection in mice. BMC Complement Altern Med 2015;15:248. https://doi.org/10.1186/s12906-015-0788-z
29. Pellegrino J, Oliveira CA, Faria J, Cunha AS. New approach to the screening of drugs in experimental schistosomiasis mansoni in mice. Am J Trop Med Hyg 1962;11:201-15. https://doi.org/10.4269/ajtmh.1962.11.201
30. El-Kott AF, Mohammed RT, Ismail NR. Efficacy of garlic and mirazid in treatment of the liver granuloma in mice infected with *Schistosoma mansoni*. Res J Parasitol 2011;6:151-9. https://doi.org/10.3923/jp.2011.151.159
31. Ali EM, Abdalameer NK, Khalaph KA, et al. Green reduction approach

for the synthesis of copper oxide nanoparticles using ginger extract and evaluation of their free radical scavenging activity. Eur Phys J Plus 2025;140:928. https://doi.org/10.1140/epjp/s13360-025-06873-1

32. Ali SB, Mohamed AS, Fahmy SR, Eet al. Anthelmintic and hepatoprotective activities of the green-synthesized zinc oxide nanoparticles against *Parascaris equorum* infection in rats. Acta Parasitol 2024;69:283-301. https://doi.org/10.1007/s11686-023-00728-4
33. Abd Jabar NA, Nor-Khaizura MAR, Ismail SI, et al. Are *Bentong* ginger (*Zingiber officinale*) biosynthesized silver nanoparticles safe and effective? An optimization, characterization, and toxicity evaluation study. OpenNano 2025;21:100224. https://doi.org/10.1016/j.onano.2024.100224
34. Cherik IT, Divsalar A, Angaji SA, et al. Green synthesis and characterization of ginger-extract-based oxali-palladium nanoparticles for colorectal cancer: downregulation of REG4 and apoptosis induction. Nanotechnol Rev 2023;12:20230154. https://doi.org/10.1515/ntrev-2023-0154
35. Mehrotra S, Goyal V, Dimkpa CO, Chhokar V. Green synthesis and characterization of ginger-derived silver nanoparticles and evaluation of their antioxidant, antibacterial, and anticancer activities. Plants (Basel) 2024;13:1255. https://doi.org/10.3390/plants13091255

https://doi.org/10.3347/PHD.26003

Original Article

Parasites Hosts Dis 2026;64(3):215-228
https://doi.org/10.3347/PHD.26026

Parasites, Hosts and Diseases

pISSN 2982-5164 • eISSN 2982-6799

Exploratory evaluation of candidate metabolites identified in *Clonorchis sinensis* preparations in psoriasis-like inflammatory models

Yu Jeong Lee[1,2], Moon-Ju Kim[2], Sung Min Yu[1,2], Je-Hwang Ryu[3], Eun Jeong Won[4,5,*], Tae-Jong Kim[1,2,*]

[1]BioMedical Sciences Graduate Program (BMSGP), Chonnam National University, Hwasun, Korea; [2]Department of Rheumatology, Chonnam National University Medical School and Hospital, Gwangju, Korea; [3]Department of Pharmacology and Dental Therapeutics, School of Dentistry, Chonnam National University, Gwangju, Korea; [4]Department of Laboratory Medicine, Asan Medical Center, University of Ulsan College of Medicine, Seoul, Korea; [5]Department of Molecular Genetics and Microbiology, Duke University Medical Center, Durham, NC, USA

Psoriasis is a chronic inflammatory seronegative disease closely associated with ankylosing spondylitis and inflammatory bowel disease. This study aimed to investigate the anti-inflammatory effects of candidate metabolites, such as D-proline, L-iditol, and propionylcarnitine, identified in *Clonorchis sinensis* preparations, in in vitro and in vivo models. None of the 3 metabolites exhibited cytotoxicity within the tested concentration range. In LPS-stimulated RAW 264.7 cells, D-proline and L-iditol significantly reduced the expression of pro-inflammatory cytokines, and in an imiquimod-induced psoriasis-like mouse model, L-iditol significantly reduced disease severity and histopathological scores, whereas the effects of other metabolites were inconsistent. These results suggest that L-iditol, a candidate metabolite identified in *Clonorchis sinensis* formulations, exhibits anti-inflammatory effects in both in vitro and in vivo environments and may have therapeutic potential for inflammatory skin diseases such as psoriasis.

Keywords: *Clonorchis sinensis*, D-proline, L-iditol, propionylcarnitine, psoriasis, anti-inflammation

Introduction

Psoriasis is a chronic, immune-mediated skin disorder characterized by hyperproliferation of keratinocytes and infiltration of immune cells, particularly those associated with Th1 and Th17 responses [1,2]. The disease affects approximately 0.6% to 4.8% of the global population and is driven by a complex interplay between genetic predisposition and environmental triggers such as stress, trauma, and infections [3-5]. At the molecular level, psoriasis is sustained by elevated levels of pro-inflammatory cytokines including tumor necrosis factor (TNF)-α, interleukin (IL)-6, IL-17, and IL-1β, which collectively promote epidermal thickening, immune activation, and sustained inflammation [6].

Recent advances in psoriasis management have markedly expanded therapeutic options, ranging from novel topical agents to highly specific biologics. Newly approved topicals such as tapinarof (aryl hydrocarbon receptor agonist) [7] and roflumilast (PDE4 inhibitor) [8] provide steroid-sparing alternatives for mild-to-moderate disease, while oral small molecules including deucravacitinib, a selective TYK2 inhibitor, have shown durable efficacy in moderate-to-severe cases [9]. Yet, tapinarof may trigger local irritation (e.g., folliculitis, contact dermatitis) and data on head-and-neck or intertriginous site use are limited [7]; roflumilast, although well tolerated in

Received: March 18, 2026 Accepted: April 27, 2026
*Correspondence: ejw, ejwon@amc.seoul.kr; tjk, ktj1562@jnu.ac.kr

Citation
Lee YJ, Kim MJ, Yu SM, Ryu JH, Won EJ, Kim TJ. Exploratory evaluation of candidate metabolites identified in *Clonorchis sinensis* preparations in psoriasis-like inflammatory models. Parasites Hosts Dis 2026;64(3):215-228.

short-term trials, lacks robust long-term real-world evidence [8,10]; and deucravacitinib, despite strong clinical efficacy, raises concerns about infection risk and long-term safety requiring ongoing pharmacovigilance [9,11]. Biologic therapies targeting key cytokine pathways—including TNF-α, IL-12/23 (ustekinumab), IL-17 (secukinumab, ixekizumab, brodalumab, and bimekizumab) and IL-23 (guselkumab, risankizumab, and tildrakizumab)—have revolutionized clinical outcomes [12,13]. In addition, the IL-36R inhibitor spesolimab was recently approved for generalized pustular psoriasis [14]. Nonetheless, despite these advances, several fundamental limitations remain: high cost and limited global accessibility, loss of efficacy or treatment switching due to immunogenicity, long-term safety concerns including increased infection risk, and specific contraindications such as inflammatory bowel disease (IBD) exacerbation with IL-17 blockade or psychiatric warnings with brodalumab [12,13]. Furthermore, conventional systemic agents (e.g., methotrexate, cyclosporine, acitretin) continue to be restricted by organ toxicity [13]. Collectively, these challenges highlight the ongoing need for safer, more affordable, and broadly effective therapeutic strategies.

Psoriasis is one of the 'seronegative' diseases in addition to ankylosing spondylitis (AS) and IBD. They are closely related clinically and often co-occur in patients and families, and a previous study highlighted shared genetic pathways and pleiotropic genes (genes influencing multiple traits) among these conditions [15]. Similar with IBD and AS, for psoriasis, current treatment strategies—including biologics and small molecule inhibitors—have significantly improved disease control, challenges such as high cost, immunogenicity, and partial response rates highlight the need for novel anti-inflammatory agents. Insights into the mechanisms that helminths use to modulate specific immune cells may give clues about their ability to protect against inflammatory diseases and several autoimmune diseases [16]. Reducing the inflammation associated with IBD like Crohn's and colitis has been demonstrated by *Trichuris suis* therapy [17]. Although helminth therapy has generated substantial interest in modulating excessive immune responses, concerns prevail around the implications of pathogenic effects caused by infection with live pathogens, particularly at high doses [18]. Therefore, identification of protective active helminth-derived molecules to substitute treatment with whole worm could circumvent this issue [19].

Clonorchis sinensis (CS) have garnered attention for their ability to modulate host immune responses through secreted proteins and metabolites. Previous studies from our group demonstrated that crude somatic proteins (CSp) and excretory/secretory proteins (CS-ESP) derived from CS exert therapeutic effects in a mouse model of AS, primarily through downregulation of pro-inflammatory mediators [20,21]. To identify functionally relevant metabolites, untargeted LC-MS/MS-based metabolomic analysis of CS preparations, including CSp and CS-ESP, was performed. Among the identified metabolites, D-proline, L-iditol, and propionylcarnitine were selected from the top 10 most abundant compounds in each protein fraction based on their relative abundance, consistent detection across samples, and potential biological relevance. Although these metabolites have been implicated in various metabolic and regulatory processes, their roles in modulating inflammatory responses in psoriasis have not been previously investigated. Therefore, this study aimed to evaluate the anti-inflammatory effects of these candidate metabolites in both in vitro and in vivo models and to provide initial insight into their potential as immunomodulatory agents in chronic inflammatory diseases.

Methods

Ethics statement

All animal experiments were approved by the Chonnam National University Animal Care and Use Committee (CNU IACUC-H-2018-35) and conducted in accordance with institutional guidelines.

CS protein extraction

The CS metacercariae were collected from the second intermediate host, *Pseudorasbora herzi*, caught in a stream in Korea, after artificial digestion of the fish [21,22]. Briefly, metacercariae were orally administered to rabbits (New Zealand White, both genders: 2.2–2.4 kg; Koatech). Adult CS were recovered from the rabbits after 3 months. Preparation of CSp or CS-ESP was performed as previously reported [20,21]. For obtaining CSp, harvested adult worms were washed thoroughly in sterile 1× phosphate-buffered saline (Oatech) and homogenized on ice in a lysis buffer containing protease inhibitors. The homogenate was centrifuged at high speed to remove debris, and the resulting supernatant containing crude proteins was collected. For CS-ESP preparation, live adult worms were incubated in RPMI-1640 medium (Oatech) supplemented with antibiotics at 37°C in 5% CO_2 for 24–48 h. The culture supernatant containing CS-ESP was collected, centrifuged to remove particulate debris, filtered, and concentrated using centrifugal filter units. Both CSp and CS-ESP samples were aliquoted and stored at -80°C until further analysis. Protein concentration was measured using the Pierce BCA Protein Assay Kit (Thermo Scientific).

https://doi.org/10.3347/PHD.26026

Metabolite extraction and LC-MS/MS analysis

To extract metabolites, CSp and CS-ESP samples were treated with 80% methanol and incubated at -80°C for 1 h. After centrifugation at 4,000× g for 15 min, the supernatant was collected, evaporated to dryness using a SpeedVac, and reconstituted in 100 µl of LC-MS mobile phase. LC-MS/MS analysis was conducted at Ebiogene using a Q Exactive Orbitrap mass spectrometer (Thermo Scientific) with an electrospray ionization source. Chromatographic separation was performed using a 2-column system: a C18 trapping column (1.8 µm, 2.1×5 mm) followed by an Eclipse Plus C18 RRHD analytical column (1.8 µm, 2.1×50 mm). The mobile phases were 0.1% formic acid in water (solvent A) and 0.1% formic acid in 80% acetonitrile (solvent B), and a linear gradient was applied over 26 min at 0.2 mL/min. MS data were acquired over the m/z range of 100–1,000. Spectral data were processed using Compound Discoverer 3.3 (Thermo Fisher Scientific) with the "Untargeted Metabolomics with Statistics Detect Unknowns" workflow. Metabolite annotation was based on mzCloud spectral matching. Confidence levels were assigned per metabolomics standards initiative criteria: level 2 for metabolites with <10 ppm mass error and mzCloud scores >80, and level 3 for ChemSpider matches with <5 ppm error. Redundant features were filtered by peak intensity to retain unique metabolite signals (Fig. 1A, B).

LC–MS/MS–based metabolomic analysis of candidate metabolites

LC–MS/MS–based metabolomic analysis was performed to identify significantly altered metabolites. Metabolites were initially filtered based on annotation confidence and subsequently prioritized according to their relative signal intensity (peak area) and consistent detection across samples. Due to the exploratory nature of this study and limitations of the available dataset, additional parameters such as fold change and background signal filtering were not systematically applied. Based on these criteria, D-proline (858919, Merck), L-iditol (I6035, Merck) and propionylcarnitine (AG007VN1, ChemSpace US) were selected for further experimental validation. A summary of the top candidate metabolites and their LC-MS/MS parameters is provided in Supplementary Table S1. Commercially available compounds with identical molecular structures to the selected metabolites were purchased and used for subsequent in vitro and in vivo experiments (Fig. 1).

Cell viability assay

RAW 264.7 cells were cultured in RPMI-1640 medium (Oatech) supplemented with 10% fetal bovine serum (Gibco) and 1% penicillin-streptomycin (Gibco) under standard culture conditions at 37°C in a humidified atmosphere containing 5% CO_2. For the cell viability assay, cells were seeded at a density of 1×10^5 cells per well in a 96-well plate and allowed to adhere overnight. The following day, the cells were treated with varying concentrations of 3 different compounds: D-proline, L-iditol and propionylcarnitine at 1, 10, 50, and 100 µg/ml 20 µl of Cell Titer 96 AQueous One Solution Reagent (MTS reagent, G3580, Promega) was added to each well and the cells were further incubated for 2 h. Absorbance was then measured at 490 nm using a Reader 96-well microplate reader (Molecular Devices) to determine cell viability based on metabolic activity. All samples were measured in triplicate [21].

Determination of experimental concentrations of candidate metabolites

To determine the experimental concentrations of the selected candidate metabolites, preliminary concentration-screening experiments were performed following cell viability assessment. Cells were treated with increasing concentrations of each metabolite to identify a concentration range without cytotoxic effects. Based on these results, a single concentration that showed no cytotoxicity and demonstrated reproducible anti-inflammatory effects was selected and used for all subsequent in vitro experiments, including cytokine expression analysis. Detailed concentration-screening data are provided in the Supplementary Figs. S1-S3.

Cytokine expression level

RAW 264.7 cells were seeded at a density of 5×10^5 cells per well in a 6-well plate and allowed to adhere overnight. To investigate the anti-inflammatory effects of selected compounds, cells were co-cultured for 24 h in the presence of LPS (4 µg/ml) to induce an inflammatory response. The treatment groups included D-proline (50 µg/ml), L-iditol (10 µg/ml), and propionylcarnitine (5 µg/ml), each added to the culture medium along with LPS. Following the incubation period, total RNA was extracted from the cells using a standard RNA isolation protocol. Complementary DNA was synthesized from the extracted RNA using a PrimeScript 1st stand complementary DNA Synthesis kit (Takara). Real-time quantitative PCR was subsequently performed to evaluate the mRNA expression levels of inflammation-related cytokines and enzymes, including IL-1β, TNF-α, IL-6, inducible nitric oxide synthase (iNOS) and cyclooxygenase-2 (COX2) (Table 1). The relative gene expression levels were analyzed to assess the modulatory effects of each compound on LPS-induced inflammation in RAW 264.7 cells. All quantifi-

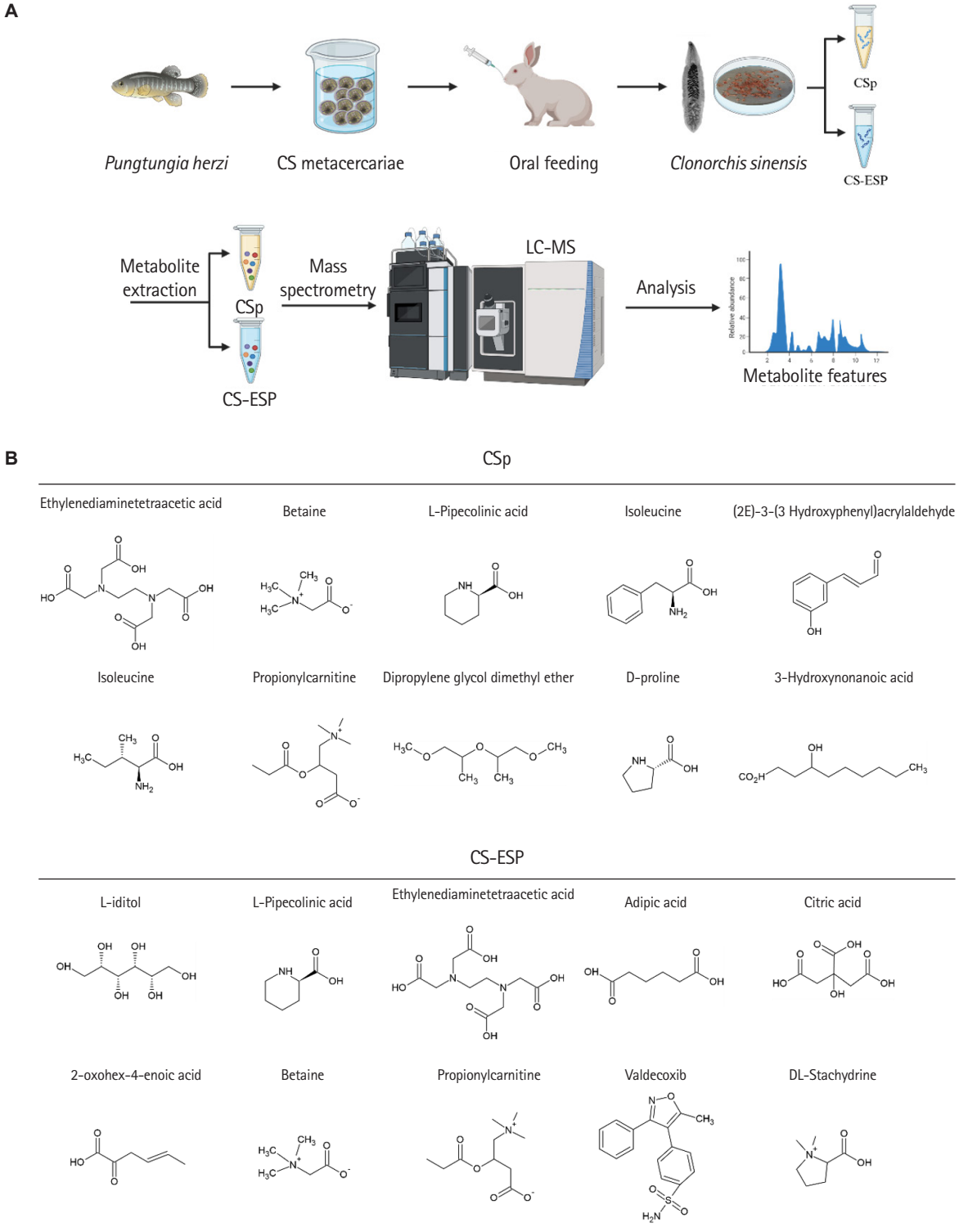

Fig. 1. Workflow of metabolite analysis of candidate metabolites from *Clonorchis sinensis* crude somatic proteins (CSp) and excretory/secretory proteins (CS-ESP). (A) Schematic representation of the overall experimental workflow, including the extraction of CSp and CS-ESP from *Clonorchis sinensis*, followed by metabolite extraction for subsequent profiling. Both protein fractions were subjected to methanol-based extraction procedures to isolate small molecule metabolites suitable for LC-MS/MS analysis. (B) Comparison of the top 10 most abundant metabolites identified in the CSp and CS-ESP samples based on untargeted LC-MS/MS profiling. Metabolite abundance was ranked according to signal intensity, and key metabolites were selected for further functional evaluation based on biological relevance and literature support.

https://doi.org/10.3347/PHD.26026

Table 1. Primer sequences for cytokine gene expression analysis

Target primer		Oligonucleotide sequence (5' → 3')
GAPDH	Forward	CAACTTTGGCATTGTGGAAGG
	Reverse	ACACATTGGGGGTAGGAACAC
TNF-α	Forward	TCTTGTGTTTCTGAGTAGTTGT
	Reverse	CCTTTACTCTGACCCCTTTATT
IL-1β	Forward	ATGGTGAAGTCAATTATGTCCT
	Reverse	ACAAGATAGAAGTCAAGAGCAA
IL-6	Forward	AGGTAGCTATGGTACTCCAG
	Reverse	GCACTTGCAGAAAACAATCT
iNOS	Forward	GGAAATAGAAACAACAGGAACC
	Reverse	CATTGTTGGTGGCATAAAGTAT
COX2	Forward	AGAAGGGTTCCCAATTAAAGAT
	Reverse	AACAGAAAAACTGTTTCGAAGT

GAPDH, glyceraldehyde-3-phosphate dehydrogenase; TNF, tumor necrosis factor; IL, interleukin; iNOS, inducible nitric oxide synthase; COX, cyclooxygenase.

cations were normalized versus endogenous GAPDH. The relative quantitation value of each target gene after normalizing to GAPDH as compared with the calibrator for that target was calculated using $2^{-\Delta\Delta Ct}$. All samples were measured in triplicate.

Experimental mice model

Male SKG mice (8–10 weeks old) of the BALB/c strain were reared in a specific pathogen-free environment and randomly assigned to 6 experimental groups. In the initial preliminary experiment, the study was conducted with a negative control (NC) group ($n=5$), a positive control (PC) group ($n=10$), a dexamethasone (DEX) group ($n=5$), D-proline ($n=5$), L-iditol ($n=5$), and propionylcarnitine ($n=5$). Subsequently, in the additional experiment, propionylcarnitine was excluded as it did not show a significant effect, and the study was conducted with NC ($n=5$), PC ($n=9$), DEX ($n=4$), D-proline ($n=11$), and L-iditol ($n=11$). The dorsal hair of the mice was completely removed, and 5% imiquimod (IMQ) cream was topically applied to the shaved area daily from day 1 to day 7 to induce psoriasis-like skin inflammation. From day 3 to day 7, D-proline (50 mg/kg), L-iditol (10 mg/kg), and propionylcarnitine (5 mg/kg) were topically co-applied with IMQ. In addition, DEX (1 mg/kg) was administered intraperitoneally once daily from day 3 to day 7. Psoriasis Area and Severity Index (PASI) scores were measured daily from day 1 to day 7 before topical application of IMQ to the dorsal skin of mice. Two independent observers evaluated skin condition in a randomized and blinded manner. Erythema (redness), induration (thickness) and desquamation (scale) were each scored on a scale from 0 to 4 (0, none; 1, slight; 2, moderate; 3, severe; 4, very severe). The total PASI score was calculated as the sum of these 3 items [23]. The scores from the observers were averaged to derive the final value.

Histological analysis

After the mice were sacrificed, dorsal skin tissues were carefully excised and immediately fixed in 10% formalin for 24 h at room temperature to preserve tissue morphology. Following fixation, the samples underwent a graded ethanol series for dehydration, were cleared in xylene, and then embedded in paraffin to prepare tissue blocks. The paraffin-embedded tissues were sectioned at a thickness of 10 μm using a microtome. The sections were mounted on glass slides and stained with hematoxylin and eosin to evaluate histopathological changes associated with psoriasis. Histological evaluation was performed by 4 independent observers using the Psoriasis Histopathological Score (PHS) in a randomized, blinded manner. Inflammatory cell infiltration, incomplete keratosis, hyperkeratosis, epidermal thickness, and Monroe microabscesses were each scored on a scale of 0 to 3 (0, none; 1, mild; 2, moderate; 3, severe). The total PHS score was calculated as the sum of these individual items [24]. The scores from the observers were averaged to derive the final value.

Statistical analysis

Statistical analyses were performed using GraphPad Prism 10 (GraphPad Software). Normality of the data was assessed using the Shapiro-Wilk test. For normally distributed data, comparisons among groups were performed using one-way or two-way ANOVA followed by Bonferroni multiple comparisons test. For data that did not meet normality assumptions, non-parametric tests were used as appropriate: the Friedman test was applied for overall comparisons of repeated measures within the same group, followed by the Wilcoxon signed-rank test for post-hoc pairwise comparisons. The Kruskal-Wallis test was used for independent group comparisons. $P<0.05$ was considered to indicate a statistically significant difference: $^{*}P<0.05$, $^{**}P<0.01$, $^{***}P<0.001$, and $^{****}P<0.0001$.

Results

Cell viability of D-proline, L-iditol, and propionylcarnitine in RAW 264.7 macrophages

Cell viability and anti-inflammatory effects were confirmed for each candidate substance in RAW 264.7 cells (Figs. 2-4). To determine the cytotoxicity of the selected candidate me-

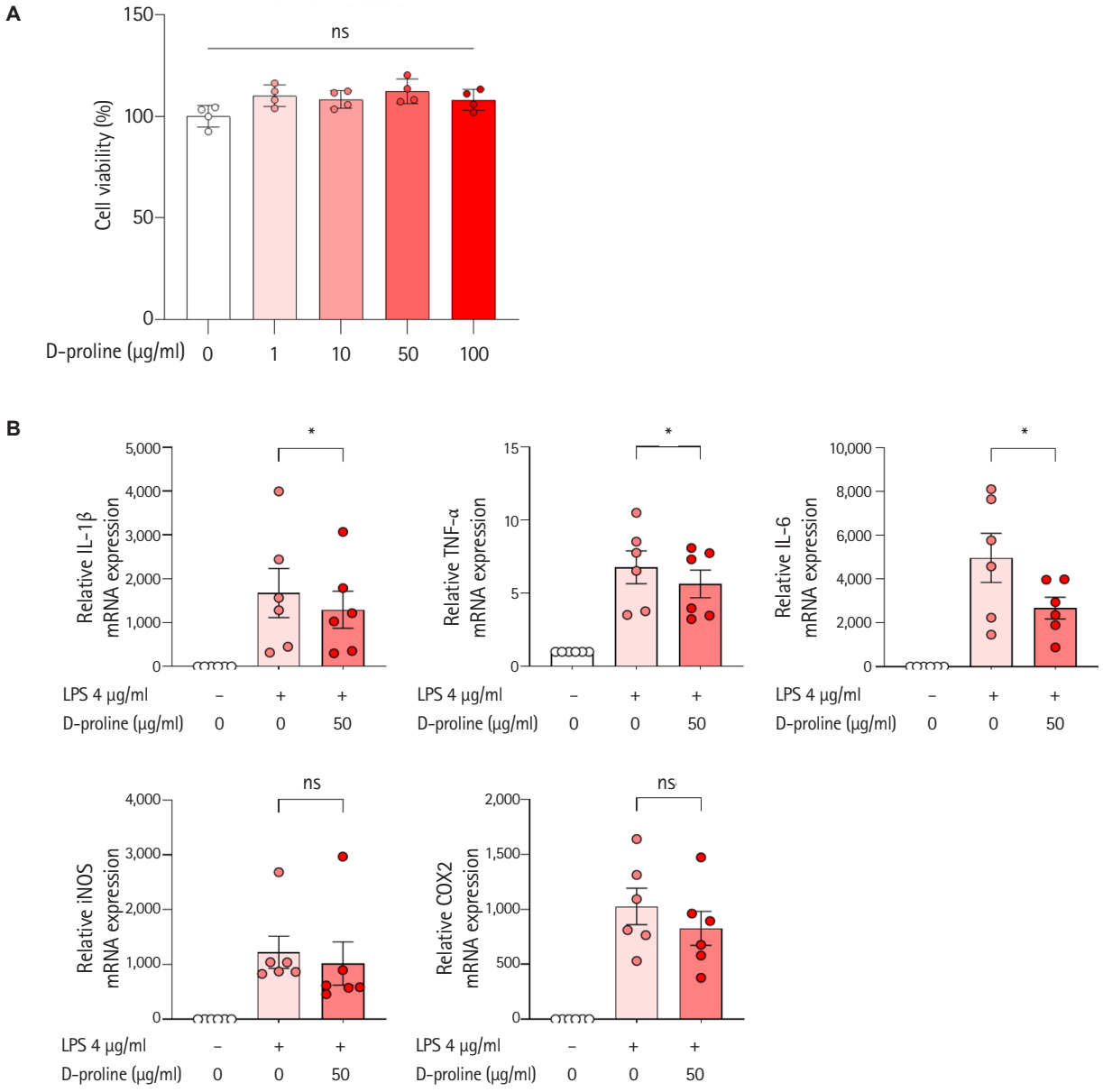

Fig. 2. Anti-inflammatory effect of D-proline in vitro. (A) Effect of D-proline on cell viability in RAW 264.7 macrophages. Cells were treated with D-proline for 24 h, and viability was assessed using an MTS assay. D-proline treatment did not result in any significant cytotoxicity at the tested concentrations, indicating it is well tolerated by RAW 264.7 cells under these conditions. (B) Gene expression analysis of inflammatory markers in RAW 264.7 cells treated with 4 μg/ml LPS and 50 μg/ml D-proline for 24 h. RT-PCR was performed to evaluate the expression levels of key pro-inflammatory genes. D-proline treatment led to a reduction in the expression of several LPS-induced genes, suggesting its potential anti-inflammatory effect. Statistical analysis was performed using the Friedman test with multiple comparisons, followed by Wilcoxon signed-rank test for pairwise comparisons. Data are presented as mean±SD (n=6). Statistical analysis was performed using the Kruskal-Wallis test followed by Dunn's multiple comparisons test. $^{*}P<0.05$. Each symbol represents an individual biological replicate. IL, interleukin; TNF, tumor necrosis factor; iNOS, inducible nitric oxide synthase; COX, cyclooxygenase; ns, not significant.

tabolites identified in CS preparations, RAW 264.7 murine macrophages were treated with increasing concentrations of D-proline, L-iditol, or propionylcarnitine. Cell viability was assessed after 24 h using the MTS reagent. As shown in Figs. 2A, 3A, and 4A, none of the compounds exhibited significant cytotoxic effects at their respective treatment concentrations. Viability remained comparable to the untreated control group, even at the highest tested doses. These results indicate that all 3 metabolites are well tolerated by macrophages under the experimental conditions and are suitable for further investigation of their functional effects.

https://doi.org/10.3347/PHD.26026

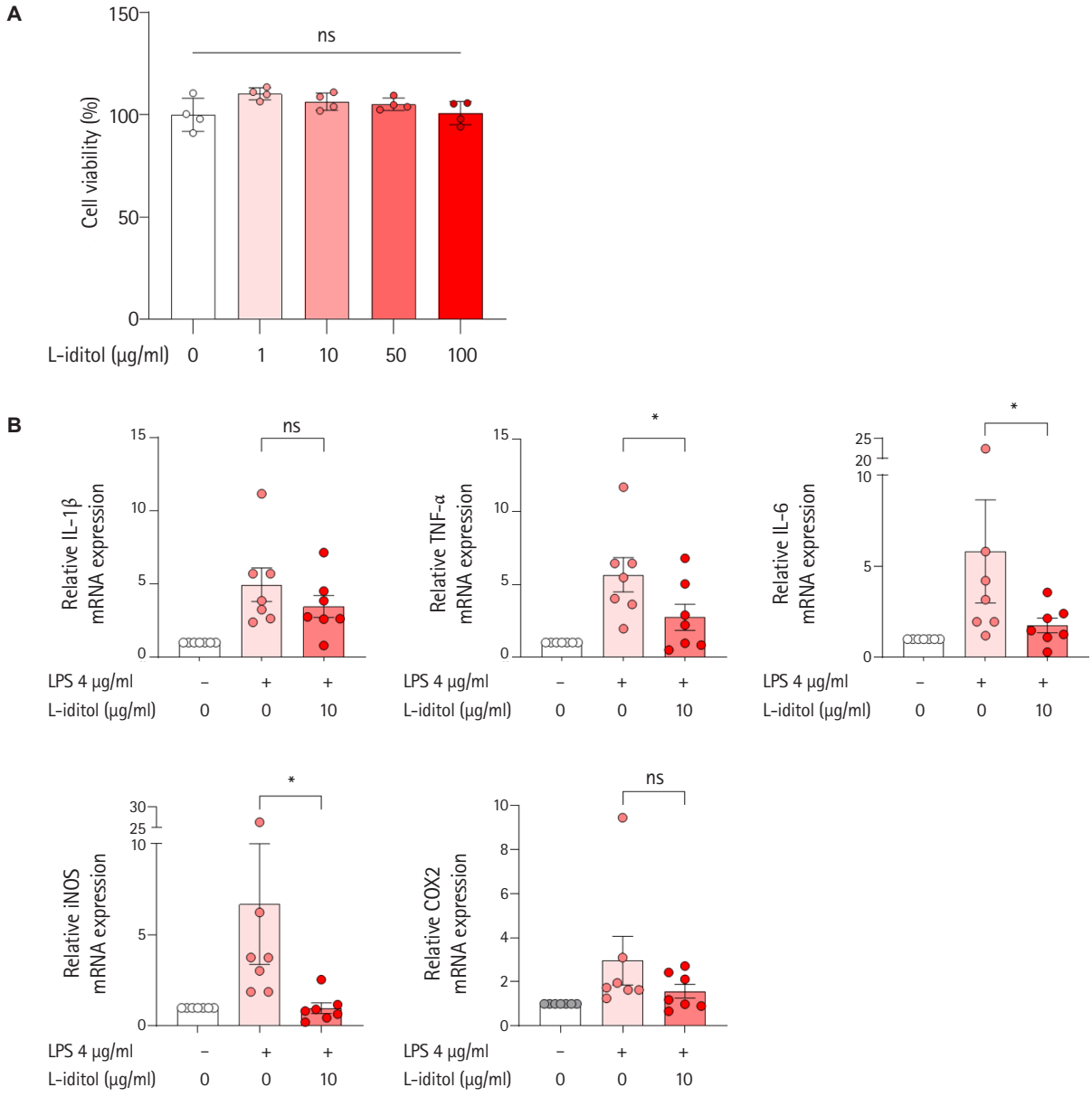

Fig. 3. Anti-inflammatory effect of L-iditol in vitro. (A) Effect of L-iditol on cell viability in RAW 264.7 macrophages. Cells were treated with L-iditol for 24 h, and viability was assessed using an MTS assay. L-iditol treatment did not result in any significant cytotoxicity at the tested concentrations, indicating it is well tolerated by RAW 264.7 cells under these conditions. (B) Gene expression analysis of inflammatory markers in RAW 264.7 cells treated with 4 μg/ml LPS and 10 μg/ml L-iditol for 24 h. RT-PCR was performed to evaluate the expression levels of key pro-inflammatory genes. L-iditol treatment led to a reduction in the expression of several LPS-induced genes, suggesting its potential anti-inflammatory effect. Statistical analysis was performed using the Friedman test with multiple comparisons, followed by Wilcoxon signed-rank test for pairwise comparisons. Data are presented as mean±SD (n=7). Statistical analysis was performed using the Kruskal-Wallis test followed by Dunn's multiple comparisons test. $^{*}P$<0.05. Each symbol represents an individual biological replicate. IL, interleukin; TNF, tumor necrosis factor; iNOS, inducible nitric oxide synthase; COX, cyclooxygenase; ns, not significant.

Determination of optimal concentrations of candidate metabolites

To determine the optimal experimental concentration of the selected candidate metabolites, preliminary dose-response experiments were performed. RAW 264.7 cells were treated with 1, 10, 50, and 100 μg/ml of each metabolite, concentrations that did not affect cell viability. The concentrations used in these experiments were pre-screened to ensure they did not induce cytotoxicity, with cell viability maintained at levels comparable to the untreated control (as shown in Figs. 2A, 3A, and 4A of the main manuscript), and inflammatory cytokine expression levels were measured (Figs. 2B, 3B, 4B).

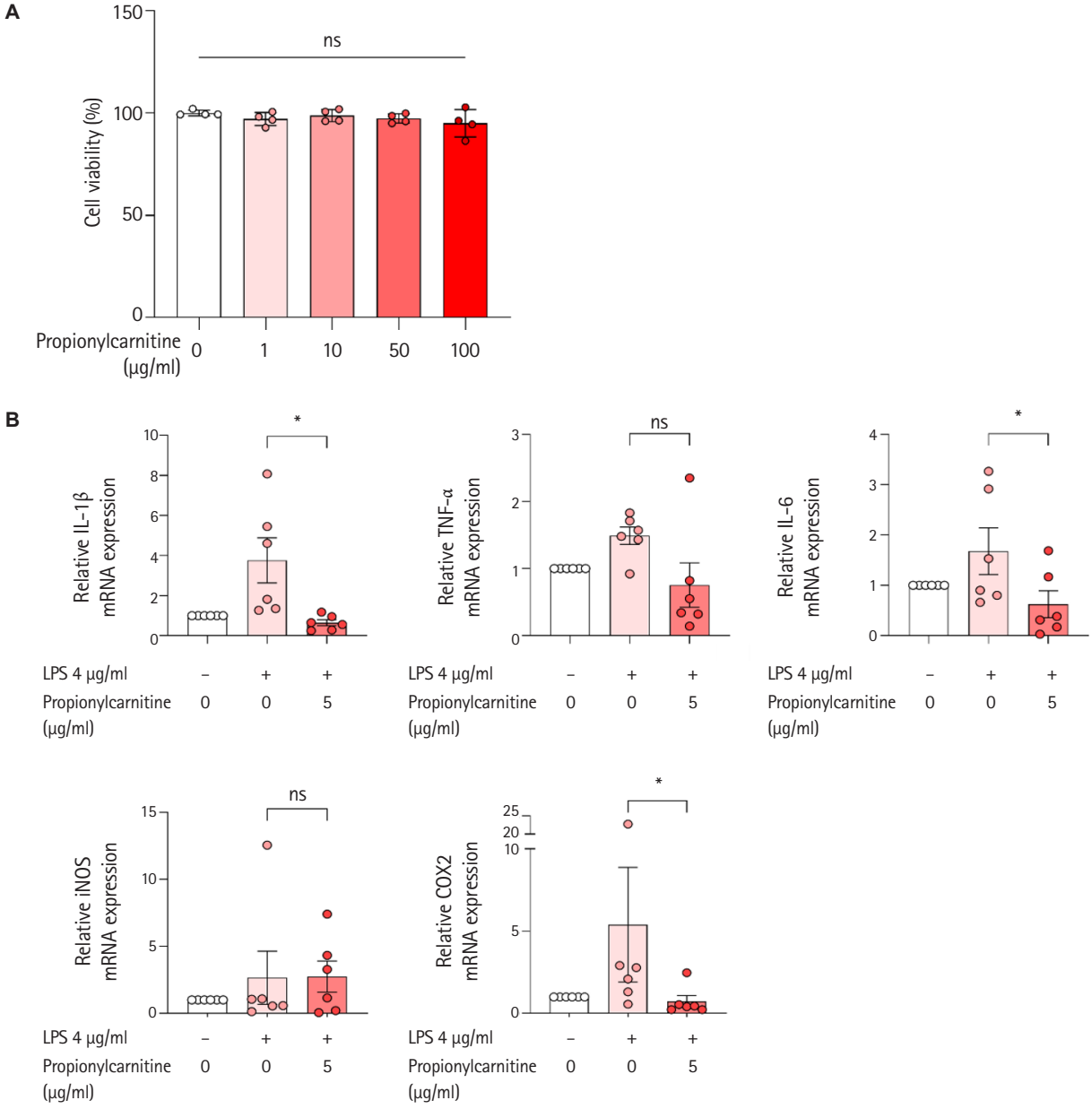

Fig. 4. Anti-inflammatory effect of propionylcarnitine in vitro. (A) Effect of propionylcarnitine on cell viability in RAW 264.7 macrophages. Cells were treated with propionylcarnitine for 24 h, and viability was assessed using an MTS assay. Propionylcarnitine treatment did not result in any significant cytotoxicity at the tested concentrations, indicating it is well tolerated by RAW 264.7 cells under these conditions. (B) Gene expression analysis of inflammatory markers in RAW 264.7 cells treated with 4 μg/ml LPS and 5 μg/ml propionylcarnitine for 24 h. RT-PCR was performed to evaluate the expression levels of key pro-inflammatory genes. Propionylcarnitine treatment led to a reduction in the expression of several LPS-induced genes, suggesting its potential anti-inflammatory effect. Statistical analysis was performed using the Friedman test with multiple comparisons, followed by Wilcoxon signed-rank test for pairwise comparisons. Data are presented as mean± SD (n=6). Statistical analysis was performed using the Kruskal-Wallis test followed by Dunn's multiple comparisons test. $^{*}P<0.05$. Each symbol represents an individual biological replicate. ns, not significant; IL, interleukin; TNF, tumor necrosis factor; iNOS, inducible nitric oxide synthase; COX, cyclooxygenase.

Among the tested concentrations, D-proline showed reduced inflammatory cytokine levels at 50 and 100 μg/ml, L-iditol at 10 and 50 μg/ml, and propionylcarnitine at 1, 5, and 10 μg/ml. Based on these results, additional preliminary experiments were conducted for each metabolite to determine a single optimal concentration. Finally, a single concentration for each metabolite that did not affect cell viability and showed consistent anti-inflammatory effects in the preliminary screening was selected and used for all subsequent in vitro and in vivo experiments.

https://doi.org/10.3347/PHD.26026

Anti-inflammatory effects of the 3 metabolites on LPS-stimulated macrophages

To evaluate the anti-inflammatory properties of D-proline, L-iditol, and propionylcarnitine, RAW 264.7 cells were pre-stimulated with LPS to induce a robust inflammatory response and then treated with each metabolite at their effective non-toxic concentrations. Quantitative real-time PCR was performed to analyze the mRNA expression levels of key inflammatory mediators. Treatment with D-proline (50 μg/ml) significantly reduced the expression of IL-1β, TNF-α, and IL-6 compared to LPS-only controls (Wilcoxon signed-rank test, W=-21.00, n=6 pairs, P=0.031). Mean±SD values were as follows: IL-1β, 1,678±1,377 versus 1,295±1,034; TNF-α, 6.78±2.75 versus 5.66±2.31; IL-6, 4,967±2,740 versus 2,673±1,216 (Fig. 2B). However, treatment with D-proline could not show statistically significant changes in the mRNA expression levels of iNOS and COX2, respectively.

Treatment with L-iditol (10 μg/ml) significantly reduced the expression of TNF-α (W=-28.00, 5.67±3.12 versus 2.75±2.38, P=0.016), IL-6 (W=-26.00, 5.81±7.48 versus 1.75±1.06, P=0.031), iNOS (W=-28.00, 6.68±8.76 versus 0.97±0.76, P=0.016), compared to LPS-only (Fig. 3B). However, treatment with L-iditol could not show statistically significant changes in the mRNA expression levels of IL-1β and COX2, respectively.

Treatment with propionylcarnitine (5 μg/ml) significantly reduced the expression of IL-1β, IL-6 and COX2 compared to LPS-only controls (Wilcoxon signed-rank test, W=-21.00, n=6 pairs, P=0.031). Mean±SD values were as follows: IL-1β, 3.76±2.76 versus 0.65±0.37; IL-6, 1.68±1.14 versus 0.63±0.66; COX2, 5.39±8.53 versus 0.72±0.87 (Fig. 4B). However, treatment with propionylcarnitine could not show statistically significant changes in the mRNA expression levels of TNF-α and iNOS, respectively. Collectively, these data demonstrate that all 3 metabolites can suppress the expression of inflammatory genes in activated macrophages, indicating their potential as immunomodulatory compounds.

Psoriasis treatment effect in experimental animals

To evaluate the therapeutic effect of the candidate metabolites, an IMQ-induced psoriasis mouse model was constructed (Fig. 5A). Evaluation of clinical skin severity based on the total PASI score revealed that treatment with specific candidate metabolites identified in CS preparations attenuated psoriatic inflammation to varying degrees (Fig. 5B). A high PASI score (mean±SEM, 6.25±0.33) was yielded in the PC groups, showing pronounced erythema, epidermal thickening, and scaling. This confirmed the successful induction of psoriasis-like pathology. At the end of the experiment, the DEX group showed the lower PASI score than the PC groups (4.50±0.29 versus PC, P=0.004), supporting its effectiveness as a systemic anti-inflammatory agent. Treatment of D-proline or L-iditol exhibited the significantly lower PASI scores than the PC groups (4.66±0.49 and 5.19±0.42 versus PC, P<0.0001 and P=0.002). However, treatment of propionylcarnitine did not show significant change in the PASI score compared to that of PC group. Collectively, we found that D-proline and L-iditol harbored notable anti-inflammatory activity in vivo and may contribute as therapeutics in psoriatic skin inflammation. In support of these observations, two-way ANOVA revealed a significant treatment effect, primarily driven by D-proline and L-iditol groups ($F_{(6, 252)}$=68.36, P<0.0001).

Dorsal skin analysis reveals anti-inflammatory effects of candidate metabolites identified in CS preparations

The anti-psoriatic effects of candidate metabolites identified in CS preparations were further supported by visual and histological evaluations of dorsal skin on day 7 (Fig. 6A-C). Mice in the PC group exhibited pronounced erythema and substantial keratin accumulation compared to the NC, clearly confirming the successful induction of psoriasis-like skin pathology. In contrast, the DEX group displayed visibly reduced redness and keratin buildup, consistent with its known anti-inflammatory efficacy. Among the metabolite-treated groups, both D-proline and L-iditol led to a reduction in skin redness relative to the PC group. However, propionylcarnitine showed inconsistent results, with decreased keratin deposition but persistent erythema in several cases (Fig. 6A). Histopathological examination of skin tissues (Fig. 6B) further corroborated these clinical observations. The PC group displayed marked dermal thickening, dense immune cell infiltration, and increased epidermal thickness, accompanied by evident hyperkeratosis and parakeratosis. While both D-proline and L-iditol treatments showed partial improvements, L-iditol led to a more substantial reduction in dermal thickness and inflammatory infiltration compared to D-proline, suggesting a more pronounced histological benefit. In contrast, propionylcarnitine did not improve keratin-related changes despite a slight reduction in dermal thickness. Quantitative analysis using the PHS supported these findings (Fig. 6C). The PC group exhibited significantly elevated PHS compared to NC (mean±SD, 6.87±0.46 for the PC group versus 0.16±0.08 for the NC group, P<0.0001), confirming the severity of induced pathology. Among the treatment groups, only L-iditol showed

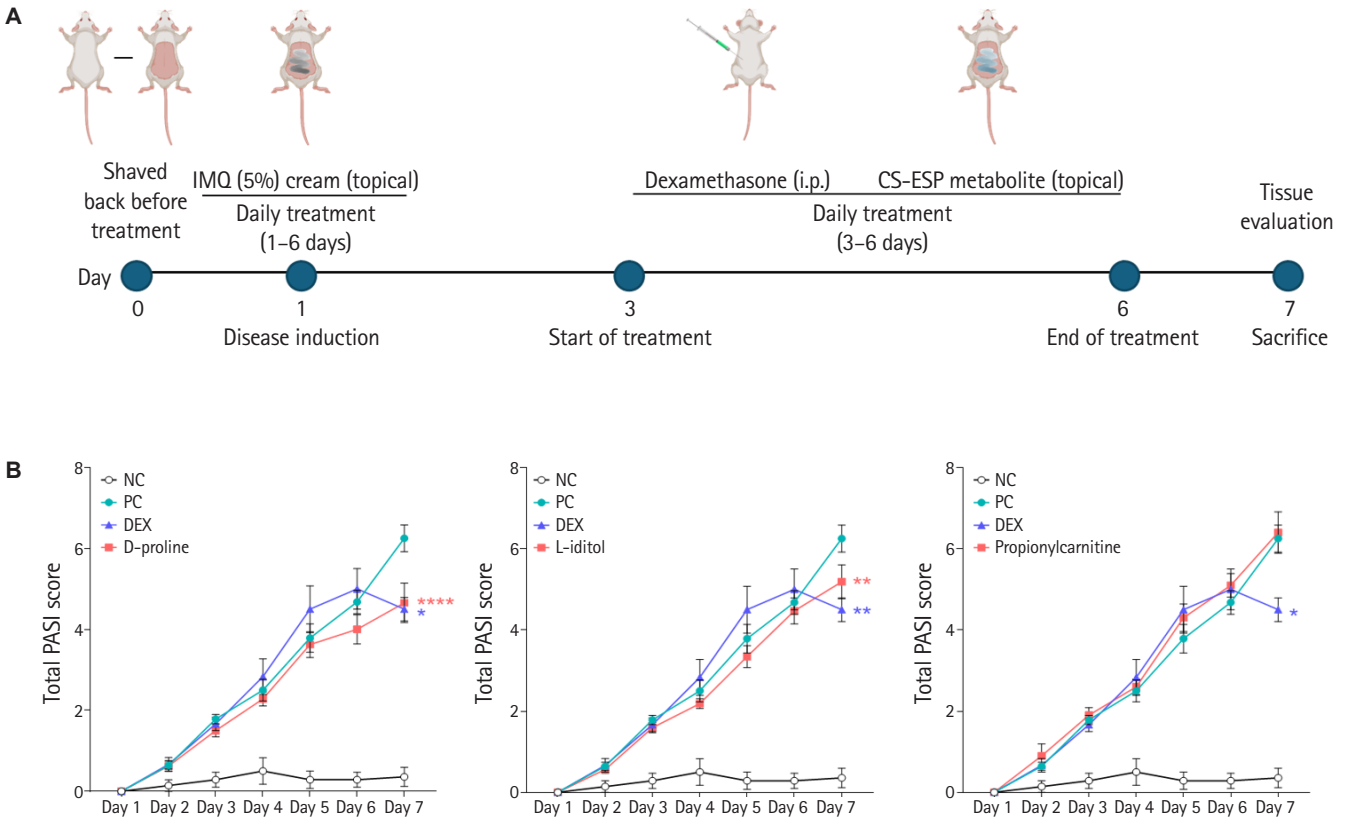

Fig. 5. Psoriasis-like skin inflammation model and treatment in SKG mice. (A) Experimental timeline for psoriasis induction and treatment. Imiquimod (IMQ) cream was applied daily to the shaved dorsal skin of SKG mice from day 1 to day 6. From day 3 to 6, mice received either intraperitoneal dexamethasone (DEX) or topical IMQ mixed with candidate metabolites identified in *Clonorchis sinensis* preparations (D-proline, L-iditol, or propionylcarnitine). (B) Psoriasis Area and Severity Index (PASI) scores, reflecting erythema, thickness, and scaling, were assessed daily before IMQ application to evaluate treatment efficacy. Statistical analysis was performed using two-way ANOVA with Bonferroni's multiple comparisons test. NC, negative control group; PC, positive control group. $^{*}P<0.05$, $^{**}P<0.01$, $^{***}P<0.001$, $^{****}P<0.0001$.

a statistically significant reduction in PHS (5.41 ± 0.46 versus PC, $P=0.038$), highlighting its potential as a promising candidate for mitigating psoriatic histopathology. Collectively, these results demonstrate a divergence between clinical and histological efficacy; while both D-proline and L-iditol attenuated clinical severity (PASI), L-iditol provided a more robust and consistent anti-inflammatory effect at the tissue level, as evidenced by the significant improvement in PHS.

Discussion

In this study, we identified and evaluated the anti-inflammatory potential of the candidate metabolites identified in CS preparations—D-proline, L-iditol, and propionylcarnitine. When tested in vitro, all 3 compounds showed no cytotoxicity at their effective concentrations, and subsequent assays confirmed their ability to suppress key pro-inflammatory mediators in LPS-stimulated macrophages. In vivo, among the tested metabolites, L-iditol emerged as the most promising candidate due to its consistent efficacy in both clinical (PASI) and histological (PHS) assessments. Although D-proline attenuated visual skin severity, it did not lead to a significant improvement in the composite histopathological score, highlighting the superior immunomodulatory potential of L-iditol in this psoriasiform model. The anti-psoriatic efficacy of L-iditol was particularly notable, as these compounds not only reduced visual erythema and keratin buildup but also mitigated histological features such as dermal thickening and immune cell infiltration. These improvements were comparable to or approaching those observed with dexamethasone, a known systemic immunosuppressant. Although propionylcarnitine showed partial effects by reducing keratin deposition, it did not lead to a statistically significant reduction in PASI or PHS scores, suggesting a more limited therapeutic potential in this model.

Previous studies have demonstrated that CS-derived fractions, including CSp [20] and CS-ESP [21], exert significant

https://doi.org/10.3347/PHD.26026

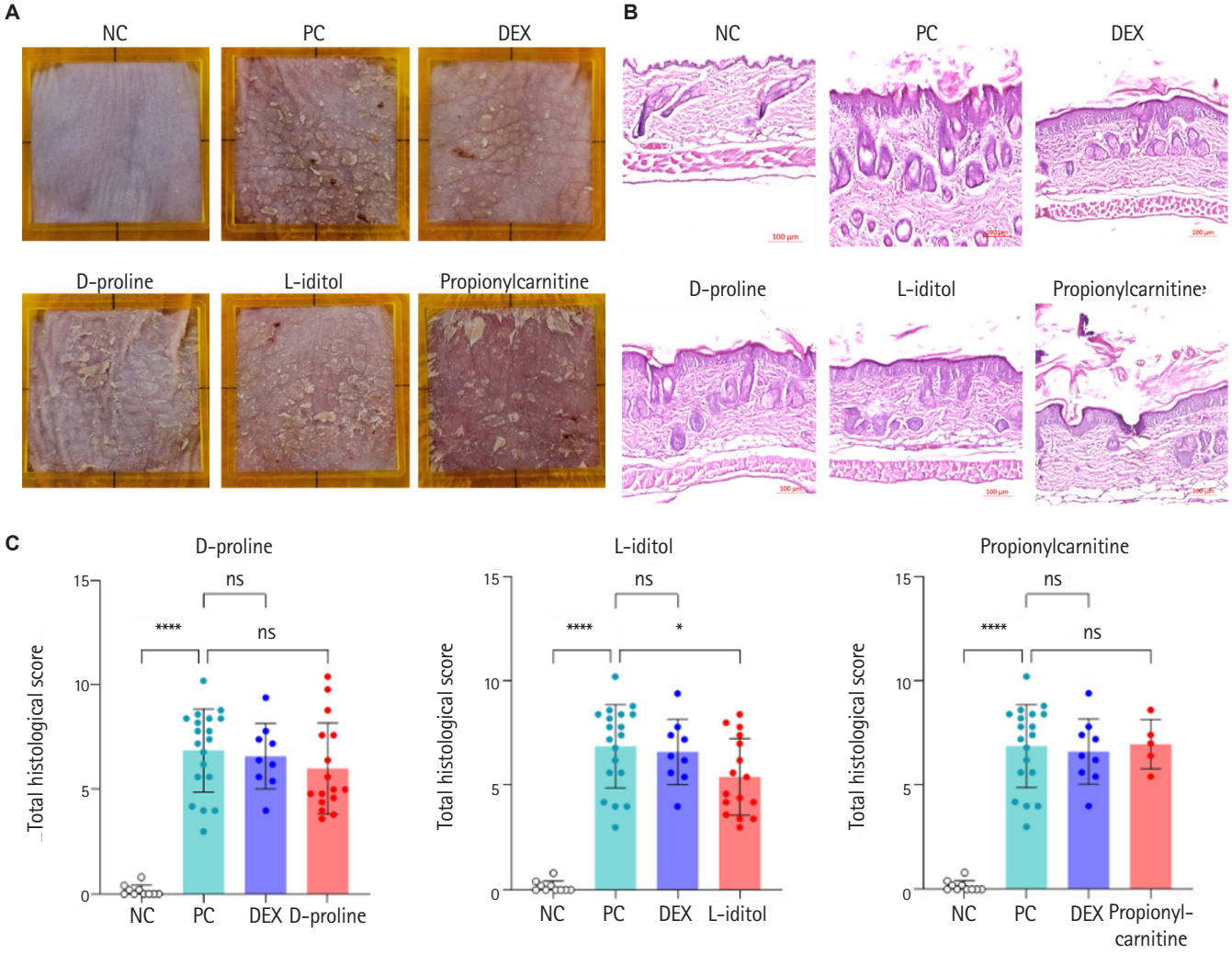

Fig. 6. Anti-inflammatory effects of candidate metabolites identified in *Clonorchis sinensis* preparations in the imiquimod-induced psoriasis model. (A) Representative images of dorsal skin from SKG mice taken on day 7. The positive control group (PC, imiquimod only) showed marked erythema and keratin buildup, while dexamethasone (DEX), D-proline, and L-iditol treatments reduced redness; propionylcarnitine reduced keratin but not erythema. (B) Hematoxylin and eosin staining of dorsal skin sections revealed dermal thickening, immune cell infiltration, and keratin abnormalities in the PC, which were alleviated by DEX and partially by D-proline and L-iditol. L-iditol showed greater improvement than D-proline, while propionylcarnitine had limited effect. (C) Psoriasis Histopathological Score was significantly increased in the PC versus negative control group (NC) and significantly reduced only in the L-iditol. Statistical analysis was performed using one-way ANOVA with Bonferroni's multiple comparisons test. ns, not significant. $^{*}P<0.05$, $^{**}P<0.01$, $^{***}P<0.001$, $^{****}P<0.0001$.

anti-inflammatory effects in various inflammatory disease models, suggesting that parasite-derived components can modulate host immune responses. Building upon these findings, our group previously performed proteomic analyses of CS-ESP and demonstrated that several proteins identified through this approach also exhibited anti-inflammatory activity [21]. These results indicate that the immunomodulatory properties of parasite-derived products are not restricted to a single molecular class but may arise from multiple molecular layers, including proteins and other bioactive components. In this context, the present study further expanded the analytical scope to the metabolomic level. Using LC-MS/MS–based metabolomic profiling, we identified candidate metabolites identified in CS preparations and subsequently evaluated their anti-inflammatory effects. Our findings demonstrate that selected parasite-derived metabolites significantly modulate inflammatory responses, supporting the concept that metabolites contribute to the overall anti-inflammatory activity previously observed for CSp and CS-ESP. The anti-inflammatory effects observed in this study are consistent with previous findings regarding metabolite-mediated immune modulation. Proline has been reported to inhibit inflammatory re-

sponses, including a reduction in TNF-α levels, under inflammatory conditions [25]. Although direct evidence for L-iditol is limited, structurally related metabolites such as myo-inositol have been shown to inhibit pro-inflammatory cytokines, including TNF-α, IL-1β, and IL-6 [26]. Additionally, carnitine-related metabolites have been reported to exhibit anti-inflammatory effects by reducing cytokine production and regulating macrophage activation [27]. These findings support the potential for the identified metabolites to modulate key inflammatory mediators associated with psoriasis.

The differential expression patterns of cytokines observed in response to LPS stimulation may reflect distinct regulatory mechanisms and expression kinetics. It is well known that cytokines such as TNF-α are rapidly induced, whereas others, including IL-6 and IL-1β, may exhibit delayed or sustained expression depending on transcriptional regulation [28-31]. Due to these temporal variations, measurements taken at a specific time point (e.g., 24 h) may show significant reductions in certain cytokines while others remain less affected. Psoriasis is driven by a complex inflammatory network, in which the TNF-α, IL-6, and IL-23/IL-17 axis play central roles [5,32,33]. In this study, candidate metabolites identified in CS preparations significantly reduced the expression of key pro-inflammatory cytokines, including TNF-α and IL-6, in activated macrophages. Given that TNF-α amplifies IL-17-mediated responses and IL-6 facilitates Th17 differentiation, these results suggest a potential modulatory effect on the broader psoriatic inflammatory milieu. However, as this study focused primarily on cytokine expression in LPS-stimulated macrophages and phenotypic changes in an acute IMQ model, direct evidence for the modulation of IL-23/IL-17 signaling or keratinocyte-specific pathways was not obtained. Therefore, while the reduction of early-stage inflammatory mediators provides a plausible basis for the observed therapeutic effects, the definitive involvement of the Th17 axis remains to be further validated through protein-level analysis and targeted mechanistic studies.

The current study has several limitations. First, although the tested metabolites exhibited anti-inflammatory effects, the specific molecular targets and signaling pathways involved were not directly identified. The involvement of the Th17 pathway could not be clarified directly based on the current data. because IL-17 expression was not evaluated. To elucidate the protein-level dynamics and downstream signaling, additional validation using ELISA or Western blot is warranted in future studies. Second, due to the small sample size of the propionylcarnitine administration group, in vivo results should be interpreted cautiously. The lack of significant effects in PASI and PHS may be due to insufficient statistical power, as the corresponding compound was excluded from subsequent experiments following the initial preliminary study. Third, the IMQ-induced psoriasis model used in this study primarily reflects an acute inflammatory response characterized by rapid onset and cytokine-driven keratinocyte hyperproliferation. This model may not fully capture the complex, long-term pathophysiology of chronic human psoriasis, which involves persistent T-cell memory and systemic comorbidities. Therefore, while our results demonstrate the potent anti-inflammatory potential of the candidate metabolites, further studies using chronic or genetic psoriasis models are warranted to evaluate their long-term therapeutic efficacy and safety. Finally, metabolite identification was performed based on LC-MS/MS spectral matching (metabolomics standards initiative levels 2–3) without verification using orthogonal analysis methods [5]. Although LC-MS/MS–based annotation are widely used [34], it remains a major bottleneck in metabolomics research due to limitations in confirming structural identity [34,35]. Therefore, these results must be interpreted cautiously. Nevertheless, the use of commercially available high-purity compounds for subsequent functional validation partially compensates for the identification uncertainty by confirming the biological activity of the predicted molecular structures.

In conclusion, our data highlights the potential of specific candidate metabolites identified in CS preparations, particularly L-iditol, as candidates for anti-inflammatory drug development. Despite the limitations, these findings contribute to a growing body of evidence supporting the role of helminth-derived molecules in immune modulation and encourage further exploration into their therapeutic applications in chronic inflammatory diseases such as psoriasis.

Data availability

Data will be made available on request.

Author contributions

Conceptualization: Won EJ, Kim TJ. Data curation: Lee YJ, Kim MJ, Yu SM, Won EJ, Kim TJ. Formal analysis: Lee YJ. Funding acquisition: Ryu JH, Won EJ, Kim TJ. Investigation: Lee YJ. Methodology: Lee YJ, Kim MJ, Yu SM, Won EJ, Kim TJ. Project administration: Won EJ, Kim TJ. Resources: Won EJ, Kim TJ. Software: Won EJ, Kim TJ. Supervision: Ryu JH, Won EJ, Kim TJ. Writing – original draft: Lee YJ, Won EJ, Kim TJ. Writing – review & editing: Kim MJ, Yu SM, Ryu JH, Won EJ,

https://doi.org/10.3347/PHD.26026

Kim TJ.

Conflict of interest

The authors have no conflicts of interest to declare.

Funding

This study was supported by the grants from the National Research Foundation of Korea (NRF) funded by the Ministry of Education, Science and Technology (NRF-2022R1C1C1002741 and RS-2024-00410713) and the grants of Chonnam National University Hospital Biomedical Research Institute (BCRI26054 and BCRI25056).

Supplementary information

Supplementary material is available with this article at https://doi.org/10.3347/PHD.26026.

ORCID

Yu Jeong Lee, https://orcid.org/0000-0003-1282-4210
Moon-Ju Kim, https://orcid.org/0000-0002-8018-6903
Sung Min Yu, https://orcid.org/0009-0005-6015-1446
Je-Hwang Ryu, https://orcid.org/0000-0002-8708-8943
Eun Jeong Won, https://orcid.org/0000-0002-8750-4257
Tae-Jong Kim, https://orcid.org/0000-0002-2871-1635

References

1. Wu M, Dai C, Zeng F. Cellular mechanisms of psoriasis pathogenesis: a systemic review. Clin Cosmet Investig Dermatol 2023;16:2503-15. https://doi.org/10.2147/CCID.S420850
2. van der Fits L, Mourits S, Voerman JS, et al. Imiquimod-induced psoriasis-like skin inflammation in mice is mediated via the IL-23/IL-17 axis. J Immunol 2009;182:5836-45. https://doi.org/10.4049/jimmunol.0802999
3. Brożyna AA, Slominski RM, Nedoszytko B, Zmijewski MA, Slominski AT. Vitamin D signaling in psoriasis: pathogenesis and therapy. Int J Mol Sci 2022;23:8575. https://doi.org/10.3390/ijms23158575
4. Ryan S. Psoriasis: characteristics, psychosocial effects and treatment options. Br J Nurs 2010;19:820-825. https://doi.org/10.12968/bjon.2010.19.13.48856
5. Zhou X, Chen Y, Cui L, Shi Y, Guo C. Advances in the pathogenesis of psoriasis: from keratinocyte perspective. Cell Death Dis 2022;13:81. https://doi.org/10.1038/s41419-022-04523-3
6. Davidovici BB, Sattar N, Prinz J, et al. Psoriasis and systemic inflammatory diseases: potential mechanistic links between skin disease and co-morbid conditions. J Invest Dermatol 2010;130:1785-96. https://doi.org/10.1038/jid.2010.103
7. Lebwohl MG, Stein Gold L, Strober B, et al. Phase 3 trials of tapinarof cream for plaque psoriasis. N Engl J Med 2021;385:2219-29. https://doi.org/
8. Lebwohl MG, Stein Gold L, Strober B, et al. Trial of roflumilast cream for chronic plaque psoriasis. N Engl J Med 2020;383:229-39. https://doi.org/10.1056/NEJMoa2103629
9. Strober B, Thaci D, Sofen H, et al. Deucravacitinib versus placebo and apremilast in moderate to severe plaque psoriasis: efficacy and safety results from the 52-week, randomized, double-blinded, phase 3 Program fOr Evaluation of TYK2 inhibitor psoriasis second trial. J Am Acad Dermatol 2023;88:40-51. https://doi.org/10.1016/j.jaad.2022.08.061
10. Stein Gold L, Adam DN, Albrecht L, et al. Long-term safety and effectiveness of roflumilast cream 0.3% in adults with chronic plaque psoriasis: a 52-week, phase 2, open-label trial. J Am Acad Dermatol 2024;91:273-80. https://doi.org/10.1016/j.jaad.2024.03.030
11. Armstrong AW, Lebwohl M, Warren RB, et al. Safety and efficacy of deucravacitinib in moderate to severe plaque psoriasis for up to 3 years: an open-label extension of randomized clinical trials. JAMA Dermatol 2025;161:56-66. https://doi.org/10.1001/jamadermatol.2024.4688
12. Armstrong AW, Read C. Pathophysiology, clinical presentation, and treatment of psoriasis: a review. JAMA 2020;323:1945-60. https://doi.org/10.1001/jama.2020.4006
13. Griffiths CEM, Armstrong AW, Gudjonsson JE, Barker JNWN. Psoriasis. Lancet 2021;397:1301-15. https://doi.org/10.1016/S0140-6736(20)32549-6
14. Bachelez H, Choon SE, Marrakchi S, et al. Trial of spesolimab for generalized pustular psoriasis. N Engl J Med 2021;385:2431-40. https://doi.org/10.1056/NEJMoa2111563
15. Ellinghaus D, Jostins L, Spain SL, et al. Analysis of five chronic inflammatory diseases identifies 27 new associations and highlights disease-specific patterns at shared loci. Nat Genet 2016;48:510-8. https://doi.org/10.1038/ng.3528
16. Kuijk LM, van Die I. Worms to the rescue: can worm glycans protect from autoimmune diseases? IUBMB Life 2010;62:303-12. https://doi.org/10.1002/iub.304
17. Summers RW, Elliott DE, Urban JF Jr, Thompson RA, Weinstock JV. *Trichuris suis* therapy for active ulcerative colitis: a randomized controlled trial. Gastroenterology 2005;128:825-32. https://doi.org/10.1053/j.gastro.2005.01.005
18. Navarro S, Pickering DA, Ferreira IB, et al. Hookworm recombinant protein promotes regulatory T cell responses that suppress experimental asthma. Sci Transl Med 2016;8:362ra143. https://doi.org/10.1126/scitranslmed.aaf8807
19. Ahangari Maleki M, Malek Mahdavi A, Soltani-Zangbar MS, Yousefi M, Khabbazi A. Randomized double-blinded controlled trial on the

effect of synbiotic supplementation on IL-17/IL-23 pathway and disease activity in patients with axial spondyloarthritis. Immunopharmacol Immunotoxicol 2023;45:43-51. https://doi.org/10.1080/08923973.2022.2112220

20. Lee YJ, Kim MJ, Jo S, et al. *Clonorchis sinensis*-derived protein attenuates inflammation and new bone formation in ankylosing spondylitis. Front Immunol 2021;12:615369. https://doi.org/10.3389/fimmu.2021.615369
21. Kim MJ, Yoo HM, Lee YJ, et al. *Clonorchis sinensis* excretory/secretory proteins ameliorate inflammation in rheumatoid arthritis and ankylosing spondylitis. Parasit Vectors 2025;18:85. https://doi.org/10.1186/s13071-025-06677-3
22. Hong SJ, Seong KY, Sohn WM, Song KY. Molecular cloning and immunological characterization of phosphoglycerate kinase from *Clonorchis sinensis*. Mol Biochem Parasitol 2000;108:207-16. https://doi.org/10.1016/s0166-6851(00)00220-6
23. Jabeen M, Boisgard AS, Danoy A, et al. Advanced characterization of imiquimod-induced psoriasis-like mouse model. Pharmaceutics 2020;12:789. https://doi.org/10.3390/pharmaceutics12090789
24. Karamani C, Antoniadou IT, Dimou A, et al. Optimization of psoriasis mouse models. J Pharmacol Toxicol Methods 2021;108:107054. https://doi.org/10.1016/j.vascn.2021.107054
25. Obayashi Y, Arisaka H, Yoshida S, Mori M, Takahashi M. Proline protects liver from D-galactosamine hepatitis by activating the IL-6/STAT3 survival signaling pathway. Amino Acids 2012;43:2371-80. https://doi.org/10.1007/s00726-012-1317-8
26. Seif M, Dahabiyeh L, Al-Hunaiti A, et al. Anti-inflammatory activity and metabolite profiling of myo-inositol in LPS-stimulated macrophages. PLoS One 2026;21:e0341193. https://doi.org/10.1371/journal.pone.0341193
27. Bollati C, Tosi M, d'Adduzio L, et al. Antioxidant and anti-inflammatory activity of a new formulation of slow-release amino acids in human intestinal Caco-2 cells. Antioxidants (Basel) 2025;14:271. https://doi.org/10.3390/antiox14030271
28. DeForge LE, Remick DG. Kinetics of TNF, IL-6, and IL-8 gene expression in LPS-stimulated human whole blood. Biochem Biophys Res Commun 1991;174:18-24. https://doi.org/10.1016/0006-291x(91)90478-p
29. Wong S, Schwartz RC, Pestka JJ. Superinduction of TNF-alpha and IL-6 in macrophages by vomitoxin (deoxynivalenol) modulated by mRNA stabilization. Toxicology 2001;161:139-49. https://doi.org/10.1016/s0300-483x(01)00331-6
30. Hobbs S, Reynoso M, Geddis AV, Mitrophanov AY, Matheny RW Jr. LPS-stimulated NF-κB p65 dynamic response marks the initiation of TNF expression and transition to IL-10 expression in RAW 264.7 macrophages. Physiol Rep 2018;6:e13914. https://doi.org/10.14814/phy2.13914
31. Zimmermann M, Aguilera FB, Castellucci M, et al. Chromatin remodelling and autocrine TNFα are required for optimal interleukin-6 expression in activated human neutrophils. Nat Commun 2015;6:6061. https://doi.org/10.1038/ncomms7061
32. Baliwag J, Barnes DH, Johnston A. Cytokines in psoriasis. Cytokine 2015;73:342-50. https://doi.org/10.1016/j.cyto.2014.12.014
33. Goodman WA, Levine AD, Massari JV, et al. IL-6 signaling in psoriasis prevents immune suppression by regulatory T cells. J Immunol 2009;183:3170-6. https://doi.org/10.4049/jimmunol.0803721
34. Theodoridis G, Gika H, Raftery D, et al. Ensuring fact-based metabolite identification in liquid chromatography-mass spectrometry-based metabolomics. Anal Chem 2023;95:3909-16. https://doi.org/10.1021/acs.analchem.2c05192
35. Wang X, Liu Y, Jiang C, et al. TidyMass2: advancing LC-MS untargeted metabolomics through metabolite origin inference and metabolic feature-based functional module analysis. Nat Commun 2026;17:1755. https://doi.org/10.1038/s41467-026-68464-7

Original Article

Parasites Hosts Dis 2026;64(3):229-236
https://doi.org/10.3347/PHD.26021

Parasites, Hosts and Diseases

pISSN 2982-5164 • eISSN 2982-6799

Acanthamoeba profilin as a novel airway allergen with diverse sensitization patterns including pollen cross-reactivity

Mi-Kyung Park[1], Hye-Kyung Park[2,*], Hak Sun Yu[1,3,*]

[1]Department of Parasitology and Tropical Medicine, School of Medicine, Pusan National University, Yangsan, Korea; [2]Department of Internal Medicine, School of Medicine, Pusan National University, Yangsan, Korea; [3]Research Institute for Convergence of Biomedical Science and Technology, Pusan National University Yangsan Hospital, Yangsan, Korea

Profilins are ubiquitous pan-allergens responsible for cross-reactivity between pollens and plant foods. While we previously demonstrated that recombinant *Acanthamoeba* profilin (rAc-PF) drives allergic airway inflammation via Th2/Th17 pathways in murine models, its clinical relevance in human allergic disease remains unclear. This study investigated rAc-PF as a novel inhalant allergen and its immunological impact on patients with allergic airway diseases. A total of 176 patients with allergic airway diseases underwent skin prick tests with rAc-PF and a standard panel of 55 common aeroallergens. *Acanthamoeba*-specific and rAc-PF–specific serum IgE levels were quantified using ELISA. To elucidate immune mechanisms, peripheral blood mononuclear cells from atopic asthma patients were stimulated with rAc-PF, and Th2/Th17 cytokine production was analyzed. Thirteen patients (7.4%) showed positive skin prick tests reactions to rAc-PF. This sensitization was significantly associated with tree, grass, and weed pollens, indicating a pan-allergen characteristic due to high cross-reactivity. Notably, one patient sensitized to rAc-PF reacted to no other common inhalants, suggesting rAc-PF as a unique causative agent. Patients exhibited significantly elevated levels of serum *Acanthamoeba*-specific and rAc-PF–specific IgE compared to healthy controls. Furthermore, rAc-PF stimulation of peripheral blood mononuclear cells from asthmatic patients induced robust production of IL-4, IL-5, IL-13, and IL-17A in humans. rAc-PF is identified as a novel allergen capable of inducing IgE-mediated sensitization and mixed Th2/Th17 responses. The strong association with pollen sensitization supports its role as an environmental pan-allergen. Therefore, rAc-PF should be considered a clinically relevant diagnostic target, especially in patients with polysensitization or unidentified triggers.

Keywords: *Acanthamoeba*, profilins, allergens, respiratory hypersensitivity, immunoglobulin E

Introduction

Asthma is a heterogeneous chronic airway disease characterized by variable airflow obstruction, airway hyperresponsiveness, and persistent airway inflammation [1,2]. IgE-mediated sensitization to environmental allergens represents a major immunologic feature of allergic asthma, and cumulative IgE responses to inhalant allergens are strongly associated with disease expression and treatment outcomes [3]. Exposure to airborne allergens such as pollens, house dust mites, molds, and animal dander plays a critical role in triggering and perpetuating airway inflammation, and is strongly influenced by environmental and climatic conditions [4]. Allergen-driven Th2 inflammation contributes to the development and progression of asthma through IL-4/IL-13–mediated IgE class switching, eosinophilic recruitment, and mast-cell activation [5]. More re-

Received: March 12, 2026 Accepted: April 30, 2026
*Correspondence: hkp, parkhk@pusan.ac.kr; hsy, hsyu@pusan.ac.kr

Citation
Park MK, Park HK, Yu HS. *Acanthamoeba* profilin as a novel airway allergen with diverse sensitization patterns including pollen cross-reactivity. Parasites Hosts Dis 2026;64(3):229-236.

cently, Th17 cells and IL-17–associated pathways have emerged as additional contributors to airway inflammation, particularly in more severe phenotypes [6]. Together, these findings underscore the central role of environmental allergen exposure and IgE sensitization in the immunopathogenesis of asthma.

Despite extensive characterization of major aeroallergens, growing evidence suggests that additional, previously unrecognized allergens may contribute to airway disease in certain populations [4-7]. Environmental risk factors, including allergens, pollutants, and pathogenic microbes, have the potential to disrupt airway epithelial barrier functions and promote sensitization, thereby amplifying susceptibility to allergic airway inflammation [8,9]. Moreover, the presence of sensitization patterns that cannot be fully explained by known aeroallergens suggests that unidentified or overlooked allergens may also play a role in allergic disease development.

Profilins are a ubiquitous family of proteins, approximately 12–16 kDa in size, found in eukaryotic cells and play a role in actin polymerization control [10]. Profilin was first identified as an allergen in birch pollen in 1991 [11]. Both natural and recombinant forms were shown to react with IgE from birch pollen-allergic patients in immunoblot assays. Subsequently, profilin was identified as an allergen in grass (*Phleum pratensis*) and weed (*Artemisia vulgaris*) pollens [12]. Allergenic profilins have since been detected in various pollen types, latex, and plant-derived foods. They are recognized as panallergens due to their highly similar tertiary structures, which leads to significant cross-reactivity even among plant species that are taxonomically distant [13].

Acanthamoeba profilin, comprising 125 amino acids, exists in 2 isoforms (profilin-I and profilin-II) and exhibits partial sequence homology with vertebrate profilin [14]. Although previous studies utilizing various protein mapping analyses have identified significant differences between the sequences of profilin-I and profilin-II, both profilins interact with monoclonal antibodies and inhibit actin polymerization similarly. We have confirmed that allergic airway disease can be induced through repeated exposure to *Acanthamoeba* induces allergic airway disease in a murine model; importantly, recombinant *Acanthamoeba* profilin (rAc-PF) alone can elicit similar airway inflammatory responses, supporting its role as a principal allergenic determinant [9,15]. Additionally, our findings suggest that rAc-PF has the potential to induce airway inflammatory disease by enhancing Th2 immune responses and airway hyper-responsiveness via toll-like receptor 2 (TLR2) [16]. However, there is currently no allergenicity data for humans regarding rAc-PF. In this study, we evaluated the sensitization rate to rAc-PF using skin prick test (SPT) in patients with allergic rhinitis and asthma to investigate its potential role as an inhalant allergen. We also investigated the interaction of rAc-PF allergens with IgE in these patients and measured cytokine production levels following rAc-PF stimulation in the patients' peripheral blood mononuclear cells (PBMCs).

Methods

Ethics statement

The ethics committee of Pusan National University Hospital approved the experimental protocols (IRB 2012-029-098), and this study adhered to the Helsinki Declaration.

Subjects and skin prick test

To investigate the sensitivity of rAc-PF in patients with respiratory allergic diseases, we recruited subjects from January 2021 to December 2022. A total of 176 patients who underwent SPT for symptoms of asthma and allergic rhinitis during the study period were included in this study (Table 1). The SPT was conducted using a panel of 55 common aeroallergens (Allergopharma), *Acanthamoeba* protein [15], and rAc-PF [14] according to adapted methods from Oryszczyn et al. [17]. The SPT re-

Table 1. Clinical characteristics of study population (*n*=176)

Characteristics	Value
Age (yr)	45.5 ± 16.4
20–30	1
31–40	27 (15.3)
41–50	27 (15.3)
51–60	31 (17.6)
61–70	39 (22.2)
71–80	6 (3.4)
Sex	
Male	58 (33.0)
Female	118 (67.0)
Atopy (%)	103 (58.5)
Diagnosis	
Allergic rhinitis	37 (21)
Asthma	107 (60.8)
Eosinophilic bronchitis	13 (7.4)
Nonallergic rhinitis	11 (6.3)
Chronic rhinosinusitis	8 (4.5)
Total IgE (IU/ml)	209.5 ± 291.6
FeNO (ppb, *n* = 161)	37.2 ± 43.56
FEV1 (%)	86.2 ± 15.9

Values are presented as mean±SD or number (%).
FeNO, fractional exhaled nitric oxide; ppb, parts per billion; FEV1, forced expiratory volume in 1 second.

https://doi.org/10.3347/PHD.26021

actions to 55 common aeroallergens were graded by the ratio of the allergen wheal diameter to the histamine wheal diameter, and were considered positive when the ratio was ≥ 1. Atopy was defined as a positive skin test response to at least 1 allergen.

Fifteen minutes after administering the SPT, the average diameter of the wheals formed by histamine and rAc-PF was measured. A skin response to rAc-PF was deemed positive if the wheal diameter measured at least 2 mm.

Acanthamoeba-specific or rAc-PF–specific serum IgE level

To determine the relationship between airway diseases and *Acanthamoeba*-specific or rAc-PF–specific antibodies, we detected the levels of rAc-PF–specific IgE in patient serum. The rAc-PF was produced and purified as previously described [Song, 2018 #1]. rAc-PF–specific IgE was measured by ELISA in 8 patients among 13 patients with a positive skin test result to rAc-PF. Normal controls consisted of non-atopic individuals with no history of allergic diseases, negative SPT results to common aeroallergens, and an age range comparable to the patient group. The ELISA cut-off value was determined as the mean +2 SD of the normal controls. Ninety-six-well immune plates (Nunc) were coated with *Acanthamoeba* antigens or rAc-PF protein (final concentration, 1 μg/ml). Microplates were coated with *Acanthamoeba* antigen or rAc-PF (1 μg/ml). Following coating, the ELISA was performed using an in-house protocol, while subsequent steps, including blocking, incubation, and detection, were carried out according to the manufacturer's instructions for the ELISA reagents (eBioscience). The biospecimens used for this study were provided by the Biobank of Pusan National University Hospital, a member of the Korea Biobank Network.

PBMC isolation, stimulation, and evaluation of cytokine production

PBMCs were isolated from blood samples using SepMate-50 (STEMCELL Technologies). The isolated PBMCs (1×10^6 cells/ml) were cultured either untreated or stimulated with phytohemagglutinin or rAc-PF. After 72 hours of culture, the supernatant was harvested for cytokine analysis. The levels of IL-4, IL-5, IL-13, and IL-17A in the PBMC culture supernatants were measured using ELISA kits (eBioscience), according to the manufacturer's recommended protocols.

Statistical analysis

The statistical analysis was conducted using Prism 6 (GraphPad Prism) and IBM SPSS Statistics version 30.0 (IBM Corp.). The Phi coefficient was utilized to estimate the correlation between rAc-PF and other common allergens. Mean ± SD was calculated, and significant differences were determined using Student's *t*-test or one-way analysis of variance with Dunnett's multiple comparison post hoc test comparing all groups to controls.

Results

Clinical characteristics of the study population

A total of 176 subjects were analyzed (Table 1). The mean age was 45.5 ± 16.4 years, and 67.0% were female. Sensitization to at least 1 aeroallergen was observed in 58.5% of the subjects. The most common diagnoses included asthma, allergic rhinitis, non-allergic rhinitis, eosinophilic bronchitis, and chronic rhinosinusitis. Among all subjects, the most common sensitizing allergens were house dust mites, with 38.1% showing positive responses. Sensitization to animals and insects was observed in 5.5%, mold in 1.9%, pollens in 7.5%, and other allergens in 3.7%. Positive responses to rAc-PF were observed in 13 out of 176 patients (7.4%). These patients included 5 with allergic rhinitis, 7 with atopic asthma accompanied by allergic rhinitis, and 1 with non-atopic asthma.

Sensitization patterns in rAc-PF–positive patients

Among rAc-PF–positive subjects, sensitization profiles were heterogeneous (Table 2). House dust mites were the most frequently detected co-sensitizing allergens. Both monosensitization and polysensitization patterns were observed, involving combinations of indoor and outdoor aeroallergens. Some subjects demonstrated sensitization restricted to indoor allergens, whereas others exhibited additional sensitization to seasonal pollens or mixed indoor–outdoor allergen profiles. Notably, one subject with rAc-PF positivity showed no sensitization to any of the tested inhalant allergens.

Patients exhibiting sensitivity to the rAc-PF antigen

Positive reactions to rAc-PF were observed in 13 out of 176 patients (7.4%) including 5 with allergic rhinitis, 7 with atopic asthma accompanied by allergic rhinitis, and 1 with non-atopic asthma. The results of SPT with common inhalant allergens in patients positive to rAc-PF are summarized in Table 2. Sensitization patterns demonstrated marked heterogeneity among rAc-PF–positive patients. House dust mites were the most frequently identified allergens, with *Dermatophagoides pteronyssinus* and *D. farinae* detected in 42.6% and 48.3% of patients, respectively. Three patients exhibited sensitization exclusively to indoor allergens, such as house dust mites, storage mites,

Table 2. Inhalant allergen skin test results in recombinant *Acanthamoeba* profilin positive patients

Positive inhalant allergens
Dp, *Df*, tyrophagus, cockroach
Df, alder, hazel, poplar, willow tree, birch, plane tree, ash, gasses, velvet grass, rye grass, orchard grass, Kentucky blue grass, meadow grass, mugwort
Dp, *Df*, alder, poplar, hazel, birch, beech, mugwort, chrysanthemum
Dp, *Df*, tyrophagus, cow epithelium
Alder, hazel, willow tree, birch, beech, orchard grass, meadow grass
Birch, beech
Df
Cockroach, willow tree, elder, dandelion, weed mix
Dp, *Df*, tyrophagus, dog, pig, cow, *Alternaria*, *Cladosporium*, *Aspergillus*, *Penicillium*, alder, hazel, elm, willow tree, birch, beech, oak, plane tree, ash, elder, gasses, velvet grass, orchard grass, rye grass, meadow grass, ragweed, mugwort, chrysanthemum, dandelion, nettle, weed mix
Cockroach, oak, orchard grass, rye grass, Kentucky blue grass, meadow grass, ragweed, weed mix
Dp, *Df*, tyrophagus, cat, dog, pig, cow, horse, cockroach, *Alternaria tenuis*, alder, poplar, birch, grasses, orchard grass, Kentucky blue grass, meadow grass, Hop Japanese, weed mix
None
Hazel, beech, ash

Dp, Dermatophagoides pteronyssinus; Df, Dermatophagoides farina.

cockroach or animal dander. Furthermore, one patient showed negative results to all common inhalant allergens, indicating absence of sensitization to commercially tested inhalant allergens despite rAc-PF positivity, suggesting *Acanthamoeba* as a unique or primary sensitizer in this patient. Another 3 patients showed sensitization only to seasonal pollens, with positive reactions to tree, grass, or weed pollens. In contrast, 6 patients showed cosensitization to both indoor allergens such as house dust mites, cockroach, animal dander, or molds and outdoor allergens including tree, grass, and weed pollens.

Correlation between rAc-PF and common inhalant allergens

To investigate the relationship between rAc-PF and common inhalant allergens, the chi-square test was used to determine the correlation between rAc-PF and other allergens. Although the highest number of positive reactions was observed for *D. pteronyssinus* and *D. farinae*, no significant correlation was found between rAc-PF positivity and these allergens. However, rAc-PF positivity was significantly associated with several pollen-derived allergens. Notably, positive reactions to poplar ($r=0.34$, $P<0.001$), willow tree ($r=0.36$, $P<0.001$), plane tree ($r=0.25$, $P<0.001$), ash tree ($r=0.28$, $P<0.001$), orchard grass ($r=0.38$, $P<0.001$), and meadow grass ($r=0.30$, $P<0.001$) were observed (Table 3).

Titer of rAc-PF–specific IgE of patients with airway disease was significantly higher than in normal controls

The mean levels of *Acanthamoeba*-specific or rAc-PF–specific IgE titers in patient sera were significantly higher than those in normal controls (Fig. 1). Compared to the control group, the mean *Acanthamoeba*-specific IgE levels in the patient group showed a greater than 3.2-fold increase, while the titer of rAc-PF–specific IgE exhibited an increase exceeding 1.5-fold. ($P<0.001$) Additionally, these patients were found to have a higher positive reaction to pollen in the SPT results compared to other patients.

The rAc-PF increased Th2 and Th17 cytokines production

The control group used PBMCs from individuals who tested negative in the SPT to common aeroallergens. The cytokine production analysis of PBMCs showed that the levels of Th2 and Th17-related genes IL-4, IL-5, IL-13, and IL-17A were higher in the positive group compared to the control group (Fig. 2). Although the cytokine levels in the rAc-PF treated group were minimal compared to the phytohemagglutinin (nonspecific stimuli) treated group, they were significantly ($P<0.05$) increased compared to the control group. These findings indicate that rAc-PF affects cytokine production in PBMCs from patients with airway disease.

Discussion

Previous studies have demonstrated that *Acanthamoeba*-derived profilin acts as an allergen capable of inducing airway inflammation through the activation of Th2 and Th17 pathways, primarily mediated by TLR2 signaling in mouse models [14,18]. Consistent with these findings, the present study confirmed that 13 of 176 patients with airway diseases exhibited positive skin prick reactions to rAc-PF, accompanied by significantly higher levels of rAc-PF–specific IgE compared with healthy nonatopic controls. These results provide further evidence supporting the relevance of rAc-PF as an allergen in humans.

In this study, sensitization patterns among rAc-PF positive patients were heterogeneous. Although house dust mites were the most frequently detected allergens among rAc-PF–positive patients, no significant correlation was found be-

https://doi.org/10.3347/PHD.26021

Table 3. Positive rates of rAc-PF and mean square contingency (ϕ) coefficients of rAc-PF and other allergens (*n*=176)

Type of allergen	Allergen	SPT positive	rAc-PF positive	*r* (*P*-value)
Mites	*Dermatophagoides pteronyssinus*	75 (42.6)	5 (38.5)	-0.024 (0.753)
	Dermatophagoides farinae	85 (48.3)	7 (53.8)	0.028 (0.709)
	Tyrophagus	41 (23.3)	4 (30.8)	0.050 (0.508)
Animals and insects	Cat epithelium	22 (12.5)	1 (7.6)	-0.041 (0.586)
	Dog epithelium	18 (10.2)	2 (15.3)	0.048 (0.524)
	Pig epithelium#	6 (3.4)	2 (15.3)	0.186 (0.013)
	Cow epithelium	17 (9.7)	3 (23.1)	0.128 (0.089)
	Rabbit epithelium	4 (2.3)	1 (7.6)	0.103 (0.173)
	Horse epithelium#	2 (1.1)	1 (7.6)	0.175 (0.020)
	Sheep's wool	0 (0.0)	0 (0.0)	-
	Feathers	0 (0.0)	0 (0.0)	-
	Cockroach#	18 (10.2)	4 (30.8)	0.191 (0.011)
Molds	Moulds I	0 (0.0)	0 (0.0)	-
	Moulds II	0 (0.0)	0 (0.0)	-
	Alternaria tenuis	5 (2.8)	2 (15.3)	0.213 (0.005)
	Cladosporium herbar	2 (1.1)	1 (7.6)	0.175 (0.020)
	Fusarium moniliforme	3 (1.7)	0 (0.0)	-
	Aspergillus fumigatus	3 (1.7)	1 (7.6)	0.131 (0.083)
	Mucor mucedo	0 (0.0)	0 (0.0)	-
	Neurospora sitophila	0 (0.0)	0 (0.0)	-
	Penicillium notatum	2 (1.1)	1 (7.6)	0.175 (0.020)
	Rhizopus stolonifer	0 (0.0)	0 (0.0)	-
	Trichophyton	15 (8.5)	0 (0.0)	-
Pollen	Alder#	32 (18.2)	5 (38.5)	0.145 (0.049)
	Hazel#	27 (15.3)	5 (38.5)	0.181 (0.016)
	Poplar#	5 (2.8)	3 (23.1)	0.34 (<0.001)
	Elm	8 (4.5)	1 (7.6)	0.043 (0.0571)
	Willow tree#	8 (4.5)	4 (30.8)	0.356 (<0.001)
	Birch#	30 (17.0)	5 (38.5)	0.161 (0.033)
	Beech#	25 (14.2)	5 (38.5)	0.196 (0.009)
	Oak	23 (13.1)	2 (15.3)	0.019 (0.797)
	Plane tree#	8 (4.5)	3 (23.1)	0.251 (0.001)
	Ash#	7 (4.0)	3 (23.1)	0.276 (<0.001)
	Elder#	9 (5.1)	3 (23.1)	0.230 (0.002)
	Grasses#	13 (7.4)	3 (23.1)	0.169 (0.025)
	Herbs	0 (0.0)	0 (0.0)	-
	Velvet grass	8 (4.5)	2 (15.3)	0.147 (0.051)
	Orchard grass#	11 (6.3)	5 (38.5)	0.379 (<0.001)
	Rye grass#	11 (6.3)	3 (23.1)	0.196 (0.009)
	Kentucky blue grass#	15 (8.5)	4 (26.7)	0.225 (0.003)
	Meadow grass#	15 (8.5)	5 (38.5)	0.303 (<0.001)
	Ragweed	7 (4.0)	2 (15.3)	0.165 (0.029)
	Mugwort#	14 (8.0)	3 (21.4)	0.158 (0.036)
	Chrysanthemum#	11 (6.3)	3 (21.4)	0.196 (0.009)
	Dandelion	8 (4.5)	2 (15.3)	0.147 (0.051)
	Nettle#	6 (3.4)	2 (15.3)	0.186 (0.013)
	Hop Japanese#	2 (1.1)	1 (7.6)	0.175 (0.020)
Other	Latex	1 (0.6)	0 (0.0)	-
	Weed mix#	12 (6.8)	4 (33.3)	0.27 (<0.001)

Values are presented as numbers unless otherwise indicated.
rAc-PF, recombinant *Acanthamoeba* profilin; SPT, skin prick tests; Φ, coefficients value (*r*) between rAc-PF and other allergens; #, significantly correlated with rAc-PF.

tween rAc-PF reactivity and mite sensitization. Instead, significant associations were identified with several pollen derived allergens including poplar, willow, plane tree, ash tree, orchard grass, and meadow grass. These findings indicate that rAc-PF-specific IgE may be influenced by sensitization to pollen allergens rather than indoor allergens.

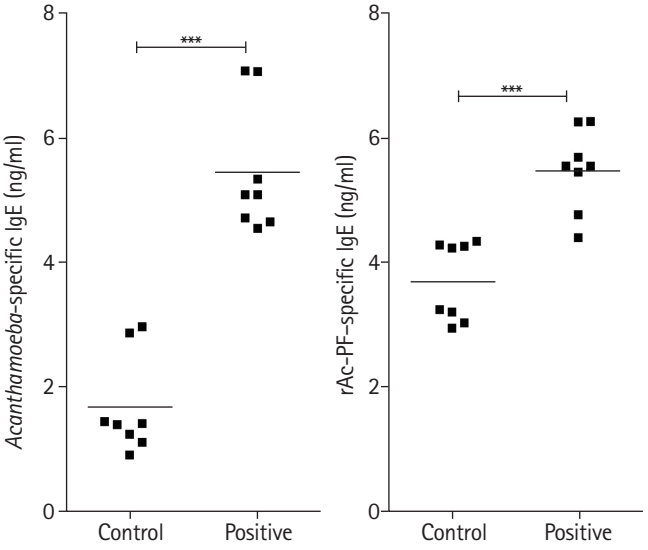

Fig. 1. Serum levels of *Acanthamoeba*-specific and recombinant *Acanthamoeba* profilin (rAc-PF)–specific IgE in patients with airway disease and normal controls. Serum samples from 8 patients with positive skin prick tests responses to rAc-PF and 8 non-atopic normal controls were analyzed. Microplates were coated with *Acanthamoeba* extract or rAc-PF (1 μg/ml), and IgE levels were measured using ELISA. Serum samples were diluted 1:2 in PBS. IgE levels are presented as ng/ml. Data are expressed as mean±SD (***P<0.001).

The distribution of sensitization patterns provided additional insights into the potential mechanisms underlying rAc-PF reactivity Patients restricted. Patients restricted to seasonal pollen sensitization likely represent cases in which rAc-PF recognition results from IgE cross-reactivity, as many tree and grass pollens share homologous allergenic epitopes with profilin-like proteins. The broad polysensitization to tree, grass, and weed pollens observed in these individuals supports this interpretation. Several recent studies have documented that under specific circumstances, profilin serves as an indicator of severity and acts as an allergen capable of inducing respiratory allergic symptoms [19-21]. Considering the statistical correlation between Ac-PF and pollen, our findings suggest that rAc-PF functions as an environmental allergen. Furthermore, it is postulated that individuals with respiratory allergy who spend extended periods outdoors are more likely to come into contact with external allergens compared to those who do not, or to individuals without allergies, thereby exhibiting reactivity to specific allergens. In contrast, patients sensitized exclusively to indoor allergens such as house dust mites, storage mites, cockroach, or animal dander and those without sensitization to any common inhalant allergens represent a distinct phenotype. In these individuals, rAc-PF positivity is less likely to be explained by cross-reactivity. Instead, their responses show the possibility of primary sensitization to *Acanthamoeba*-derived antigens. These findings suggest that rAc-PF may function not only as a cross-reactive profilin but also as a primary allergen in a subset of patients with airway disease.

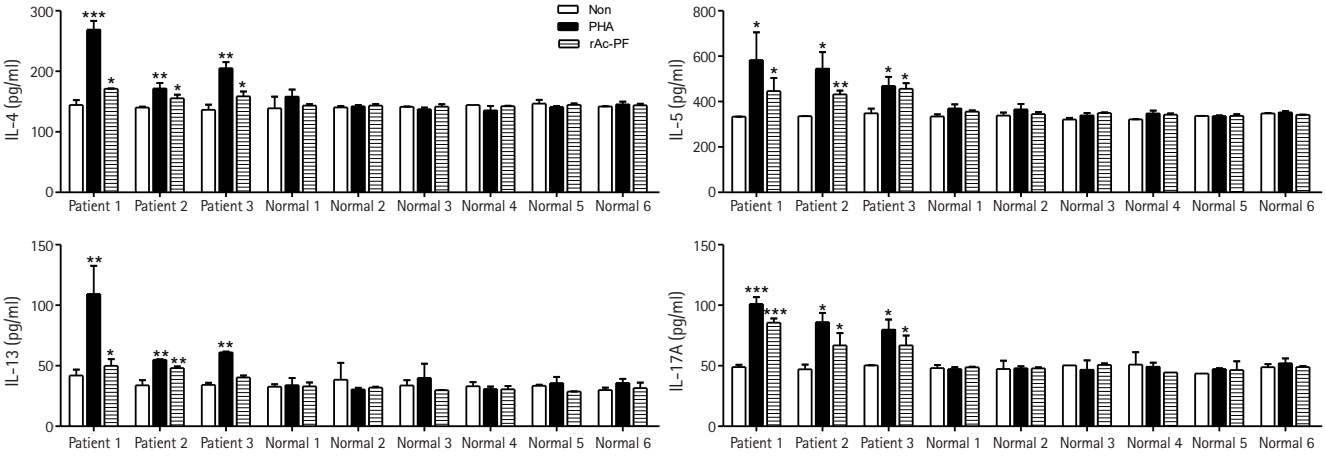

Fig. 2. Cytokine production in peripheral blood mononuclear cells (PBMCs) stimulated with recombinant *Acanthamoeba* profilin (rAc-PF) in patients with airway disease. PBMCs isolated from patients with airway disease were cultured (1×10^6 cells/ml) and stimulated with rAc-PF (1 μg/ml) or phytohemagglutinin (PHA) as a positive control for 72 hours. PBMCs from non-atopic individuals were used as controls. Levels of Th2 cytokines (IL-4, IL-5, and IL-13) and Th17 cytokine (IL-17A) in culture supernatants were measured using ELISA. Data are presented as mean±SD. Statistical significance was analyzed using one-way ANOVA with Dunnett's post hoc test ($^{*}P$<0.05, $^{**}P$<0.01, $^{***}P$<0.001).

https://doi.org/10.3347/PHD.26021

In our prior mouse model study, exposure to rAc-PF induced airway inflammatory phenotypes, including airway hyperresponsiveness, peribronchial immune cell infiltration, histological alterations, and increased production of pro-inflammatory cytokines [14]. We also demonstrated that TLR2 contribute the production of dendritic cell-derived Th2/17 cell-polarizing cytokines in response to rAc-PF stimulation [18]. Consistent with these findings, the present study reveals that rAc-PF elicits comparable immune responses in human PBMCs. rAc-PF stimulation significantly increased the production of Th2-related cytokines (IL-4, IL-5, and IL-13) and the Th17-related cytokine (IL-17A) in PBMCs obtained from patients with atopic asthma supporting its role in promoting type 2 and type 17 inflammatory pathways. Taken together, these findings demonstrate that rAc-PF induces prominent type 2 and type 17 inflammatory responses in human immune cells, supporting its relevance to the immunopathogenesis of human allergic airway disease.

Previous studies have demonstrated that patients with allergic diseases exhibit allergen-specific Th2-mediated responses, and that clinical resolution is often associated with a shift toward a Th1 response [22,23]. Th2 cytokines play pivotal roles in allergic inflammation, including the propagation of the Th2 phenotype, IgE isotype switching, eosinophil recruitment, and mast cell maturation and activation [24]. Recent investigations have revealed that the Th1/Th2 paradigm in allergy extends to other T cell effector subsets, particularly Th17 cells, which are characterized by IL-17 production [25]. In humans, IL-17 expression is elevated in moderate-to-severe asthma [26]. Th17 responses contribute to neutrophilic airway inflammation through IL-17-mediated induction of IL-8, a key chemokine for neutrophil recruitment by airway epithelial cells and smooth muscle [27,28]. Moreover, IL-17 stimulates the expression of granulocyte-colony-stimulating factor in bronchial epithelial cells, promoting neutrophil development and granulopoiesis [25].

This study has several limitations. First, the number of rAc-PF–positive patients was relatively small, and the limited sample size, particularly in the PBMC experiments, may have reduced the statistical power for subgroup analyses. Second, because cross-inhibition assays and molecular epitope-mapping studies were not performed, we were unable to conclusively differentiate cross-reactivity from primary sensitization. Further structural and epitope-mapping studies are required to elucidate the shared molecular features between *Acanthamoeba*-derived profilin and pollen profilins, which may explain the observed cross-reactivity. Third, the absence of environmental and exposure data limited our ability to assess exposure-dependent patterns of sensitization. Fourth, the cross-sectional study design precludes any inference regarding the temporal sequence of sensitization or causal relationships. Finally, as our analyses were confined to in vitro PBMC responses, the in vivo functional relevance of rAc-PF in humans warrants further investigation.

In this study, we observed that a subset of patients with airway disease showed significant reactivity to rAc-PF in SPT and specific IgE assays. We also demonstrated that rAc-PF induces Th2 and Th17 cytokine production from PBMCs of patients with respiratory diseases. Although cross-reactivity with pollen profilins likely contributes to rAc-PF–specific IgE binding in many patients, evidence of primary sensitization in a subset of individuals highlights the need for further characterization of shared and unique epitopes between *Acanthamoeba*-derived and pollen-derived profilin. Overall, these findings support the identification of rAc-PF as a previously unrecognized environmental and pathogen-derived allergen with potential clinical significance in respiratory allergic disease.

Author contributions

Conceptualization: Yu HS. Data curation: Park MK. Formal analysis: Park MK. Funding acquisition: Park HK. Investigation: Park MK. Methodology: Park MK. Project administration: Park HK, Yu HS. Supervision: Yu HS. Validation: Park MK, Park HK. Visualization: Park MK, Park HK. Writing – original draft: Park MK. Writing – review & editing: Park HK, Yu HS.

Conflict of interest

Hak Sun Yu serves as an editor of Parasites, Hosts and Diseases but had no involvement in the decision to publish this article. No other potential conflicts of interest relevant to this study were reported.

ORCID

Mi-Kyung Park, https://orcid.org/0000-0003-4992-1866
Hye-Kyung Park, https://orcid.org/0000-0003-4065-2962
Hak Sun Yu, https://orcid.org/0000-0002-6696-7981

References

1. Hough KP, Curtiss ML, Blain TJ, et al. Airway remodeling in asthma. Front Med (Lausanne) 2020;7:191. https://doi.org/10.3389/fmed.2020.00191
2. Holgate ST. Pathogenesis of asthma. Clin Exp Allergy 2008;38:872-

97. https://doi.org/10.1111/j.1365-2222.2008.02971.x
3. Lambrecht BN, Hammad H. The immunology of asthma. Nat Immunol 2015;16:45-56. https://doi.org/10.1038/ni.3049
4. Pawankar R. Allergic diseases and asthma: a global public health concern and a call to action. World Allergy Organ J 2014;7:12. https://doi.org/10.1186/1939-4551-7-12
5. Fahy JV. Type 2 inflammation in asthma: present in most, absent in many. Nat Rev Immunol 2015;15:57-65. https://doi.org/10.1038/nri3786
6. Al-Ramli W, Préfontaine D, Chouiali F, et al. T(H)17-associated cytokines (IL-17A and IL-17F) in severe asthma. J Allergy Clin Immunol 2009;123:1185-7. https://doi.org/10.1016/j.jaci.2009.02.024
7. Galli SJ, Tsai M, Piliponsky AM. The development of allergic inflammation. Nature 2008;454:445-54. https://doi.org/10.1038/nature07204
8. Kim BE, Hui-Beckman JW, Nevid MZ, Goleva E, Leung DYM. Air pollutants contribute to epithelial barrier dysfunction and allergic diseases. Ann Allergy Asthma Immunol 2024;132:433-9. https://doi.org/10.1016/j.anai.2023.11.014
9. Kang SA, Yu HS. Microarray-based characterization of airway inflammation induced by environmental *Acanthamoeba* exposure versus the ovalbumin-alum model. Parasites Hosts Dis 2025;63:327-39. https://doi.org/10.3347/PHD.25050
10. Davey RJ, Moens PD. Profilin: many facets of a small protein. Biophys Rev 2020;12:827-49. https://doi.org/10.1007/s12551-020-00723-3
11. Valenta R, Duchêne M, Pettenburger K, et al. Identification of profilin as a novel pollen allergen; IgE autoreactivity in sensitized individuals. Science 1991;253:557-60. https://doi.org/10.1126/science.1857985
12. Barderas R, Villalba M, Rodríguez R. Recombinant expression, purification and cross-reactivity of chenopod profilin: rChe a 2 as a good marker for profilin sensitization. Biol Chem 2004;385:731-7. https://doi.org/10.1515/BC.2004.089
13. Valenta R, Duchêne M, Vrtala S, et al. Profilin, a novel plant pan-allergen. Int Arch Allergy Immunol 1992;99:271-3. https://doi.org/10.1159/000236263
14. Song SM, Kang SA, Park HK, et al. *Acanthamoeba* profilin elicits allergic airway inflammation in mice. PLoS Negl Trop Dis 2018;12:e0006979. https://doi.org/10.1371/journal.pntd.0006979
15. Park MK, Cho MK, Kang SA, et al. *Acanthamoeba* protease activity promotes allergic airway inflammation via protease-activated receptor 2. PLoS One 2014;9:e92726. https://doi.org/10.1371/journal.pone.0092726
16. Park MK, Park HK, Yu HS. Toll-like receptor 2 mediates *Acanthamoeba*-induced allergic airway inflammatory response in mice. PLoS Negl Trop Dis 2023;17:e0011085. https://doi.org/10.1371/journal.pntd.0011085
17. Oryszczyn MP, Annesi I, Neukirch F, Doré MF, Kauffmann F. Longitudinal observations of serum IgE and skin prick test response. Am J Respir Crit Care Med 1995;151:663-8. https://doi.org/10.1164/ajrccm.151.3.7881653
18. Park MK, Park HK, Yu HS. The recombinant profilin from free-living amoebae induced allergic immune responses via TLR2. J Inflamm Res 2024;17:2915-25. https://doi.org/10.2147/JIR.S450866
19. Menz G, Dolecek C, Schönheit-Kenn U, et al. Serological and skin-test diagnosis of birch pollen allergy with recombinant Bet v I, the major birch pollen allergen. Clin Exp Allergy 1996;26:50-60. https://doi.org/10.1111/j.1365-2222.1996.tb00056.x
20. Scheurer S, Wangorsch A, Haustein D, Vieths S. Cloning of the minor allergen Api g 4 profilin from celery (*Apium graveolens*) and its cross-reactivity with birch pollen profilin Bet v 2. Clin Exp Allergy 2000;30:962-71. https://doi.org/10.1046/j.1365-2222.2000.00821.x
21. Gunning PW, Ghoshdastider U, Whitaker S, Popp D, Robinson RC. The evolution of compositionally and functionally distinct actin filaments. J Cell Sci 2015;128:2009-19. https://doi.org/10.1242/jcs.165563
22. Borish L, Aarons A, Rumbyrt J, et al. Interleukin-10 regulation in normal subjects and patients with asthma. J Allergy Clin Immunol 1996;97:1288-96. https://doi.org/10.1016/s0091-6749(96)70197-5
23. Rissoan MC, Soumelis V, Kadowaki N, et al. Reciprocal control of T helper cell and dendritic cell differentiation. Science 1999;283:1183-6. https://doi.org/10.1126/science.283.5405.1183
24. Elias JA, Lee CG, Zheng T, et al. New insights into the pathogenesis of asthma. J Clin Invest 2003;111:291-7. https://doi.org/10.1172/JCI17748
25. Zhao J, Lloyd CM, Noble A. Th17 responses in chronic allergic airway inflammation abrogate regulatory T-cell-mediated tolerance and contribute to airway remodeling. Mucosal Immunol 2013;6:335-46. https://doi.org/10.1038/mi.2012.76
26. Molet S, Hamid Q, Davoine F, et al. IL-17 is increased in asthmatic airways and induces human bronchial fibroblasts to produce cytokines. J Allergy Clin Immunol 2001;108:430-8. https://doi.org/10.1067/mai.2001.117929
27. Fossiez F, Djossou O, Chomarat P, et al. T cell interleukin-17 induces stromal cells to produce proinflammatory and hematopoietic cytokines. J Exp Med 1996;183:2593-603. https://doi.org/10.1084/jem.183.6.2593
28. Vanaudenaerde BM, Wuyts WA, Dupont LJ, et al. Interleukin-17 stimulates release of interleukin-8 by human airway smooth muscle cells in vitro: a potential role for interleukin-17 and airway smooth muscle cells in bronchiolitis obliterans syndrome. J Heart Lung Transplant 2003;22:1280-3. https://doi.org/10.1016/s1053-2498(02)01234-2

Original Article

Parasites Hosts Dis 2026;64(3):237-247
https://doi.org/10.3347/PHD.25003

Parasites, Hosts and Diseases

pISSN 2982-5164 • eISSN 2982-6799

Influence of livestock keeping on feeding behavior, host choice, and spatial distribution of malaria vectors in rural northwestern Tanzania

Diana Zakayo[1], Deokary J. Matiya[1,2], Winifrida Kidima[1], Jaeyul Kwon[3], Bo-In Kwon[4,5,*], Ernest Mazigo[6,*]

[1]Department of Zoology, College of Natural and Applied Sciences, University of Dar es Salaam, Dar es Salaam, Tanzania; [2]Department of Biological Sciences, Dar es Salaam University College of Education, Dar es Salaam, Tanzania; [3]Department of Medical Science, College of Medicine, Chungnam National University, Daejeon, Korea; [4]Department of Pathology, College of Korean Medicine, Sangji University, Wonju, Korea; [5]Massachusetts General Hospital, Harvard Medical School, Boston, MA, USA; [6]Department of Parasitic Diseases and Vector Control, National Institute for Medical Research, Dar es Salaam, Tanzania

Malaria transmission remains high in rural Tanzania despite widespread use of insecticide-treated nets and indoor residual spraying. Outdoor biting and flexible host-feeding behavior of *Anopheles* mosquitoes reduce the effectiveness of these interventions. Livestock near households may influence vector behavior, but evidence from high-transmission rural settings is limited. A cross-sectional study was conducted from November 2022 to February 2023 in 5 villages of Misungwi District, involving 44 households (22 livestock-keeping and 22 non-livestock-keeping). Adult *Anopheles* mosquitoes were collected indoors and outdoors using Center for Disease Control light traps, identified morphologically and by PCR, and blood-meal sources were determined by ELISA. Host-feeding patterns were assessed using the human blood index, bovine blood index, and foraging ratios. A total of 611 female mosquitoes were collected, dominated by *An. gambiae* s.l. (96.1%) and *An. funestus* s.l. (3.9%). Livestock households had more mosquitoes (61.5%) and higher outdoor activity (67.3%), while non-livestock households had higher indoor collections (73.6%). Among 231 blood-fed mosquitoes, 150 (64.9%) were from livestock households and 81 (35.1%) from non-livestock households. In livestock households, 108 (72.0%) had animal blood only, 27 (18.0%) mixed blood, and 15 (10.0%) human blood only. In non-livestock households, 44 (54.3%) had human blood only, 24 (29.6%) mixed blood, and 13 (16.0%) animal blood only. *An. arabiensis* was opportunistic, while *An. gambiae* s.s. and *An. funestus* s.s. remained strongly anthropophilic. Livestock shifts feeding toward animals and increases outdoor activity but does not eliminate human feeding, highlighting the need for integrated malaria control strategies.

Keywords: Malaria vectors, *Anopheles*, livestock, blood meal, Tanzania

Introduction

Malaria remains a major global health challenge, with an estimated 263 million cases and nearly 597,000 deaths in 2023, most occurring in sub-Saharan Africa [1]. Tanzania remains highly endemic, with 93% of the population at risk and 3.6 million cases reported in 2023 [1]. Despite widespread use of insecticide-treated nets (ITNs) and indoor residual spraying (IRS), residual transmission persists [2,3], driven in part by behavioral adaptations in vectors such as the *Anopheles gambiae* complex and *An. funestus*, which increasingly feed outdoors, bite earlier, and exhibit flexible host preferences [4,5].

Received: December 18, 2025 Accepted: February 19, 2026
*Correspondence: bik, kbi34812@sangji.ac.kr; em, mazigoernest72@gmail.com

Citation
Zakayo D, Matiya DJ, Kidima W, Kwon J, Kwon BI, Mazigo E. Influence of livestock keeping on feeding behavior, host choice, and spatial distribution of malaria vectors in rural northwestern Tanzania. Parasites Hosts Dis 2026;64(3):237-247.

Livestock keeping is common in rural Tanzania, where more than 60% of households own domestic animals [6]. In the Lake Zone, particularly Mwanza Region, cattle, goats, sheep, dogs and poultry are often kept within or near household compounds [7,8]. In Misungwi District, livestock corrals are frequently located within 20 meters of human dwellings [8]. This close proximity increases opportunities for human–animal–vector interactions, yet limited empirical evidence exists on how livestock ownership influences mosquito host choice and feeding behavior in such settings.

Studies across sub-Saharan Africa suggest that livestock may divert mosquito feeding away from humans (zooprophylaxis) or, conversely, sustain vector populations by providing alternative blood sources (zoopotentiation) [8,9]. These effects vary widely across ecological contexts, and it remains unclear how livestock presence interacts with household factors, vector species composition, and vector control measures to shape mosquito feeding patterns.

Blood meal analysis provides a direct method to assess host use and can reveal species-specific feeding behavior and associations with household characteristics [10-12]. This study examined blood meals of female *Anopheles* mosquitoes collected from livestock-keeping and non-livestock households in Misungwi District, northwestern Tanzania. Specifically, we aimed to (i) quantify human, animal, and mixed blood meals; (ii) compare indoor and outdoor feeding patterns relative to livestock presence; and (iii) assess how vector species identity and abundance relate to host choice. Findings will support improved malaria control strategies in livestock-keeping communities and similar ecological settings.

Methods

Ethics statement

The protocols for this study were approved by the National Institute for Medical Research (NIMR), a department of the Ministry of Health in Tanzania (NIMR/HQ/R.8a/Vol. IX/4114). All household owners were consulted and consented prior to their involvement in the study. Center for Disease Control (CDC) traps were placed indoors or outdoors in only those households that consented to participate.

Study area

The study was conducted in Misungwi District, Mwanza Region, northwestern Tanzania (Fig. 1). Geographically, the district lies at approximately 2°51′59″S and 33°05′60″E, covering an area of 2,553 km^2 and hosting a population of 467,867 people [13]. Misungwi is largely rural, with most residents engaged in mixed farming and livestock keeping. The district hosts a substantial livestock population, including cattle, goats, sheep, poultry, and dogs. Misungwi and Mabuki wards were purposively selected due to their high malaria transmission and close

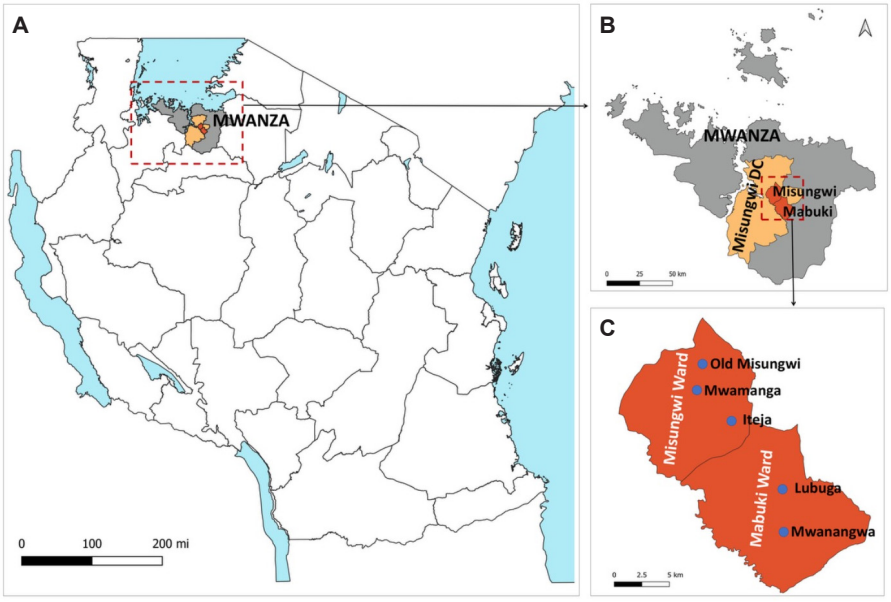

Fig. 1. Study sites. (A) Map of Tanzania showing the location of Mwanza Region and associated study sites. (B) Mwanza Region highlighting Misungwi District Council and the 2 purposively selected wards for the study, Misungwi and Mabuki. (C) Misungwi and Mabuki wards indicating the 5 villages chosen for the study, with 3 villages from Misungwi ward and 2 from Mabuki ward. Villages were purposively selected based on previous reports identifying crop cultivation and pastoralism as the primary economic activities in the areas. The maps were created using QGIS version 3.34.1.

https://doi.org/10.3347/PHD.25003

proximity of livestock to human dwellings, characteristics that provide suitable conditions for investigating vector feeding behavior (Fig. 1B). Malaria transmission remains moderate to high, peaking after the 2 rainy seasons, with a reported prevalence of approximately 52% across all age groups [14]. ITNs are the primary malaria control tool, while IRS has not been conducted since 2015. The coexistence of persistent malaria transmission, high vector densities, and widespread livestock ownership makes Misungwi an important site for examining vector–host interactions.

Villages and household selection

A total of 44 households from 5 villages were selected for mosquito collection: 3 villages from Misungwi ward (Old Misungwi, Mwamanga, and Iteja) and 2 from Mabuki ward (Lubuga and Mwanangwa) (Fig. 1C). The villages were purposively selected based on previous reports identifying crop cultivation and pastoralism as the primary economic activities in these areas. Households were randomly selected from lists provided by district authorities. Among the selected households, 22 kept livestock and 22 did not. Using a structured questionnaire and field measurements, the number of vertebrate hosts and the distances between livestock corrals and human dwellings were recorded. In the study setting, livestock enclosures are typically constructed in close proximity to sleeping structures due to cultural husbandry practices, land-use constraints, and security considerations, resulting in natural spatial clustering within short peri-domestic distances. Field measurements indicated that most corrals were located within approximately 10–15 meters of human dwellings. Accordingly, the distance between corrals and human dwellings was categorized into 2 groups: 1–12 meters and ≥13 meters. Corrals located within 1–12 meters were classified as "close," while those ≥13 meters were classified as "distant." This classification was informed by both the observed settlement structure and biologically plausible attraction ranges of host-seeking mosquitoes. Mosquito host-seeking behavior in peri-domestic environments typically operates at short spatial scales, with attraction gradients frequently documented within 10–20 meters of host sources [15,16]. Similar short-range thresholds have been used in studies examining livestock proximity, zooprophylaxis, and household-level malaria exposure [17].

Mosquito collection

Mosquito collections were conducted over a 4-month period, from November 2022 to February 2023. In the selected households, adult mosquitoes were sampled both indoors and outdoors using CDC miniature light traps. The traps were set in the evening and operated between 18:00 and 06:00 hours, following standard protocols for malaria surveillance [18]. Each household had 2 CDC light traps set per night, one indoors and one outdoors. The indoor trap was suspended about 1.5 meters above the floor at the foot end of a bed in a sleeping area, as described previously [19]. For outdoor collections in livestock-keeping households, the trap was positioned within the livestock corral at approximately 1.5 meters above ground level and at least 1 meter away from large animals to prevent physical obstruction, while remaining within the host odor plume zone. In households without livestock, the outdoor trap was placed within 10 meters of the main house at approximately 1.5 meters above ground level in an open peri-domestic area. To ensure comparability across households, traps were positioned in similar heights across all selected houses, away from artificial light sources, dense vegetation, cooking areas, and obvious mosquito resting sites, and were placed in locations with similar exposure to human activity and airflow. Placement criteria were standardized across households to minimize environmental heterogeneity and reduce sampling bias related to microhabitat differences [20].

Morphological identifications of mosquitoes

Collected mosquitoes were morphologically identified to distinguish *Anopheles* species from other mosquito genera. Identification was based on standard African vector identification keys including body colouration, sex, presence of pale or dark scales on the palps and proboscis, wing scale patterns (notably black scales), and the structure of the terminal abdominal segments [21,22]. All adult female *Anopheles* were preserved individually in silica gel and transported to the NIMR Mwanza Centre for molecular confirmation and blood meal analysis. At the NIMR laboratory, each mosquito was examined under a dissecting microscope, and dissection was performed by transversely separating the thorax from the abdomen. The legs were preserved for species-specific molecular identification, and the abdomens of blood-fed mosquitoes were used for blood meal source analysis. For downstream analyses, including blood meal source identification, host preference, and foraging ratio (FR) calculations, mosquito species identity was assigned based on molecular confirmation whenever available. Specimens that failed PCR amplification were retained under their morphologically identified group. This approach allowed maximal inclusion of specimens while maintaining species-level resolution [23].

Molecular confirmation of *An. gambiae* complex and *An. funestus* group sibling species

For species confirmation within the *An. gambiae* and *An. funestus* complexes, PCR targeting the ITS2 region was conducted using species-specific primers following established protocols [17,22]. Briefly, genomic DNA was mixed with the following primers in a 20 µl reaction: a universal forward primer common for all species (UN: 5'-GTG TGC CCC TTC CTC GAT GT-3') and species-specific reverse primers for *An. gambiae* s.s. (GA: 5'-CTG GTT TGG TCG GCA CGT TT-3'), *An. arabiensis* (AR: 5'-AAG TGT CCT TCT CCA TCC TA-3'), *An. funestus* (FUN: CTC GGG CAT CGA TGG GTT AAT CATG), and (PAR: GCC CTG CGG TCC CAA GCT AGA TT) for *An. parensis*. The selection of primers was based on previous entomological surveys [24,25]. Reactions were carried out in a 20 µl volume using AccuPower PCR PreMix (Bioneer). A 1 µl of extracted gDNA was used as a template for the PCR reaction, mixed with 25 pmol of primers GA, AR, FUN and PAR and 0.25 pmol of UN (Eurogentec). The PCR conditions were as follows: pre-denaturation at 94°C for 4 min, followed by 30 cycles of denaturation for 30 sec at 94°C, annealing for 30 sec at 58°C, and extension for 45 sec at 72°C, plus a final extension at 72°C for 7 min. Amplified PCR products were visualized on 2% agarose gels, stained with ethidium bromide. A known *An. arabiensis* strain from the Sekoru colony (Jimma, Ethiopia), was used as a positive control and double-distilled water used as negative control. These molecular analyses provided confirmatory evidence supporting the morphological identification.

Identification of blood meal sources

To identify the vertebrate host sources of blood-fed *Anopheles* mosquitoes collected both indoors and outdoors, ELISA was performed on the abdomens of morphologically and molecular identified specimens using established methods [26]. The analysis utilized species-specific antibodies targeting human, bovine, caprine, and canine antigens, corresponding to the most commonly kept domestic animals in the study area [12]. Briefly, each dissected mosquito abdomen was homogenized in 50 µl of grinding buffer and applied to ELISA plates pre-coated with capture monoclonal antibodies. Plates were then blocked with 200 µl of blocking buffer and incubated at room temperature for 1 h. Following this, homogenized samples, along with positive and double-distilled water as negative controls, were added to the wells and incubated for 2 h. After incubation, the plates were washed twice, and 50 µl of peroxidase-conjugated monoclonal antibody was added to each well, followed by a 1-h incubation in the dark. Plates were then washed 3 times with phosphate-buffered saline containing 0.05% Tween-20, and 100 µl of substrate solution was added to each well. After a final 30-min incubation in the dark, absorbance was measured at 405 nm using an ELISA plate reader. Samples with optical density values exceeding the negative control threshold were classified as positive for the corresponding host. This method provided reliable confirmation of mosquito host-feeding preferences and supported further analysis of vector–host interactions within the ecological and household contexts of the study area.

Data analysis

Data were entered and cleaned in MS Excel file (Microsoft), then analyzed using GraphPad Prism version 8.0.2 (GraphPad Software). Prior to statistical comparisons, data on blood meal sources (host types), human blood index (HBI), and bovine blood index (BBI) were tested for normality and log-transformed. HBI and BBI were calculated as the proportions of mosquitoes with human and bovine blood meals, respectively, among the total blood-fed specimens identified. Mixed (human + bovine) meals were included in both HBI and BBI calculations. Differences in HBI and BBI between indoor and outdoor collections were assessed using independent *t*-tests ($P<0.05$). Variation in mosquito host choices was analyzed using one-way ANOVA, followed by Tukey's HSD test for post hoc comparisons ($P<0.05$). FRs were calculated to assess host selection by mosquitoes [27], using the formula: FR = (NAE/NTE)/(NAP/NTP), where NAE is the number of engorged mosquitoes feeding on a specific host, NTE is the total engorged mosquitoes, NAP is the number of that host in the area, and NTP is the total number of all host types [27]. An FR ≈1 indicates opportunistic feeding; FR >1 suggests preference, and FR <1 indicates avoidance [12,28]. FRs were computed for humans, cattle, goat, sheep, chicken and dogs. Host feeding indices (HFIs) were also calculated to compare feeding preferences between host pairs using the formula: HFI = (Nx/Ny)/(Ax/Ay), where Nx and Ny are the mean number of mosquitoes feeding on hosts x and y, and Ax and Ay are the corresponding host abundances. An HFI of 1 indicates no preference; >1 suggests preference for host x; <1 suggests preference for host y. In this study, HFI was calculated specifically for humans versus cattle.

https://doi.org/10.3347/PHD.25003

Results

Collection, identification and distribution of *Anopheles* mosquitoes

Morphological identification confirmed 611 female *Anopheles* mosquitoes. PCR successfully amplified 553 specimens (90.5%), while 58 (9.5%) did not amplify (Table 1). Of the 587 mosquitoes morphologically identified as *An. gambiae* s.l., 535 (91%) amplified, revealing 446 (75.9%) *An. arabiensis* and 89 (15.1%) *An. gambiae* s.s., with 52 (9%) unamplified. Among 24 mosquitoes identified morphologically as *An. funestus* s.l., 18 (75%) amplified and were all confirmed as *An. funestus* s.s. Overall, 376 mosquitoes (61.5%) were collected from livestock-keeping households and 235 (38.5%) from non-livestock households ($P=0.5445$), indicating no evidence of a difference in overall mosquito abundance between household types. In livestock-keeping households, more mosquitoes were collected outdoors (253, 67.3%) than indoors (123, 32.7%); however, this difference was not statistically significant ($P>0.05$). In contrast, non-livestock households had significantly higher indoor collections (173, 73.6%) than outdoor (62, 26.4%) ($P=0.0361$). Spatial distribution across villages did not differ significantly ($P>0.05$), indicating no detectable variation in mosquito abundance between villages during the study period (Table 2).

Abdominal status of female *Anopheles* mosquitoes

The abdominal status of the 611 adult female *Anopheles* mosquitoes collected is summarized in Table 3 and Fig. 2. The majority of the collected *Anopheles* were unfed (362, 59.2%), followed by fed (231, 37.8%), gravid (11, 1.8%), and half-gravid (7, 1.1%). A higher proportion of fed (150, 64.9%), unfed (217, 59.9%) and gravid (7, 63.6%) female *Anopheles* mosquitoes were collected from livestock-keeping households compared to non-livestock-keeping households that had 81 (35.1%), 145 (40.1%), and 4 (36.4%), respectively. In the livestock-keeping

Table 1. Morphological vs. molecular species identification

Morphological ID	Molecular ID	No. of specimens	Discrepancies
Anopheles gambiae s.l.	*An. arabiensis*	446	Matches molecular confirmation
An. gambiae s.l.	*An. gambiae* s.s.	89	Matches molecular confirmation
An. gambiae s.l.	Not amplified	52	Potential discrepancy; retained as morphological ID
An. funestus s.l.	*An. funestus* s.s.	18	Matches molecular confirmation
An. funestus s.l.	Not amplified	6	Potential discrepancy; retained as morphological ID

Table 2. Composition and abundance of vertebrate hosts in studied villages

Villages (*n*)	Host					
	Human	Cow	Sheep	Goat	Chicken	Dog
Old Misungwi (4,324)	537	3,598	14	11	120	44
Iteja (1,295)	238	610	175	210	52	10
Mwamanga (905)	146	429	169	91	63	7
Mwanangwa (3,710)	840	2,543	98	12	104	113
Lubuga (2,154)	492	1,046	524	18	47	27
Total (12,388)	2,253	8,226	980	342	386	201
Mean ± SE	451 ± 122	1,645 ± 614	196 ± 87	68 ± 38	77 ± 15	40 ± 19

Values are presented as numbers unless otherwise indicated.

Table 3. Abdominal status of female *Anopheles* mosquitoes by place of collection

Blood digestion stage (*n*)	Livestock keeping households			Non-livestock keeping households		
	Total	Indoor	Outdoor	Total	Indoor	Outdoor
Fed (231)	150 (64.9)	48 (48.0)	102 (52.0)	81 (35.1)	52 (64.2)	29 (35.8)
Unfed (362)	217 (61.9)	96 (30.3)	121 (69.7)	145 (39.1)	124 (85.5)	21 (14.5)
Gravid (11)	7 (63.6)	2 (28.6)	5 (71.4)	4 (36.4)	3 (75.0)	1 (25.0)
Half gravid (7)	2 (28.6)	1 (50.0)	1 (50.0)	5 (71.4)	4 (80.0)	1 (20.0)
Total (611)	376 (61.5)	147 (32.7)	229 (67.3)	235 (38.5)	183 (73.6)	52 (26.4)

Values are presented as number (%).

households, the fed, unfed and gravid *Anopheles* mosquitoes were significantly found outdoors, 229 (60.9%), than indoors, 147 (39.1%) ($P<0.05$). This was contrary to the observation in non-livestock-keeping households where a large proportion of *Anopheles* mosquitoes were collected from indoors 183 (77.9%) than outdoors 52 (22.1%) ($P<0.05$).

Compositions and abundances of potential vertebrate hosts for *Anopheles* mosquitoes

A total of 12,388 hosts were recorded across the 44 surveyed houses in 5 villages, of which 6,524 (52.7%) were from Misungwi ward and the remainder from Mabuki ward. Of the 3 villages from Misungwi ward, Old Misungwi accounted for 4,324 (34.9%) followed by Iteja 1,295 (10.5%) and Mwamanga 905 (7.3%). From Mabuki ward, the number of hosts were large in Mwanangwa 3,710 (29.9%) than Lubuga 2,154 (17.4%). The identified hosts included cows 8,226 (66.4%), humans 2,253 (18.2%), sheep (7.9%), chickens (3.1%), goats (2.8%), and dogs 201 (1.6%). A large proportion of the domesticated animals, 6,939/10,135 (68.4%), were kept in corrals located less than 12 meters from human dwellings, compared to 3,196 (31.5%) housed more than 12 meters away ($P=0.0062$). Overall, a higher proportion of human and cattle hosts was recorded in the study area ($F_{5,20}=5,927$, $P=0.0016$) (Table 2).

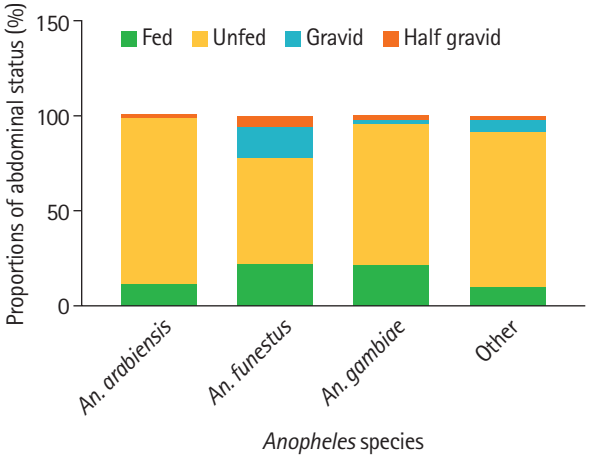

Fig. 2. Proportions of abdominal status of female *Anopheles* species collected in the study areas. Bars represent the relative proportions of fed, unfed, gravid, and half-gravid females within each *Anopheles* species group (*An. arabiensis*, *An. funestus*, *An. gambiae*, and other *Anopheles* species). "Fed" indicates females with freshly ingested blood, "unfed" those without visible blood, "gravid" females with fully developed eggs, and "half-gravid" females with partially developed eggs.

Distribution of bloodmeals across villages and place of collection

As indicated in Table 3, fed *Anopheles* mosquitoes were 231/611 (37.8%) and all were assayed for bloodmeal source analysis using ELISA. Of the assayed mosquitoes, 150 (64.9%) were collected from livestock-keeping houses and 81 (35.1%) from non-livestock-keeping households. A large proportion of the fed *Anopheles* mosquitoes were from Mabuki ward (159; 68.8%), which comprised Mwanangwa and Lubuga villages. Of these 159 mosquitoes, 114 (71.7%) from Mwanangwa village and 45 (28.3%) from Lubuga village. The remaining 72 (31.2%) fed *Anopheles* mosquitoes were from Misungwi ward, consisting of Old Misungwi (33, 45.8%), Iteja (18, 25.0%), and Mwamanga (21, 29.2%). Although numerical differences were observed in the distribution of fed mosquitoes across villages, these differences were not statistically significant ($P>0.05$).

Among the 150 fed *Anopheles* collected from livestock-keeping households, 108 (72.0%) contained animal blood, 27 (18.0%) had mixed human and other animal blood, and 15 (10.0%) had human blood. This was contrary to non-livestock keeping households where of the 81-fed *Anopheles*, 44 (54.3%) had human blood, 24 (29.6%) had human and other animal blood, and 13 (16.0%) had only animal blood (Fig. 3). Comparatively, the proportion of mosquitoes fed on human blood was higher in non-livestock keeping houses 68 (29.4%) compared to those from livestock-keeping houses 42 (18.2%) and the difference was significant ($P=0.0200$). Likewise, mosquitoes with animal blood only were significantly higher in livestock keeping houses 108 (46.8%) compared to non-livestock

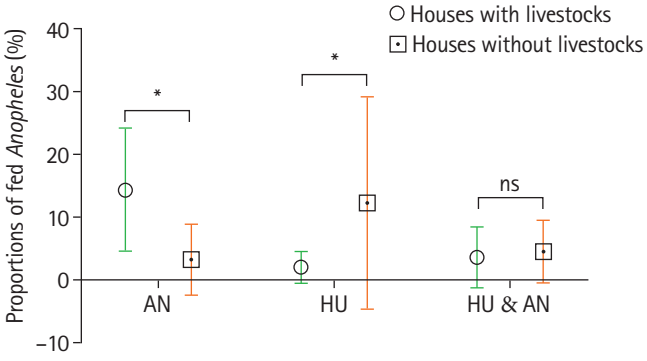

Fig. 3. Proportions of fed *Anopheles* mosquitoes collected from houses with and without livestock. Bars show the mean±SE proportions of blood-fed *Anopheles* in different host categories: animal husbandry host (AN), human host (HU), and HU & AN (mixed blood meal index of human and animal hosts). Circles represent livestock-keeping households, while squares represent non–livestock-keeping households. Asterisks indicate statistically significant differences ($P<0.05$), and "ns" denotes a non-significant difference between the 2 household groups by Mann–Whitney test at 95% confidence interval.

https://doi.org/10.3347/PHD.25003

keeping houses 13 (5.6%) (P=0.0317) (Fig. 4). Mosquitoes collected from corrals situated closer to houses (<12 m) showed a higher proportion of animal, mixed (animal + human), and human blood meals compared to those from corrals located farther away (>12 m) (Fig. 5).

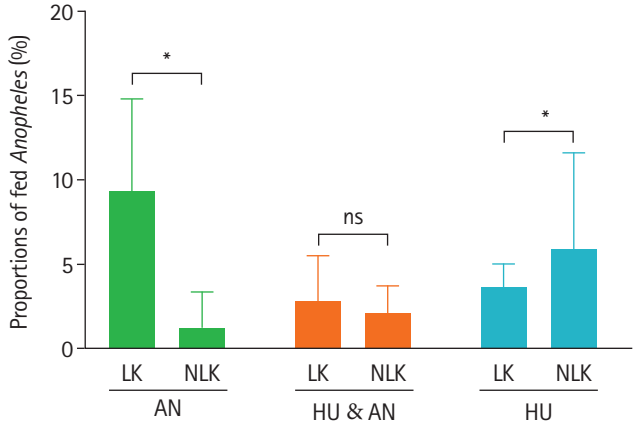

Fig. 4. Proportions of fed *Anopheles* mosquitoes collected from livestock-keeping (LK) and non-livestock-keeping (NLK) households. Bars represent the mean proportions (±SD) of fed *Anopheles* associated with different host categories: animal hosts (AN), human and animal hosts (HU & AN), and human hosts (HU). Statistical comparisons between LK and NLK groups were performed using the Mann–Whitney test. Asterisks indicate statistically significant differences (P<0.05). ns, not significant at 95% confidence interval.

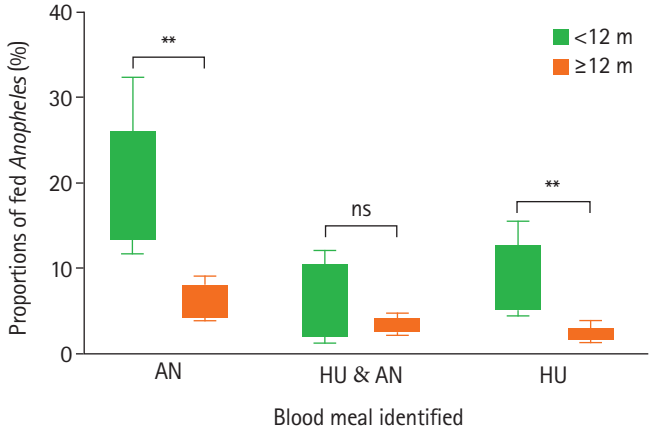

Fig. 5. Proportions of fed *Anopheles* mosquitoes based on the identified blood-meal sources and distance of animal corrals from human dwellings. Bars show the mean±SE proportions of blood-fed *Anopheles* collected from corrals located at less than 12 meters and those at 12 meters and above from human dwellings. Animal host (AN), human host (HU), and mixed blood meal index of human and animal hosts (HU & AN). Asterisks indicate statistically significant differences (P<0.05), and "ns" denotes a non-significant difference between the 2 household groups by Mann–Whitney test at 95% confidence interval.

FRs and host selection dynamics among *Anopheles* species

The FR analysis was calculated for all identified vertebrate hosts (humans, cattle, goats, sheep, chickens, and dogs) to evaluate feeding preference relative to host availability (Table 4). Distinct host-selection patterns were observed among the 3 *Anopheles* species. *An. gambiae* s.s. and *An. funestus* exhibited strong anthropophilic tendencies, with high FR values for humans (FR=4.4 and 4.95, respectively), despite relatively lower human availability. Both species showed consistent avoidance of livestock hosts (FR <1 across cattle, goats, sheep, chickens, and dogs). In contrast, *An. arabiensis* demonstrated opportunistic feeding behavior, with a moderate preference for goats (FR=2.86), a slight preference for humans (FR=1.38), and near-random feeding on sheep, chickens, and dogs. Although cattle represented the most abundant host type (66.4%), their FR values remained below 1 across all vector species, suggesting relative avoidance rather than proportional feeding. These findings indicate that host selection was not solely determined by host abundance but reflected species-specific behavioral traits and ecological flexibility (Table 4).

Discussion

In many African settings, particularly in rural and peri-urban areas where livestock ownership is common, close human–livestock cohabitation provides multiple blood-meal sources that can influence mosquito host-seeking behavior and feeding preferences. Increasing evidence indicates that malaria vectors historically associated with indoor feeding and resting are shifting toward outdoor and animal-associated behaviors, thereby reducing the effectiveness of indoor-based interventions such as ITNs and IRS [29]. Studies from Ethiopia, Kenya, and Tanzania have consistently shown that *An. arabiensis*, a key member of the *An. gambiae* complex, exhibits substantial behavioral plasticity, switching between human and animal hosts depending on host availability and environmental conditions [8,30,31]. Understanding the role of livestock in shaping vector behavior is therefore essential for designing effective malaria control strategies in settings where residual transmission persists despite high ITN and IRS coverage.

Our findings indicate that livestock keeping was associated with differences in vector feeding behavior and indoor–outdoor distribution patterns; however, not all observed differences, particularly in overall mosquito abundance and village-level distribution, reached statistical significance. *An.*

Table 4. FR and host preference of *Anopheles* mosquitoes collected in Misungwi, Tanzania

	Host type	Host availability (%)	Proportion of blood meals (%)	Foraging ratio (BBI and HBI)	Feeding preference	Interpretation
An. arabiensis (*n*=47, 57.6%)	Humans	18.2	25	1.38	Slight preference	Opportunistic, feeds on both humans and livestock; higher tendency outdoors
	Cattle	66.4	55	0.83	Random–avoidance	Reflects zoophilic tendency when livestock are near houses
	Goats	2.8	8	2.86	Strong preference	Indicates opportunistic feeding near small ruminants
	Sheep	7.9	7	0.89	Neutral	No significant bias
	Chickens	3.1	3	0.97	Neutral	Minor feeding
	Dogs	1.6	2	1.25	Mild preference	Possible opportunistic feeding outdoors
An. gambiae s.s. (*n*=31, 38.4%)	Humans	18.2	80	4.4	Strong preference	Highly anthropophilic; main malaria vector indoors
	Cattle	66.4	15	0.23	Avoidance	Avoids livestock; prefers humans
	Goats	2.8	2	0.71	Slight avoidance	Rarely feeds on small ruminants
	Sheep	7.9	1	0.13	Avoidance	Prefers humans
	Chickens	3.1	1	0.32	Avoidance	Prefers humans
	Dogs	1.6	1	0.63	Avoidance	Avoids livestock; prefers humans
An. funestus (*n*=3, 3.9%)	Humans	18.2	90	4.95	Very strong preference	Strictly anthropophilic, indoor feeder
	Cattle	66.4	8	0.12	Avoidance	Minimal feeding on livestock
	Goats	2.8	1	0.36	Avoidance	Minimal feeding on livestock
	Sheep	7.9	1	0.13	Avoidance	Minimal feeding on livestock
	Chickens	3.1	–	–	Avoidance	Minimal feeding on livestock
	Dogs	1.6	–	–	Avoidance	Minimal feeding on livestock

FR >1 → mosquitoes are selectively feeding on that host (preference); FR=1 → feeding is random relative to host abundance; FR <1 → mosquitoes avoid that host.
FR, foraging ratio; BBI, bovine blood index; HBI, human blood index.

arabiensis was the predominant vector species and was more frequently encountered outdoors in livestock-keeping households, consistent with its documented exophagic and zoophilic tendencies [32,33]. In contrast, *An. gambiae* s.s. and *An. funestus* s.s. remained strongly anthropophilic, reinforcing their continued role in sustaining indoor malaria transmission even in areas with widespread indoor vector control [34]. Statistically significant differences in indoor–outdoor mosquito densities were observed in non-livestock households, whereas the corresponding pattern in livestock-keeping households did not reach statistical significance. Therefore, while livestock presence may influence host-seeking and resting behavior, this interpretation should be made cautiously and primarily with respect to feeding patterns, which showed clearer statistical support.

Blood-meal analysis further revealed distinct feeding patterns between household types. Mosquitoes collected from livestock-keeping households exhibited a higher proportion of animal or mixed blood meals, whereas those from non-livestock households fed more frequently on humans. The reduced HBI observed in livestock-keeping settings is consistent with a potential zooprophylactic effect, whereby domestic animals divert mosquito feeding away from humans [27]. However, HBI reflects feeding behavior rather than transmission intensity, and a reduction in HBI alone does not necessarily translate into a measurable reduction in malaria transmission risk. Transmission dynamics depend on multiple entomological and epidemiological parameters, including vector density, survival rates, sporozoite prevalence, entomological inoculation rates, and human infection prevalence. In some settings, livestock-associated blood sources may sustain or even increase vector populations despite reduced anthropophily, thereby maintaining transmission potential [27,35]. Because this study did not assess sporozoite rates, entomological inoculation rates, or human malaria prevalence, we cannot directly determine whether the observed behavioral shift results in reduced malaria risk. These findings should therefore be interpreted as evidence of altered vector feeding patterns rather

https://doi.org/10.3347/PHD.25003

than definitive evidence of a protective zooprophylactic effect. Future studies integrating behavioral, entomological, and epidemiological indicators will be essential to clarify the net impact of livestock ownership on malaria transmission dynamics.

Host preference analysis revealed clear interspecific differences in feeding behavior. *An. gambiae* s.s. and *An. funestus* s.s. remained highly anthropophilic, with FR values exceeding 4 for humans and consistent avoidance of livestock hosts, reinforcing their established role as primary indoor malaria vectors. In contrast, *An. arabiensis* exhibited greater behavioral plasticity, showing a strong preference for goats (FR = 2.86), a slight preference for humans (FR = 1.38), and largely neutral or random feeding on other domestic animals. Despite the numerical dominance of cattle in the study area, their FR values were consistently below one across species, indicating that feeding patterns were not strictly proportional to host availability. These results underscore the ecological adaptability of *An. arabiensis* and its capacity to exploit multiple host types, a trait that may facilitate its persistence in livestock-associated and outdoor environments under sustained indoor vector control pressure [34].

These findings have important implications for malaria control in Tanzania. The continued presence of highly anthropophilic vectors underscores the ongoing importance of ITNs and IRS for reducing indoor transmission. However, the predominance of *An. arabiensis*, particularly in outdoor collections, highlights a potential behavioral gap that may contribute to residual transmission beyond the reach of indoor interventions. This interpretation is primarily supported by species composition and feeding data rather than differences in overall mosquito abundance, which were not statistically significant. The close proximity of livestock shelters to human dwellings further increases opportunities for mosquito feeding and resting near both hosts. Addressing this challenge will require integrated vector management strategies that complement indoor tools with targeted outdoor and livestock-based approaches, including insecticide-treated livestock, improved corral management, increased separation between animal shelters and human dwellings, larval source management, and other outdoor control measures. Such integrated approaches may enhance the effectiveness of existing interventions and contribute to reducing residual malaria transmission in endemic rural settings.

Study limitations

Despite its strengths, this study has several limitations. The cross-sectional design and 4-month data collection during the rainy season limit assessment of temporal dynamics and seasonal variability in mosquito populations and host–vector interactions, and may not reflect year-round fluctuations in abundance, species composition, and livestock–human contact patterns. The relatively small sample size ($n = 44$ households) may have reduced statistical power, increased the risk of type II error, and limited generalizability. Additionally, categorizing livestock–dwelling distance into 2 groups (1–12 m and ≥13 m), although informed by settlement patterns and biologically plausible mosquito attraction ranges, may oversimplify a potentially continuous and nonlinear relationship with mosquito density. This approach was partly driven by analytical constraints, as further stratification could have produced sparse data and unstable estimates. A small proportion of specimens (≈9.5%) could not be confirmed molecularly, and were retained under their morphological classification, which may have introduced minor misclassification in species-level analyses, including host preference and FRs. Future longitudinal studies across multiple seasons, with larger samples and spatially explicit analyses modeling distance as a continuous variable, are needed to better characterize temporal and distance-dependent vector dynamics and strengthen causal inference and external validity.

Author contributions

Conceptualization: Zakayo D, Matiya DJ, Kidima W, Mazigo E. Data curation: Kidima W, Mazigo E. Formal analysis: Zakayo D, Kidima W, Mazigo E. Funding acquisition: Kwon BI. Investigation: Zakayo D, Matiya DJ, Kidima W, Mazigo E. Methodology: Zakayo D, Matiya DJ, Kidima W, Mazigo E. Project administration: Matiya DJ, Kidima W, Mazigo E. Resources: Mazigo E. Software: Matiya DJ, Mazigo E. Supervision: Matiya DJ, Kidima W, Mazigo E. Validation: Zakayo D, Matiya DJ, Kidima W, Kwon J, Kwon BI, Mazigo E. Visualization: Zakayo D, Matiya DJ, Kidima W, Kwon J, Mazigo E. Writing – original draft: Zakayo D, Kidima W. Writing – review & editing: Matiya DJ, Kidima W, Kwon J, Kwon BI, Mazigo E.

Conflict of interest

The authors have no conflicts of interest to declare.

Funding

This research was supported by the Regional Innovation System and Education (RISE) program through the Gangwon RISE Center, funded by the Ministry of Education and the Gangwon State, Republic of Korea (2025-RISE-10-005).

Acknowledgments

We thank the study communities in Misungwi District for their cooperation and participation. We are grateful to the local leaders for facilitating field activities and to the field and laboratory teams for their technical support during mosquito collection, identification, and laboratory analyses. We also acknowledge the support of the NIMR Mwanza Centre for providing laboratory facilities and logistical assistance throughout the study.

ORCID

Diana Zakayo, https://orcid.org/0009-0006-2406-5943
Deokary J. Matiya, https://orcid.org/0000-0001-6692-479X
Winifrida Kidima, https://orcid.org/0000-0003-3344-7725
Jaeyul Kwon, https://orcid.org/0000-0002-2452-4111
Bo-In Kwon, https://orcid.org/0000-0003-3949-3052
Ernest Mazigo, https://orcid.org/0000-0002-8044-7384

References

1. World Health Organization. World malaria report 2024. World Health Organization; 2025.
2. Kapfunde A. The effectiveness of indoor residual spraying program in reducing malaria incidence in Mutasa District, 2020 to 2022 [dissertation]. Africa University; 2024.
3. Bachan EG, Adokiya MN, Tobin-West C. Challenges of implementing malaria control interventions in resource limited countries: a systematic review. P H J Public Health 2025;1:57-69.
4. Takken W, Charlwood D, Lindsay SW. The behaviour of adult *Anopheles gambiae*, sub-Saharan Africa's principal malaria vector, and its relevance to malaria control: a review. Malar J 2024;23:161. https://doi.org/10.1186/s12936-024-04982-3
5. Tung GA, Fonseca DM. Internal and external drivers interact to create highly dynamic mosquito blood-feeding behaviour. Proc Biol Sci 2024;291:20241105. https://doi.org/10.1098/rspb.2024.1105
6. Kitole FA, Sesabo JK. Smallholder livestock keepers' breeding choices and its implication on poverty reduction in developing countries: empirical evidence from Tanzania. Glob Soc Welf 2022;9:241-51. https://doi.org/10.1007/s40609-022-00252-9
7. Mramba RP, Mapunda PE. Management factors associated with the prevalence of gastrointestinal parasites in cattle: a case study of small-scale farms of the Nyamagana District in Mwanza, Tanzania. Ghana J Anim Sci 2024;14:108-19. https://doi.org/10.4314/gjansci.v14i1.11
8. Mwalugelo YA, Mponzi WP, Muyaga LL, et al. Livestock keeping, mosquitoes and community viewpoints: a mixed methods assessment of relationships between livestock management, malaria vector biting risk and community perspectives in rural Tanzania. Malar J 2024;23:213. https://doi.org/10.1186/s12936-024-05039-1
9. Kemibala EE, Mafra-Neto A, Dekker T, et al. A zooprophylaxis strategy using L-lactic acid (Abate) to divert host-seeking malaria vectors from human host to treated non-host animals. Malar J 2020;19:52. https://doi.org/10.1186/s12936-020-3136-9
10. Adugna T, Yewhelew D, Getu E. Bloodmeal sources and feeding behavior of anopheline mosquitoes in Bure district, northwestern Ethiopia. Parasit Vectors 2021;14:166. https://doi.org/10.1186/s13071-021-04669-7
11. Lardeux F, Loayza P, Bouchité B, Chavez T. Host choice and human blood index of *Anopheles pseudopunctipennis* in a village of the Andean valleys of Bolivia. Malar J 2007;6:8. https://doi.org/10.1186/1475-2875-6-8
12. Reeves LE, Burkett-Cadena ND. Mosquito blood meal analysis. Cold Spring Harb Protoc 2024;2024:pdb.top107706. https://doi.org/10.1101/pdb.top107706
13. National Bureau of Statistics. The 2022 population and housing census. Ministry of Finance and Planning; 2022.
14. Mosha JF, Kulkarni MA, Messenger LA, et al. Protocol for a four parallel-arm, single-blind, cluster-randomised trial to assess the effectiveness of three types of dual active ingredient treated nets compared to pyrethroid-only long-lasting insecticidal nets to prevent malaria transmitted by pyrethroid insecticide-resistant vector mosquitoes in Tanzania. BMJ Open 2021;11:e046664. https://doi.org/10.1136/bmjopen-2020-046664
15. Gillies MT, Wilkes TJ. The range of attraction of animal baits and carbon dioxide for mosquitoes: studies in a freshwater area of West Africa. Bull Entomol Res 1972;61:389-404. https://doi.org/10.1017/S0007485300047295
16. Takken W, Knols BG. Odor-mediated behavior of Afrotropical malaria mosquitoes. Annu Rev Entomol 1999;44:131-57. https://doi.org/10.1146/annurev.ento.44.1.131
17. Donnelly B, Berrang-Ford L, Ross NA, Michel P. A systematic, realist review of zooprophylaxis for malaria control. Malar J 2015;14:313. https://doi.org/10.1186/s12936-015-0822-0
18. Sadanandane C, Jambulingam P, Subramanian S. Role of modified CDC miniature light-traps as an alternative method for sampling adult anophelines (Diptera: Culicidae) in the National Mosquito Surveillance Programme in India. Bull Entomol Res 2004;94:55-63. https://doi.org/10.1079/ber2003281
19. Kakilla C, Manjurano A, Nelwin K, et al. Malaria vector species composition and entomological indices following indoor residual spraying in regions bordering Lake Victoria, Tanzania. Malar J 2020;19:383. https://doi.org/10.1186/s12936-020-03452-w
20. Service MW. Mosquito ecology: field sampling methods. Applied Science Publishers; 1976.

21. Gillies MT, Coetzee M. A supplement to the Anophelinae of Africa south of the Sahara. South African Institute for Medical Research; 1987.
22. Coetzee M. Key to the females of Afrotropical *Anopheles* mosquitoes (Diptera: Culicidae). Malar J 2020;19:70. https://doi.org/10.1186/s12936-020-3144-9
23. Coetzee M, Hunt RH, Wilkerson R, et al. *Anopheles coluzzii* and *Anopheles amharicus*, new members of the *Anopheles gambiae* complex. Zootaxa 2013;3619:246-74. https://doi.org/10.11646/zootaxa.3619.3.2
24. Philbert A, Lyantagaye SL, Pradel G, Ngwa CJ, Nkwengulila G. Pyrethroids and DDT tolerance of *Anopheles gambiae* s.l. from Sengerema District, an area of intensive pesticide usage in north-western Tanzania. Trop Med Int Health 2017;22:388-98. https://doi.org/10.1111/tmi.12850
25. Woyessa D, Yewhalaw D. *Anopheles* mosquito fauna, blood meal sources and transmission intensity from high and moderate malaria endemic areas of Ethiopia. Sci Rep 2025;15:10636. https://doi.org/10.1038/s41598-025-94739-y
26. Wirtz RA, Zavala F, Charoenvit Y, et al. Comparative testing of monoclonal antibodies against *Plasmodium falciparum* sporozoites for ELISA development. Bull World Health Organ 1987;65:39-45.
27. Ashine T, Kochora A, Shibru H, et al. Plasticity of blood feeding behavior of *Anopheles* mosquitoes in Ethiopia: a systematic review. Parasit Vectors 2024;17:408. https://doi.org/10.1186/s13071-024-06493-1
28. Riccetti N, Fasano A, Ferraccioli F, Gomez-Ramirez J, Stilianakis NI. Host selection and forage ratio in West Nile virus-transmitting *Culex* mosquitoes: challenges and knowledge gaps. PLoS Negl Trop Dis 2022;16:e0010819. https://doi.org/10.1371/journal.pntd.0010819
29. Rashmi P, Anupama M, Jayakrishnan TV, Jiji Joseph V. Mosquito diversity and disease transmission in Kerala: an integrated review of species ecology, habitat, and public health impact. Int J Mosq Res 2025;12:1-13. https://doi.org/10.22271/23487941.2025.v12.i2a.827
30. Chan K, Cano J, Massebo F, Messenger LA. Cattle-related risk factors for malaria in southwest Ethiopia: a cross-sectional study. Malar J 2022;21:179. https://doi.org/10.1186/s12936-022-04202-w
31. Nyangau PN, Nzuma JM, Irungu P, Kassie M. Evaluating livestock farmers knowledge, beliefs, and management of arboviral diseases in Kenya: a multivariate fractional probit approach. PLoS Negl Trop Dis 2021;15:e0009786. https://doi.org/10.1371/journal.pntd.0009786
32. Belay AK, Asale A, Sole CL, et al. Feeding habits and malaria parasite infection of *Anopheles* mosquitoes in selected agroecological areas of Northwestern Ethiopia. Parasit Vectors 2024;17:412. https://doi.org/10.1186/s13071-024-06496-y
33. Mayagaya VS, Nkwengulila G, Lyimo IN, et al. The impact of livestock on the abundance, resting behaviour and sporozoite rate of malaria vectors in southern Tanzania. Malar J 2015;14:17. https://doi.org/10.1186/s12936-014-0536-8
34. Machani MG, Ochomo E, Amimo F, et al. Behavioral responses of pyrethroid resistant and susceptible *Anopheles gambiae* mosquitoes to insecticide treated bed net. PLoS One 2022;17:e0266420. https://doi.org/10.1371/journal.pone.0266420
35. Mburu MM, Zembere K, Mzilahowa T, et al. Impact of cattle on the abundance of indoor and outdoor resting malaria vectors in southern Malawi. Malar J 2021;20:353. https://doi.org/10.1186/s12936-021-03885-x

Original Article

Parasites Hosts Dis 2026;64(3):248-259
https://doi.org/10.3347/PHD.26028

Parasites, Hosts and Diseases

pISSN 2982-5164 • eISSN 2982-6799

Tick-borne bacterial pathogens in wildlife and their parasitizing ticks in Korea: A molecular epidemiological study

You-Jeong Lee[1], Beoul Kim[1], Yong Sun Hyun[2], Jae Woong Heo[2], Hyo-Min Woo[1], Jae-Woo Choi[1], Insu Choi[1], Yong-Myung Kang[1], Man Hee Rhee[1], Dongmi Kwak[1], Kyoo-Tae Kim[1,*], Min-Goo Seo[1,*]

[1]College of Veterinary Medicine & Institute for Veterinary Biomedical Science, Kyungpook National University, Daegu, Korea; [2]Jeonnam Wildlife and Management Center, Suncheon, Korea

Ticks are important vectors of numerous zoonotic pathogens, yet integrated molecular surveillance of wildlife hosts and their parasitizing ticks remains limited in Korea. In this study, we investigated the occurrence of major tick-borne bacterial pathogens in wildlife and their associated ticks. Blood samples were collected from Korean water deer (*Hydropotes inermis*), raccoon dogs (*Nyctereutes procyonoides*), and wild boars (*Sus scrofa*), and a total of 246 ticks were obtained from these 34 animals. Molecular analyses identified multiple bacterial pathogens, including *Anaplasma phagocytophilum*, *Ehrlichia canis*, *Bartonella schoenbuchensis*, *Rickettsia raoultii*, *Rickettsia monacensis*, and *Candidatus* Rickettsia longicornii. Notably, *E. canis* was detected for the first time in blood samples from raccoon dogs and wild boars in Korea, and *B. schoenbuchensis* was identified in ticks for the first time in the country. In addition, *R. monacensis* exhibited a remarkably high minimum infection rate in *Ixodes nipponensis*, and all positive ticks were collected from raccoon dogs. Strikingly, *Ca*. R. longicornii was detected at a very high prevalence (94.1%) in wildlife blood samples, suggesting extensive circulation among wildlife hosts in the study area. These findings indicate that wildlife and their parasitic ticks may serve as important reservoirs of diverse tick-borne bacteria in Korea and highlight the importance of continuous molecular surveillance within a One Health framework.

Keywords: Tick-borne diseases, ticks, wildlife, One Health

Introduction

Ticks are hematophagous ectoparasites that parasitize a wide range of vertebrate hosts and serve as important vectors for numerous zoonotic pathogens. The transmission of tick-borne pathogens is influenced not only by complex interactions among vectors, pathogens, and hosts, but also by environmental and ecological factors as well as human behavior [1]. Rickettsial diseases are caused by obligate intracellular bacteria transmitted by arthropod vectors and have re-emerged as significant threats to both human and animal health worldwide. Bacteria belonging to the order Rickettsiales, including *Anaplasma*, *Ehrlichia*, and *Rickettsia*, are transmitted to humans, livestock, companion animals, and wildlife through the bites of infected ticks [2].

Anaplasma phagocytophilum, the causative agent of human granulocytic anaplasmosis, has been detected in various tick species in Korea [3]. Ehrlichiosis is also recognized as an emerging tick-borne zoonotic disease of clinical significance in both humans and animals. Most human cases are caused by *Ehrlichia chaffeensis*, which primarily infects monocytes [4]. *Rickettsia* species, particularly those belonging to the spotted fever group,

Received: March 18, 2026 Accepted: June 2, 2026
*Correspondence: ktk, kyootae@knu.ac.kr; mgs, koreasmg@knu.ac.kr

Citation
Lee YJ, Kim B, Hyun YS, Heo JW, Woo HM, Choi JW, Choi I, Kang YM, Rhee MH, Kwak D, Kim KT, Seo MG. Tick-borne bacterial pathogens in wildlife and their parasitizing ticks in Korea: A molecular epidemiological study. Parasites Hosts Dis 2026;64(3):248-259.

are of growing public health concern as tick-borne rickettsioses continue to emerge and re-emerge worldwide [5]. Among tick-associated rickettsiae, *Candidatus* Rickettsia longicornii has recently attracted attention as a potential emerging pathogen detected in *Haemaphysalis longicornis* ticks in East Asia [6]. Although several molecular studies have reported its presence in ticks, information regarding its occurrence in wildlife hosts and its ecological circulation between ticks and wildlife remains limited. In Korea, several rickettsial pathogens have been identified in both ticks and animals. In ticks, *A. phagocytophilum* [3,7] *Rickettsia raoultii* [6,8], *Rickettsia monacensis* [8,9], *Candidatus* Rickettsia longicornii [6] and *Ehrlichia canis* [6,8] have been detected, whereas in animals *A. phagocytophilum* [10,11], *E. canis* [12], *Candidatus* Rickettsia longicornii [11], and *Bartonella schoenbuchensis* [13] have been reported.

Although several studies in Korea have investigated tick-borne pathogens, most have focused on domestic animals or single wildlife species. Integrated research that simultaneously examines wildlife hosts and their parasitic ticks remains limited. Wildlife plays a crucial role in maintaining zoonotic pathogens, and habitats located near agricultural areas and human settlements provide important ecological settings for the transmission of tick-borne infections.

In this study, we conducted molecular surveillance to detect major bacterial pathogens transmitted by ticks, including *Anaplasma*, *Ehrlichia*, *Bartonella*, and *Rickettsia*, in Korean water deer (*Hydropotes inermis*), raccoon dogs (*Nyctereutes procyonoides*), and wild boars (*Sus scrofa*), as well as in ticks collected from these hosts. The findings of this study provide insights into the distribution patterns and ecological roles of these pathogens within wildlife–tick interfaces and offer baseline data for developing future One Health-based strategies for the control of zoonotic tick-borne diseases.

Methods

Ethical approval

All experimental procedures involving animals were approved by the Institutional Animal Care and Use Committee of Kyungpook National University (approval No. KNU-2024-0407). Tick samples were collected from wild animals captured by the Jeonnam Wildlife Management Center as part of routine wildlife management activities. Ticks were removed from the animals during routine handling procedures performed by wildlife management personnel. All procedures were conducted in accordance with institutional ethical guidelines, and no additional animal handling was required for this study. No endangered or protected species were included in this study.

Tick collection and species identification

From July to November 2024, ticks and blood samples were collected from wild animals in Jeonnam province, Korea, as part of a wildlife health surveillance program. A total of 34 wild animals captured during routine wildlife management activities were included for blood sampling, including 16 Korean water deer, 7 raccoon dogs, and 11 wild boars. A total of 246 ticks were collected: 33 from Korean water deer, 113 from raccoon dogs, and 100 from wild boars. All ticks were collected while attached to host animals at the time of sampling, indicating active or recent feeding. Ticks at different feeding stages, including partially fed and fully engorged individuals, were included in the analysis.

For molecular analysis, the collected ticks were grouped into 186 pools based on host individual, tick species, developmental stage (larva, nymph, and adult), and sex (for adult ticks). Only ticks sharing identical characteristics were grouped into the same pool to ensure biological homogeneity and to minimize potential bias in pathogen detection. Tick species were initially identified based on morphological characteristics using previously described taxonomic keys [14]. Species identification was further confirmed by molecular analysis. Molecular identification of ticks was performed by PCR amplification of the mitochondrial cytochrome c oxidase subunit I (*cox1*) gene using previously described primers [15]. All samples were stored at -70°C until genomic DNA extraction.

DNA extraction and molecular detection

Genomic DNA from tick samples and blood samples from wild animals was extracted using the Biniprep Pathogen DNA/RNA Kit (InvirusTech) according to the manufacturer's instructions. *Anaplasma* spp., *Ehrlichia* spp., and *Rickettsia* spp. were detected using the AccuPower Rickettsiales 3-Plex PCR Kit (Bioneer), which targets the 16S rRNA gene. The exact primer sequences are proprietary information of the manufacturer. *Bartonella* spp. [16] were detected using commercially available primers obtained from Thermo Fisher Scientific targeting the 23S rRNA gene. PCR amplification was performed using the AccuPower PCR Premix Kit (Bioneer).

DNA sequencing and phylogenetic analysis

Positive PCR products were sequenced by a commercial sequencing service (Macrogen) using the same primers employed for PCR amplification. The obtained sequences were compared with reference nucleotide sequences available in the GenBank database using the BLASTn algorithm for species

identification. Multiple sequence alignments were performed using CLUSTAL Omega version 1.2.1 and manually edited using BioEdit version 7.2.5. Phylogenetic analyses were performed using MEGA software version 6.0 based on the maximum likelihood method with the Kimura 2-parameter model. The reliability of phylogenetic groupings was evaluated using 1,000 bootstrap replicates.

Statistical analysis

Statistical analyses were performed using GraphPad Prism version 5.04 (GraphPad Software). Differences in pathogen prevalence among animal species were assessed using the chi-square test. A P-value of <0.05 was considered statistically significant. Ninety-five percent confidence intervals (95% CI) were calculated for prevalence estimates.

Results

Identification of tick species and tick counts per animal species

A total of 246 ticks were collected from wild animals and grouped into 186 pools for molecular analysis. Three tick species were identified: *Amblyomma testudinarium* (100 ticks, 100 pools), *H. longicornis* (129 ticks, 69 pools), and *Ixodes nipponensis* (17 ticks, 17 pools) (Table 1). *A. testudinarium* ($n=100$) was collected exclusively from wild boars. *H. longicornis* was collected from Korean water deer ($n=33$ ticks) and raccoon dogs ($n=96$ ticks), whereas *I. nipponensis* ($n=17$) was detected only on raccoon dogs. Among the 186 tick pools, 169 were adult pools, 9 were nymph pools, and 8 were larval pools.

The prevalence of tick-borne pathogens by tick species

The overall positivity rates for *A. phagocytophilum*, *B. schoenbuchensis*, *E. canis*, *R. raoultii*, and *R. monacensis* were 8.1% (15/186 pools), 5.4% (10/186 pools), 34.9% (65/186 pools), 91.4% (170/186 pools), and 8.6% (16/186 pools), respectively (Table 1). The corresponding minimum infection rates (MIRs) were 6.1% (15/246), 4.1% (10/246), 26.4% (65/246), 69.1% (170/246), and 6.5% (16/246), respectively. The detection results by tick species were as follows: in *A. testudinarium*, *B. schoenbuchensis* was detected in 1.0% of pools (1/100; 95% CI, 0–3.0), *E. canis* in 55.0% (55/100; 95% CI, 45.2–64.8), and *R. raoultii* in 100% (100/100). *A. phagocytophilum* and *R. monacensis* were not detected. In *H. longicornis*, *A. phagocytophilum* was detected in 2.9% of pools (2/69; 95% CI, 0–6.9), *E. canis* in 8.7% (6/69; 95% CI, 2–15.3), and *R. raoultii* in 100% (69/69). *B.*

Table 1. Molecular detection of tick-borne pathogens in ticks collected from wild animals in Korea

Species	Stage	Tested ticks (pool)	No. positive tick pool/tick pool tested (minimum infection rate[a])																			
			Korean water deer					Raccoon dog					Wild boar					Total				
			A.p	B.s	E.c	R.r	R.m	A.p	B.s	E.c	R.r	R.m	A.p	B.s	E.c	R.r	R.m	A.p	B.s	E.c	R.r	R.m
Amblyomma testudinarium	Adult male	61 (61)	-	-	-	-	-	-	-	-	-	-	0/61	1/61	37/61	61/61	0/61	0/61	1/61 (1.6)	37/61 (60.7)	61/61 (100)	0/61
	Adult female	39 (39)	-	-	-	-	-	-	-	-	-	-	0/39	0/39	18/39	39/39	0/39	0/39	0/39	18/39 (46.2)	39/39 (100)	0/39
	Subtotal	100 (100)	-	-	-	-	-	-	-	-	-	-	0/100	1/100	55/100	100/100	0/100	0/100	1/100 (1.0)	55/100 (55.0)	100/100 (100)	0/100
Haemaphysalis longicornis	Adult male	22 (10)	0/5	0/5	3/5	5/5	0/5	0/5	0/5	0/5	5/5	0/5	-	-	-	-	-	0/10	0/10	3/10 (13.6)	10/10 (45.5)	0/10
	Adult female	62 (42)	2/12	0/12	1/12	12/12	0/12	0/30	0/30	0/30	30/30	0/30	-	-	-	-	-	2/42 (3.2)	0/42	1/42 (1.6)	42/42 (67.7)	0/42
	Nymph	24 (9)	0/3	0/3	2/3	3/3	0/3	0/6	0/6	0/6	6/6	0/6	-	-	-	-	-	0/9	0/9	2/9 (8.3)	9/9 (37.5)	0/9
	Larva	21 (8)	0/1	0/1	0/1	1/1	0/1	0/7	0/7	0/7	7/7	0/7	-	-	-	-	-	0/8	0/8	0/8	8/8 (38.1)	0/8
	Subtotal	129 (69)	2/21	0/21	6/21	21/21	0/21	0/48	0/48	0/48	48/48	0/48	-	-	-	-	-	2/69 (1.6)	0/69	6/69 (4.7)	69/69 (53.5)	0/69
Ixodes nipponensis	Adult male	2 (2)	-	-	-	-	-	1/2	0/2	0/2	0/2	2/2	-	-	-	-	-	1/2 (50.0)	0/2	0/2	0/2	2/2 (100)
	Adult female	15 (15)	-	-	-	-	-	12/15	9/15	4/15	1/15	14/15	-	-	-	-	-	12/15 (80.0)	9/15 (60.0)	4/15 (26.7)	1/15 (6.7)	14/15 (93.3)
	Subtotal	17 (17)	-	-	-	-	-	13/17	9/17	4/17	1/17	16/17	-	-	-	-	-	13/17 (76.5)	9/17 (52.9)	4/17 (23.5)	1/17 (5.9)	16/17 (94.1)
Total		246 (186)	2/21 (0.8)	0/21	6/21 (2.4)	21/21 (8.5)	0/21	13/61 (5.3)	9/61 (3.7)	4/61 (1.6)	49/61 (19.9)	16/61 (6.5)	0/100	1/100 (0.4)	55/100 (22.4)	100/100 (40.7)	0/100	15/186 (6.1)	10/186 (4.1)	65/186 (26.4)	170/186 (69.1)	16/186 (6.5)

A.p, *Anaplasma phagocytophilum*; B.s, *Bartonella schoenbuchensis*; E.c, *Ehrlichia canis*; R.r, *Rickettsia raoultii*; R.m, *Rickettsia monacensis*; -, not applicable.
[a]Calculated as the number of positive tick pools divided by the total number of ticks tested, multiplied by 100.

https://doi.org/10.3347/PHD.26028

schoenbuchensis and *R. monacensis* were not detected. In *I. nipponensis*, *A. phagocytophilum* was detected in 76.5% of pools (13/17; 95% CI, 56.3–96.6), *B. schoenbuchensis* in 52.9% (9/17; 95% CI, 29.2–76.7), *E. canis* in 23.5% (4/17; 95% CI, 3.4–43.7), *R. raoultii* in 5.9% (1/17; 95% CI, 0–17.1), and *R. monacensis* in 94.1% (16/17; 95% CI, 82.9–100).

Based on MIR calculations, *B. schoenbuchensis*, *E. canis*, and *R. raoultii* showed MIRs of 1.0%, 55.0%, and 100%, respectively, in *A. testudinarium*. In *H. longicornis*, the MIRs were 1.6% for *A. phagocytophilum*, 4.7% for *E. canis*, and 53.5% for *R. raoultii*. In *I. nipponensis*, MIRs were 76.5% for *A. phagocytophilum*, 52.9% for *B. schoenbuchensis*, 23.5% for *E. canis*, 5.9% for *R. raoultii*, and 94.1% for *R. monacensis*.

The prevalence of tick-borne pathogens in blood samples by animal species

Blood samples were collected from a total of 34 wild animals, including 16 Korean water deer, 7 raccoon dogs, and 11 wild boars (Table 2). In Korean water deer, the following pathogens were detected: *A. phagocytophilum* in 75.0% of samples (12/16; 95% CI, 53.8–96.2), *B. schoenbuchensis* in 6.3% (1/16; 95% CI, 0–18.1), *E. canis* in 12.5% (2/16; 95% CI, 0–28.7), and *Ca*. Rickettsia longicornii in 87.5% (14/16; 95% CI, 71.3–100). In raccoon dogs, *E. canis* was detected in 28.6% of samples (2/7; 95% CI, 0–62.0), and *Ca*. R. longicornii was detected in all samples (100%, 7/7). *A. phagocytophilum* and *B. schoenbuchensis* were not detected in this species. In wild boars, *E. canis* was detected in 9.1% of samples (1/11; 95% CI, 0–26.1), and *Ca*. R. longicornii was detected in all samples (100%, 11/11). No positive results were observed for *A. phagocytophilum* or *B. schoenbuchensis* in wild boars. Across all sampled animals, *Ca*. R. longicornii showed the highest overall prevalence (94.1%, 32/34). A significantly higher prevalence of *A. phagocytophilum* was observed in Korean water deer compared with other animal species ($P<0.0001$).

Molecular and phylogenetic analyses

Two *cox1* sequences of *H. longicornis* obtained in this study were identical (100% sequence identity) (Fig. 1) and showed 98.8%–100% identity with reference sequences retrieved from the GenBank database. These reference sequences corresponded to the same gene and species and were selected based on high similarity identified through BLAST analysis. Similarly, 2 *cox1* sequences of *I. nipponensis* were identical to each other and shared 99.2%–99.7% identity with corresponding GenBank sequences. Four *cox1* sequences of *A. testudinarium* also showed complete identity (100%) among themselves and exhibited 99.7%–100% identity when compared with reference sequences in GenBank. All *cox1* sequences generated in this study were deposited in GenBank under accession numbers PX389923–PX389930.

Phylogenetic analysis of 5 samples based on the 16S rRNA gene confirmed their classification as *A. phagocytophilum* in both wildlife hosts and ticks (Fig. 2). These sequences shared 98.8%–100% identity among themselves and showed 98.8%–100% identity with previously reported *A. phagocytophilum* isolates in GenBank. The sequences obtained in this study were deposited in GenBank under accession numbers PX279206–PX279210.

Phylogenetic analysis of the 23S rRNA gene sequences identified 2 samples as *B. schoenbuchensis* (Fig. 3). These sequences showed 99.6%–100% identity to each other and 98.1%–100% identity with previously reported *B. schoenbuchensis* isolates in GenBank. The sequences were deposited under accession numbers PX280588–PX280589.

Similarly, phylogenetic analysis of the 16S rRNA gene sequences classified 2 samples as *E. canis* (Fig. 4). These sequences shared 99.7%–100% identity with each other and with previously reported *E. canis* isolates in GenBank. The sequences obtained in this study were deposited under accession numbers PX279204–PX279205.

Phylogenetic analysis of the 16S rRNA gene sequences of Rickettsia revealed 3 sequences belonging to *R. raoultii*, eleven sequences belonging to *Ca*. Rickettsia longicornii, and one sequence belonging to *R. monacensis* (Fig. 5). The *R. raoultii* sequences shared 100% identity with each other and showed

Table 2. Prevalence of tick-borne pathogens detected in blood samples of wild animals

Animal species	No. tested	Positive samples, No. (%)				
		Anaplasma phagocytophilum	*Bartonella schoenbuchensis*	*Ehrlichia canis*	*Candidatus* Rickettsia longicornii	Total
Korean water deer	16	12 (75.0)[a]	1 (6.3)	2 (12.5)	14 (87.5)	16 (100)
Raccoon dog	7	0	0	2 (28.6)	7 (100)	7 (100)
Wild boar	11	0	0	1 (9.1)	11 (100)	11 (100)
Total	34	12 (35.3)	1 (2.9)	5 (14.7)	32 (94.1)	34 (100)

[a]Statistically significant difference compared with other animal species ($P<0.05$).

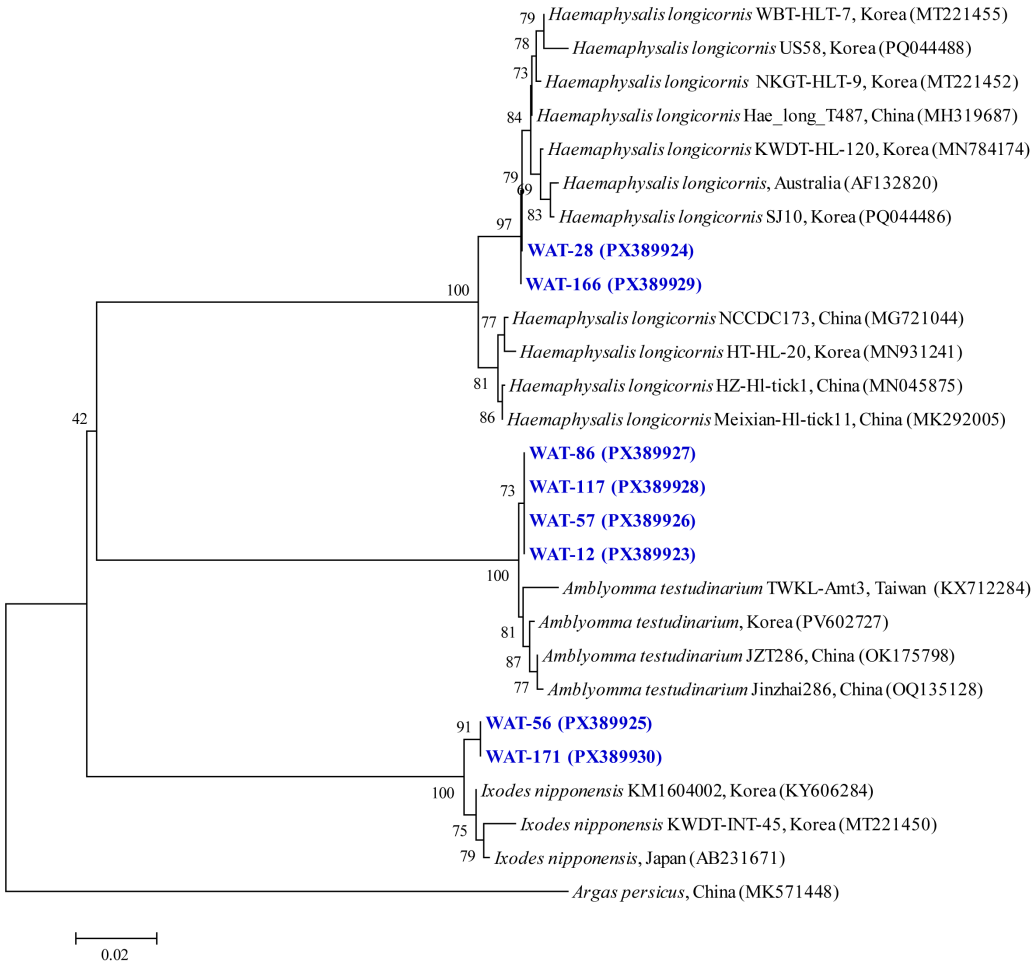

Fig. 1. Phylogenetic tree of tick species based on mitochondrial cytochrome c oxidase subunit I sequences constructed using the maximum likelihood method. Sequences obtained in this study are highlighted in blue. GenBank accession numbers and collection countries are shown for reference sequences. *Argas persicus* was used as the outgroup. Bootstrap values based on 1,000 replicates are indicated at the nodes, and the scale bar represents genetic distance.

99.6%–100% identity with reference sequences in GenBank. The *Ca*. R. longicornii sequences shared 99.6%–100% identity among themselves and with previously reported isolates. The *R. monacensis* sequence showed 100% identity with previously reported sequences.

These sequences were deposited in GenBank under accession numbers PX279455–PX279457 (*R. raoultii*), PX279444–PX279454 (*Ca*. R. longicornii), and PX279458 (*R. monacensis*).

Comparison of pathogen detection between host blood and attached ticks in paired samples

Paired samples consisting of host blood and corresponding attached ticks were analyzed to evaluate host-tick associations. A total of 8 host individuals had paired samples (8 blood samples and 105 tick pools), allowing direct comparison between host blood and parasitizing ticks. In contrast, 26 of 34 host samples and 81 of 186 tick pools were not paired, limiting individual-level comparisons. Among the paired samples, simultaneous detection of identical pathogens in both host blood and attached ticks was observed in 2 Korean water deer individuals (Korean water deer #1 and #2) (Table 3). In these cases, *A. phagocytophilum* and *E. canis* were detected in both host blood and corresponding tick pools. In contrast, in the remaining 6 host individuals, although several pathogens were detected either in tick pools or in host blood, no matched detection was observed. Notably, *R. raoultii* showed high positivity in tick pools across most hosts, whereas it was not detected in the corresponding host blood samples. Conversely, *Ca*. Rickettsia longicornii was consistently detected in host blood samples but was not identified in the attached ticks.

Sequence comparison revealed high nucleotide identity between host- and tick-derived sequences, ranging from 98.8% to 100% for *A. phagocytophilum* and 99.7% for *E. canis*.

https://doi.org/10.3347/PHD.26028

Fig. 2. Phylogenetic tree of *Anaplasma* species based on 16S rRNA gene sequences constructed using the maximum likelihood method. Sequences obtained in this study are labeled as "WB" (wildlife blood) and "WAT" (wildlife-attached ticks) to indicate their origin and are highlighted in blue. GenBank accession numbers are provided for reference sequences. *Rickettsia raoultii* was used as the outgroup. Bootstrap values (1,000 replicates) are shown at the nodes, and the scale bar represents genetic distance.

In addition, phylogenetic analysis showed that sequences obtained from host blood and ticks clustered closely together, indicating high genetic similarity.

Discussion

In this study, ticks and blood samples collected from wildlife in Korea were analyzed to investigate the distribution of major tick-borne bacterial pathogens, including *Anaplasma*, *Ehrlichia*, *Bartonella*, and *Rickettsia* species. The wildlife examined included Korean water deer, raccoon dogs, and wild boars. A total of 246 ticks were collected, comprising 129 *H. longicornis*, 100 *A. testudinarium*, and 17 *I. nipponensis*.

Among the 3 tick species identified, *A. testudinarium* is primarily distributed in the southern regions of Korea, whereas reports from other regions remain relatively limited [17]. Because all samples in this study were collected in Jeonnam Province, the regional distribution of this tick species may have contributed to its detection. In addition, *A. testudinarium* was found exclusively in wild boars in this study, which is consistent with previous reports indicating that this species commonly infests large wild mammals such as wild boars [18]. Wild boars frequently move between forested areas and agricultural lands, increasing opportunities for contact with diverse tick species. Such ecological characteristics likely influence the host association patterns of *A. testudinarium*.

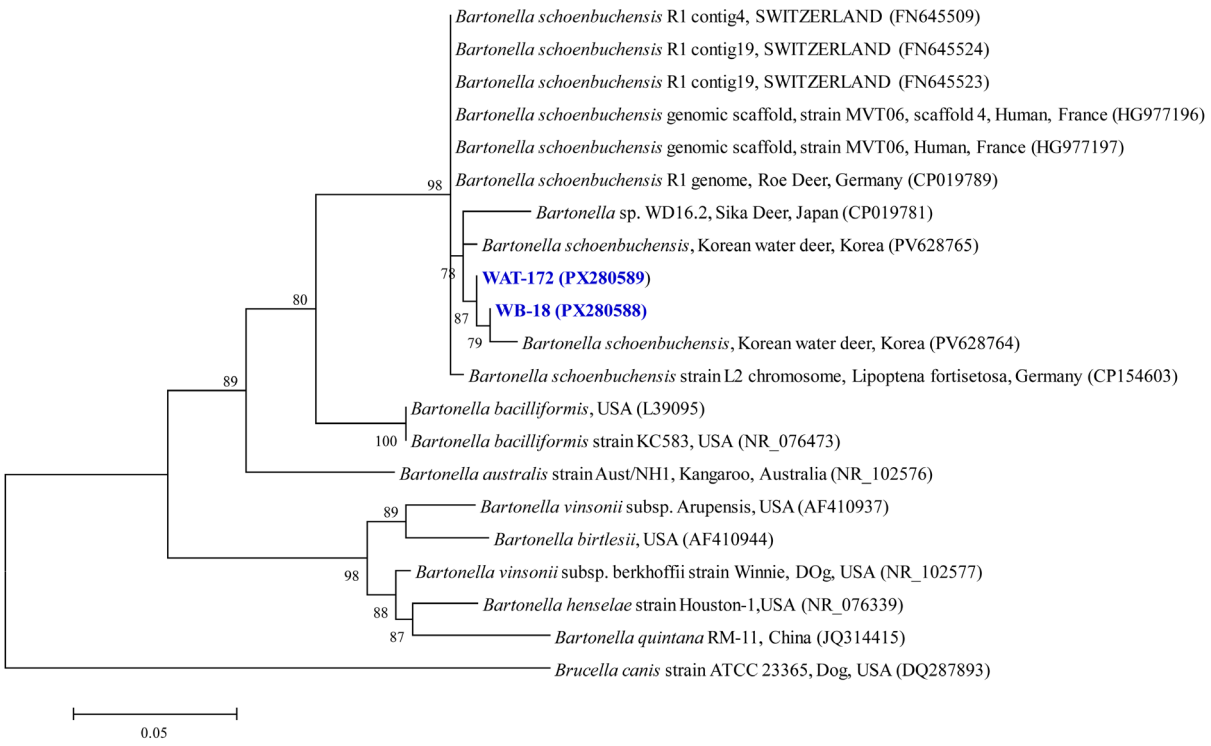

Fig. 3. Phylogenetic tree of *Bartonella* species based on 23S rRNA gene sequences constructed using the maximum likelihood method. Sequences obtained in this study are labeled as "WB" (wildlife blood) and "WAT" (wildlife-attached ticks) to indicate their origin and are highlighted in blue. GenBank accession numbers are indicated for reference sequences. *Brucella canis* was used as the outgroup. Bootstrap values (1,000 replicates) are shown at the nodes, and the scale bar represents genetic distance.

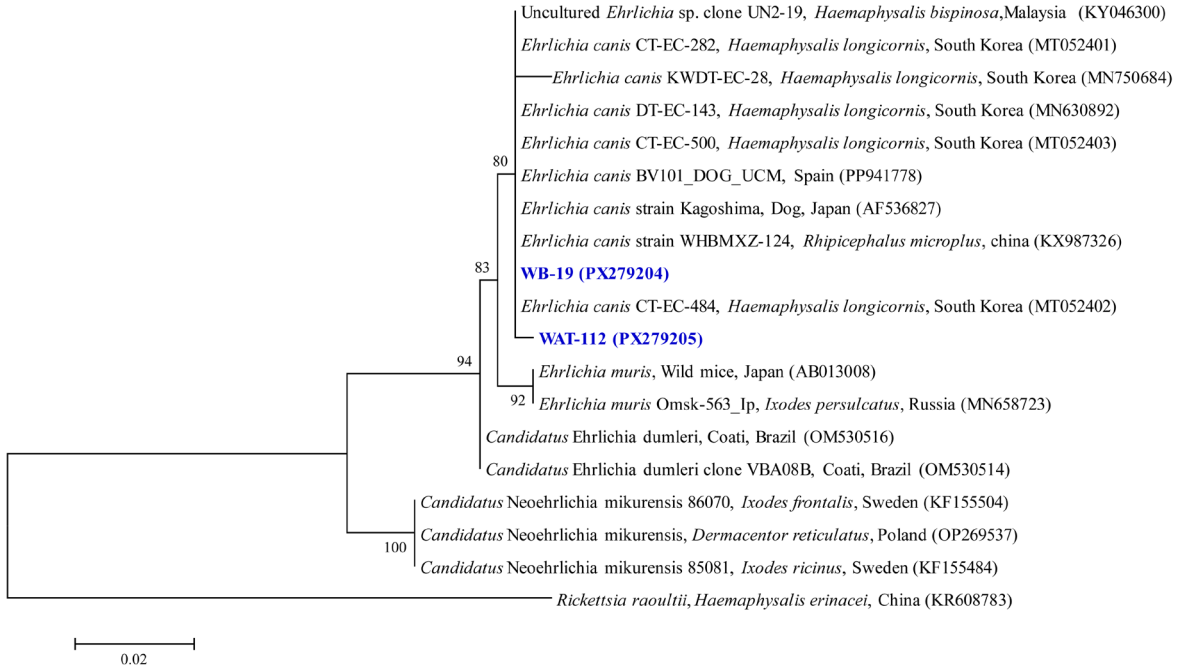

Fig. 4. Phylogenetic tree of *Ehrlichia* species based on 16S rRNA gene sequences constructed using the maximum likelihood method. Sequences obtained in this study are labeled as "WB" (wildlife blood) and "WAT" (wildlife-attached ticks) to indicate their origin and are highlighted in blue. GenBank accession numbers are indicated for reference sequences. *Rickettsia raoultii* was used as the outgroup. Bootstrap values (1,000 replicates) are shown at the nodes, and the scale bar represents genetic distance.

https://doi.org/10.3347/PHD.26028

Fig. 5. Phylogenetic tree of *Rickettsia* species based on 16S rRNA gene sequences constructed using the maximum likelihood method. Sequences obtained in this study are labeled as "WB" (wildlife blood) and "WAT" (wildlife-attached ticks) to indicate their origin and are highlighted in blue. GenBank accession numbers are indicated for reference sequences. *Anaplasma phagocytophilum* was used as the outgroup. Bootstrap values (1,000 replicates) are shown at the nodes, and the scale bar represents genetic distance.

Table 3. Detection of tick-borne pathogens in paired host blood and attached ticks from the same individuals

Host ID	No. positive tick pools/total tick pools					No. positive host blood				Matched detection[a]
	A.p	B.s	E.c	R.r	R.m	A.p	B.s	E.c	Ca.R.l	
Wild boar #1	0/27	1/27	0/27	27/27	0/27	0	0	0	1	No
Raccoon dog #1	0/21	0/21	0/21	21/21	0/21	0	0	0	1	No
Raccoon dog #2	0/8	0/8	0/8	8/8	0/8	0	0	0	1	No
Wild boar #2	0/20	0/20	17/20	20/20	0/20	0	0	0	1	No
Korean water deer #1	0/5	0/5	2/5	5/5	0/5	1	0	1	1	Yes
Raccoon dog #3	0/5	0/5	0/5	5/5	0/5	0	0	1	1	No
Raccoon dog #4	0/7	0/7	0/7	7/7	0/7	0	0	0	1	No
Korean water deer #2	2/12	0/12	1/12	12/12	2/12	1	0	1	1	Yes

A.p, *Anaplasma phagocytophilum*; B.s, *Bartonella schoenbuchensis*; E.c, *Ehrlichia canis*; R.r, *Rickettsia raoultii*; R.m, *Rickettsia monacensis*; Ca.R.l, *Candidatus* Rickettsia longicornii.

[a]Indicates simultaneous detection of the same pathogen in both host blood and attached ticks from the same individual.

I. nipponensis showed the highest prevalence of *R. monacensis*, which is consistent with previous studies identifying this species as a primary vector of *R. monacensis* [9]. Notably, all *R. monacensis*–positive specimens in this study were detected exclusively in ticks collected from raccoon dogs, representing the first report of this pathogen associated with raccoon dogs in Korea, to our knowledge. This finding emphasizes the importance of region-specific surveillance considering host ecology and tick–pathogen interactions.

H. longicornis is the most commonly encountered tick species in Korea and is widely recognized as an important vector of multiple pathogens affecting both humans and animals [18,19]. This species is known to transmit a wide range of pathogens, such as *Rickettsia*, *Anaplasma*, *Borrelia*, *Babesia*, *Bartonella*, *Coxiella*, and severe fever with thrombocytopenia syndrome virus [20]. Consistent with previous studies, *H. longicornis* was the predominant tick species identified in this study [21]. Therefore, *H. longicornis* may function as a key vector linking diverse hosts and pathogens, potentially increasing the risk of pathogen transmission among humans, livestock, and wildlife. These findings highlight the importance of continuous surveillance of tick-borne pathogens from a One Health perspective.

In Korea, *A. phagocytophilum*—the etiological agent of human granulocytic anaplasmosis—has been detected across diverse tick species [3]. In the present study, *A. phagocytophilum* were detected only in *H. longicornis* and *I. nipponensis* ticks, with *I. nipponensis* showing the highest prevalence. These findings are consistent with previous studies conducted in Korea [22]. The overall MIR of *A. phagocytophilum* in ticks in this study was 6.1%. Similarly, a previous study in Korea reported a positivity rate of 24.5% (89/363) based on the MIR in ticks collected from Korean water deer carcasses [7]. The detection of *A. phagocytophilum* in ticks associated with wildlife suggests that these hosts may play an important role in maintaining the natural enzootic cycle of tick-borne pathogens. In addition, the prevalence of *A. phagocytophilum* in blood samples from Korean water deer reached 75.0% in the present study. Previous investigations have also reported *A. phagocytophilum* in Korean water deer [10,23,24]. Taken together, these findings suggest that Korean water deer may act as important reservoir hosts of *A. phagocytophilum* in the Republic of Korea, providing valuable evidence for assessing the risk of tick-borne zoonoses and for developing effective control strategies.

Bacteria of the genus *Bartonella* are Gram-negative organisms that parasitize erythrocytes and endothelial cells, among which *B. schoenbuchensis* has been identified as a pathogen with zoonotic potential [25]. This bacterium has been detected in various wildlife hosts, including European roe deer (*Capreolus capreolus*) in Germany [26], and in larvae of the ectoparasitic deer ked *Lipoptena cervi* collected from red deer (*Cervus elaphus*) [27]. In the present study, the MIR of *B. schoenbuchensis* was 1.0% in *A. testudinarium* and 52.9% in *I. nipponensis*, with an overall MIR of 5.4%. In addition, *B. schoenbuchensis* was detected in 6.3% of blood samples from Korean water deer. To date, no studies have reported the detection of this pathogen in ticks in Korea. However, a previous study reported a detection rate of 12.9% in Korean water deer collected between 2008 and 2009 [28], and another study identified *B. schoenbuchensis* with a prevalence of 6.8% (13/192) in Korean water deer [16]. This study therefore provides the first evidence of *B. schoenbuchensis* detection in ticks in Korea, highlighting the potential role of ticks as vectors of this pathogen. These findings highlight the need for comprehensive molecular epidemiological studies and long-term surveillance incorporating broader geographic coverage, diverse host species, and seasonal factors to clarify the transmission ecology and assess the public health risks associated with *B. schoenbuchensis*.

E. canis is the causative agent of canine monocytic ehrlichiosis [29]. In the present study, *E. canis* was detected in ticks collected from wild animals. Based on MIR values, the positivity rates were 2.4% in Korean water deer, 1.6% in raccoon dogs, and 22.4% in wild boars, with an overall MIR of 26.4%. In animal blood samples, the prevalence was 12.5% in Korean water deer, 28.6% in raccoon dogs, and 9.1% in wild boars, with an overall prevalence of 14.7%. A previous study conducted in Korea reported *E. canis* positivity in 20% (2/10) of Korean water deer [23], whereas another investigation reported a prevalence of 0.5% (1/192) in Korean water deer [16]. However, previous studies conducted in Korea did not detect *E. canis* in blood samples from raccoon dogs [30] or wild boars [13]. In the present study, *E. canis* was detected in blood samples from raccoon dogs and wild boars for the first time in Korea. Furthermore, the infections detected in Korean water deer indicate that the pathogen may circulate not only through tick-mediated transmission but also within wildlife host populations. Therefore, further studies are required to identify the specific tick species involved in the transmission of *E. canis*. Broader epidemiological investigations involving wildlife hosts and their associated ticks will be essential to clarify the ecological dynamics of this zoonotic pathogen and to assess its potential public health significance.

Rickettsia species, particularly those belonging to the spot-

https://doi.org/10.3347/PHD.26028

ted fever group, have become an important public health concern as tick-borne rickettsioses continue to occur and re-emerge worldwide [5]. In Korea, *R. raoultii* was identified in 40.9% of ticks collected from dogs between 2010 and 2015 [8]. In addition, a study conducted in Korea in 2021 reported the detection of *R. raoultii* in 20% of ticks collected from Korean water deer [6]. Similarly, in the present study, this pathogen was detected in all 3 tick species. These findings suggest that *R. raoultii* may circulate among wildlife hosts and ticks in Korea. Because *R. raoultii* is a zoonotic pathogen capable of causing human disease, continuous molecular epidemiological surveillance is required to assess the potential risk of human infection and to establish appropriate public health response strategies.

R. monacensis is widely distributed across Europe, Asia, and Africa and is mainly transmitted by *Ixodes* spp. [31]. In Korea, a study conducted between 2005 and 2006 reported the detection of *R. monacensis* in *I. nipponensis* collected from small mammals [9,32]. More recently, a domestic study conducted in 2024 also reported a high detection rate of *R. monacensis* in *I. nipponensis* [33]. Similarly, in the present study, *I. nipponensis* was the only tick species in which the pathogen was detected, with a MIR of 94.1%. Notably, *R. monacensis* has also been isolated directly from human patient blood samples in Korea, highlighting its importance as a zoonotic pathogen [34]. The high detection rate of *R. monacensis* in *I. nipponensis* observed in this study suggests that this pathogen is maintained within local tick populations. These findings highlight the need for continuous surveillance to assess the potential risk of infection in both humans and animals.

Candidatus Rickettsia longicornii has been identified in *H. longicornis* in East Asia and is increasingly recognized as an emerging tick-borne pathogen [6]. Most previous studies in Korea have focused on the detection of *Ca*. R. longicornii in ticks. For example, this pathogen was detected at prevalences of 21.5% in ticks in 2021 [35], and 31% in ticks collected from Korean water deer between 2013 and 2017 [6]. In contrast, information on the occurrence of *Ca*. R. longicornii in animal blood samples remains limited. A recent study reported the detection of this pathogen in only 0.2% (2/906) of dog blood samples in Korea [11]. In the present study, however, *Ca*. R. longicornii was detected in 94.1% of wildlife blood samples, including Korean water deer, raccoon dogs, and wild boars, representing an unexpectedly high prevalence. Interestingly, *Ca*. R. longicornii was not detected in tick samples in the present study. This discrepancy between animal blood and tick samples may be related to several ecological factors, including transient bacteremia in wildlife hosts, host-associated circulation of the pathogen, or limitations in tick sample size. It is also possible that certain wildlife species may act as reservoir hosts, maintaining the pathogen within local ecosystems even when detection in ticks is relatively low. Taken together, these findings suggest that *Ca*. R. longicornii may circulate widely among wildlife hosts in Korea and may represent an under-recognized component of the local tick–wildlife transmission cycle. Future studies should expand molecular epidemiological surveillance using multilocus genetic markers such as *gltA*, *ompA*/*ompB*, and *sca4* to better clarify the transmission dynamics and potential zoonotic risk of this pathogen from a One Health perspective.

To investigate the association between pathogens in wildlife hosts and their parasitizing ticks, paired samples were analyzed at the individual level. Among 8 host individuals with paired samples, simultaneous detection of identical pathogens in both host blood and attached ticks was observed in only 2 Korean water deer individuals. In these cases, *A. phagocytophilum* and *E. canis* were detected in both host blood and tick pools, suggesting potential host–tick sharing of these pathogens. However, for the majority of hosts, no matched detection was observed. Notably, *R. raoultii* was widely detected in tick pools but was not identified in the corresponding host blood samples, whereas *Ca*. Rickettsia longicornii was consistently detected in host blood but not in attached ticks. These contrasting patterns may reflect differences in pathogen transmission dynamics, host specificity, or temporal variation in infection status. Overall, these findings suggest that direct concordance between host infection and tick infection is not consistently observed at the individual level. Although the matched cases provide limited molecular evidence supporting potential host–tick pathogen sharing, the low number of such cases and the use of pooled tick samples warrant cautious interpretation. Further studies based on larger sample sizes and individual-level analyses of both ticks and hosts are required to better elucidate transmission dynamics within wildlife–tick systems.

This study provides a molecular epidemiological overview of multiple tick-borne bacterial pathogens in wildlife and their associated ticks in Korea. *H. longicornis* was identified as the predominant tick species, and several pathogens—including *Anaplasma*, *Ehrlichia*, *Bartonella*, and *Rickettsia*—were detected in Korean water deer, raccoon dogs, and wild boars. Notably, some pathogens were identified for the first time in wildlife or ticks in Korea, highlighting previously unrecognized transmission dynamics within the wildlife-tick inter-

face. These findings suggest that wildlife may serve as important reservoirs of tick-borne pathogens and may contribute to the maintenance of zoonotic cycles in natural ecosystems. Continued molecular surveillance and broader epidemiological studies are therefore required to better understand the ecology and potential public health implications of tick-borne pathogens in Korea.

Author contributions

Conceptualization: Lee YJ, Kim KT, Seo MG. Data curation: Kim B, Woo HM, Choi JW. Formal analysis: Kim B, Woo HM, Choi JW. Investigation: Lee YJ, Choi I. Methodology: Choi I. Project administration: Kang YM, Rhee MH, Kwak D. Resources: Hyun YS, Heo JW. Software: Choi I. Supervision: Kang YM, Rhee MH, Kwak D. Validation: Hyun YS, Heo JW. Visualization: Choi I, Hyun YS, Heo JW. Writing – original draft: Lee YJ, Kim KT, Seo MG. Writing – review & editing: Kim KT, Seo MG.

Conflict of interest

Dongmi Kwak serves as an editor of Parasites, Hosts and Diseases but had no involvement in the decision to publish this article. No other potential conflicts of interest relevant to this study were reported.

ORCID

You-Jeong Lee, https://orcid.org/0009-0009-8058-570X
Beoul Kim, https://orcid.org/0009-0001-5159-4801
Yong Sun Hyun, https://orcid.org/0009-0007-8820-7469
Jae Woong Heo, https://orcid.org/0009-0001-3024-3463
Hyo-Min Woo, https://orcid.org/0009-0009-5637-5681
Jae-Woo Choi, https://orcid.org/0009-0005-8707-5076
Insu Choi, https://orcid.org/0009-0003-0043-4167
Yong-Myung Kang, https://orcid.org/0000-0002-0353-9138
Man Hee Rhee, https://orcid.org/0000-0002-3088-1318
Dongmi Kwak, https://orcid.org/0000-0003-0876-3179
Kyoo-Tae Kim, https://orcid.org/0000-0001-8103-9887
Min-Goo Seo, https://orcid.org/0000-0003-1752-5105

References

1. de la Fuente J, Estrada-Pena A, Venzal JM, Kocan KM, Sonenshine DE. Overview: ticks as vectors of pathogens that cause disease in humans and animals. Front Biosci 2008;13:6938-46. https://doi.org/10.2741/3200
2. Low VL, Tan TK, Khoo JJ, Lim FS, AbuBakar S. An overview of rickettsiae in Southeast Asia: vector-animal-human interface. Acta Trop 2020;202:105282. https://doi.org/10.1016/j.actatropica.2019.105282
3. Seo MG, Lee H, Alkathiri B, et al. Tick populations and molecular analysis of *Anaplasma* species in ticks from the Republic of Korea. Microorganisms 2023;11:820. https://doi.org/10.3390/microorganisms11040820
4. Demma LJ, Holman RC, McQuiston JH, Krebs JW, Swerdlow DL. Epidemiology of human ehrlichiosis and anaplasmosis in the United States, 2001-2002. Am J Trop Med Hyg 2005;73:400-9.
5. Parola P, Paddock CD, Raoult D. Tick-borne rickettsioses around the world: emerging diseases challenging old concepts. Clin Microbiol Rev 2005;18:719-56. https://doi.org/10.1128/cmr.18.4.719-756.2005
6. Seo MG, Kwon OD, Kwak D. Molecular detection of *Rickettsia raoultii*, *Rickettsia tamurae*, and associated pathogens from ticks parasitizing water deer (*Hydropotes inermis argyropus*) in South Korea. Ticks Tick Borne Dis 2021;12:101712. https://doi.org/10.1016/j.ttbdis.2021.101712
7. Kang JG, Ko S, Kim HC, et al. Prevalence of *Anaplasma* and *Bartonella* spp. in ticks collected from Korean water deer (*Hydropotes inermis argyropus*). Korean J Parasitol 2016;54:87-91. https://doi.org/10.3347/kjp.2016.54.1.87
8. Seo MG, Kwon OD, Kwak D. High prevalence of *Rickettsia raoultii* and associated pathogens in canine ticks, South Korea. Emerg Infect Dis 2020;26:2530-2. https://doi.org/10.3201/eid2610.191649
9. Shin SH, Seo HJ, Choi YJ, et al. Detection of *Rickettsia monacensis* from *Ixodes nipponensis* collected from rodents in Gyeonggi and Gangwon Provinces, Republic of Korea. Exp Appl Acarol 2013;61:337-47. https://doi.org/10.1007/s10493-013-9699-1
10. Han YJ, Park J, Lee YS, et al. Molecular identification of selected tick-borne pathogens in wild deer and raccoon dogs from the Republic of Korea. Vet Parasitol Reg Stud Reports 2017;7:25-31. https://doi.org/10.1016/j.vprsr.2016.12.001
11. Kim KT, Seo MG. Molecular analysis of *Rickettsia* spp. and related tick-borne pathogens detected in dogs in Korea. Acta Trop 2023;243:106934. https://doi.org/10.1016/j.actatropica.2023.106934
12. Miranda EA, Han SW, Rim JM, et al. Serological evidence of *Anaplasma* spp., *Borrelia burgdorferi* and *Ehrlichia canis* in dogs from the Republic of Korea by rapid diagnostic test kits. J Vet Sci 2022;23:e20. https://doi.org/10.4142/jvs.21215
13. Byun HR, Ji SR, Kang JG, et al. Circulation of tick-borne pathogens in wildlife of the Republic of Korea. One Health 2024;19:100913. https://doi.org/10.1016/j.onehlt.2024.100913
14. Truong AT, Yun BR, Lim J, et al. Real-time PCR biochip for on-site detection of *Coxiella burnetii* in ticks. Parasit Vectors 2021;14:239. https://doi.org/10.1186/s13071-021-04744-z
15. Folmer O, Black M, Hoeh W, Lutz R, Vrijenhoek R. DNA primers for amplification of mitochondrial cytochrome c oxidase subunit I

from diverse metazoan invertebrates. Mol Mar Biol Biotechnol 1994;3:294-9.
16. Kim B, Chae SJ, Lee YJ, et al. Expanding the wildlife reservoir landscape: a high-throughput molecular surveillance study of zoonotic pathogens in Korean water deer. One Health 2025;21:101187. https://doi.org/10.1016/j.onehlt.2025.101187
17. Seo JW, Han SY, Sung SH, et al. Survey on tick distribution and tick-borne pathogens in Daejeon and adjacent areas in South Korea. Ticks Tick Borne Dis 2021;12:101711. https://doi.org/10.1016/j.ttbdis.2021.101711
18. Kim CM, Yi YH, Yu DH, et al. Tick-borne rickettsial pathogens in ticks and small mammals in Korea. Appl Environ Microbiol 2006;72:5766-76. https://doi.org/10.1128/aem.00431-06
19. Lee MJ, Chae JS. Molecular detection of *Ehrlichia chaffeensis* and *Anaplasma bovis* in the salivary glands from *Haemaphysalis longicornis* ticks. Vector Borne Zoonotic Dis 2010;10:411-3. https://doi.org/10.1089/vbz.2008.0215
20. Rosenberg R, Lindsey NP, Fischer M, et al. Vital signs: trends in reported vectorborne disease cases: United States and Territories, 2004-2016. MMWR Morb Mortal Wkly Rep 2018;67:496-501. https://doi.org/10.15585/mmwr.mm6717e1
21. Chae JB, Cho YS, Cho YK, et al. Epidemiological investigation of tick species from near domestic animal farms and cattle, goat, and wild boar in Korea. Korean J Parasitol 2019;57:319-24. https://doi.org/10.3347/kjp.2019.57.3.319
22. Truong AT, Noh J, Park Y, et al. Molecular detection and phylogeny of tick-borne pathogens in ticks collected from dogs in the Republic of Korea. Pathogens 2021;10:613. https://doi.org/10.3390/pathogens10050613
23. Seong G, Han YJ, Oh SS, et al. Detection of tick-borne pathogens in the Korean water deer (*Hydropotes inermis argyropus*) from Jeonbuk Province, Korea. Korean J Parasitol 2015;53:653-9. https://doi.org/10.3347/kjp.2015.53.5.653
24. Kim B, Chae SJ, Lee YJ, et al. Nationwide geographical and temporal distribution of tick-borne diseases in Korean water deer (*Hydropotes inermis argyropus*). Animals (Basel) 2025;15:1499. https://doi.org/10.3390/ani15101499
25. Vayssier-Taussat M, Moutailler S, Féménia F, et al. Identification of novel zoonotic activity of *Bartonella* spp., France. Emerg Infect Dis 2016;22:457-62. https://doi.org/10.3201/eid2203.150269
26. Wijburg SR, Fonville M, de Bruin A, et al. Prevalence and predictors of vector-borne pathogens in Dutch roe deer. Parasit Vectors 2022;15:76. https://doi.org/10.1186/s13071-022-05195-w
27. de Bruin A, van Leeuwen AD, Jahfari S, et al. Vertical transmission of *Bartonella schoenbuchensis* in *Lipoptena cervi*. Parasit Vectors 2015;8:176. https://doi.org/10.1186/s13071-015-0764-y
28. Ko S, Kim SJ, Kang JG, et al. Molecular detection of *Bartonella grahamii* and *B. schoenbuchensis*-related species in Korean water deer (*Hydropotes inermis argyropus*). Vector Borne Zoonotic Dis 2013;13:415-8. https://doi.org/10.1089/vbz.2012.1105
29. Perez M, Rikihisa Y, Wen B. *Ehrlichia canis*-like agent isolated from a man in Venezuela: antigenic and genetic characterization. J Clin Microbiol 1996;34:2133-9. https://doi.org/10.1128/jcm.34.9.2133-2139.1996
30. Taili I, Kim S, Jeong DH, Na KJ. Prevalence of Rickettsiales in raccoon dogs (*Nyctereutes procyonoides koreensis*) in South Korea: a three-year survey. J Vet Sci 2025;26:e57. https://doi.org/10.4142/jvs.25046
31. Parola P, Paddock CD, Socolovschi C, et al. Update on tick-borne rickettsioses around the world: a geographic approach. Clin Microbiol Rev 2013;26:657-702. https://doi.org/10.1128/cmr.00032-13
32. Lee KM, Choi YJ, Shin SH, et al. Spotted fever group rickettsia closely related to *Rickettsia monacensis* isolated from ticks in South Jeolla province, Korea. Microbiol Immunol 2013;57:487-95. https://doi.org/10.1111/1348-0421.12062
33. Kim KG, Hwang DJ, Park JW, et al. Distribution and pathogen prevalence of field-collected ticks from south-western Korea: a study from 2019 to 2022. Sci Rep 2024;14:12336. https://doi.org/10.1038/s41598-024-61126-y
34. Kim YS, Choi YJ, Lee KM, et al. First isolation of *Rickettsia monacensis* from a patient in South Korea. Microbiol Immunol 2017;61:258-63. https://doi.org/10.1111/1348-0421.12496
35. Park HJ, Kim J, Choi YJ, et al. Tick-borne rickettsiae in Midwestern region of Republic of Korea. Acta Trop 2021;215:105794. https://doi.org/10.1016/j.actatropica.2020.105794

Brief Communication

Parasites Hosts Dis 2026;64(3):260-264
https://doi.org/10.3347/PHD.26006

Parasites, Hosts and Diseases

pISSN 2982–5164 • eISSN 2982–6799

Three-year survey of *Enterobius vermicularis* infection among preschool children in Jeollanam-do, Korea (2023–2025)

Ji-Yoon Jeon[1,2], Yeon-Ju Lee[1], Hye-Rin Kim[1], Hye-Lin Yang[1], Yun-Ji Park[1], Hye-Jin Kim[1], Tae-Man Ha[1], Jin-Yeong Kim[1], Gwi-Nim Park[1], Sook Park[1], Yang-Joon An[1], Yeongjin Hong[2,*]

[1]Jeollanam-do Institute of Health and Environment, Muan, Korea; [2]Department of Microbiology and Immunology, Chonnam National University Medical School, Gwangju, Korea

The purpose of this study was to ascertain the status and patterns of pinworm *Enterobius vermicularis* infection among preschool children in Jeollanam-do from 2023 to 2025. Further, it aimed to assess changes in infection rates during the implementation of the test-and-treatment strategy. Cellophane tape swabs were collected from 12,608 children aged 0–6 years enrolled in daycare or kindergarten facilities in 8 cities and counties of Jeollanam-do. The samples were examined under a light microscope to diagnose pinworm infection. The overall infection rate over the 3-year period was 0.22% (28/12,608). The annual infection rate declined continuously from 0.35% in 2023 to 0.06% in 2025 (trend $P<0.05$). The infection rate did not vary significantly with sex ($P>0.05$), but was significantly higher in the 4–6 year age group ($P<0.05$), and was highest in Jangheung-gun (0.65%) and Goheung-gun (0.37%). The overall infection rate in this study was substantially lower than previously reported. However, this may represent a transient phenomenon reflecting environmental or behavioral factors associated with this specific period. Therefore, continuous monitoring is necessary.

Keywords: *Enterobius vermicularis*, enterobiasis, cellophane tape method, preschool children, Jeollanam-do

Enterobiasis, caused by the pinworm *Enterobius vermicularis*, is one of the most commonly reported helminthic infections in humans worldwide, and infection rates are especially high among preschool children and children of school age [1-3]. Infections spread via objects contaminated with *E. vermicularis* eggs or by direct contact with an infected person. The risk of spreading is especially high in communal settings such as daycare facilities [4,5]. The main clinical symptom is perianal itching, sometimes accompanied by sleep disturbance or weight loss, and rare complications such as appendicitis can occur [6]. In Korea, surveys have been conducted continuously in several regions, and overall infection rates have declined in recent years [7]. However, sporadic localized clusters are still observed in some regions, suggesting the need for sustained surveillance and intervention [8,9]. As such, the purpose of this study was to ascertain the status and patterns of *E. vermicularis* infection during the 3-year study period among preschool children in Jeollanam-do, and to assess changes in infection rates during the implementation of the test-and-treatment strategy.

This study was approved by the Chonnam National University Hwasun Hospital Institutional Review Board (approval No. CNUHH-2025-250). The participants were 12,608 preschool children, aged 0–6 years, enrolled in daycare or kindergarten facilities in 8 cities and counties of Jeollanam-do (Yeosu-si, Damyang-gun, Gurye-gun, Goheung-gun, Jangheung-gun, Yeongam-gun, Jangseong-gun, and Jindo-gun) between 2023

Received: January 14, 2026 Accepted: April 1, 2026
*Correspondence: yjhong@jnu.ac.kr

Citation
Jeon JY, Lee YJ, Kim HR, Yang HL, Park YJ, Kim HJ, Ha TM, Kim JY, Park GN, Park S, An YJ, Hong Y. Three-year survey of *Enterobius vermicularis* infection among preschool children in Jeollanam-do, Korea. Parasites Hosts Dis 2026;64(3):260-264.

and 2025 (Fig. 1). Cellophane tape samples were collected by caregivers from the perianal region before washing or bathing and submitted to local public health centers. The samples were transferred to the Jeollanam-do Institute of Health and Environment and examined under a light microscope to identify *E. vermicularis* eggs based on typical morphological characteristics (asymmetric oval shape, approximately 50–60 μm long and 20–30 μm wide) [1,2]. Caregivers of diagnosed children were advised to administer anthelmintic medication provided by the public health center. The ratio of egg-positive results among all tested children was estimated as the infection rate. Statistical analysis was performed using the chi-squared test and the Cochran–Armitage test for linear trend with a significance level of 0.05 using IBM SPSS Statistics version 31.0 (IBM Corp.).

The overall infection rate was 0.22% (28/12,608), and all the infected children ($n=28$) tested negative after anthelmintic treatment. The annual infection rate was 0.35% (18/5,077) in 2023, 0.20% (8/3,940) in 2024, and 0.06% (2/3,591) in 2025, reflecting a significant continuous decline over time (trend $P<0.05$) (Table 1). The infection rate was 0.24% (15/6,325) for boys and 0.21% (13/6,283) for girls, with no significant difference ($P>0.05$) (Table 2). By age, no infected children were detected in the 0–3 year age group, whereas the 4–6 year age group showed a significantly higher infection rate of 0.29% (28/9,494, $P<0.05$) (Table 2). By region, the infection rate was highest in Jangheung-gun (0.65%; 7/1,071), followed by Goheung-gun (0.37%; 3/816), Yeongam-gun (0.37%; 4/1,089), Yeosu-si (0.21%; 12/5,815), and Gurye-gun (0.19%; 2/1,057), with significant differences among the regions ($P<0.05$). No infected children were detected in Damyang-gun, Jangseong-gun, or Jindo-gun (Table 2).

The overall infection rate declined in preschool children of Jeollanam-do over the study period, from 0.35% in 2023 to 0.06% in 2025. The rates observed in this study were substantially lower than the previous nationwide infection rate in 2008–2019 (1.6%) [7], and lower than those reported in some European regions such as eastern Slovakia (3.59%, 2018) [10] and north-eastern Poland (10.1%, 2013–2015) [11]. The continuous decline in infection rates from 2023 to 2025 may be partly

Table 1. Annual infection rates of *Enterobius vermicularis* among preschool children in Jeollanam-do, 2023–2025

Year	No. positive/ No. examined	Infection rate (%, 95% CI[a])	Trend P^b
2023	18/5,077	0.35 (0.22–0.56)	0.003
2024	8/3,940	0.20 (0.10–0.40)	
2025	2/3,591	0.06 (0.02–0.20)	

[a]Calculated using Wilson score method; [b]Trend *P* calculated using the Cochran–Armitage test.

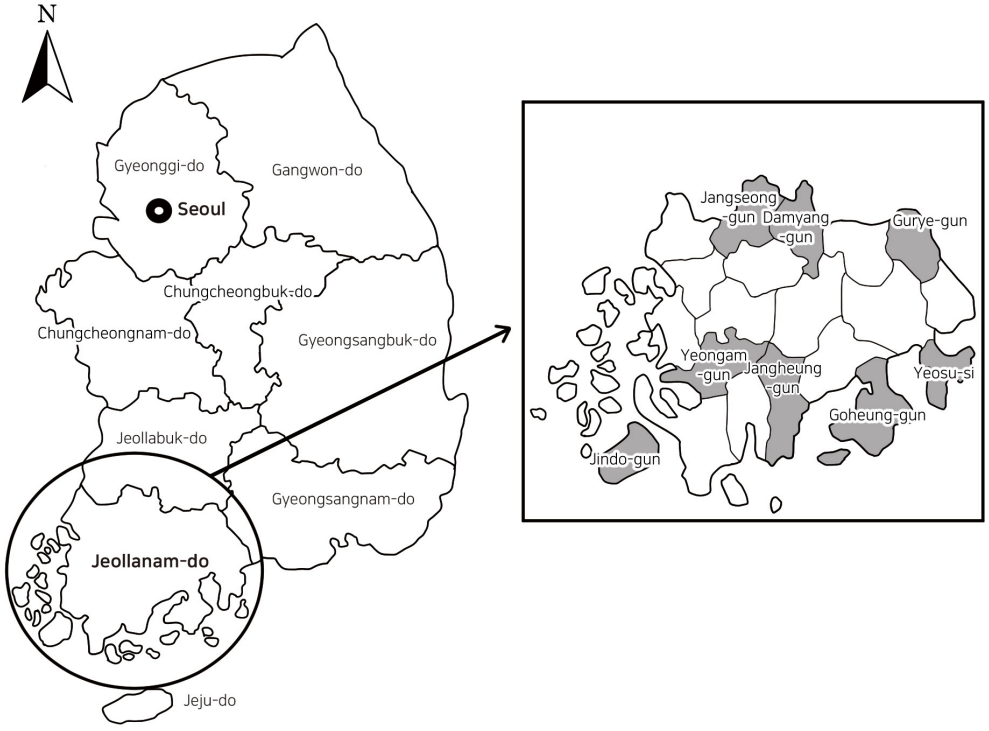

Fig. 1. Surveyed regions for *Enterobius vermicularis* infection monitoring in Jeollanam-do, Korea.

attributable to the sustained implementation of the test-and-treatment strategy. This is consistent with the decline in infection rates in Yeosu-si, from 5.0% to 1.0% between 2017 and 2021 [8], and with the long-term decline in infections in Taiwan between 1990 and 2012, from 4.3% to 0.21% [4]. Although there were no significant differences by sex, some previous studies have reported a higher infection rate among boys [7,8,12-14]. It is thought that the effects of sex in this study were weakened by the decline in the overall infection rate to a very low level. The significantly higher infection rate observed in the 4–6 year age group may be related to behavioral factors that expose children to infection, such as increased group activities and frequent interpersonal contact [5]. Finally, although the infection rate varied significantly by region, this variation is thought to be attributable to localized clusters within specific daycare or kindergarten facilities rather than to broader regional characteristics. Indeed, at least 2 such localized clusters were observed in Jangheung-gun and Yeosu-si, partially contributing to the increased infection rates observed in these regions.

This study has several limitations. First, because only one sample was taken from each participant, some infections could have been missed due to the limited sensitivity of a single test, potentially resulting in false-negative results. Although standard diagnostic protocols recommend performing the test at least 3 times to maximize detection sensitivity [1,3], this survey was limited to a single sampling due to practical constraints, which is common in large-scale community-based surveys. Therefore, the reported infection rate may underestimate the true rate. In addition, because the samples were taken directly by the caregivers, consistency of the sampling process could not be completely guaranteed.

The *E. vermicularis* infection rate observed among preschool children in 8 cities and counties of Jeollanam-do was 0.22%, which is much lower than in previous studies (Table 3) [7-9,12-

Table 2. Infection rates of *Enterobius vermicularis* by sex, age, and region among preschool children in Jeollanam-do, 2023–2025

Category		No. positive/No. examined (%)				
		2023	2024	2025	Total	*P*-value
Sex	Male	11/2,552 (0.43)	4/2,000 (0.20)	0/1,773 (0)	15/6,325 (0.24)	0.718
	Female	7/2,525 (0.28)	4/1,940 (0.21)	2/1,818 (0.11)	13/6,283 (0.21)	
Age group (yr)	0–3	0/1,196 (0)	0/1,065 (0)	0/853 (0)	0/3,114 (0)	0.002
	4–6	18/3,881 (0.46)	8/2,875 (0.28)	2/2,738 (0.07)	28/9,494 (0.29)	
Region	Yeosu-si	5/1,781 (0.28)	5/2,050 (0.24)	2/1,984 (0.10)	12/5,815 (0.21)	0.017
	Damyang-gun	0/509 (0)	0/317 (0)	0/282 (0)	0/1,108 (0)	
	Gurye-gun	2/517 (0.39)	0/282 (0)	0/258 (0)	2/1,057 (0.19)	
	Goheung-gun	2/301 (0.66)	1/338 (0.30)	0/177 (0)	3/816 (0.37)	
	Jangheung-gun	6/575 (1.04)	1/179 (0.56)	0/317 (0)	7/1,071 (0.65)	
	Yeongam-gun	3/614 (0.49)	1/292 (0.34)	0/183 (0)	4/1,089 (0.37)	
	Jangseong-gun	0/345 (0)	0/160 (0)	0/129 (0)	0/634 (0)	
	Jindo-gun	0/435 (0)	0/322 (0)	0/261 (0)	0/1,018 (0)	
Overall					28/12,608 (0.22)	

Table 3. Recent trends in the infection rates of *Enterobius vermicularis* among children in Korea

Survey period	Region	Population (age, yr)	Sample size (*n*)	Infection rate (%)[a]	Reference
2008	Gangwon-do (Chuncheon-si, Inje-gun), Gyeonggi-do (Paju-si)	Preschool children (0–7)	7,048	4.0	Hong et al. (2011) [12]
2008–2009	Jeollanam-do (Muan-gun)	Preschool children (0–7)	2,347	4.4 (4.1→4.6)	Hong et al. (2012) [9]
≤2010[b]	Busan	Kindergarten children (1–7)	1,674	10.7	Kim et al. (2010) [13]
≤2011[b]	Gyeongsangnam-do (Gimhae-si)	Preschool children (≤7)	6,921	10.5	Lee et al. (2011) [14]
2011	Southeast region of Korea	Kindergarten children	3,422	6.0	Kim et al. (2013) [15]
2012–2013	Industrial, urban, suburban areas	Primary school children (7–9)	3,840	4.4	Kim et al. (2014) [16]
2014	Busan, Ulsan	Orphanage children (4–13)	117	0.85	Kim et al. (2015) [17]
2008–2019	Nationwide	Preschool children (1–6)	638,354	1.6 (1.8→0.6)	Shin et al. (2021) [7]
2017–2021	Jeollanam-do (Yeosu-si)	Preschool children (0–7)	10,392	3.2 (5.0→1.0)	Lee et al. (2023) [8]

[a]Values in parentheses represent the initial and final infection rates during the survey period; [b]Exact survey period was not specified and studies are ordered by publication year.

https://doi.org/10.3347/PHD.26006

17]. This is thought to be partially due to improvements in personal hygiene habits (such as regular handwashing, nail care, and mask-wearing) and the sustained behavioral changes aimed at infection prevention established during the COVID-19 pandemic. In fact, studies conducted in Korea have reported a significant decrease in the incidence of infectious respiratory diseases [18] and gastrointestinal infections [19] during this period. Moreover, the infection rate declined significantly from 0.35% to 0.06% (trend $P<0.05$) over the study period (2023–2025). The regular test-and-treatment strategy implemented over this period is thought to have played a role in this decline, which is consistent with previous findings [7,8]. In order to maintain this low infection rate, it will be important to conduct continuous monitoring and anthelmintic treatment programs and to gradually expand the survey region. These findings are expected to provide basic data for establishing community-based infection-control policies.

Author contributions

Data curation: Jeon JY. Formal analysis: Jeon JY. Investigation: Lee YJ, Kim HR, Yang HL, Park YJ, Kim HJ. Project administration: Park GN, Park S, An YJ. Resources: Ha TM. Supervision: Hong Y. Writing - original draft: Jeon JY. Writing - review & editing: Kim JY, Hong Y.

Conflict of interest

The authors have no conflicts of interest to declare.

Acknowledgments

The cellophane tape for *E. vermicularis* egg testing was provided by the Division of Vectors and Parasitic Diseases at the Korea Disease Control and Prevention Agency (KDCA). The authors would like to extend their deepest gratitude to the public health center workers who cooperated and assisted throughout the research process.

ORCID

Ji-Yoon Jeon, https://orcid.org/0000-0001-9447-946X
Yeon-Ju Lee, https://orcid.org/0009-0005-2614-3805
Hye-Rin Kim, https://orcid.org/0009-0005-8241-5246
Hye-Lin Yang, https://orcid.org/0009-0007-7108-1222
Yun-Ji Park, https://orcid.org/0009-0004-6851-083X
Hye-Jin Kim, https://orcid.org/0009-0007-3785-2732
Tae-Man Ha, https://orcid.org/0009-0003-4240-453X
Jin-Yeong Kim, https://orcid.org/0000-0003-0613-8951
Gwi-Nim Park, https://orcid.org/0009-0000-1265-6443
Sook Park, https://orcid.org/0000-0002-9856-9638
Yang-Joon An, https://orcid.org/0009-0008-3501-8506
Yeongjin Hong, https://orcid.org/0000-0002-8115-7362

References

1. Chai JY, Hong ST, Choi MH, et al. Clinical parasitology. Seoul National University Press; 2011.
2. Joo CY, Chung DI, Kong HH, Ock MS. Human parasitology. Keimyung University Press; 2003.
3. Yong TS, Kim GA, Kim GJ, et al. Human parasitology. Jungmunkag; 2022.
4. Chen KY, Yen CM, Hwang KP, Wang LC. *Enterobius vermicularis* infection and its risk factors among pre-school children in Taipei, Taiwan. J Microbiol Immunol Infect 2018;51:559-64. https://doi.org/10.1016/j.jmii.2016.12.013
5. Fan CK, Chuang TW, Huang YC, et al. *Enterobius vermicularis* infection: prevalence and risk factors among preschool children in kindergarten in the capital area, Republic of the Marshall Islands. BMC Infect Dis 2019;19:536. https://doi.org/10.1186/s12879-019-4159-0
6. Chhetri S, Al Mamari AH, Al Awfi MM, et al. *Enterobius vermicularis* related acute appendicitis: a case report and review of the literature. Infect Dis Rep 2023;15:417-24. https://doi.org/10.3390/idr15040042
7. Shin H, Jung BK, Ryoo S, et al. *Enterobius vermicularis* infection among preschool children: a 12-year (2008-2019) survey in large cities and provinces of the Republic of Korea. Korean J Parasitol 2021;59:421-6. https://doi.org/10.3347/kjp.2021.59.4.421
8. Lee MR, Shin HE, Back SO, et al. Positive rates for *Enterobius vermicularis* eggs among preschool children in Yeosu-si, Jeollanam-do, Korea (2017-2021). Parasites Hosts Dis 2023;61:84-8. https://doi.org/10.3347/PHD.22121
9. Hong SH, Jeong YI, Lee JH, et al. Prevalence of *Enterobius vermicularis* among preschool children in Muan-gun, Jeollanam-do, Korea. Korean J Parasitol 2012;50:259-62. https://doi.org/10.3347/kjp.2012.50.3.259
10. Dudlová A, Juriš P, Jarčuška P, et al. The incidence of pinworm (*Enterobius vermicularis*) in pre-school and school aged children in the Eastern Slovakia. Helminthologia 2018;55:275-80. https://doi.org/10.2478/helm-2018-0030
11. Kubiak K, Dzika E, Paukszto L. Enterobiasis epidemiology and molecular characterization of *Enterobius vermicularis* in healthy children in north-eastern Poland. Helminthologia 2017;54:284-91. https://doi.org/10.1515/helm-2017-0042
12. Hong SH, Lee SE, Jeong YI, Lee WJ, Cho SH. Comparison of egg positive rates of *Enterobius vermicularis* among preschool children in three Korean localities. Korean J Parasitol 2011;49:441-3. https://

doi.org/10.3347/kjp.2011.49.4.441

13. Kim DH, Son HM, Kim JY, et al. Parents' knowledge about enterobiasis might be one of the most important risk factors for enterobiasis in children. Korean J Parasitol 2010;48:121-6. https://doi.org/10.3347/kjp.2010.48.2.121
14. Lee SE, Lee JH, Ju JW, Lee WJ, Cho SH. Prevalence of *Enterobius vermicularis* among preschool children in Gimhae-si, Gyeongsangnam-do, Korea. Korean J Parasitol 2011;49:183-5. https://doi.org/10.3347/kjp.2011.49.2.183
15. Kim DH, Cho MK, Park MK, et al. Environmental factors related to enterobiasis in a southeast region of Korea. Korean J Parasitol 2013;51:139-42. https://doi.org/10.3347/kjp.2013.51.1.139
16. Kim DH, Yu HS. Effect of a one-off educational session about enterobiasis on knowledge, preventative practices, and infection rates among schoolchildren in South Korea. PLoS One 2014;9:e112149. https://doi.org/10.1371/journal.pone.0112149
17. Kim DH, Son HM, Lee SH, et al. Negligible egg positive rate of *Enterobius vermicularis* and no detection of head lice among orphanage children in Busan and Ulsan, Korea (2014). Korean J Parasitol 2015;53:497-9. https://doi.org/10.3347/kjp.2015.53.4.497
18. Kim DH, Nguyen TM, Kim JH. Infectious respiratory diseases decreased during the COVID-19 pandemic in South Korea. Int J Environ Res Public Health 2021;18:6008. https://doi.org/10.3390/ijerph18116008
19. Ahn SY, Park JY, Lim IS, et al. Changes in the occurrence of gastrointestinal infections after COVID-19 in Korea. J Korean Med Sci 2021;36:e180. https://doi.org/10.3346/jkms.2021.36.e180

https://doi.org/10.3347/PHD.26006

Brief Communication

Parasites Hosts Dis 2026;64(3):265-269
https://doi.org/10.3347/PHD.25002

Parasites, Hosts and Diseases

pISSN 2982-5164 • eISSN 2982-6799

Infections of digenetic trematode metacercariae in freshwater fish from Banbyeon-cheon (stream) in Yeongyang-gun, Gyeongsangbuk-do, Korea

Emmanuel Opara[1], Ha-Eun Lee[1], Heon Woo Lee[1], Mohammed Mebarek Bia[2], Myoung-Ro Lee[3], Sunmin Kim[1], Seongjun Choe[1,4,*]

[1]Department of Parasitology, School of Medicine, Chungbuk National University, Cheongju, Korea; [2]International Parasite Resources Bank, Cheongju, Korea; [3]Division of Vectors and Parasitic Diseases, Korea Disease Control and Prevention Agency, Osong, Korea; [4]Biomedical Research Institute, Chungbuk National University Hospital, Cheongju, Korea

The present study investigated the infection status of digenetic trematode metacercariae (DTM) in freshwater fish from Banbyeon-cheon in Yeongyang-gun, Gyeongsangbuk-do, Korea. A total of 211 freshwater fish representing 11 species were examined using the artificial digestion method in October 2023. Six taxa of DTM, including *Clonorchis sinensis*, *Metagonimus* spp., *Centrocestus armatus*, echinostomes, *Exorchis oviformis*, and Metacercaria hasegawai, were detected. The overall prevalence of DTM was 92.4% among the fish examined. The prevalence of *C. armatus* was the highest (52.8%), followed by *E. oviformis* (51.6%), M. hasegawai (35.6%), echinostomes (31.0%), *C. sinensis* (16.1%), and *Metagonimus* spp. (6.9%) in positive fish species. The infection intensity of *C. armatus* was 126 metacercariae per infected fish, whereas those of *C. sinensis* and *Metagonimus* spp. were 20 and 5.8 per infected fish, respectively. These findings indicate that at least 6 taxa of DTM, including *C. sinensis* and *Metagonimus* spp., are prevalent to varying degrees in fish from Banbyeon-cheon in Yeongyang-gun, Gyeongsangbuk-do, Korea. However, the potential risk of fishborne zoonotic trematodes, particularly *C. sinensis*, appears to be markedly lower than that reported in previous studies.

Keywords: Banbyeon-cheon, digenetic trematode metacercariae, *Clonorchis sinensis*, freshwater fish, Yeongyang-gun

Infections caused by fishborne zoonotic trematodes are widely recognized as important public health problems in Korea. Among these, clonorchiasis caused by *Clonorchis sinensis* remains one of the most significant parasitic diseases, particularly in riparian areas, as reported by the Korea Disease Control and Prevention Agency [1]. Although the endemicity of these infections has reportedly decreased over time, they continue to pose a substantial public health concern [2].

Beyond their zoonotic significance, digenetic trematode metacercariae (DTM) are also useful for characterizing trematode transmission in freshwater ecosystems. Infections are caused by trematodes whose infective larval stage, the metacercaria, commonly utilizes fish as an intermediate host and serves as a source of infection for definitive hosts, including humans [3]. In addition, DTM species in fish intermediate hosts serve as important bioindicators of ecosystem health and reflect the infection status of adult trematodes in definitive hosts.

In Korea, numerous surveys have investigated the infection status of DTM in freshwater fish across diverse ecological habitats to evaluate their endemicity, particularly within various re-

Received: December 15, 2025 Accepted: March 9, 2026
*Correspondence: parasite@chungbuk.ac.kr

Citation
Opara E, Lee HE, Lee HW, Bia MM, Lee MR, Kim S, Choe S. Infections of digenetic trematode metacercariae in freshwater fish from Banbyeon-cheon (stream) in Yeongyang-gun, Gyeongsangbuk-do, Korea. Parasites Hosts Dis 2026;64(3):265-269.

gions of Nakdong-gang ("gang" means river). These studies, spanning both the upper and lower reaches of the river, have documented the prevalence and distribution of DTM infections [4-9].

Banbyeon-cheon ("cheon" means stream) in Yeongyang-gun ("gun" means county) is located among agricultural fields, villages, and townships and forms part of the tributary network of the Nakdong-gang basin, where previous studies have reported persistent endemicity of DTM infections [5]. Adjacent tributaries, including Wi-cheon in Gunwi-gun, Yongjeon-cheon in Cheongsong-gun, and Gilan-cheon in Andong-si ("si" means city), Gyeongsangbuk-do ("do" means province), have been identified as endemic hotspots for zoonotic DTM species, particularly *C. sinensis* [10-12]. However, investigations specifically examining DTM prevalence in Banbyeon-cheon remain limited. To date, studies of DTM infections, including *C. sinensis*, *Centrocestus armatus*, and *Metagonimus* spp., in fish from this area have only been included as part of broader regional investigations [13-15]. Comprehensive analyses of other DTM species and overall parasite assemblages in this river have not yet been conducted. Therefore, the present study aimed to investigate the infection status of DTM species in freshwater fish from Banbyeon-cheon in Yeongyang-gun, Gyeongsangbuk-do.

Fish collection was conducted at 3 sites along Banbyeon-cheon in Yeongyang-gun, Gyeongsangbuk-do (site A: Hyeong-ri in Yeongyang-eup, latitude 36.6477°, longitude 129.1177°; site B: Hapgang-ri in Ibam-myeon, latitude 36.5870°, longitude 129.0744°; and site C: Bangjeon in Ibam-myeon, latitude 36.5535°, longitude 129.0900°) (Fig. 1). All lakes and rivers in the map figure were represented using consistent line widths.

A total of 211 freshwater fish representing 11 species were collected, including 139 individuals from site A, 67 individuals from site B (9 species), and 5 individuals from site C (4 species). Fish were collected using gill nets, casting nets, and stake nets at all surveyed sites in October 2023 with permission from the local government authorities. Because all 3 collection sites were located within close proximity and exhibited no ecologically significant differences, they were considered part of a single water system. The collected fish were transported on ice to the laboratory of the Department of Parasitology, School of Medicine, Chungbuk National University, Cheongju, Korea. Fish species were identified according to a published atlas [16], and each specimen was individually weighed and measured for length (Supplementary Tables S1-S7). Subsequently, each fish was homogenized using a mortar and pestle. The homogenized tissue was transferred to a beaker, mixed with 1% acid pepsin solution, and incubated for 2 h at 36°C for digestion. After incubation, the digested material was filtered through a 1×1 mm²

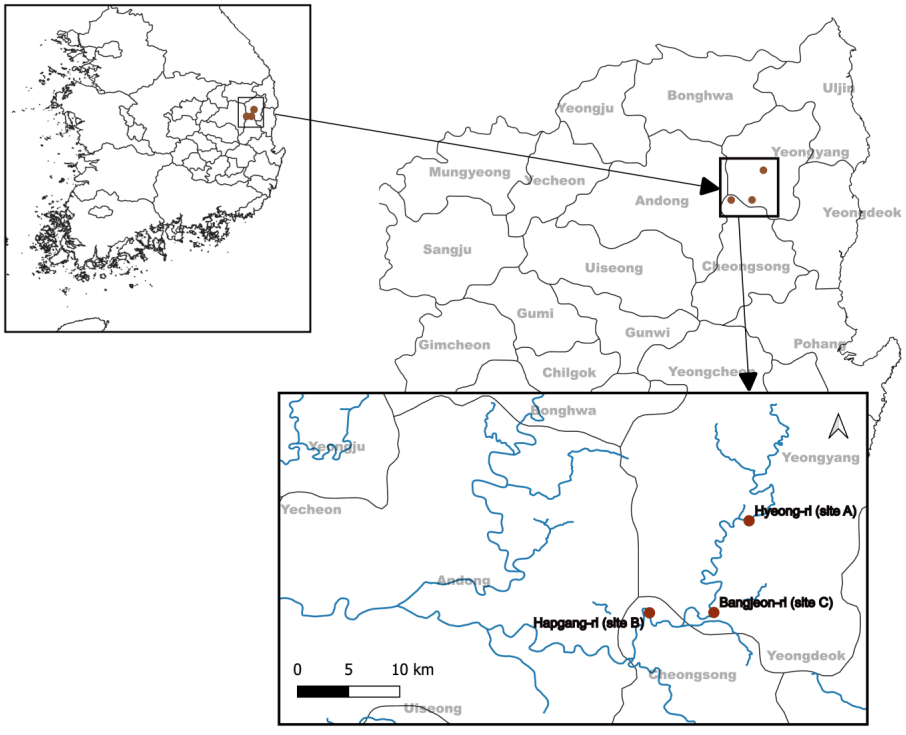

Fig. 1. Map of the surveyed sites in the water systems of Banbyeon-cheon in Yeongyang-gun, Gyeongsangbuk-do, Korea.

https://doi.org/10.3347/PHD.25002

mesh and rinsed with 0.85% saline until the supernatant became clear. The sediment was then carefully examined under a stereomicroscope. All DTM specimens were individually collected and identified according to their general morphological characteristics [17]. Thereafter, the prevalence (%) and mean intensity of infection (number of DTM per infected fish) were calculated.

Six taxa of DTM, including *C. sinensis*, *Metagonimus* spp., *C. armatus*, echinostomes, *Exorchis oviformis*, and M. hasegawai, were detected. The overall prevalence of DTM was 92.4% among all fish examined (Table 1). For each trematode taxon, prevalence was calculated as the proportion of infected fish relative to the total number of examined individuals within host species in which the parasite was detected.

Among the detected parasite taxa, *C. armatus* metacercariae exhibited the highest prevalence (52.8%), with 94 infected individuals among 178 fish from 9 positive fish species (PFS), and an average density of 126 per infected fish (PFI). *E. oviformis* was the second most prevalent species 51.6%, recorded in 108 infected fish among 209 individuals from 9 PFS, with an average density of 88.8. M. hasegawai (35.6%; 62 infected individuals among 174 fish from 8 PFS; average density, 40.3). This was followed closely by echinostomes having a prevalence of 31.0%; 26 infected individuals among 84 fish from 5 PFS with an average density of 17. *C. sinensis* (16.1%; 26 infected individuals among 167 fish from 7 PFS; average density, 20) and *Metagonimus* spp. (6.9%; 13 infected individuals among 186 fish from 6 PFS; average density, 5.8). The overall prevalence and infection intensities of DTM according to fish species are summarized in Table 1 and Supplementary Tables S8-S13.

In the present investigation, 6 taxa of DTM were detected in 11 fish species collected from Banbyeon-cheon in Yeongyang-gun, Gyeongsangbuk-do, Korea. The prevalence of individual parasite taxa varied markedly, with some species showing comparatively high infection rates, whereas others exhibited relatively low prevalence compared with findings from adjacent environments.

Consistent with the results of previous studies, our findings suggest that the overall infection levels, particularly those of *C. sinensis*, may have declined compared with previous reports from nearby tributaries within the Nakdong-gang system. Adjacent streams, including Wi-cheon and Yongjeon-cheon, have been reported to show prevalence rates of 59.9% with an infection intensity of 677.1 PFI (2011 and 2013–2017) and 65.5% with an intensity of 453.0 PFI (2019–2020), respectively [10,11]. Similarly, Lee et al. [12] reported that the prevalence of *C. sinensis* metacercariae (CsMc) in fish from Yongjeon-cheon was 50% (125 PFI), whereas that in fish from Gilan-cheon was 49% (79 PFI), indicating sustained high transmission in neighbouring streams. Furthermore, Sohn et al. [13] reported a prevalence of 81.6% and an infection intensity of 190.1 PFI in Banbyeon-cheon between 2010 and 2020. Although their investigation was conducted at a single site, the present study included 3 sampling sites and observed a substantially lower prevalence. The reason for this marked difference remains uncertain but may reflect spatial and temporal differences in sampling and DTM transmission dynamics. Overall, the present findings indicate a lower prevalence of CsMc than that reported in earlier investigations conducted in the upper reaches of Nakdong-gang.

Consequently, the susceptibility index (SI; prevalence/100 × average intensity of DTM PFI) [18] in the present study was 3.2, which was substantially lower than the values reported previously for Banbyeon-cheon (SI, 155.1), Yongjeon-cheon (SI, 402.9 and 40.3), Gilan-cheon (SI, 62.3), and Wi-cheon (SI, 297.2). In the present study, *Pungtungia herzi*, a recognized in-

Table 1. Infection status of digenetic trematode metacercariae in freshwater fish from Banbyeon-cheon in Yeongyang-gun, Gyeongsangbuk-do, Korea

Fish species examined	Fish infected	*Clonorchis sinensis*		*Metagonimus* spp.		*Centrocestus armatus*		Echinostomes		*Exorchis oviformis*		Metacercaria hasegawai	
		Fish infected	Average	Fish infected	Average	Fish infected	Average	Fish infected	Average	Fish infected	Average	Fish infected	Average
Acheilognathus lanceolatus	32	1 (3.1)	8	5 (15.6)	2	-	-	-	-	25 (78.1)	9	13 (40.6)	126.7
Acheilognathus majusculus	12	2 (16.7)	5.5	1 (8.3)	1	1 (8.3)	1	4 (33.3)	2.5	12 (100)	11	12 (100)	6
Carassius auratus	1	-	-	-	-	-	-	-	-	-	-	-	-
Coreoperca herzi	7	-	-	-	-	2 (28.5)	1,068	-	-	3 (42.8)	3	1 (14.2)	1
Misgurnus anguillicaudatus	1	-	-	-	-	1 (100)	2	-	-	-	-	-	-
Nipponocypris temminckii	35	-	-	2 (5.7)	9	33 (92.4)	139	-	-	2 (6.1)	5	-	-
Pungtungia herzi	51	14 (27.4)	16.6	3 (6)	3.3	2	12	16 (31.3)	34	45 (88.2)	139	18 (35.3)	6.4
Pseudogobio esocinus	5	1 (20)	6	1 (20)	26	1 (20)	1	3 (60)	3.5	5 (100)	19	2 (40)	3.5
Sarcocheilichthys nigripinnis morii	8	5 (62.5)	8	-	-	1 (37.5)	2	1 (12.5)	1	5 (33.3)	39	6 (75)	4
Squalidus japonicus koreanus	8	2 (25)	13	-	-	4 (50)	3.8	2 (25)	4	3 (100)	44	7 (85.7)	4.7
Zacco platypus	51	2 (3.9)	1	1 (1.9)	1	48 (94.1)	144	-	-	3 (17.3)	5.3	3 (5.8)	1
Total	211	27 (16.1)	20	13 (6.9)	5.8	94 (52.8)	126	26 (31)	17	108 (51.6)	88.8	62 (35.6)	40.3

Values are presented as number or number (%).

dex species for CsMc in Korea, showed an SI of only 4.5, which was markedly lower than values reported previously from other streams, some of which exceeded 1,000 [10-12]. For example, Sohn et al. [11] reported an SI of 1,060.7 for *P. herzi* from Yongjeon-cheon. These findings suggest a potential reduction in clonorchiasis risk in this environment, although continuous surveillance is required to confirm this trend. This decline may be associated with changes in fish community composition, including reductions in highly susceptible species such as *P. herzi*, as well as broader national control programs aimed at interrupting the parasite life cycle through fecal management and related interventions implemented by the Korea Disease Control and Prevention Agency.

Among the other DTM species, *Centrocestus armatus* metacercariae (CaMc) showed the highest prevalence (52.8%) in PFS, whereas *Metagonimus* spp. showed the lowest prevalence (6.9%). The remaining taxa, including echinostomes (31.0%), *E. oviformis* (51.6%), and M. hasegawai (35.6%), exhibited intermediate prevalence levels. The high prevalence of CaMc in *Zacco platypus* (94.1%) is consistent with previous reports from Nakdong-gang, where CaMc was reported to be nearly ubiquitous in Zacco species [14]. Persistent high infection rates in chub fish suggest that this parasite remains widespread and may serve as a reliable indicator of DTM burden in the region. In contrast, the very low prevalence of *Metagonimus* spp. may reflect the limited distribution of highly susceptible host species, particularly *Plecoglossus altivelis*. This low endemicity is consistent with findings from other Nakdong-gang studies, excluding Deokcheon-gang, where prevalence reached 87.5% [15,18]. These results suggest that host fish distribution may influence local parasite transmission.

These results support continued monitoring of DTM infections in fish from the Nakdong-gang water system. In the present study, 6 taxa of DTM, including *C. sinensis* and *Metagonimus* spp., were detected in fish from Banbyeon-cheon in Yeongyang-gun. However, compared with earlier reports from Banbyeon-cheon and adjacent streams in the upper reaches of Nakdong-gang, the potential risk of fishborne zoonotic trematodes, particularly *C. sinensis*, appears to have decreased substantially.

Author contributions

Conceptualization: Opara E, Choe S. Data curation: Opara E, Lee HE, Lee MR, Choe S. Formal analysis: Opara E, Kim S, Choe S. Funding acquisition: Choe S. Investigation: Opara E, Lee HE, Lee HW. Methodology: Lee HW, Opara E. Project administration: Bia MM, Choe S. Supervision: Choe S. Writing – original draft: Opara E, Choe S. Writing – review & editing: Kim S, Choe S.

Conflict of interest

The authors have no conflicts of interest to declare.

Funding

This work was supported by the Brain Korea Scholarship 21 and Korea Disease Control and Prevention Agency (grant No. 6331-311-260-01, 2023).

Supplementary information

Supplementary material is available with this article at https://doi.org/10.3347/PHD.25002.

ORCID

Emmanuel Opara, https://orcid.org/0000-0003-1535-3581
Ha-Eun Lee, https://orcid.org/0009-0007-1301-9666
Heon Woo Lee, https://orcid.org/0000-0002-5925-4246
Mohammed Mebarek Bia, https://orcid.org/0000-0003-2495-6800
Myoung-Ro Lee, https://orcid.org/0000-0003-3369-0063
Sunmin Kim, https://orcid.org/0000-0002-3855-8785
Seongjun Choe, https://orcid.org/0000-0002-9204-2173

References

1. Korea Centers for Disease Control and Prevention; Korea National Institute of Health. National survey of the prevalence of intestinal parasitic infections in Korea, 2012: the 8th report. Korea Centers for Disease Control and Prevention; 2013.
2. Lee MR, Shin HE, Back SO, et al. Status of helminthic infections in residents around river basins in the Republic of Korea for 10 years (2011-2020). Korean J Parasitol 2022;60:187-93. https://doi.org/10.3347/kjp.2022.60.3.187
3. Gibson DI. Subclass digenea Carus. In: Gibson DI, Jones A, Bray RA, editors. Keys to the Trematoda. Vol. 1. CABI and Natural History Museum; 2001. p. 15-8.
4. Chun SK. Studies on some trematodes whose intermediate hosts are fish in the Naktong River. Bull Fish Coll Pusan Natl Univ 1962;4:21-38.
5. Lee JT. Studies on the metacercariae from freshwater fishes in the Kum-Ho River. Korean J Parasitol 1968;6:77-99. https://doi.org/10.3347/kjp.1968.6.3.77
6. Hwang JT, Choi DW. Changing pattern of infestation with larval trematodes from freshwater fish in river Kumho, Kyungpook Province, Korea. Kyungpook Univ Med J 1980;21:460-75.
7. Kong HH, Choi BR, Moon CH, Choi DW. Larval digenetic trema-

todes from fresh water fish in river Miryang, Korea. Jpn J Parasitol 1995;44:112-8.
8. Sohn WM, Choi YS. Infection status with trematode metacercariae in the fresh-water fish from Chunamchosuchi (pond), Uichang-gun, Kyongsangnam-do, Korea. Korean J Parasitol 1997;35:165-70. https://doi.org/10.3347/kjp.1997.35.3.165
9. Sohn WM, Na BK. Infections with digenetic trematode metacercariae in freshwater fishes from two visiting sites of migratory birds in Gyeongsangnam-do, Republic of Korea. Korean J Parasitol 2019;57:273-81. https://doi.org/10.3347/kjp.2019.57.3.273
10. Sohn WM, Na BK, Cho SH, Ju JW, Son DC. Prevalence and intensity of *Clonorchis sinensis* metacercariae in freshwater fish from Wicheon stream in Gunwi-gun, Gyeongsangbuk-do, Korea. Korean J Parasitol 2018;56:41-8. https://doi.org/10.3347/kjp.2018.56.1.41
11. Sohn WM, Na BK, Cho SH, et al. High endemicity with *Clonorchis sinensis* metacercariae in fish from Yongjeon-cheon (stream) in Cheongsong-gun, Gyeong-sangbuk-do, Korea. Korean J Parasitol 2021;59:97-101. https://doi.org/10.3347/kjp.2021.59.1.97
12. Lee MR, Ju JW, Baek SO, Lee YJ, Lee HI. The survey of infection status of *Clonorchis sinensis* metacercariae of freshwater fish in 2022. Jugan Geongang Gwa Jilbyeong 2023;16:1455-63. https://doi.org/10.56786/PHWR.2023.16.43.1
13. Sohn WM. Infection characteristics of *Clonorchis sinensis* metacercariae in fish from Republic of Korea. Korean J Parasitol 2022;60:79-96. https://doi.org/10.3347/kjp.2022.60.2.79
14. Sohn WM, Na BK, Cho SH, et al. Infections with *Centrocestus armatus* metacercariae in fishes from water systems of major rivers in Republic of Korea. Korean J Parasitol 2018;56:341-9. https://doi.org/10.3347/kjp.2018.56.4.341
15. Sohn WM. Infection characteristics of *Metagonimus* species (Digenea: Heterophyidae) metacercariae in fish from major rivers of Korea. Parasites Hosts Dis 2024;62:1-29. https://doi.org/10.3347/PHD.23096
16. Kim IS, Kang EJ. Coloured fishes of Korea. Academy Publishing Company; 1993.
17. Sohn WM. Fish-borne zoonotic trematode metacercariae in the Republic of Korea. Korean J Parasitol 2009;47 Suppl:S103-13. https://doi.org/10.3347/kjp.2009.47.S.S103
18. Sohn WM, Na BK, Cho SH, et al. Endemicity of zoonotic trematode metacercariae in fish from Deokcheon-gang (river) in Sancheong-gun, Gyeongsangnam-do, Republic of Korea. Korean J Parasitol 2021;59:523-9. https://doi.org/10.3347/kjp.2021.59.5.523

Brief Communication

Parasites Hosts Dis 2026;64(3):270-273
https://doi.org/10.3347/PHD.26047

Parasites, Hosts and Diseases

pISSN 2982-5164 • eISSN 2982-6799

Accession-level reassessment of *cox1* identity in the first Korean case of *Echinococcus multilocularis*

Jihun Kim[1], Dongmi Kwak[1,2,*]

[1]College of Veterinary Medicine, Kyungpook National University, Daegu, Korea; [2]Institute for Veterinary Biomedical Science, College of Veterinary Medicine, Kyungpook National University, Daegu, Korea

The first Korean case of *Echinococcus multilocularis* interpreted the probable origin of the isolate on the basis of *cox1* sequence similarity, originally reporting 99.8%–99.9% similarity to Asian isolates and 99.5%–99.6% similarity to European isolates. To examine whether this similarity-based interpretation remains epidemiologically informative, we re-evaluated currently available *cox1* sequences with high sequence identity at the accession level. Using AB780998.1 as the query, BLAST hits with ≥99.5% identity were collected, and 110 non-self accessions were manually annotated according to clade classifications reported in the source literature. Sequence alignment and phylogenetic assessment were performed with MAFFT and IQ-TREE. Across the re-evaluated dataset, sequences with identities from 99.5025% to 99.6269% were predominantly classified as European, whereas all sequences from 99.6891% to 99.9378% were classified as Asian. The only 2 exceptions to this overall pattern were OR263180 and OR263183, which were classified as Asian despite falling within the lower identity band. These 2 accessions were reported in a study using a concatenated mitochondrial framework including *cox1*, *cob*, and *nad2*, suggesting that single-marker interpretation may be limited in such borderline cases. In the 1,608 bp alignment, 1,544 sites were constant and only 19 were parsimony-informative. Despite this limited variation, *cox1* percent identity showed strong concordance with classification of Asian and European groups reported in the source literature. These findings indicate that high *cox1* identity may serve as a practical proxy for broad lineage discrimination between Asian and European groups of *E. multilocularis*, although rare borderline cases may require confirmation with multiple mitochondrial markers.

Keywords: *Echinococcus multilocularis*, alveolar echinococcosis, mitochondrial DNA, sequence analysis, phylogeny

Echinococcus multilocularis is the causative agent of alveolar echinococcosis, a potentially fatal zoonotic disease in humans, and is distributed predominantly throughout the Northern Hemisphere [1]. A previous mitochondrial phylogeographic study has identified the broad geographic structuring of *E. multilocularis* corresponding to European, Asian, and North American clades [2]. In Korea, where indigenous infection had not previously been documented, the first reported case of *E. multilocularis* was interpreted epidemiologically on the basis of cytochrome c oxidase subunit 1 (*cox1*) sequence similarity [3]. The present study re-examines whether this similarity-based interpretation remains epidemiologically valid in light of currently available accession-level sequence data.

The original Korean report demonstrated that the Korean isolate shared 99.8%–99.9% *cox1* sequence similarity with Asian isolates, with the highest similarity to an isolate from Sichuan,

Received: May 31, 2026 Accepted: June 8, 2026
*Correspondence: dmkwak@knu.ac.kr

Citation
Kim J, Kwak D. Accession-level reassessment of *cox1* identity in the first Korean case of *Echinococcus multilocularis*. Parasites Hosts Dis 2026;64(3):270-273.

China, whereas similarity with European isolates ranged from 99.5% to 99.6% [3]. In this regional context, *E. multilocularis* populations from the Western Sichuan Plateau have been reported to exhibit low genetic variation based on microsatellite and mitochondrial markers, with partial *cox1* haplotypes assigned to the Asian clade [4]. Although the original interpretation has been regarded as epidemiologically informative, its validity at the accession level has not been reassessed against the larger number of highly similar *cox1* accessions currently available in public databases. Accordingly, we revisited this issue by evaluating whether the identity ranges described in the original Korean case remain concordant with Asian and European classifications in the source literature when currently retrievable accessions with high sequence identity are examined individually. Therefore, the present study focused on an accession-level re-evaluation of the epidemiologic interpretation of the first Korean case, rather than proposing a revised phylogeographic framework for *E. multilocularis*.

Using AB780998.1 as the query sequence, BLAST hits with ≥99.5% identity were collected. After excluding the query sequence itself, 110 accessions remained for evaluation. This study was intentionally restricted to the high-identity interval relevant to the original Korean report and was not designed to assess the full sequence diversity of *E. multilocularis*. For each accession, geographic metadata were compiled, and the corresponding source study was manually identified. Lineage assignments were adopted from the corresponding source literature and were not inferred de novo from geographic origin or phylogenetic reconstruction in the present study. The lineage terminology used here follows the continental-scale grouping framework for *E. multilocularis* originally described by Nakao et al. [2]. Complete accession-level annotations are presented in Supplementary Table S1. Geographic metadata (geo_loc_name) were obtained from NCBI, whereas lineage classification was based on a manual review of the corresponding source studies listed in Supplementary Table S1.

As a complementary analysis, the 110 *cox1* sequences were aligned using MAFFT [5] and analyzed in IQ-TREE 3 by ModelFinder and ultrafast bootstrap analysis [6-8]. In the resulting alignment comprising 1,608 bp, 1,544 sites were constant, and only 19 sites were parsimony-informative. ModelFinder identified HKY+F+G4 as the best-fit model according to the Bayesian information criterion [6,7]. The small number of informative sites indicated limited phylogenetic resolution from this marker alone, particularly for finer internal relationships [9]. Consistent with this observation, bootstrap support across internal nodes was generally low (median, 17; mean, 32.77; range, 1–99). Nevertheless, despite the weak internal support caused by high sequence homogeneity, the distribution of percent identity values showed clear separation between the 2 broad geographical groups.

Despite the limited phylogenetic signal, a distinct pattern of segregation by percent identity was observed. Accessions with percent identities ranging from 99.5025% to 99.6269% were predominantly classified as European in the source literature, with only 2 Asian-classified exceptions (OR263180 and OR263183). In contrast, all accessions with identities ranging from 99.6891% to 99.9378% were classified as Asian. Therefore, within the ≥99.5% identity interval, lower identity values corresponded predominantly to European-classified sequences, whereas higher identity values were exclusively associated with Asian-classified sequences (Fig. 1). These findings support the epidemiologic interpretation proposed in the original Korean report [3].

The 2 exceptional accessions (OR263180 and OR263183) were both reported in a study conducted in Yili Prefecture, Xinjiang [10]. In that study, lineage interpretation was based on a concatenated mitochondrial framework incorporating *cox1*, cytochrome b (*cob*), and NADH dehydrogenase subunit 2 (*nad2*); notably, both accessions were linked to the same *cob* accession (OR243690) rather than being evaluated on the basis of *cox1* alone [10]. Therefore, these cases may be more appropriately regarded as boundary cases illustrating the limitations of single-marker interpretation rather than as direct contradictions to the overall segregation pattern. The purpose of identifying these exceptions is not to resolve their phylogeographic origin but to demonstrate that *cox1* identity can still provide a practical epidemiologic proxy under conditions of limited sequence information. However, in borderline or discordant cases, lineage interpretation should be approached cautiously and supported by additional mitochondrial markers (e.g., *cob* and *nad2*) or by previously established multi-marker classification frameworks.

Even within this highly homogeneous dataset, percent identity retained substantial classificatory signal. Beyond simply expanding the comparison set, the present study shows that even within a narrow high-identity interval, *cox1* percent identity in *E. multilocularis* remained informative at a broad phylogeographic level, with lower identity values corresponding predominantly to European-classified accessions and higher identity values confined to Asian-classified accessions. This observation is notable because, despite the limited number of parsimony-informative sites and generally low internal bootstrap support, these identity ranges remained strongly concordant

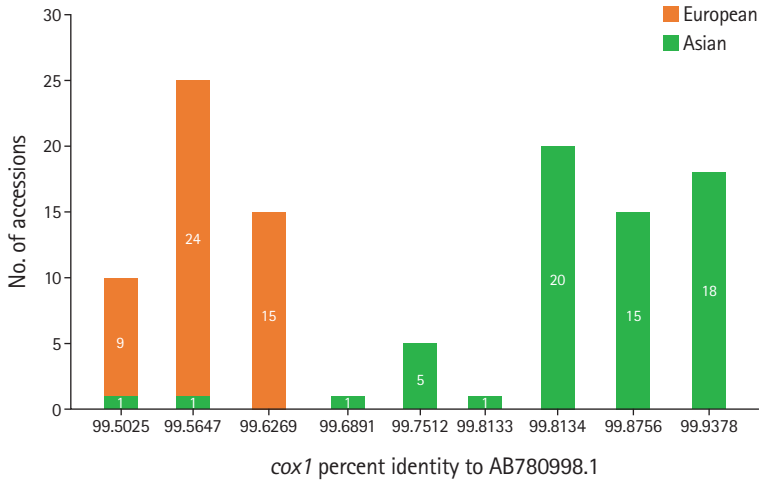

Fig. 1. Frequency distribution of *cox1* percent identity values relative to AB780998.1 among 110 non-self *Echinococcus multilocularis* accessions classified as Asian or European in the source literature. Bars indicate the number of accessions assigned to each group at each observed percent identity value.

with source-based continental classification. Although variation across the 1,608 bp region was limited, identity values remained strongly associated with annotation as Asian or European in the source literature. Taken together, these findings suggest that the *cox1* similarity ranges reported for the first Korean case were not merely descriptive but were broadly consistent with later evidence evaluated at the accession level [3]. The present analysis does not argue that percent identity should replace phylogenetic or haplotype-based inference in general. Rather, it shows that in the present *E. multilocularis* dataset, *cox1* percent identity was strongly concordant with source-based classification of Asian and European groups, allowing percent identity to function as a practical epidemiologic proxy, while rare borderline cases may benefit from confirmation with additional mitochondrial markers such as *cob* or *nad2* [10].

Author contributions

Conceptualization: Kim J. Data curation: Kim J. Formal analysis: Kim J. Investigation: Kim J. Methodology: Kim J. Supervision: Kwak D. Validation: Kim J, Kwak D. Visualization: Kim J. Writing-original draft: Kim J. Writing-review & editing: Kim J, Kwak D.

Conflict of interest

Dongmi Kwak serves as an editor of Parasites, Hosts and Diseases but had no involvement in the decision to publish this article. No other potential conflicts of interest relevant to this study were reported.

Supplementary information

Supplementary material is available with this article at https://doi.org/10.3347/PHD.26047.

ORCID

Jihun Kim, https://orcid.org/0009-0001-7303-2033
Dongmi Kwak, https://orcid.org/0000-0003-0876-3179

References

1. Baumann S, Shi R, Liu W, et al. Worldwide literature on epidemiology of human alveolar echinococcosis: a systematic review of research published in the twenty-first century. Infection 2019;47:703-27. https://doi.org/10.1007/s15010-019-01325-2
2. Nakao M, Xiao N, Okamoto M, et al. Geographic pattern of genetic variation in the fox tapeworm *Echinococcus multilocularis*. Parasitol Int 2009;58:384-9. https://doi.org/10.1016/j.parint.2009.07.010
3. Jeong JS, Han SY, Kim YH, et al. Serological and molecular characteristics of the first Korean case of *Echinococcus multilocularis*. Korean J Parasitol 2013;51:595-7. https://doi.org/10.3347/kjp.2013.51.5.595
4. Shang JY, Zhang GJ, Liao S, et al. Low genetic variation in *Echinococcus multilocularis* from the Western Sichuan Plateau of China revealed by microsatellite and mitochondrial DNA markers. Acta Trop 2021;221:105989. https://doi.org/10.1016/j.actatropica.2021.105989
5. Katoh K, Misawa K, Kuma K, Miyata T. MAFFT: a novel method for rapid multiple sequence alignment based on fast Fourier transform. Nucleic Acids Res 2002;30:3059-66. https://doi.org/10.1093/nar/gkf436
6. Wong TKF, Ly-Trong N, Ren H, et al. IQ-TREE 3: phylogenomic inference software using complex evolutionary models [Preprint]. Posted

2025 Apr 7. EcoEvoRxiv. https://doi.org/10.32942/X2P62N

7. Kalyaanamoorthy S, Minh BQ, Wong TKF, von Haeseler A, Jermiin LS. ModelFinder: fast model selection for accurate phylogenetic estimates. Nat Methods 2017;14:587-9. https://doi.org/10.1038/nmeth.4285
8. Hoang DT, Chernomor O, von Haeseler A, Minh BQ, Vinh LS. UFBoot2: improving the ultrafast bootstrap approximation. Mol Biol Evol 2018;35:518-22. https://doi.org/10.1093/molbev/msx281
9. Townsend JP, Su Z, Tekle YI. Phylogenetic signal and noise: predicting the power of a data set to resolve phylogeny. Syst Biol 2012;61:835-49. https://doi.org/10.1093/sysbio/sys036
10. Guo B, Cairen, Wu J, et al. The A2 haplotype of *Echinococcus multilocularis* is the predominant variant infecting humans and dogs in Yili Prefecture, Xinjiang. Infect Genet Evol 2024;119:105581. https://doi.org/10.1016/j.meegid.2024.105581

Brief Communication

Parasites Hosts Dis 2026;64(3):274-280
https://doi.org/10.3347/PHD.26010

Parasites, Hosts and Diseases

pISSN 2982-5164 • eISSN 2982-6799

Molecular detection of *Bartonella* species and *Coxiella* endosymbiont in human-biting *Haemaphysalis longicornis* ticks in Korea

Choon-Mee Kim[1,†], Merlin Jayalal Lawrence Panchali[2,†], You Mi Lee[2], Na Ra Yun[2], Dong-Min Kim[2,*]

[1]Premedical Science, College of Medicine, Chosun University, Gwangju, Korea; [2]Department of Internal Medicine, College of Medicine, Chosun University, Gwangju, Korea

Bartonella species are vector-borne pathogens that infect a wide range of hosts, including humans. Although several *Bartonella* species have been identified in rodents and arthropods in Korea, information on *Bartonella* detection in ticks removed from human patients remains limited. This study investigated the presence of *Bartonella* species DNA in human-biting ticks collected in Korea and screened for other tick-associated bacteria, including *Coxiella* endosymbiont. From January to December 2018, 35 ticks were removed from 29 tick-bitten patients in Jeollanam-do and Gwangju, Korea. Ticks were identified morphologically and molecularly by *16S rRNA* gene PCR. The presence of *Bartonella* species was assessed using nested PCR targeting the 16S-23S internal transcribed spacer (*ITS*) region. The ticks were identified as *Haemaphysalis longicornis* (17/35, 48.6%), *Amblyomma testudinarium* (14/35, 40.0%), and *Ixodes nipponensis* (4/35, 11.4%). Two *H. longicornis* ticks tested positive for *Bartonella* species. Sequencing revealed 99.5% identity with *B. bacilliformis* isolate GJR*ITS*124 in one tick and 98.9% identity with *B. taylorii* isolate 190731_HC2 in the other, both previously identified in *Apodemus agrarius* rodents in Korea. One *B. bacilliformis*-positive tick was also positive for *Coxiella* spp., and sequence analysis indicated a *Coxiella* endosymbiont showing 100.0% identity with the *Coxiella*-like endosymbiont strain 580. Phylogenetic analysis supported these findings; however, bacterial cultures from PCR-positive tick lysates were negative. This study provides baseline evidence of *B. bacilliformis* and *B. taylorii*, as well as *Coxiella* endosymbiont DNA in human-biting *H. longicornis* ticks in Korea and highlights the need for continued surveillance.

Keywords: Ticks, *Bartonella*, *Coxiella*, tick-borne infections, polymerase chain reaction

Ectoparasites, such as ticks, are prominent vectors of numerous infectious diseases, including those caused by bacteria, viruses, and protozoans. Ticks are haematophagous arthropods, and their ability to acquire and maintain pathogens is influenced by complex tick-pathogen interactions and vector competence-related mechanisms [1]. However, for *Bartonella* species, the role of ticks as vectors remains uncertain and has not been conclusively demonstrated. *Bartonella* species are zoonotic bacteria present in various mammals, including rodents, cats, ruminants, and humans [2]. Although several studies have suggested possible tick-associated transmission, their role as definitive vectors remains controversial [3]. Molecular surveys have detected *Bartonella* DNA in multiple tick genera, including *Haemaphysalis* and *Ixodes* across different geographic regions [4,5]. However, direct transmission of *Bartonella* species from ticks to mammalian hosts has not been conclusively demonstrated [3].

Received: February 9, 2026 Accepted: March 9, 2026
*Correspondence: drongkim@chosun.ac.kr
†These authors contributed equally to this work.

Citation
Kim CM, Panchali MJL, Lee YM, Yun NR, Kim DM. Molecular detection of *Bartonella* species and *Coxiella* endosymbiont in human-biting *Haemaphysalis longicornis* ticks in Korea. Parasites Hosts Dis 2026;64(3):274-280.

Among *Bartonella* species, *B. bacilliformis* is a human-pathogenic organism typically associated with sandfly transmission, whereas *B. taylorii* is mainly maintained in rodent-flea cycles [6,7]. The involvement of ticks in the ecology of these species has not been established.

In East Asia, *Bartonella* DNA has been detected in ticks, including *H. longicornis*, collected in China, indicating that this tick species can harbor *Bartonella* in the region [5]. In Korea, multiple *Bartonella* species, including *B. grahamii*, *B. henselae*, *B. taylorii*, *B. tribocorum*, and *B. phoceensis*, have been identified in *Apodemus agrarius* rodents [8]. Additionally, *H. longicornis*, a dominant tick species in East Asia, is known to transmit several pathogens, including *Rickettsia*, *Anaplasma*, and severe fever with thrombocytopenia syndrome virus [5,9-11]. Given the increasing reports of *Bartonella* species in ticks globally, it is crucial to investigate their potential involvement in the transmission of *Bartonella* species. Understanding the interaction between *Bartonella* species and their potential tick vectors is critical for evaluating the epidemiological impact of tick-borne *Bartonella* infections. Therefore, this study investigated the molecular detection of *Bartonella* species DNA in ticks removed from human patients in Korea and performed additional screening PCR assays for other tick-associated pathogens, including *Rickettsia* spp., *Orientia tsutsugamushi*, *Anaplasma* spp., and *Coxiella* spp., to evaluate their occurrence at the human–tick interface.

Between January and December 2018, ticks removed from humans in Jeollanam-do and Gwangju, Korea, were collected during routine clinical care for tick-bitten patients at Chosun University Hospital, and sampling was based on clinical presentation rather than a predefined geographic or temporal survey design. The study was approved by the Ethics in Human Research Committee of Chosun University Hospital under an institutional review board that approves all experiments involving ticks and tick-bitten humans (No. CHOSUN 2013-10-001-018). Ticks were morphologically identified to the species and developmental stage (adult female, adult male, nymph, or larva) using standard taxonomic parameters and morphological features under a microscope [12]. Each identified tick was individually processed and subjected to molecular identification using conventional PCR (C-PCR) targeting mitochondrial *16S rRNA* [13].

Ticks at all developmental stages were washed in 70% ethanol and rinsed twice with sterile phosphate-buffered saline. Each tick was transferred to a hard tissue grinding MK28 tube (Bertin Technology) containing 800 μl of phosphate-buffered saline with 1× PC/SM (penicillin and streptomycin), ground using a FastPrep-24 Classic instrument (MP Biomedicals), and then stored at -80°C until DNA extraction. For DNA extraction, 150 μl of the homogenized tick lysate was mixed with 150 μl ATL buffer and 20 μl proteinase K and incubated at 56°C overnight for lysis; genomic DNA was extracted using the QIAamp Tissue & Blood Mini Kit (Qiagen) according to the manufacturer's instructions.

PCR amplification was performed using target-specific primers and AmpliTaq Gold 360 Master Mix (Applied Biosystems) on an AB thermal cycler (Applied Biosystems). The 16S-23S internal transcribed spacer (*ITS*) region was targeted for detection of *Bartonella* species [8], and PCR reactions included positive controls (*B. henselae* DNA) and negative controls (molecular-grade water). Additional screening PCR assays were performed for *Rickettsia* spp., *Orientia tsutsugamushi*, *Anaplasma* spp., and *Coxiella* spp. using previously described primers and conditions (Supplementary Table S1) [8,13-17]. For nested PCR, the reaction mixture was identical to that used for C-PCR, except that the first PCR product was used as template DNA with nested PCR primers, and the screening results are presented in Table 1.

The amplified PCR products were purified using the QIAquick PCR Purification Kit (Qiagen) and sequenced with PCR primers (Solgent). Obtained sequences were compared with GenBank database entries using the Basic Local Alignment Search Tool (BLAST) provided by the National Center for Biotechnology Information and aligned using Lasergene version 8

Table 1. Identification of ticks and detection of tick-borne pathogens in ticks collected from human patients

Tick No.	Tick species	Tick developmental stage	*Rickettsia spp.*	*Orientia tsutsugamushi*	*Anaplasma spp.*		*Coxiella spp.*		*Bartonella spp.*
			ompA	*56 kDa*	*groEL*	*ankA*	*16S rRNA*	*IS1111*	*ITS*
Tick 1	*Haemaphysalis longicornis*	Adult female	-	-	-	-	-	-	*Bartonella taylorii*
Tick 2	*H. longicornis*	Adult female	-	-	-	-	*Coxiella* endosymbiont	-	*Bartonella bacilliformis*

ompA, outer membrane protein A gene; *56 kDa*, 56-kDa type-specific antigen gene; *groEL*, heat shock protein gene; *ankA*, ankyrin-related protein gene; *16S rRNA*, 16S ribosomal RNA gene; *IS1111*, *htpAB*-associated repetitive element; *ITS*, 16S-23S internal transcribed spacer region; -, not detected.

(DNASTAR). Phylogenetic trees were constructed by the neighbor-joining method based on ClustalW alignments using the MegAlign program (DNASTAR). Bootstrap analysis (1,000 replicates) was performed using the Kimura 2-parameter model. Pairwise alignments were performed with an open-gap penalty of 10 and a gap extension penalty of 0.5. Bacterial culture of *Bartonella* species PCR-positive tick lysates was performed on heart infusion agar blood plates using 200 μl of the homogenized tick lysate [18].

All ticks examined in this study were fed or partially fed ticks that had been removed from human patients during clinical visits. From 29 tick-bitten patients, a total of 35 ticks were obtained, of which 19 ticks (54.3%) were adults, including 16 (45.7%) females and 3 males (8.6%). Thirteen ticks (37.1%) were nymphs, and 3 (8.6%) were larvae based on morphological examination using a microscope for tick identification. The ticks were identified as *H. longicornis* (17 ticks, 48.6%; 12 adult females, 2 nymphs, and 3 larvae), *Amblyomma testudinarium* (14 ticks, 40.0%; 3 adult males and 11 nymphs), and *Ixodes nipponensis* (4 ticks, 11.4%; 4 adult females), as described in Table 2. Tick identification using 16S rDNA C-PCR and DNA sequencing yielded the same results as microscopic examination (Table 2).

A total of 35 ticks were examined for the detection of *Bartonella* species using *Bartonella*-specific 16S-23S *ITS* nested PCR. Among these, 2 ticks (2 out of 35, 5.7%) tested positive for *Bartonella* species. Both *Bartonella*-positive ticks were identified as *H. longicornis* (Table 1; Supplementary Fig. S1). The positive PCR products were sequenced, and the resulting sequences were aligned with reference sequences obtained from the GenBank database to identify known sequences with a high degree of similarity using ClustalW. The DNA sequence analysis revealed the presence of *B. taylorii* in tick 1 and *B. bacilliformis* in tick 2. Homology testing showed that the *B. taylorii*-positive tick 1 exhibited 98.9% identity with *B. taylorii* isolate 190731_HC2 (GenBank accession No. OR288191.1), and the *B. bacilliformis*-positive tick 2 exhibited 99.5% identity with *B. bacilliformis* isolate GJR*ITS*124 (GenBank accession No. PQ888831.1), both previously identified in *A. agrarius* rodents in Korea. A phylogenetic tree was constructed based on the alignment of 16S–23S *ITS* sequences obtained from the 2 *Bartonella*-positive *H. longicornis* ticks together with reference *Bartonella* sequences retrieved from GenBank. In the phylogenetic analysis, the sequence from tick 1 clustered with *B. taylorii*, whereas the sequence from tick 2 clustered with *B. bacilliformis* (Fig. 1), supporting the species identification based on sequence similarity. The 16S–23S *ITS* nested PCR product sequences generated in this study were deposited in the GenBank database under accession numbers PX864259 (*B. taylorii*, tick 1) and PX864260 (*B. bacilliformis*, tick 2).

No DNA of *Rickettsia* spp., *O. tsutsugamushi*, or *Anaplasma* spp. was detected in any of the examined ticks. One tick (tick 2) tested positive by PCR for *Coxiella* spp.; however, sequence analysis indicated that this signal corresponded to a *Coxiella* endosymbiont rather than *Coxiella burnetii* (Table 1). Homology analysis demonstrated that the *Coxiella* endosymbiont–positive tick 2 exhibited 100.0% identity with the *Coxiella*-like endosymbiont strain 580 chromosome (GenBank accession No. CP084737.1). The partial *16S rRNA* gene sequence of the *Coxiella* endosymbiont detected in *H. longicornis* tick 2 was deposited in the GenBank database under accession number PZ039301 (*Coxiella* endosymbiont, tick 2). A phylogenetic tree based on the partial *16S rRNA* sequence obtained from the *Coxiella* endosymbiont-positive tick 2 was constructed with reference sequences from GenBank, and the sequence clustered with *Coxiella* endosymbionts (Fig. 2). No viable *Bartonella* colonies were obtained from PCR-positive tick lysates, indicating the difficulty of isolating viable *Bartonella* organisms from tick vectors under the culture conditions used.

Detection of *B. bacilliformis* and *B. taylorii* DNA and *Coxiella* endosymbiont DNA in human-biting *H. longicornis* ticks demonstrates the presence of tick-associated bacterial DNA at the human-tick interface in Korea. However, molecular detection alone does not demonstrate transmission by ticks. Previous studies have also detected *Bartonella* DNA in various tick genera worldwide [4,5], indicating that ticks may harbor the organism under natural conditions [4].

Table 2. 16S rDNA-targeting conventional PCR and morphological identification of ticks collected from patients

Development stage/tick species	*Haemaphysalis longicornis*	*Amblyomma testudinarium*	*Ixodes nipponensis*	Species total
Adult female	12 (70.6)	0 (0)	4 (100)	16 (45.7)
Adult male	0 (0)	3 (21.4)	0 (0)	3 (8.6)
Nymph	2 (11.8)	11 (78.6)	0 (0)	13 (37.1)
Larva	3 (17.6)	0 (0)	0 (0)	3 (8.6)
Stage total	17 (48.6)	14 (40.0)	4 (11.4)	35 (100)

Values are presented as number (%).

https://doi.org/10.3347/PHD.26010

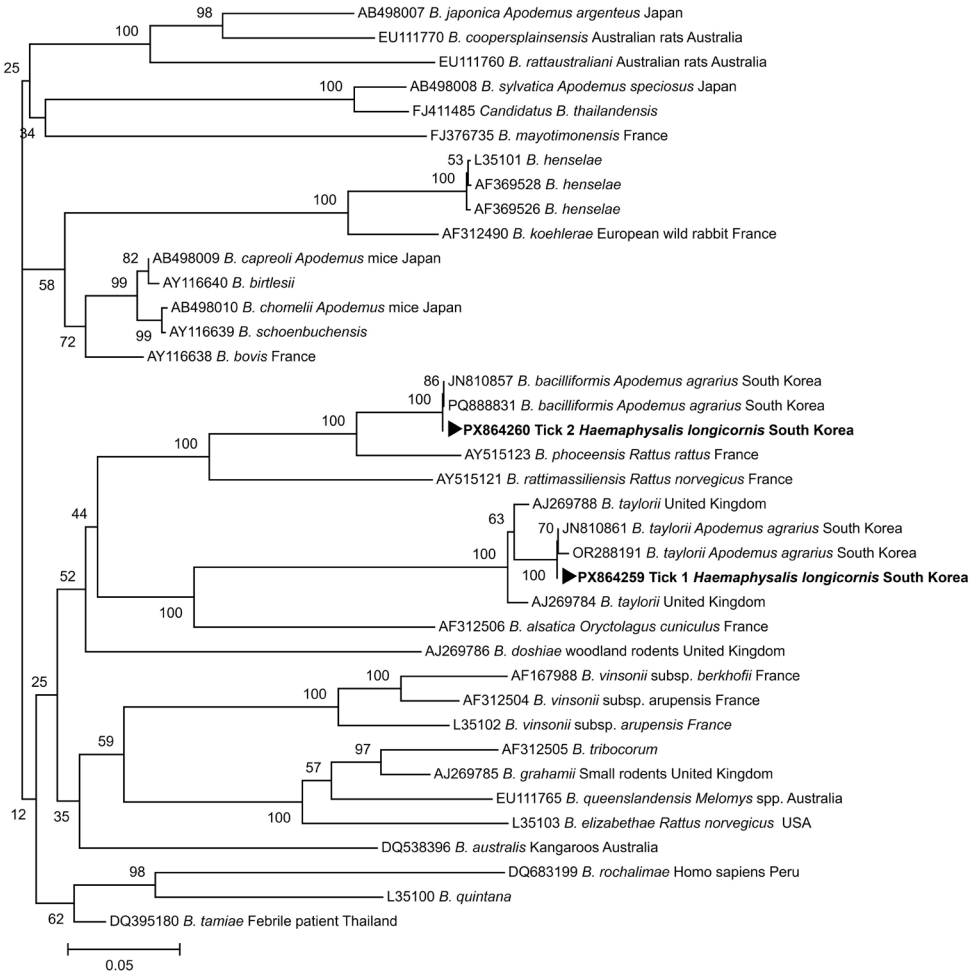

Fig. 1. Phylogenetic tree constructed based on partial 16S–23S internal transcribed spacer (*ITS*) sequences of the *Bartonella* spp. detected in 2 *Haemaphysalis longicornis* ticks (tick 1 and tick 2) removed from human patients in Korea (►), together with reference *Bartonella* sequences retrieved from the GenBank database. The phylogenetic tree was constructed using the neighbor-joining method. Bootstrap values based on 1,000 replicates are shown at the branch nodes.The scale bar represents 0.05 nucleotide substitutions per site. GenBank accession numbers are indicated for all reference sequences. Host and country information for the reference sequences are provided. For some reference sequences retrieved from GenBank, information on the host and/or country of origin was not available in the original database records.

Phylogenetic analysis showed that the *Bartonella* sequences detected in human-biting ticks were closely related to strains previously reported from *A. agrarius* rodents in Korea, showing 99.5% identity for *B. bacilliformis* and 98.9% identity for *B. taylorii*. These findings suggest that the *Bartonella* DNA detected in ticks removed from human patients showed sequence similarity to strains previously detected in rodents in Korea. However, the ecological or epidemiological relationships among rodents, ticks, and humans cannot be determined based solely on the molecular data obtained in this study.

The 2 *Bartonella*-positive *H. longicornis* ticks were collected from different patients. One tick (tick 1) positive for *B. taylorii* was removed from a patient (2018-Lee01) who presented solely for tick removal without fever or other systemic symptoms suggestive of bartonellosis. The other tick (tick 2), which tested positive for *B. bacilliformis*, was removed from a different patient (2018-505) who presented with fever; however, no clinical features characteristic of bartonellosis, such as Oroya fever, verruga peruana, endocarditis, or lymphadenopathy, were identified during clinical evaluation. No laboratory or clinical evidence of confirmed human *Bartonella* infection was documented in either patient.

One possible explanation for this sequence similarity is that the detected *Bartonella* DNA may have originated from the blood meal of infected rodent hosts, such as *A. agrarius*, rather than reflecting active infection or transmission by the tick, as previous studies have emphasized that detection of *Barton-*

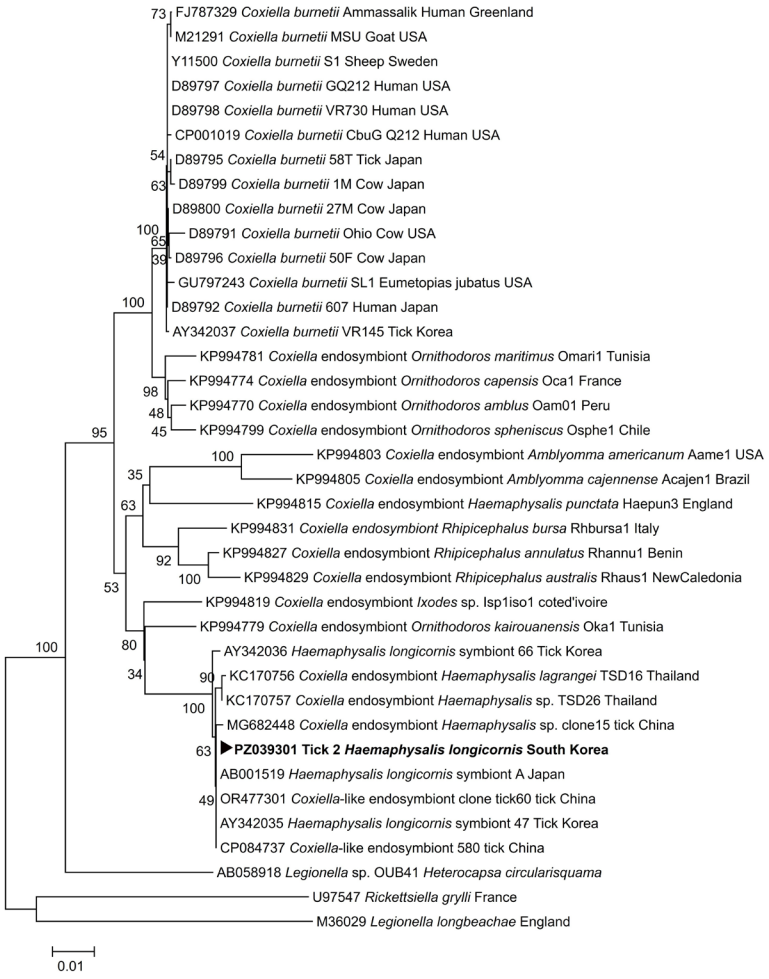

Fig. 2. Phylogenetic tree constructed based on partial *16S rRNA* gene sequences of the *Coxiella* endosymbiont detected in a *Haemaphysalis longicornis* tick (tick 2) removed from human patients in Korea (►), together with reference sequences of *Coxiella burnetii* and *Coxiella* endosymbionts retrieved from the GenBank database. The phylogenetic tree was constructed using the neighbor-joining method. Bootstrap values based on 1,000 replicates are shown at the branch nodes. The scale bar represents 0.01 nucleotide substitutions per site. GenBank accession numbers are indicated for all reference sequences.

ella DNA in ticks does not necessarily indicate vector competence [3]. Consistent with this interpretation, bacterial cultures of PCR-positive tick lysates were negative in this study, further illustrating the difficulty of isolating viable *Bartonella* organisms and highlighting the limitations of current culture-based approaches.

This study has several limitations, including the relatively small number of ticks examined, the restriction of sampling to a single year, and the clinical-based consecutive collection of ticks from patients at a single hospital, which limits epidemiological interpretation. Nevertheless, previous studies in Korea have reported the presence of *Bartonella* DNA in various tick species and rodents, and human infections have also been reported, supporting the zoonotic relevance of these organisms [4,19]. Similar molecular findings from other regions, including the detection of *B. taylorii* in rodent species such as *A. flavicollis*, *A. sylvaticus*, and *Clethrionomys glareolus* in Slovenia, indicate that these pathogens occur across diverse geographic settings and host species [20]. Future studies incorporating quantitative PCR to estimate bacterial load, multilocus sequence typing, or metagenomic approaches would help further validate species identification and provide a more comprehensive understanding of *Bartonella* diversity detected in human-biting ticks.

In conclusion, this study provides baseline evidence for the presence of *B. bacilliformis* and *B. taylorii*, as well as *Coxiella* endosymbiont DNA in *H. longicornis* ticks removed from human patients in Korea. The findings are limited to molecular detection in a small number of fed ticks and do not demonstrate transmission by ticks. These results provide baseline

https://doi.org/10.3347/PHD.26010

detection data for tick-associated bacterial DNA, including *Bartonella* and *Coxiella* endosymbiont, in human-biting ticks in Korea and support further studies to clarify the ecological relevance of these findings in human exposure settings.

Data availability

Data and materials are available upon request to the corresponding author.

Author contributions

Conceptualization: Kim DM. Data curation: Kim CM, Lee YM. Formal analysis: Kim CM, Panchali MJL. Funding acquisition: Kim DM. Investigation: Kim CM, Panchali MJL, Lee YM. Methodology: Lee YM. Project administration: Kim DM. Resources: Lee YM, Yun NR. Supervision: Kim DM, Yun NR. Validation: Kim CM, Panchali MJL. Visualization: Lee YM, Yun NR. Writing - original draft: Kim CM, Panchali MJL. Writing - review & editing: Kim DM, Kim CM, Panchali MJL.

Conflict of interest

The authors have no conflicts of interest to declare.

Funding

This study was supported by a research fund from Chosun University Hospital (2025).

Supplementary information

Supplementary material is available with this article at https://doi.org/10.3347/PHD.26010.

ORCID

Choon-Mee Kim, https://orcid.org/0000-0003-4404-6214
Merlin Jayalal Lawrence Panchali, https://orcid.org/0009-0006-8714-3611
You Mi Lee, https://orcid.org/0009-0002-4202-8282
Na Ra Yun, https://orcid.org/0000-0002-4219-0127
Dong-Min Kim, https://orcid.org/0000-0001-6373-0922

References

1. de la Fuente J, Antunes S, Bonnet S, et al. Tick-pathogen interactions and vector competence: identification of molecular drivers for tick-borne diseases. Front Cell Infect Microbiol 2017;7:114. https://doi.org/10.3389/fcimb.2017.00114
2. Deng H, Pang Q, Zhao B, Vayssier-Taussat M. Molecular mechanisms of *Bartonella* and mammalian erythrocyte interactions: a review. Front Cell Infect Microbiol 2018;8:431. https://doi.org/10.3389/fcimb.2018.00431
3. Angelakis E, Billeter SA, Breitschwerdt EB, Chomel BB, Raoult D. Potential for tick-borne bartonelloses. Emerg Infect Dis 2010;16:385-91. https://doi.org/10.3201/eid1603.081685
4. Kim CM, Kim JY, Yi YH, et al. Detection of *Bartonella* species from ticks, mites and small mammals in Korea. J Vet Sci 2005;6:327-34. https://doi.org/10.4142/jvs.2005.6.4.327
5. Sun J, Liu Q, Lu L, et al. Coinfection with four genera of bacteria (*Borrelia*, *Bartonella*, *Anaplasma*, and *Ehrlichia*) in *Haemaphysalis longicornis* and *Ixodes sinensis* ticks from China. Vector Borne Zoonotic Dis 2008;8:791-5. https://doi.org/10.1089/vbz.2008.0005
6. Bai Y, Kosoy MY, Boonmar S, et al. Enrichment culture and molecular identification of diverse *Bartonella* species in stray dogs. Vet Microbiol 2010;146:314-9. https://doi.org/10.1016/j.vetmic.2010.05.017
7. Marié JL, Fournier PE, Rolain JM, et al. Molecular detection of *Bartonella quintana*, *B. elizabethae*, *B. koehlerae*, *B. doshiae*, *B. taylorii*, and *Rickettsia felis* in rodent fleas collected in Kabul, Afghanistan. Am J Trop Med Hyg 2006;74:436-9. https://doi.org/10.4269/ajtmh.2006.74.436
8. Ko S, Kang JG, Kim HC, et al. Prevalence, isolation and molecular characterization of *Bartonella* species in Republic of Korea. Transbound Emerg Dis 2016;63:56-67. https://doi.org/10.1111/tbed.12217
9. Kim CM, Kim MS, Park MS, Park JH, Chae JS. Identification of *Ehrlichia chaffeensis*, *Anaplasma phagocytophilum*, and *A. bovis* in *Haemaphysalis longicornis* and *Ixodes persulcatus* ticks from Korea. Vector Borne Zoonotic Dis 2003;3:17-26. https://doi.org/10.1089/153036603765627424
10. Lee J, Moon K, Kim M, et al. Seasonal distribution of *Haemaphysalis longicornis* (Acari: Ixodidae) and detection of SFTS virus in Gyeongbuk Province, Republic of Korea, 2018. Acta Trop 2021;221:106012. https://doi.org/10.1016/j.actatropica.2021.106012
11. Stanley HM, Ford SL, Snellgrove AN, et al. The ability of the invasive Asian longhorned tick *Haemaphysalis longicornis* (Acari: Ixodidae) to acquire and transmit *Rickettsia rickettsii* (Rickettsiales: Rickettsiaceae), the agent of Rocky Mountain spotted fever, under laboratory conditions. J Med Entomol 2020;57:1635-9. https://doi.org/10.1093/jme/tjaa076
12. Yamaguti N, Tipton VJ, Keegan HL, Toshioka S. Ticks of Japan, Korea, and the Ryukyu Islands. Brigh Young Univ Sci Bull Biol Ser 1971;15:Article 1.
13. Tian Z, Liu G, Xie J, et al. Discrimination between *Haemaphysalis longicornis* and *H.s qinghaiensis* based on the partial 16S rDNA and the second internal transcribed spacer (ITS-2). Exp Appl Acarol 2011;54:165-72. https://doi.org/10.1007/s10493-010-9423-3
14. Bang MS, Kim CM, Park JW, et al. Prevalence of *Orientia tsut-*

sugamushi, *Anaplasma phagocytophilum* and *Leptospira interrogans* in striped field mice in Gwangju, Republic of Korea. PLoS One 2019;14:e0215526. https://doi.org/10.1371/journal.pone.0215526

15. Fenollar F, Fournier PE, Raoult D. Molecular detection of *Coxiella burnetii* in the sera of patients with Q fever endocarditis or vascular infection. J Clin Microbiol 2004;42:4919-24. https://doi.org/10.1128/JCM.42.11.4919-4924.2004
16. Regnery RL, Spruill CL, Plikaytis BD. Genotypic identification of rickettsiae and estimation of intraspecies sequence divergence for portions of two rickettsial genes. J Bacteriol 1991;173:1576-89. https://doi.org/10.1128/jb.173.5.1576-1589.1991
17. Roux V, Fournier PE, Raoult D. Differentiation of spotted fever group rickettsiae by sequencing and analysis of restriction fragment length polymorphism of PCR-amplified DNA of the gene encoding the protein rOmpA. J Clin Microbiol 1996;34:2058-65. https://doi.org/10.1128/jcm.34.9.2058-2065.1996
18. Minnick MF, Smitherman LS, Samuels DS. Mitogenic effect of *Bartonella bacilliformis* on human vascular endothelial cells and involvement of GroEL. Infect Immun 2003;71:6933-42. https://doi.org/10.1128/IAI.71.12.6933-6942.2003
19. Durey A, Kwon HY, Im JH, et al. *Bartonella henselae* infection presenting with a picture of adult-onset Still's disease. Int J Infect Dis 2016;46:61-3. https://doi.org/10.1016/j.ijid.2016.03.014
20. Knap N, Duh D, Birtles R, et al. Molecular detection of *Bartonella* species infecting rodents in Slovenia. FEMS Immunol Med Microbiol 2007;50:45-50. https://doi.org/10.1111/j.1574-695X.2007.00226.x

https://doi.org/10.3347/PHD.26010

Case Report

Parasites Hosts Dis 2026;64(3):281-284
https://doi.org/10.3347/PHD.26031

Parasites, Hosts and Diseases

pISSN 2982-5164 • eISSN 2982-6799

A case of severe strongyloidiasis complicating immunosuppressive therapy initiated for IgA vasculitis

Limei Hu[1,#], Yihe Chen[2,#], Ying Liang[1], Li Zhao[1,*]

[1]Department of Laboratory Medicine, The People's Hospital of Guangxi Zhuang Autonomous Region, Nanning, China; [2]Department of Emergency, The People's Hospital of Guangxi Zhuang Autonomous Region, Nanning, China

IgA vasculitis (IgAV) and *Strongyloides stercoralis* infection may both present with abdominal pain and purpura; however, glucocorticoid, the treatment for IgAV, is a major risk factor for *S. stercoralis* hyperinfection syndrome and disseminated strongyloidiasis. To date, only 2 cases of IgAV with concurrent *S. stercoralis* infection have been reported globally, both in children. We report a 72-year-old man presenting with abdominal pain and purpura. Diagnosed with IgAV during this admission, he received glucocorticoid therapy. However, the patient's condition did not improve as expected. Subsequently, *S. stercoralis* was detected in the patient's sputum and stool. We report the first adult case of IgAV with concurrent *S. stercoralis* infection, highlighting the importance of screening patients with IgAV for strongyloidiasis before initiating immunosuppressive therapy.

Keywords: IgA vasculitis, *Strongyloides stercoralis*, severe strongyloidiasis, immunosuppressive therapy

Introduction

IgA vasculitis (IgAV) is a systemic small-vessel vasculitis characterized by a clinical tetrad that includes palpable purpura, arthralgia and/or arthritis, abdominal pain, and renal disease [1]. Pathogens are known to induce IgAV. However, the relationship between IgAV and parasites has rarely been reported [2]. *Strongyloides stercoralis* is a soil-transmitted helminth widely distributed in tropical and subtropical regions worldwide. Its clinical manifestations can involve the skin, respiratory system, and digestive system. Immunosuppressive conditions can cause life-threatening hyperinfection syndrome and disseminated strongyloidiasis [3]. Given the similar clinical manifestations of IgAV and strongyloidiasis, and the use of glucocorticoids in IgAV [4], we report the first case of IgAV complicated by *S. stercoralis* infection in an adult, highlighting the importance of screening for strongyloidiasis in patients with IgAV.

Case Report

A 72-year-old man was admitted to the People's Hospital of Guangxi Zhuang Autonomous Region presenting with a 10-day history of upper mid-abdominal pain and nausea. He had a medical history of coronary heart disease, hypertension, and diabetes mellitus. Two months earlier, the patient had been evaluated at another hospital for a hepatic hilar mass, which was suspected to be caused by IgG4-related cholangitis. Treatment was initiated with oral methylprednisolone (glucocorticoid) 32 mg daily, with tapering by 4 mg every 2 weeks. He was admitted to the gastroenterology department for abdominal

Received: April 1, 2026 Accepted: May 12, 2026
*Correspondence: ZHAOzhao88356@163.com

[#]These authors contributed equally to this work.

Citation
Hu L, Chen Y, Liang Y, Zhao L. A case of severe strongyloidiasis complicating immunosuppressive therapy initiated for IgA vasculitis. Parasites Hosts Dis 2026;64(3):281-284.

pain evaluation. Physical examination revealed extensive non-blanching purpura and epigastric tenderness without significant rebound (Fig. 1A). Laboratory tests showed elevated inflammatory markers (C-reactive protein, 32.13 mg/L; normal range, 0–10 mg/L), hyperglycemia (blood glucose, 10.44 mmol/L; normal range, 3.9–6.1 mmol/L), and impaired cardiac function (high-sensitivity cardiac troponin, 39.13 ng/L; normal range, 0–14 ng/L); coagulation, liver and renal function, tumor markers, and autoimmune antibodies were all unremarkable. Fecal microscopy was not performed due to the patient's inability to defecate. Computed tomography imaging confirmed right lung inflammatory changes (Fig. 1B), and abdominal radiography revealed incomplete bowel obstruction (Fig. 1C). The presentation of typical palpable purpura with abdominal pain met the EULAR/PRINTO/PRES criteria for IgAV. Admission laboratory studies ruled out thrombotic thrombocytopenic purpura and other hemorrhagic rash disorders, as well as antineutrophil cytoplasmic antibody-associated vasculitis. Clinical and laboratory findings substantiated the diagnosis of IgAV, and methylprednisolone was initiated; concomitantly, right-sided pneumonia was treated with piperacillin-tazobactam, and incomplete bowel obstruction was managed by nasogastric decompression and therapeutic enemas.

On hospital day 7, the patient developed acute respiratory failure and was managed with endotracheal intubation and mechanical ventilation. Later the same day, *S. stercoralis* were identified in sputum under microscopic examination (Fig. 2A). Given the limited availability of ivermectin in China, albendazole was administered for the treatment of *S. stercoralis* infection. Blood agar culture of sputum showed bacterial colonies arranged in numerous serpiginous tracts, suggestive of multiple live, motile parasites (Fig. 2B). Gram staining of the smear prepared from the bacterial colony revealed the presence of Gram positive bacilli and *S. stercoralis* under the microscope (Fig. 2C). Bacteria were identified as *Corynebacterium striatum* by MALDI TOF mass spectrometry (Supplementary Fig. S1). The metagenomic next-generation sequencing of tracheal aspirate showed consistency with above identification (Supplementary Table S1). On hospital day 9, the family obtained ivermectin from overseas. Ivermectin was subsequently administered to treat *S. stercoralis* infection. On hospital day 11, *Aspergillus fumigatus* was isolated from tracheal aspirate cultures (Fig. 2D). On hospital day 13, stool examination demonstrated significant quantities of lifeless *S. stercoralis* (Fig. 2E) and Strongyloides-like eggs (Fig. 2F). Unfortunately, the patient's condition failed to improve. On hospital day 15, gastrointestinal bleeding was indicated by dark red gastric aspirate and melena. Emergency bedside endoscopy revealed diffuse bleeding of the rectal mucosa. On hospital day 16, the patient's family chose automatic discharge due to the poor prognosis and multiple comorbidities. Regrettably, the patient died following discharge. Written informed consent for publication was obtained from the patient.

Discussion

S. stercoralis is a soil-transmitted helminth found worldwide. It is mainly prevalent in tropical and subtropical areas. The parasite has a complex life history. It parasitizes the human small intestine and reproduces by parthenogenesis. In the intestine,

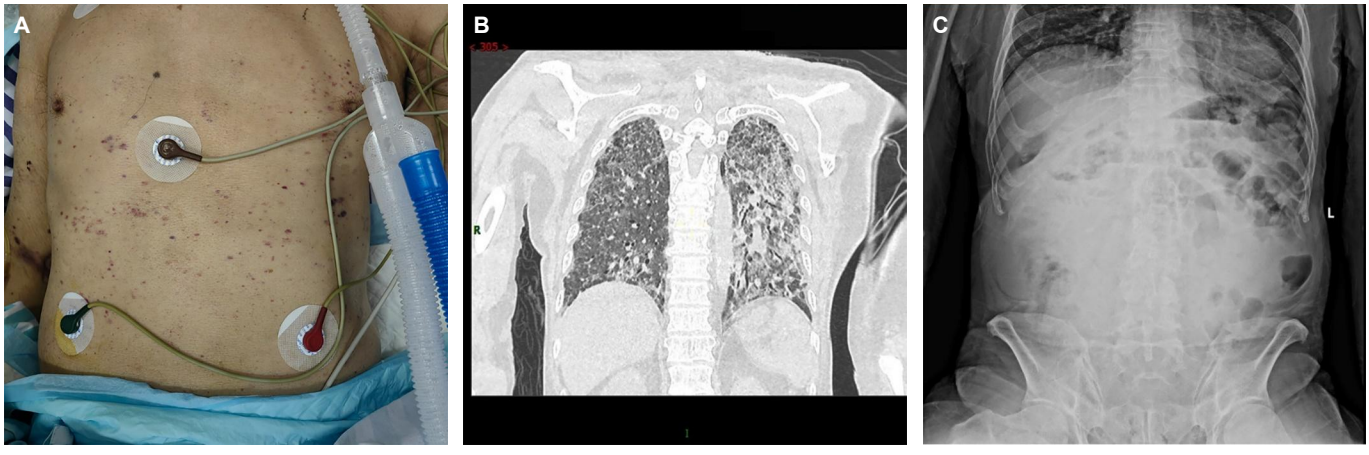

Fig. 1. Cutaneous manifestations and radiological features. (A) Diffuse non-blanching purpuric macules and petechiae involved the trunk and bilateral thighs. (B) Multiple small patchy and cord-like opacities with indistinct margins scattered in all lobes of the right lung, indicating pulmonary inflammation. (C) Mild bowel dilatation with short air-fluid levels and residual intra-abdominal bowel gas, suggesting incomplete bowel obstruction. Written informed consent for publication was obtained from the patient.

https://doi.org/10.3347/PHD.26031

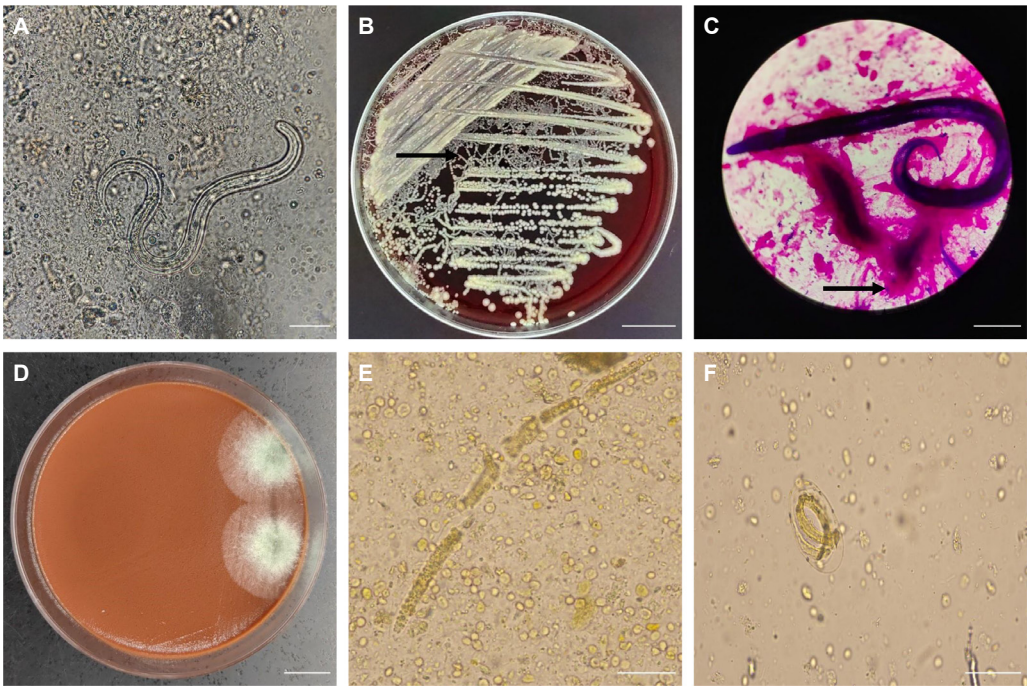

Fig. 2. Pathogenic microscopic and culture findings. (A) Filariform larva of *Strongyloides stercoralis* recovered from clinical sputum specimen, characterized by slender somatic form and a lengthy esophagus devoid of posterior esophageal bulb. Scale bar=50 μm. (B) Sputum cultured on blood agar exhibited extensive serpiginous bacterial trails (arrow), signifying active larval migration. Scale bar=1 cm. (C) Gram staining of bacterial colony smear revealed Gram-positive bacilli (arrow) and *S. stercoralis*. Scale bar=50 μm. (D) Tracheal aspirate cultured on chocolate agar showed *Aspergillus fumigatus* with smoky green, velvety colonies. Scale bar=1 cm. (E) Stool smear revealed numerous non-viable larvae of *S. stercoralis* with degenerated internal structures. Scale bar=30 μm. (F) Stool smear revealed numerous *S. stercoralis*-like eggs that were oval, thin-shelled, and larvated. Scale bar=30 μm.

eggs hatch into non-infective rhabditiform larvae. Most of these larvae leave the host through feces and enter the environment. Some can develop directly into infectious filariform larvae in the intestine, leading to autoinfection. Autoinfection enables *S. stercoralis* to persist within the host, potentially resulting in lifelong infection [5]. A case report showed that an 83-year-old man had been infected with *S. stercoralis* for 75 years [6]. In this case, the patient reported soil exposure over a decade ago that likely led to chronic *S. stercoralis* infection, which remained latent until worsening comorbidities and long-term corticosteroid use triggered hyperinfection.

IgAV is a multifactorial leukocytoclastic vasculitis characterized by IgA-dominant immune complex deposition within or around small vessels. It exhibits 4 clinical manifestations: non-thrombocytopenic palpable purpura, arthralgia or arthritis, abdominal pain, and renal impairment [1]. A variety of factors, such as infections, medications, genetic susceptibility, malignancies, and monoclonal gammopathy, have been implicated in the pathogenesis of IgAV [7]. IgAV with parasitic infection is extremely rare. Currently, only 2 cases of IgAV with *S. stercoralis* infection have been described, both in children [8,9]. This is the first adult case of IgAV with strongyloidiasis, providing further evidence for the role of *S. stercoralis* in the pathogenesis of IgAV. In addition, the clinical manifestations of strongyloidiasis are similar to those of IgAV. The glucocorticoid used to treat IgAV may induce *S. stercoralis* hyperinfection syndrome and disseminated strongyloidiasis. Thus, clinicians must perform *S. stercoralis* screening before starting immunosuppressive treatment for IgAV.

The diagnosis of strongyloidiasis is challenging. To date, there is neither a recognized 'gold standard' nor a standardized testing process. The best diagnosis approach often varies according to the patient's disease status. Current diagnostic methods include microscopic examination, immunological detection, and molecular technology. The sensitivity of microscopic examination is limited, and as shown in this case, severe strongyloidiasis can be manifested as intestinal obstruction and constipation; the patient's stool cannot be obtained for microscopic examination. Immune diagnosis is of great value for chronic strongyloidiasis, but false negatives may occur in patients with acute infection, early infection, or who are immunocompromised. In addition, the antigen of *S. stercoralis* is prone to cross-reaction with other helminth antigens. Generally speaking, molecular techniques have high sensitivity and spec-

ificity, but the cost is high [10]. A comprehensive understanding of the diagnostic method is very important for clinicians because missing *S. stercoralis* may lead to serious consequences.

There are several shortcomings in this case. First, the patient comes from the epidemic area of *S. stercoralis*, and ivermectin is not available locally; there is a possibility of exposure. However, the possibility of strongyloidiasis was not considered before immunosuppressive treatment was started. Second, the fecal sample could not be sent in time after an enema and gastrointestinal decompression. Third, given the known association between severe strongyloidiasis and HTLV-1 infection, HTLV-1 testing was not performed. In summary, the lack of awareness of strongyloidiasis led to diagnostic and therapeutic delays.

Author contributions

Conceptualization: Zhao L, Hu L. Data curation: Liang Y. Investigation: Liang Y. Resources: Zhao L, Hu L, Chen Y. Supervision: Chen Y. Writing – original draft: Hu L, Chen Y. Writing – review & editing: Zhao L.

Conflict of interest

The authors have no conflicts of interest to declare.

Supplementary information

Supplementary material is available with this article at https://doi.org/10.3347/PHD.26031.

ORCID

Limei Hu, https://orcid.org/0000-0003-0643-7361
Yihe Chen, https://orcid.org/0009-0000-3571-8870
Ying Liang, https://orcid.org/0009-0005-3781-8839
Li Zhao, https://orcid.org/0009-0008-5212-5274

References

1. Xu L, Li Y, Wu X. IgA vasculitis update: epidemiology, pathogenesis, and biomarkers. Front Immunol 2022;13:921864. https://doi.org/10.3389/fimmu.2022.921864
2. Mastroianni A, Greco S, Vangeli V, et al. Lambliasis-associated Schönlein-Henoch purpura in an Italian traveller: first case report in Italy. Int Marit Health 2023;74:89-91. https://doi.org/10.5603/IMH.2023.0013
3. Buonfrate D, Bradbury RS, Watts MR, Bisoffi Z. Human strongyloidiasis: complexities and pathways forward. Clin Microbiol Rev 2023;36:e0003323. https://doi.org/10.1128/cmr.00033-23
4. Floege J, Barratt J, Cook HT, et al. Executive summary of the KDIGO 2025 Clinical Practice Guideline for the Management of Immunoglobulin A Nephropathy (IgAN) and Immunoglobulin A Vasculitis (IgAV). Kidney Int 2025;108:548-54. https://doi.org/10.1016/j.kint.2025.04.003
5. Lo NC, Addiss DG, Buonfrate D, et al. Review of the WHO guideline on preventive chemotherapy for public health control of strongyloidiasis. Lancet Infect Dis 2025;25:e146-52. https://doi.org/10.1016/S1473-3099(24)00595-4
6. Prendki V, Fenaux P, Durand R, Thellier M, Bouchaud O. Strongyloidiasis in man 75 years after initial exposure. Emerg Infect Dis 2011;17:931-2. https://doi.org/10.3201/eid1705.100490
7. Stichert VR, Santoso B, Winters BG, et al. Updates on the diagnosis, prognosis, and management of IgA vasculitis in adults: a narrative review. J Am Acad Dermatol 2026;S0190-9622(26):00170-2. https://doi.org/10.1016/j.jaad.2026.02.007
8. Janković S, Nikolić M, Simović A, Vujić A. Henoch-Schönlein purpura associated with *Strongyloides stercoralis* infection. Vojnosanit Pregl 2016;73:491-5. https://doi.org/10.2298/vsp140821028j
9. Konstantopoulou A, Tsoliakos I, Berikopoulou MM, et al. A case-based review of IgA vasculitis complicated with gastrointestinal infections: insights from a norovirus-associated case in an adolescent. Rheumatol Int 2025;45:114. https://doi.org/10.1007/s00296-025-05876-6
10. Gordon CA, Utzinger J, Muhi S, et al. Strongyloidiasis. Nat Rev Dis Primers 2024;10:6. https://doi.org/10.1038/s41572-023-00490-x

Case Report

Parasites Hosts Dis 2026;64(3):285-290
https://doi.org/10.3347/PHD.26020

Parasites, Hosts and Diseases

pISSN 2982-5164 • eISSN 2982-6799

Cerebral cystic echinococcosis in Vietnam

Tran Thi Thu Huong[1], Vu Thi Lam Binh[2], Nguyen Van Lam[1], Vu Thanh Trung[3], Veronique Dermauw[4,*], Pierre Dorny[4]

[1]National Paediatric Hospital, Ha Noi, Vietnam; [2]National Institute of Malariology, Parasitology and Entomology, Ha Noi, Vietnam; [3]Bach Mai Hospital, Ha Noi, Vietnam; [4]Institute of Tropical Medicine, Antwerp, Belgium

In Vietnam, only few cases of cystic echinococcosis have been reported up to now. We report on the first case of cystic echinococcosis involving the central nervous system reported in Vietnam. Our patient, a 14-year-old child, presented with symptoms of headache and progressive tremor in the right hand that had lasted for 1 month and had worsened in the last days before admission. Following the demonstration of a large space occupying brain cyst by computed tomography, a presumptive diagnosis of a brain tumour was made, that was later overruled. Magnetic resonance imaging, a biopsy and serological analysis allowed for the diagnosis of a giant hydatid brain cyst. The patient underwent surgical removal of the cyst and was treated for 6 months post-surgery with albendazole. On follow-up, the clinical symptoms gradually improved, serology became negative and 1.5 years after the surgical intervention the patient was declared to be cured. This case highlights the importance of considering hydatid disease in differential diagnoses, even in regions where *Echinococcus* infections are considered rare.

Keywords: *Echinococcus granulosus*, hydatidosis, brain, Vietnam

Introduction

Cystic echinococcosis (CE) is a zoonotic disease caused by the metacestode larval stage of *Echinococcus granulosus* s.l. [1]. Dogs are the definitive hosts of *E. granulosus*, in which the tapeworm develops in the small intestine. These tapeworms release eggs that are excreted via faeces of the definitive host [2]. The eggs are infective to intermediate hosts, mainly domestic herbivores and omnivores. Once ingested, the larvae develop into hydatid cysts, which form in various organs. Within these cysts, the parasites undergo asexual multiplication. Dogs become infected by eating cyst-infected offal, perpetuating the life cycle [3].

Humans can become accidental intermediate hosts following ingesting of parasite eggs in contaminated food or water or after direct contact with infected dogs [1]. This disease mostly occurs in sheep breeding areas with low economic situation and hygiene such as, Western China, Central Asia, South America, Mediterranean countries, and Eastern Africa [4,5]. Out of the 10 known *E. granulosus* s.l. strains/genotypes, the *E. granulosus* s.s. G1 strain, mainly transmitted between dogs and sheep, accounts for nearly 90% of human infections [6].

In humans, hydatid cysts are mainly found in the liver and lungs, accounting for over 90% of cases. Cysts can also establish in other organs, including the spleen, kidneys, heart, bones, and the central nervous system [3,7]. CE can occur in all age classes, from under 1 year old to 75 years old, of which paediatric patients account for a fairly high rate [8]. The pathogenesis

Received: March 11, 2026 Accepted: April 27, 2026
*Correspondence: vdermauw@itg.be

Citation
Huong TTT, Binh VTL, Lam NV, Trung VT, Dermauw V, Dorny P. Cerebral cystic echinococcosis in Vietnam. Parasites Hosts Dis 2026;64(3):285-290.

of CE is the result of functional changes of organs resulting from pressure caused by the growing cysts, as well as from anaphylactic reactions when the cyst wall breaks, releasing their content [7]. For treatment, the World Health Organization recommends the surgical removal of cysts combined with chemotherapy to avoid recurrence. However, some cases can be treated by anthelmintics only, by ultrasound-guided percutaneous aspiration of cyst fluid followed by instillation and re-aspiration of a scolicidal agent (PAIR [puncture, aspiration, injection, and re-aspiration] technique) or are left untreated [7,8].

Although CE is endemic in many parts of the world, it remains rarely reported in Vietnam. To date, only 5 confirmed human cases have been described in literature: 3 cases of pulmonary, 1 case of cardiac CE, and 1 case with concomitant cardiac and hepatic CE [9-11]. These reports are notable not only for their rarity but also because all but one could be attributed to *E. ortleppi* (G5), commonly referred to as the cattle strain. This strain is infrequently associated with human infection worldwide but seems to be emerging in Asia [12]. Despite these isolated reports, the true burden of CE in Vietnam is likely underestimated due to limited surveillance, non-specific clinical presentation, and restricted access to diagnostic tools. Moreover, the disease is not notifiable in many areas, and transmission risks—such as close human-animal contact and lack of veterinary inspection—persist in rural settings. These conditions suggest that sporadic cases may be overlooked.

Here we present a case of cerebral CE in a 14-year-old Vietnamese child and the outcome of surgical and anthelmintic treatment.

Case Report

On 22 February 2023 a 14-year-old boy was admitted to the National Paediatric Hospital. Upon clinical examination by the physician, the boy presented with symptoms of dull headache in the back of the neck, right hand tremor, and difficulties in writing that lasted for 1 month. A few days before being admitted to the hospital, the patient suffered from progressively worsening severe headache. He vomited several times a day and had a blurred vision. His medical history was normal. The patient lived in a rural area of Quynh Luu district, Nghe An province, and often played with his grandparents' dog. He had no travel history.

Blood, urine and cerebrospinal fluid samples were obtained, and abdominal ultrasound, chest X-ray and brain computed tomography (CT)-scan were performed on the same day. Hematological and blood biochemical analysis revealed an inflammatory reaction with a high WBC (14,230 cells/mm^3) and a neutrophil rate of 81%. Blood and cerebrospinal fluid cultures were negative. Urine tests, abdominal ultrasound, and chest X-ray were normal. A brain CT scan showed a large cyst of 100 × 71 mm in the left temporo-parietal region compressing the left lateral ventricle and shifting the midline to the right; with dilation of the right lateral ventricle (Fig. 1A).

The patient was diagnosed with a cystic brain tumour, and it was decided to perform a surgical removal on 27 February 2023. However, during surgery it appeared that the presumed tumour was a large cyst suspected to be caused by a parasite; therefore, no action was taken while waiting for further investigation. Brain magnetic resonance imaging (MRI), performed immediately after the first surgical intervention showed a cystic mass in the left temporal lobe. The cyst was compartmented with membranes dividing the interior into small cysts of different sizes. The cyst fluid was clear and homogeneous, and the cyst was surrounded by a thin wall. The cyst measured 87 × 64 mm (Fig. 1B). Serological examination showed a positive result for a commercial *Echinococcus* IgG ELISA (Diagnostic Automation/Cortez Diagnostics), with an optical density of 0.532 and a cut-off of 0.3, hinting to the possibility of a brain hydatid cyst.

Based on the presumptive diagnosis, the child underwent a second surgical intervention on 6 March 2023, whereby the cyst was completely excised. The procedure was successful with no rupture of the cyst wall. Intraoperatively, a soft, pinkish-white cyst was identified in the left temporo-occipital region. After removal, the cyst was opened, and it was found to contain multiple smaller cysts, each with a thick and white wall. The cyst fluid appeared transparent, and slightly viscous. A biopsy was subsequently performed to confirm the diagnosis. Histological examination of the biopsy specimen, following hematoxylin and eosin (H&E) staining revealed the presence of *Echinococcus* spp. protoscolices (Fig. 1C, D).

After surgery, the patient was treated for 2 weeks with ceftriaxone 50 mg/kg twice a day, and with albendazole 15 mg/kg/day divided in 2 doses for 6 months. Ten days after the second operation, the number of WBCs and the rate of neutrophils had become normal (WBCs 9,110 cells/mm^3 and neutrophil rate 51.9%). Clinically, the patient no longer suffered from headaches. Moreover, the hand tremors gradually decreased over time, and he could go back to school. The patient was invited for re-examination periodically once a month for 3 months, then every 3 months, to monitor clinical symptoms, blood count and liver enzymes. All test results were normal. On examination on 13 August 2024, all blood test results were normal, and *Echinococcus* IgG ELISA was negative. The patient was

https://doi.org/10.3347/PHD.26020

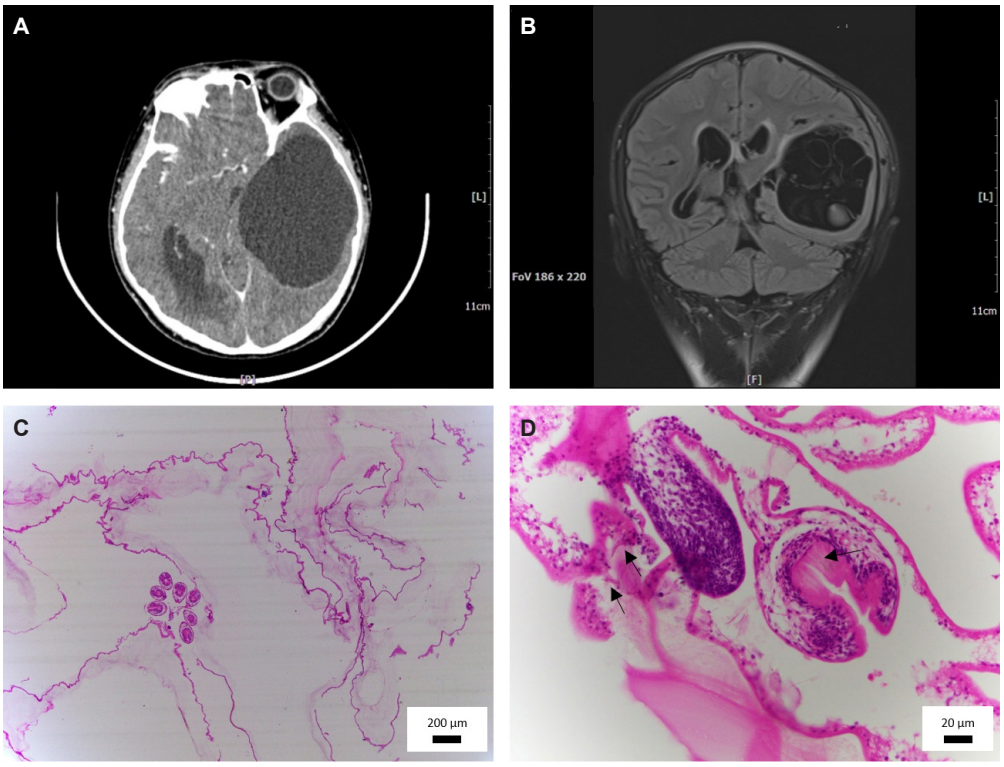

Fig. 1. Imaging results of the case. (A) Computed tomography scan prior to first surgery showing a giant cyst (100×71 mm), mimicking a brain tumour. (B) Magnetic resonance imaging image prior to second surgery revealing a giant cyst (87×64 mm) filled with cyst fluid, delineated by a thin wall, and containing membrane structures dividing it in different compartments. (C) Histological image (hematoxylin-eosin staining) of a biopsy of a membrane-like mass obtained after second surgery, showing the cyst wall and *Echinococcus* spp. protoscolices (100× magnification). (D) Histological image (hematoxylin-eosin staining) of a biopsy of a membrane-like mass obtained after second surgery, showing a *Echinococcus* spp. protoscolex with hooks (arrows) (400× magnification).

also invited for MRI/CT scans every 6 months to monitor the progression of the postoperative lesion. An MRI performed 8 months post-surgery revealed a cystic structure measuring 59×48 mm, and a CT scan almost 1.5 years post-surgery revealed the same cystic structure (83×51 mm) in the temporal lobe with mild lateral ventricle dilatation (Fig. 2A, B). The same structure (82×50 mm) was observed on a CT performed more than 2.5 years post-surgery (Fig. 2C). At that time the symptoms of headache and hand tremors had completely disappeared, but the memory and learning ability of the boy had declined.

The reporting of the case was approved by National Institute of Malariology, Parasitology and Entomology, Vietnam (No 661/QD-VSR). A consent to participate in the study is not applicable to this case report. Written informed consent was obtained from the patient's parents for the publication of this case report and accompanying images.

Discussion

This case represents an exceptional presentation of cerebral CE in a child in Vietnam, a country where *E. granulosus* infections are very rare. Notably, the 5 previously described CE cases in Vietnam, involved 3 pulmonary cases, 1 cardiac case, and 1 case with concomitant cardiac and hepatic cysts [9-11]. The distribution of these cases (where described in the papers) and our case is shown in Fig. 3. All but one of the earlier cases were attributed to *E. ortleppi* [9,10], a genotype uncommonly associated with human infections: a recent review retrieved 19 cases only globally [12]. Its recent emergence in Asia has been highlighted, yet much remains unknown about its presence in Vietnam. Unfortunately, for our case report, molecular identification of the causative species was not possible, as obtaining the paraffin block of the biopsy for genetic analysis required a formal, multi-step hospital process that was not feasible within the limited timeframe of the patient's follow-up visit.

The transmission dynamics of *Echinococcus* in Vietnam are poorly understood. Archaeological data from a 7th-millennium BP forager community suggest that *E. granulosus* may have circulated in prehistoric Vietnamese communities, who might have been accidentally exposed through contaminated water

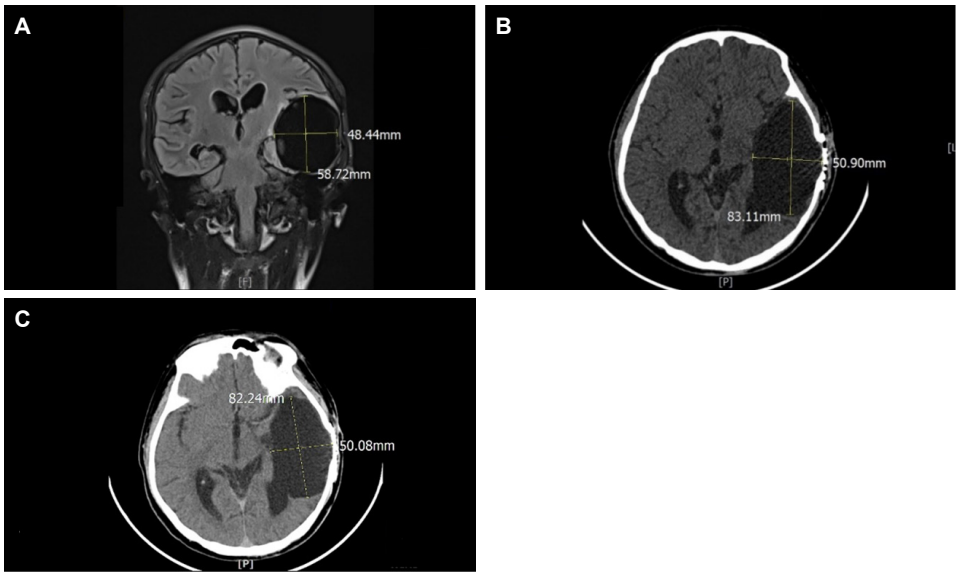

Fig. 2. Follow-up imaging of the case. (A) Magnetic resonance imaging image 8 months after the second surgery revealed a cystic structure measuring 59×48 mm. (B) Computed tomography image 1.5 years after the second surgery revealed 83×51 mm cystic structure in the temporal lobe with mild lateral ventricular dilatation. (C) Computed tomography image 2 years and 8 months after the second surgery revealed 82×50 mm cystic structure in the temporal lobe with mild lateral ventricular dilatation

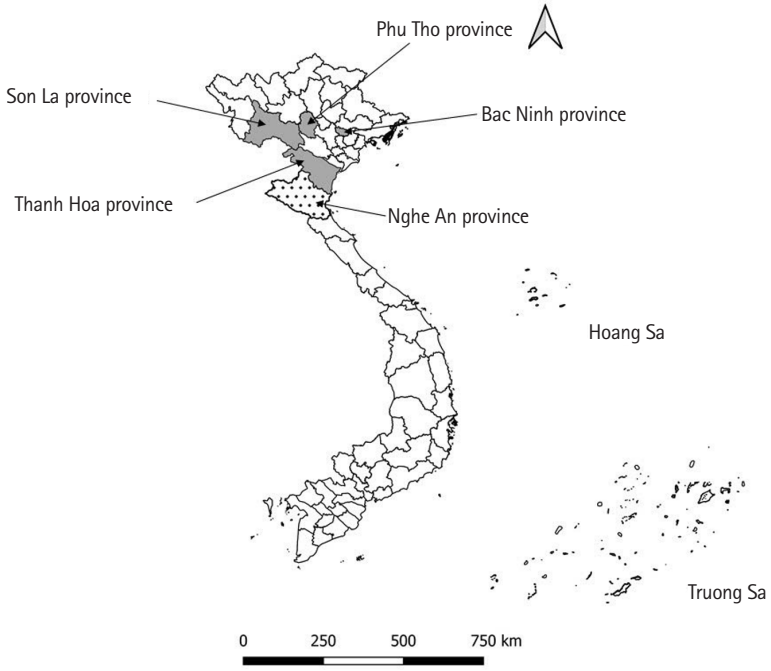

Fig. 3. Distribution of earlier cases and the current case of hydatidosis in Vietnam. Grey indicates provinces with earlier reported cases and the dotted white area denotes the province of origin of our case.

sources, shared by wild canids and ruminants (e.g., wild buffalo, deer) [13]; however, more recent data on animal involvement are scarce. The only documented infection of a final host dates back to 1967, involving a domestic dog [14], and remarkably, no reports exist of CE in livestock. More recently, *E. ortleppi* was also discovered in multiple langur species in Vietnam (*Trachypithecus hatinhensis*, *T. delacouri*, *Pygathrix nemaeus*, and *P. cinerea*) [15,16], raising the possibility of an underrecognized sylvatic reservoir and transmission route involving wild primates as intermediate hosts.

Cerebral hydatid cysts are extremely rare, occurring in only about 0.4% of human CE cases [8]. Given this context, and the

https://doi.org/10.3347/PHD.26020

fact that infections in Vietnam are equally rare, clinical familiarity with cerebral CE is limited. It is therefore unsurprising that the diagnosis was delayed and the lesion was initially mistaken for a brain tumor. Contributing further to this diagnostic challenge was the child's unusually mild symptomatology despite the presence of a large space-occupying cyst. For a considerable period, the child remained asymptomatic, and only began experiencing subtle neurological signs—such as headaches, right-hand tremors, and writing difficulties—about a month before surgery. These symptoms were non-specific and easily attributed to more common pediatric neurological conditions. In the days preceding surgical intervention, the child developed blurred vision and vomiting, which, although more suggestive of intracranial pressure, still lacked specificity. Cerebral CE was only correctly diagnosed after further imaging, histopathology, and serological testing. As no other cysts were found in this child, a primary cerebral infection is suggested rather than a secondary spread from other organs.

Following World Health Organization guidelines, the patient underwent surgery to remove the cyst, followed by a 6-month course of albendazole (15 mg/kg/day). Throughout treatment, blood tests, liver function, and enzyme levels remained stable, and serological tests eventually turned negative. Postoperative MRI and CT scans were conducted every 6 months. While the child's symptoms had fully resolved a year and a half after surgery, some cognitive difficulties, particularly with learning and memory, persisted. Neuroimaging also continued to show a residual cyst, highlighting the need for long-term monitoring.

Overall, this case highlights the importance of considering hydatid disease in differential diagnoses, even in regions where *Echinococcus* infections are considered rare. Diagnosing cerebral CE can be particularly challenging, especially when relying on clinical symptoms and basic neuroimaging, as it often mimics a brain tumour. The lack of epidemiological data on *Echinococcus* in Vietnam underscores the need for further research. Studies in domestic dogs, livestock, and wildlife are essential to understand the parasite's transmission, its intermediate hosts, and the genotypes circulating in the region. Given the presence of free-roaming dogs in rural communities, regular deworming programs could be an effective strategy to reduce the risk of human infections. This case serves as a reminder that even rare diseases can appear in unexpected places—and when they do, they can challenge both diagnosis and treatment. Continued surveillance and research will be crucial to uncovering the true burden of echinococcosis in Vietnam and beyond.

Author contributions

Conceptualization: Huong TTT, Lam NV, Trung VT, Binh VTL, Dermauw V, Dorny P. Data curation: Huong TTT, Lam NV, Trung VT. Investigation: Huong TTT, Lam NV, Trung VT. Methodology: Huong TTT, Lam NV, Trung VT. Project administration: Huong TTT. Resources: Huong TTT, Lam NV, Trung VT. Supervision: Huong TTT, Lam NV. Validation: Huong TTT, Lam NV, Trung VT. Visualization: Trung VT. Writing – original draft: Binh VTL, Dermauw V, Dorny P. Writing – review & editing: Binh VTL, Dermauw V, Dorny P.

Conflict of interest

The authors have no conflicts of interest to declare.

Acknowledgments

We thank the patient's parents for consenting to provide their son's medical information. We are grateful to National Paediatric Hospital Vietnam for treatment and closely following up the patient.

ORCID

Tran Thi Thu Huong, https://orcid.org/0009-0002-7075-9605
Vu Thi Lam Binh, https://orcid.org/0000-0001-6406-0422
Nguyen Van Lam, https://orcid.org/0000-0003-0656-6091
Vu Thanh Trung, https://orcid.org/0009-0006-5327-885X
Veronique Dermauw, https://orcid.org/0000-0001-8745-5304
Pierre Dorny, https://orcid.org/0000-0001-5381-7987

References

1. World Health Organization. Echinococcosis [Internet]. 2021 [cited 2025 Nov 25]. Available from: https://www.who.int/news-room/fact-sheets/detail/echinococcosis
2. Eckert J, Deplazes P. Biological, epidemiological, and clinical aspects of echinococcosis, a zoonosis of increasing concern. Clin Microbiol Rev 2004;17:107-35. https://doi.org/10.1128/CMR.17.1.107-135.2004
3. Moro P, Schantz PM. Echinococcosis: a review. Int J Infect Dis 2009;13:125-33. https://doi.org/10.1016/j.ijid.2008.03.037
4. Wen H, Vuitton L, Tuxun T, et al. Echinococcosis: advances in the 21st century. Clin Microbiol Rev 2019;32:e00075-18. https://doi.org/10.1128/CMR.00075-18
5. Hogea M, Ciomaga BF, Muntean A, et al. Cystic echinococcosis in the early 2020s: a review. Trop Med Infect Dis 2024;9:36. https://doi.org/10.3390/tropicalmed9020036

6. Alvarez Rojas CA, Romig T, Lightowlers MW. *Echinococcus granulosus* sensu lato genotypes infecting humans: review of current knowledge. Int J Parasitol 2014;44:9-18. https://doi.org/10.1016/j.ijpara.2013.08.008
7. Brunetti E, Kern P, Vuitton DA; Writing Panel for the WHO-IWGE. Expert consensus for the diagnosis and treatment of cystic and alveolar echinococcosis in humans. Acta Trop 2010;114:1-16. https://doi.org/10.1016/j.actatropica.2009.11.001
8. Pawlowski Z, Eckert J, Vuitton DA, et al. Echinococcosis in humans: clinical aspects, diagnosis and treatment. In: World Organisation for Animal Health. WHO/OIE manual on echinococcosis in humans and animals: a public health problem of global concern. World Organisation for Animal Health; 2002. p. 20-66.
9. Van De N, Le Van D. The first report of two cases of cystic echinococcosis in the lung by *Echinococcus ortleppi* infection, in Vietnam. Res Rep Trop Med 2017;8:45-51. https://doi.org/10.2147/RRTM.S122014
10. De NV, Minh PN, Duyet LV, et al. Two human cases of *Echinococcus ortleppi* infection in the lung and heart in Vietnam. Korean J Parasitol 2020;58:451-6. https://doi.org/10.3347/kjp.2020.58.4.451
11. Nguyen HTT, Pham VT, Duong HD, et al. Concomitant intramyocardial and hepatic hydatid cysts diagnosed by multi-modality imaging: a rare case report. Front Cardiovasc Med 2022;9:1055000. https://doi.org/10.3389/fcvm.2022.1055000
12. Yoshida A, Irie T, Le LA, Bui KL, Nawa Y. *Echinococcus ortleppi* infection in humans: an emerging zoonosis in Asia. Parasitol Int 2024;103:102949. https://doi.org/10.1016/j.parint.2024.102949
13. Vlok M, Buckley HR, Domett K, et al. Hydatid disease (*Echinococcosis granulosis*) diagnosis from skeletal osteolytic lesions in an early seventh-millennium BP forager community from preagricultural northern Vietnam. Am J Biol Anthropol 2022;177:100-15. https://doi.org/10.1002/ajpa.24435
14. Le-Van-Hoa, Vu-Ngoc-Tan. Concerning the presence of cestodes, *Echinococcus granulosus* (Batsch, 1786), in a wild dog, Cyon primaerus (Hodgs) in South Vietnam. Bull Soc Pathol Exot Filiales 1967;60:64-71.
15. Plesker R, Nadler T, Dinkel A, Romig T. A case of an *Echinococcus ortleppi* infestation in a red-shanked douc langur (*Pygathrix nemaeus*) in northern Vietnam. Vietnam J Primatol 2009;3:75-81.
16. Thanh VD, Nam VH, Anh LTL, et al. Transmission of *Echinococcus ortleppi* at the Endangered Primate Rescue Center, Cuc Phuong National Park. Vietnam J Primatol 2020;3:53-8.

https://doi.org/10.3347/PHD.26020

Instructions for authors

Parasites, Hosts and Diseases

Enacted: June 1963
Revised: February 2023
Last revision: January 1, 2026

Parasites, Hosts and Diseases (PHD) is an open access, peer-reviewed, online journal published quarterly on the last day of January, April, July, and October (beginning in 2026, the publication dates were changed from the last day of February, May, August, and November, which had been in effect through 2025). As the official journal of The Korean Society for Parasitology and Tropical Medicine, PHD aims to generate new knowledge on parasites infecting humans and animals, disease vectors, host-parasite relationships, zoonotic diseases, and tropical medicine.

Manuscripts should adhere to the Recommendations for the Conduct, Reporting, Editing, and Publication of Scholarly Work in Medical Journals, issued by the International Committee of Medical Journal Editors (ICMJE; http://www.icmje.org/recommendations/), unless otherwise specified.

1. Article Processing Charge

Accepted manuscripts are published with the understanding that the author(s) will cover the associated publication costs, including page charges. The standard page charge is 700,000 KRW for Korean authors and 700 USD for others, covering up to 10 pages. An additional 100,000 KRW (for Korean authors) or 100 USD per page applies from the 11th page onward. The page charge for Letters to the Editor is 350 USD.

2. Research and Publication Ethics

It is available at: https://parahostdis.org/policy/ethics.php

3. Submission and Peer Review Process

A. Submission

Authors should submit their manuscripts online through the PHD submission system at https://submit.parahostdis.org/. Once logged in, the system will guide you through the submission process step-by-step. Detailed submission instructions are available on the website, and all manuscripts must comply with these guidelines. Failure to do so may result in the return of the manuscript and potential delays in publication.

B. Peer review process

PHD reviews all submitted manuscripts. Each manuscript is first assessed for format and relevance to the journal's aims and scope. If it meets these criteria, it is sent to two experts in the relevant field for review. PHD uses a single-blind process, where reviewer identities are concealed from the author, but both are visible to the decision-making editor. Reviewers make one of four recommendations: accept, minor revision, major revision, or reject. A first decision is typically made within an average of 4 weeks after the reviewers have agreed to evaluate the manuscript. In cases of review discrepancies, the editorial board will conduct an additional review to make a final determination. Authors are expected to revise their manuscripts based on reviewer feedback and provide explanations for any feedback they choose not to implement. The editorial board makes the final publication decision and may request further changes.

C. Cover Letter

The cover letter should confirm that the submitted material, in whole or in part, has neither been published previously nor is under consideration for publication elsewhere. Additionally, it should disclose any potential conflicts of interest that could influence the authors' interpretation of the data, such as financial support, affiliations with pharmaceutical companies, political pressures from interest groups, or academically related conflicts. The cover letter should also specify that all authors have approved the manuscript for submission and confirm that the manuscript complies with ethical guidelines, including IRB approval and informed consent where applicable.

4. Manuscript Preparation

A. Article types

- Original articles: Original articles present results of research investigations on parasites, parasitic diseases, host-parasite relationships and tropical medicine. They should be organized in the following sequence: Title page, Abstract (≤250 words) and Keywords, Main text (Introduction, Methods, Results, and Discussion), References, Tables, Figure legends, and Figures. Original articles should not include more than a total of 35 references.
- Reviews or mini reviews: Reviews provide a comprehensive analysis of specific topics. The text should be organized in the following sequence: Title page, Abstract (≤250

words) and Keywords, Main text (Introduction, Body text, and Conclusion), References, Tables, Figure legends, and Figures. Unsolicited reviews are also welcome. A mini-review is a shorter version of a full review article. Systematic reviews and meta-analyses should be submitted as review articles but require a structured abstract and should follow the PRISMA guidelines (http://www.prisma-statement.org/).

- Case reports: Case reports are accepted only when they present clinically important information about unique cases. Reports should describe cases not previously observed or reported. If a case involves a common condition but is deemed significant, the editorial board will review it to determine acceptance. They should be organized in the following sequence: Title page, Abstract (≤250 words) and Keywords, Introduction, Case Report, Discussion, References, Tables, Figure legends, and Figures. The number of references should not exceed 20.
- Brief communications: Brief communication is a short article detailing clinically or experimentally significant findings or major advancements. It should adhere to the guidelines for original articles, but the text should be formatted as a single section without headings or section divisions. Additionally, the number of references should be no more than 20.
- Letters to the editor: Letters offer rapid publication of new findings of unique clinical importance, recent perspectives on articles, or topics of interest published in the journal. They may also include opinions on specific topics of academic relevance. The text should be organized in the following sequence: Title page, Main text, References, Tables, Figure legends, and Figures (if applicable). The text should be formatted as a single section without headings or section divisions with no more than 10 references.
- Book reviews: Invited book reviews are eligible for publication. Submissions should provide a critical evaluation of the book's arguments and content. The text should include the title of the book reviewed, the author(s) and editor(s), and publisher, the total number of pages, and the ISBN number, followed by the main text, with no more than 10 references.

B. General requirements

- Manuscripts should be prepared using Microsoft Word (doc or docx format). They should be formatted on A4 (21.0×29.7 cm), with margins of at least 2.54 cm on all sides.
- Texts should be double-spaced with the same normal, plain font throughout, preferably 11-point Times New Roman.
- Genera and species names of parasites and living organisms should be written in italic.
- Other Latin origin words, such as "et al.", "in situ", "in vitro", and "in vivo" should not be italicized.
- Provide the names of manufacturers.
- When quoting from other sources, give a reference number after the author's surname or at the end of the quotation.
- Authors should express all measurements in conventional units, using International System of Units (SI units).
- Authors should follow International Rules for Nomenclature and, if new names are introduced, the International Code for Zoological Nomenclature. All strains and sources of hosts and parasites should be stated.
- Abbreviations should be used sparingly and unambiguously.

C. Key features

Key features and limits of articles are summarized in Table 1 below. However, the limits are negotiable with the editor.

Table 1. Key features and limits of articles

Type of article	Abstract	Text structure	References
Original Article	≤250 words	Introduction, Methods, Results, Discussion	35
Review and Mini Review	≤250 words	Introduction, Body text, Conclusion	No limit
Case Report	≤250 words	Introduction, Case report, Discussion	20
Brief Communication	≤250 words	Single section with no headings	20
Letters to the Editor	Not required	Single section with no headings	10
Book reviews	Not required	Free-form style	10

D. Reporting guidelines

For specific study designs, such as randomized controlled trials, diagnostic accuracy studies, meta-analyses, observational studies, and non-randomized studies, authors should follow the relevant reporting guidelines. Recommended sources include the EQUATOR Network (https://www.equator-network.org/) and the National Library of Medicine (https://www.nlm.nih.gov/services/research_report_guide.html).

E. Manuscript structure and format

Organize your manuscript file as follows:

Manuscript file: (1) Title page (2) Abstract & keywords, (3) Body text, (4) References list, (5) Notes (author contributions,

conflict of interest, funding, acknowledgments) (6) Tables (each beginning on a new page), (7) Figure legends (upload figures in separate files)

Supplementary materials (upload separately)

• **Title page**

The title page should include the following items:

- **Title:** The article title should be concise and precise. The title should also indicate the study design. If the study involved human participants, the country where the study was conducted should be included.
- **Running title:** Less than 50 characters
- **Authors and affiliations:** Each author's given name and surname should be provided. For authors with different affiliations, use superscripted Arabic numerals (e.g., [1], [2], [3]) placed at the top-right of each author's name and before each corresponding affiliation. If an author is associated with multiple departments or institutions, arrange affiliations in the order of the authors and indicate them with superscript numbers. The corresponding author should be marked with an asterisk (*) as a superscript.
- **ORCID:** All authors are required to provide their ORCIDs. If an author does not have an ORCID, they can register for one at the ORCID website (https://orcid.org/). Registration is free to all researchers.
- **Corresponding author:** The corresponding author's email address should be provided. If no corresponding author is specified, the editorial board will assume the first author holds this role.

• **Abstract and keywords**

- **Abstract:** For original articles, reviews and mini reviews, case reports, and brief communications, provide an unstructured abstract of less than 250 words. Ensure all data in the abstract appear in the manuscript text or tables.
- **Keywords:** Up to 6 keywords should be listed at the bottom of the abstract to be used as index terms. PHD strongly recommends using Medical Subject Headings (MeSH; https://meshb.nlm.nih.gov/) keywords.

• **Main text**

The main text of an original article must be prepared under the following subheadings: Introduction, Methods, Results, and Discussion. Case report should be organized with Introduction, Case Report, and Discussion. In addition to these types, manuscripts that fall under specific reporting guidelines must be prepared accordingly.

- **Introduction:** Provide the background and purpose of the article, emphasizing its significance. Summarize the rationale with only relevant references, avoiding diffuse listing of related topics. Do not include data or conclusions from the study itself.
- **Methods:** Authors must provide sufficient details to enable an independent researcher to reproduce the work. Previously published methods should be summarized and cited appropriately, without unnecessary repetition. If directly quoting a published method, cite the source. Any major modifications to existing methods must be clearly described. The number of experiments, replicates, and statistical tests used should be specified. An ethics statement must be included when studies involve clinical samples, human data, or animals. This statement should appear as the first subheading in the Methods section. Examples are shown in the following: "We conducted this study in compliance with the principles of the Declaration of Helsinki. The study's protocol was reviewed and approved by the Institutional Review Board of OO (No. OO). Written informed consents were obtained from the patients. The requirement for informed consent was waived."
- **Results:** Present the results in a logical sequence across the text, tables, and figures. Avoid repeating data in the text that is already provided in tables or figures; instead, highlight and summarize key findings and insights.
- **Discussion:** Emphasize the novel and important aspects of the study, along with the conclusions drawn from them. Avoid detailed repetition of data or material already presented in the Introduction or Results sections. Discuss the implications and limitations of the findings, including potential impacts on future research. Connect the conclusions to the study's objectives by comparing and discussing relevant findings from other research. Avoid unqualified statements and conclusions not fully supported by the data. Where applicable, propose new hypotheses and include recommendations as appropriate.

• **References**

In the text, references should be cited with Arabic numerals in square brackets, numbered in the order of appearance. In the References, the references should be numbered and listed in the order of appearance in the text. List all authors when there are 5 or fewer. For sources with 6 or more authors, list the first 3 authors followed by "et al." If an article has been published online, but not yet assigned an issue or page numbers, the DOI should be supplied. journals should be abbreviated according to the style used in the list of journals indexed in the NLM Journal Catalog (https://www.ncbi.nlm.nih.gov/nlmcatalog/journals). For journal titles not list-

ed in the Catalog, they should follow the ISO abbreviation as described in "ISO 4:1997 Information and documentation—Rules for the abbreviation of title words and titles of publications" (https://www.iso.org/iso/home/store/catalogue_tc/catalogue_detail.htm?csnumber=3569).

Journal articles:

1. Aung JM, Joo SY, Na BK, et al. Establishing a Cre/loxP-based genetic manipulation system for *Acanthamoeba*: targeted genome editing and stable reporter expression. Parasites Hosts Dis 2025;63:25-36. https://doi.org/10.3347/PHD.24078
2. Kim MJ, Moon EK, Jo HJ, Quan FS, Kong HH. Identifying the function of genes involved in excreted vesicle formation in *Acanthamoeba castellanii* containing *Legionella pneumophila*. Parasit Vectors 2023;16:215. https://doi.org/10.1186/s13071-023-05824-y
3. Poncet AF, Blanchard N, Marion S. Toxoplasma and dendritic cells: an intimate relationship that deserves further scrutiny. Trends Parasitol 2019;35:870-86. https://doi.org/10.1016/j.pt.2019.08.001

Book & book chapter:

4. Khan NA. *Acanthamoeba*: biology and pathogenesis. 2nd ed. Caister Academic Press; 2015.
5. Nesheim MC. Ascariasis and human nutrition. In: Crompton DW, Nesheim MC, Pawlowski ZS, editors. Ascariasis and its prevention and control. Taylor and Francis; 1989. p. 87-100.

• **Notes**

- **Conflict of interest:** Authors should disclose any potential conflict of interest. If there are no conflicts of interest to declare, authors should include the following sentence: "The authors have no conflicts of interest to declare."
- **Author contributions:** Describe contributions using the Contributor Roles Taxonomy (CRediT; https://credit.niso.org/). Contributors must meet at least one core role (conceptualization, data curation, formal analysis, investigation, methodology, software, and validation) and one writing role (original draft preparation, review, and editing). Authors who do not meet these requirements will not qualify for authorship.
- **Funding:** Funding for the research should be detailed here. Provision of a FundRef ID is recommended, including the name of the funding agency, country, and (if available) the number of the grant provided by the funding agency. If the funding agency lacks a FundRef ID, please ask that agency to contact the FundRef registry (e-mail: fundref.registry@crossref.org).
- **Data availability:** Include a statement indicating where the data supporting the article's results can be found, with hyperlinks to publicly archived datasets if applicable.
- **Acknowledgments:** All persons who have made substantial contributions, but do not meet the criteria for authorship, should be acknowledged here.

• **Tables**

Table titles and content should be concise, clear, and self-explanatory, so readers do not need to refer to the main text. The table title should be placed at the top-left corner, formatted as "Table [Arabic numeral]." Tables should not contain vertical lines.

Include abbreviations or necessary descriptions in footnotes below the table, using superscript letters (a, b, c) to indicate each footnote, ensuring each note has a corresponding marker. List abbreviations in the footnote section, explaining any empty cells. Where possible, place units directly within the table, avoiding separate listing, and use lowercase symbols for units. In the main text, the term "Table" should appear as "Table" followed by an Arabic numeral.

• **Figures**

Number figures in the order they are cited in the text, using Arabic numerals. Upload each figure as a single image file with a resolution of at least 300 dpi. For figures depicting averages or proportions, use bar or line graphs. Specify the statistical methods used in a footnote for each figure. For multiple panels within the same figure number, use English letters after the numeral to indicate order (e.g., Fig. 1A, Fig. 2B, C).

• **Permission**

If any tables or figures are taken or modified from other papers, authors should obtain permission through the Copyright Clearance Center (https://www.copyright.com/) or from the individual publisher, unless the materials are from an open access journal under the Creative Commons license. For open access journal materials, simply verify the source in the accompanying footnote. Note the distinction between free-access and open access journals: permission from the publisher is required for using tables or figures from free-access journals.

Examples:

Reprinted (Modified) from Tanaka et al. [48], with permission of Elsevier.

Reprinted (Modified) from Weiss et al. [2], according to the Creative Commons License.

• **Supplementary materials**

Supplemental material includes files provided by the au-

thors to accompany their article, typically featuring additional content not included in the print version, such as appendices or extra tables. All supplemental materials will be published online with the full-text article. List the supplemental materials at the end of the manuscript file, and ensure they are cited consecutively within the manuscript text.

5. Processing After Acceptance

Once a paper is accepted for publication, the corresponding author must submit a signed copyright transfer agreement form via email to the editorial office. The paper will not be published until the copyright transfer is complete. Around this time, the invoice for the article processing charge (APC) will also be issued. Please note that publication will proceed only after the APC has been paid in full. Failure to complete payment may result in a delay in publication or, in some cases, withdrawal of the manuscript.

After the APC has been confirmed, the manuscript editor will format the paper to meet the journal's publication standards. Authors are required to respond within 3 working days to any revision requests from the manuscript editor. Please note that delays in response may result in the publication being postponed to the next issue.

A. Galley proofs

Once all corrections have been completed, the corresponding author will receive the final version of the manuscript in PDF format.

Within 5 working days of receipt, authors must reply to the printing office of any errors found in the file. The proof may be revised more than once by the corresponding author, if needed. Authors should double-check for corrections in the content, title, affiliation, capitalization, locations of figures, and references.

6. Post-Publication Corrections

To correct errors in published articles, the corresponding author should contact the journal's editorial office with a detailed description of the proposed correction. Corrections that profoundly affect the interpretation or conclusions of the article will be reviewed by the editors. Corrections will be published as author correction or publisher correction in a later issue of the journal.

Minor errors will be corrected directly in the online version of the article. An indication of the correction, along with the date it was made, will be added to the article information in both the HTML and PDF versions. A separate correction note will not be published.

Contact Us

Editor-in-Chief: Myeong Heon Shin, MD, PhD
Email: myeong@yuhs.ac

Editorial Office

Department of Tropical Medicine, Yonsei University College of Medicine, Yonsei-ro 50-1, Seodaemun-gu, Seoul 03722 Korea
Tel: +82-2-2228-1844 Email: support@parahostdis.org

NOTICE: These instructions to authors will be effective from the January 2026 issue.